New Modelling and Control Methods with Application to Combined Cycle Power Plants

Mohammad Hasan Moradi

Industrial Control Centre

Department of Electronic and Electrical Engineering

University of Strathclyde

Graham Hills Building

50 George Street

Glasgow G1 1QE

Submitted for the Degree of Doctor of Philosophy
January 2002

Declaration of Author's Rights

"The copyright of this thesis belongs to the author under the terms of the United Kingdom Copyright Acts as qualified by the University of Strathclyde Regulation 3.49. Due to acknowledgement must always be made of the use of any material contained in, derived from, this thesis."

Abstract

This thesis reports the analysis and modelling required to build a software simulation of combine cycle power plants. A new MIMO PID controller tuning method and a novel predictive PID controller design method for MIMO systems are also described in the thesis. The emphasis of this work is on simulation; identification and controller design methods.

The thesis begins with an account of the combined cycle power plant modelling and simulation development. This culminates in a library of different blocks and subsystems of combined cycle power plants. The simulation development shows how the steady state and dynamic behaviour of combined cycle power plants can be simulated and implemented in the SIMULINK and MATLAB environment using per unit models, which are suitable for control design.

In the identification stage, the relay identification method is used to identify the critical points of the system for a newly defined criterion at bandwidth frequency. Then, the identified critical points are used to tune PID controllers. The thesis then outlines multivariable PID tuning methods and makes a comparison between these methods and the new relay identification method concerning their robustness for MIMO systems.

The last two chapter of thesis are concerned with a new predictive PID controller design method for both SISO and MIMO systems. This methodology is concerned with the design of PID controllers, which have similar features to the model-based predictive controller. Generalized Predictive Control (GPC) design principles are used to develop the PID control with predictive capabilities for both SISO and MIMO systems. The combined cycle power plant simulation, especially the boiler subsystem, is used as an example throughout the thesis.

Dedication

To my wife and my sons who have stood by my side during the research and writing of this thesis with much understanding and consideration.

To my parents and to my parents-in-law for their love and support over the many years I needed to develop my career.

To my sister and my brothers and all my family and friends for their support.

Acknowledgements

Firstly, I should like to thank my supervisors Dr. Reza Katebi and Professor Michael Johnson. I am grateful to them for the background ideas that have contributed to this thesis and advice in formal and informal discussion sessions throughout the research period.

The author acknowledges the financial support derived from the Ministry of Science Research and Technology of Iran.

Preface

Many industrial processes are inherently multivariable and need multivariable control to enhance performance. This is a strong motivation to derive a simple and effective method for tuning multivariable process controllers. PID control is one of most common control schemes for industrial MIMO plants. These controllers are usually tuned using prior knowledge of dynamics of the system. But as MIMO processes are also non-linear, changes in the set point will cause changes the dynamics of system and the controller needs to be retuned. Therefore the robustness of a MIMO controller for model uncertainties is very important criteria.

PID control is also restricted in its performance for processes with time delay effects, non-minimum phase behaviour, unusual dynamics or a multivariable system structure. For these more complex control problems, advanced techniques such as Generalized Predictive Control (GPC) or Dynamic Matrix Control (DMC) may be required to achieve better control performance. For example, in the petrochemical industries, the GPC method (Clarke et al., 1987) has become one of the most popular Model Predictive Control (MPC) methods to be implemented. Model Predictive Control (MPC) has developed considerably over the last few years, both within the research control community and in industry. The reason for this success is because MPC is a good way of posing the process control problem in the time domain. Constraints, which are frequently found in these processes, can also be handled by MPC. In many reported applications, MPC has been found to be quite a robust type of control.

However in other industries and in more routine situations, even though these advanced techniques may provide superior control, they may not be used. A common hurdle to successful implementation of advanced controllers at Distributed Control System (DCS) level is the limited support in terms of hardware, software and personnel training available within many industries. Plant personnel at the DCS level are frequently unable to provide the higher level of programming skill and the extra commitment needed to

introduce advanced controllers and their associated features like failsafe redundancy. Implementing model-based control may also require capital investment to support new hardware and software products and also resources to train personnel in the operational behaviour of the new advanced controllers.

Meanwhile, the academic control community has developed many new techniques for tuning PID controllers. Often these methods try to extend the capabilities of PID control to match the performance of the advanced controller designs. One aim of this thesis is to develop new control methods for industrial multivariable process with application to Combined Cycle Power Plants (CCPP's). This development begins from models for CCPP's processes and systems. The full background to a modular, hierarchical procedure used to model these plants is given in the first chapters of the thesis where the appropriate SIMULINK code can be found. The CCPP has become more important over recent years due to both technological advances and the changing needs of the energy market. As the CCPP is a MIMO process, its control needs MIMO control design procedures. This thesis looks at this requirement and has been organized as follows:

Chapter 1 presents a review of different ways of classifying model for Combined cycle power plants' subsystems. It starts with an explanation of different configuration of CCPPs, and continues with a review of CCPPs' subsystem models that has been found in the published literature. The physical modelling and block box modelling of each subsystem is discussed and finally a model that is suitable for control purposes is chosen.

In Chapter 2, the CCPP's model from Chapter 1 is used to simulate the steady state and dynamic behaviour of CCPPs. This chapter presents a modular and hierarchical procedure to model these plants using SIMULINK. For the model validation, the step responses of model have been compared with published experimental data. The differences between results and the experimental data are shown to be insignificant.

The PID tuning methods, which will be discussed in this thesis, can be divided to following categories, where a key criterion is the availability of a process model, Fig 1.

- Model Free Methods
- Non parametric Methods
- Parametric Methods

Model Free Methods: No model or any particular points of the process are identified.
Non-parametric Methods: Some particular points of process such as critical points are identified. The model is generally based in the frequency domain.
Parametric Methods: A transfer function model for process will be identified.

Chapter 3 begins with a description of parametric and non-parametric multivariable PID tuning methods. A new criterion to calculate the robust performance of multivariable processes is introduced. Then, nominal performance, robust stability and robust performance of eight well known multivariable PID tuning methods are compared and discussed for the boiler model described in Chapter 2.

A new relay identification method for multivariable PID tuning is introduced in Chapter 4. The chapter starts from an explanation of the critical points for MIMO processes. Calculation of the process gains at bandwidth frequency and zero frequency using decentralized relay experiments is described. 2I2O PID auto-tuning method due to Palmor *et al*, (1995a) is extended for MIMO processes. In this chapter, a new relay identification method for PID tuning at bandwidth frequency is introduced. The appropriate algorithms for PID tuning methods in zero frequency and at bandwidth frequency have been prepared. Comparison between the Palmor *et al* tuning method and proposed method is discussed at the end of this chapter.

In Chapter 5, a new type of PID controller based on the GPC approach is introduced. This method is a kind of optimal parametric methods involving Control Signal Matching (see Fig I). The proposed PID control design is used and applied to low order, high order and non-minimum phase processes. The main idea is based on calculating an equivalent

set of PID parameters from a GPC control law derived using a general process model. In this way, an optimal controller is developed which has a simple and desirable PID structure but yields the level of performance expected from GPC.

One advantage of this predictive PID control scheme is related to hardware implementation and current operators' practice. The approach of this chapter is based on an existing PID controller configuration and requires only a little extra additional hardware because the calculations can be done off-line and tested on a computer away from the actual control system and then downloaded to the appropriate storage device. Moreover, there are no changes from the point of view of operators' training; the operators can continue to manage the plant in the same manner that they used before.

The chapter begins by describing the structure of PID type predictive controller and calculates the control law for this controller. The optimal value for PID type predictive controller is presented and then the stability issues are discussed. At the end of the chapter, a comparison between the proposed and GPC method is discussed.

Chapter 6 introduces an extension of the predictive PID controller (Chapter 5) for MIMO systems. The structure of MIMO PID type predictive controller is described at the beginning of chapter and then the optimal values of the controller gain are calculated. The chapter continues with a decentralized predictive PID controller representation followed by a state space representation of the predictive PID controller. Stability issues for MIMO closed loop systems are discussed. A comparison between the proposed method and the GPC technique close the chapter.

Chapter 7 presents the conclusions that follow from the work of thesis and a future work programme is outlined.

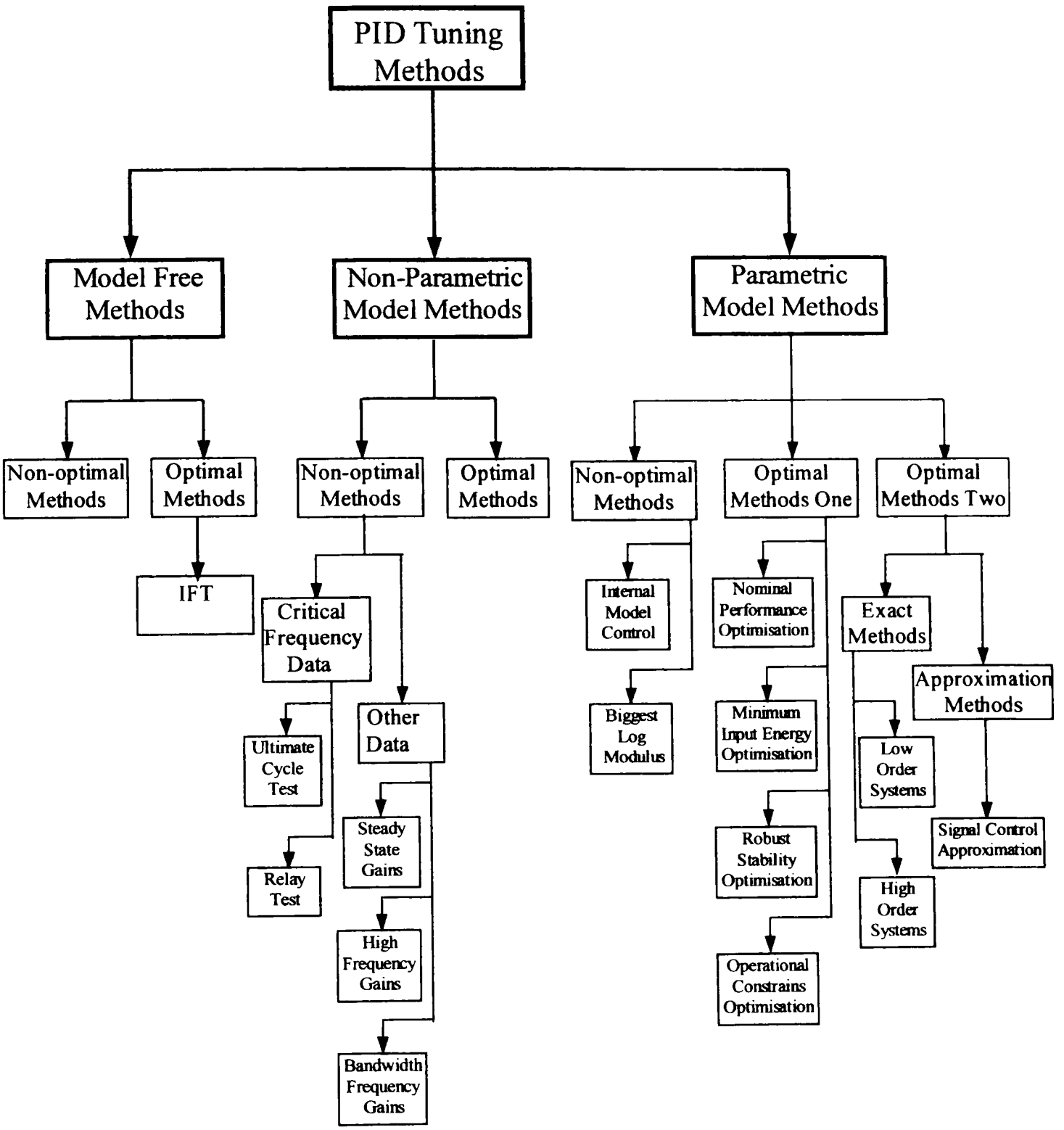

Fig I: PID tuning Methods

Original Contributions Presented in the Thesis

The research study was wide-ranging involving power plant modelling, simulation; control engineering analysis and insight in the theoretical areas. The investigations used academic software. The original contributions of this thesis are in five main areas:

1. **Simulation:** A simulation environment for combined cycle power plant was constructed. This is used throughout the thesis.

2. **Modelling:** The model structure to build a fully detailed and authentic simulation for the combined cycle power plant is recorded in Chapter2.

3. **Control Algorithm Implementation and Testing:** MIMO PID controllers were applied to combined cycle power plants. A new criterion for the discussion and comparison of robustness of PID controllers has been established.

4. **Algorithmic Improvements:** Contributions have been made to improve MIMO PID controllers tuning methods.

5. **Control Structure Design:** A new SISO predictive PID controller design method has been introduced. The method was extended to different representations of MIMO systems.

Publications

The following articles by the thesis author, arising from the work in this thesis, have been published.

Journal Papers

Moradi M.H., M.R. Katebi and M.A. Johnson, 2002a, '*The MIMO Predictive PID Controller Design*', "Advanced in PID Control" Special Issue of Asian Journal of Control, Vol.4, No. 4, 2002.

Katebi M R and M.H. Moradi, 2001, '*Predictive PID Controllers*', IEE Proceeding of Control Theory Application, Vol. 148, No. 6, November 2001, pp. 478-487.

Conference Papers

Moradi M.H., M.R. Katebi, M.A. Johnson, 2002b, *MIMO Predictive PID Controls*, The 15th IFAC World Congress, 21st – 26th July 2002, Barcelona, Spain.

Moradi M.H., M.R. Katebi, M.A. Johnson, 2001, *Predictive PID control: A new algorithm*, The 27th Annual Conference of the IEEE Industrial Electronics Society, IECON'01, 29th Nov- 2nd Dec 2001, p.p. 764-769, Colorado, USA.

Moradi M.H., M.R. Katebi, 2001, *Predictive PID control design for ship autopilot*, IFAC Conference on Control Applications for Marine Systems, CAMS 2001, 18th -20th July 2001, Glasgow, UK.

Moradi M.H., 2001a, *Multi Input Multi Output robust PID controller*, The 8th Iranian Student Seminar in Europe ISS-2001 5th -8th May 2001, Manchester, UK.

Katebi M.R., M.H. Moradi and M A Johnson, 2000c, *Controller tuning methods for industrial boilers*, IEEE International Conference on Industrial Electronics, Control and Instrumentation, (IECON) 18th to 22nd Oct. 2000, Nagoya, Aichi, Japan.

Moradi M.H., M.R. Katebi, M A Johnson, 2000b, *Combined cycle power plant, modelling, simulation and control*, UKACC International Conference on Control 2000, 4th -7th Sept. 2000, Cambridge, England.

Moradi M.H., M.R. Katebi and M A Johnson, 2000b, *Modelling, simulation and control of power plant*, International Conference for Process Control and Instrumentation (PCI2000), 26th -28th July 2000, Glasgow, Scotland, pp. 123-128.

Katebi M.R., M.H.Moradi and M A Johnson, 2000a, *On the robustness of multivariable PID tuning methods*, The Eighth Iranian Conference on Electrical Engineering, 17th-19th May 2000, Isfahan, Iran, pp. 31-38.

Katebi M.R., M.H. Moradi, M A Johnson, 2000a, *A comparison of stability and performance robustness of multivariable PID tuning method*s, IFAC Workshop on Digital Control, 5th - 7th April 2000, Terrassa, Spain, pp. 611-616.

Others

Moradi M.H., M. A. Johnson and M.R. Katebi, 1999, *Power generation simulation and control*, Advanced Control Technologies for Power Generation and Distribution: An International Training Course September 20-23, 1999, University of Strathclyde, Glasgow, UK.

Moradi M.H., M.R. Katebi and M A Johnson, 2000d, *Combined cycle power plant: modelling, simulation and control*, 7th Iranian Student Seminar in Europe ISS-2000, 20th -21st May 2000, Manchester, UK, pp. 73-78.

Moradi M.H., 2001b, *Book review: Advances in PID Control* by K.K. Tan, Q. Wang, C.C. Hang and T. Hagglund; Springer-Verlag London, ISBN: 1-85233-138-0, Published in International Journal of Adaptive Control and Signal Processing.

Moradi M.H., 2002, *Book review: "Predictive Control with Constraints"* by J.M. Maciejowski; Prentice Hall London, ISBN: 0-201-39823-0, Published in International Journal of Adaptive Control and Signal Processing.

Contents

Acronyms:

2I2O	Two-Input and Two-Output
ADC	Advanced Digital Control
ANN	Artificial Neural Network
A/C	Analogue to Digital
BC	Boiler Control
BLT	Biggest Log Modulus
CARIMA	Controlled Autoregressive Integrated Moving Average
CC	Combined Cycle
CCPP	Combined Cycle Power Plants
CHP	Combined Heat and Power
CV	Control Valve
DCP	Desired Critical Points
DMC	Dynamic Matrix Control
DNA	Direct Nyquist Array
DRF	Decentrelised Relay Feedback
DSM	Dynamic Set-point Manoeuvring
EHC	Electro-Hydraulic Control
EVA	Early Valve Actuation
FDM	Fuzzy Dynamic Modelling
GPC	Generalised Predictive Control
HP	High pressure
HRSG	Heat Recovery Steam Generator
IGCC	Integrated Gasifier Combined Cycle
IGV	Inlet Guide Vanes
IP	Intermediate Pressure
IMC	Internal Model Control
IRF	Independent single Relay Feedback
IV	Interface Valve

LP	Low Pressure
LQG	Linear Quadratic Gaussian
LQGPC	Linear Quadratic Generalised Predictive Control
LR	Load Reference
LTDS	Long term Dynamic Simulation Programs
MPC	Model Based Predictive Control
MIMO	Multi Inputs and Multi Outputs
MW	Mega Watt
MZN	Modified Ziegler-Nichols
NN	Neutral Network
NO_X	Oxides of Nitrogen
PI	Proportional and Integral
PID	Proportional, Integral and Derivative
POMC	Process Optimising Multivariable Control
QP	Quadratic Programming
RTO	Real Time Optimisation
SFR	System Frequency Response
SIGT	Steam Injection Gas Turbine
SISO	Single Input and Single Output
SRF	Sequential Relay Feedback
TC	Turbine Control
UHRSG	Unfired Heat Recovery Steam Generator
ZN	Ziegler-Nichols

Chapter 1

A Review of Modelling and Control of Combined Cycle Power Plants

1. 1 Introduction

Combined Cycle Power Plants (CCPP's) are power plant systems in which two types of turbines, namely a gas turbine and a steam turbine, are used to generate electricity. Moreover the turbines are combined in one cycle, so that the energy in the form of a heat flow or a gas flow is transferred from one of the turbines types to another. The most common type of Combined Cycle is where the exhaust gases from the gas turbine are used to provide the heat necessary to produce steam in a steam generator. The steam is then supplied to the steam turbine. However, as will be shown later, other connections between the gas turbine and the steam turbine are possible.

The purpose of introducing Combined Cycle in power plants is to reduce losses of energy. Their main role lies in the utilisation of waste heat, which may be found in exhaust gases from the gas turbine, or at some other points of the process to produce additional electricity. In this way the overall efficiency of the plant - that is the efficiency of transformation of fuel energy into electric energy - increases reaching over 50%, when for traditional steam turbine plants it is approximately 40% and 35% for gas turbines plants (Boissenin and Castanier, 1988).

Chapter 1

Combined Heat and Power (CHP) plants, sometimes called Cogeneration plants, are those, which produce both electricity and heat. In this case electricity may be generated by a steam turbine or a gas turbine or, in smaller installations, by a diesel engine. Heat is extracted as steam or hot water and exported from the system. The ratio between electric output and heat output depends on the end requirements and this influence the selection of the configuration and sizing of components. The most common installation consists of a steam turbine cycle in which part of the steam is bled from the steam turbine to provide heat. However, other combinations are also possible. In particular a Combined Heat and Power scheme may also include a Combined Cycle installation.

Some examples of CC and CHP installations may be found in (Jericha and Hoeller, 1991), (Yacobucci, 1991), (Boissenin and Castanier, 1988), (Wiggin, 1981), (Ahluvalia and Domenichini, 1990). According to (Shields, 1989) the largest Combined Cycle plant in the world is in Japan, where 14 gas turbines and 14 steam turbines (one gas turbine and one steam turbine driving one generator) generate 2000MW electric power firing natural gas.

In this chapter different configuration of CCPP's and their subsystems such as boiler, steam turbine and gas turbine will be discussed. The Chapter has been organised as follows: Section 2 describes different configuration of CCPP's, and Section 3 describes boiler modelling and different boiler control strategies. Steam turbine and gas turbine modelling and control are described in Sections 4 and 5 respectively. The conclusion is drawn at the end.

1.2 Combined Cycle Configurations

1.2.1 Combined Heat and Power Configurations

A wide variety of CHP schemes exist. The emphasis is usually on configurations, which are primarily for electricity production. Consequently, the classification is based on the type of turbine and fuel used for electricity generation. Hence, three types of plants (Basu and Cogger, 1986) are considered:

- Plants with steam turbines
- Plants with gas turbines
- Plants with diesel engines.

For steam turbines schemes the fuel may be coal, natural gas or gas obtained from coal gasification. Liquid fuels are less popular due to their higher cost. For gas turbines, the fuel is mainly gas, however, liquid fuels may be used, especially during the start-up procedure when they are much safer. In addition, in CHP schemes with gas turbines an additional firing may be provided to the boiler and for this purpose any kind of fuel is suitable. Plants operating on liquid fuel are usually small local installations using modified diesel engines with added waste heat recuperation facilities. Also in this case an additional firing may be provided to the boiler.

1.2.2 Combined Cycle Power Plants

The most popular types of CC power plants are:

- Unfired Heat Recovery Steam Generator (HRSG)
- HRSG with supplementary fired boiler
- Fully fired steam generator low excess air cycle
- Integrated Gasifier Combined Cycle (IGCC)
- Steam Injection Gas Turbine (SIGT)

In the following section the most popular types of CCPP's will be reviewed.

Unfired Heat Recovery Steam Generator (UHRSG)

The exhaust gas from the gas turbine is used for steam production in the heat recovery steam generator. The UHRSG extracts heat from exhaust gas to raise the steam parameters (temperature and pressure). In this configuration, the gas turbine plays the main role in electricity production Fig1.1.

HRSG with Supplementary-Fired Boiler

Using exhaust gas from the gas turbine alone to generate steam frequently results in inadequate flexibility for combined cycle applications. For this reason, gas turbine heat recovery boilers are often provided with an additional firing system Fig1.2. The efficiency may be lower, when compared with the standard configuration, but there is an added flexibility in that the boiler may be supplied with different kind of fuels compared with UHRSG. Finckh and pfost (1992) argued that the overall efficiency of the simple non-heated recuperative plant could be improved by supplementary firing up for large size power plant. However, few recent plants use supplementary-fired HRSG. Schobesberger *et al.* (1991) have reported a heat recovery combined cycle with supplementary firing, especially adapted to the requirements of a paper mill.

Fully Fired Steam Generator Low Excess Air Cycle:

In this case the exhaust gas from the gas turbine provides air to the boiler combustion chamber. With a high gas turbine exhaust temperature, the air pre-heater installed in the original steam plant (to preheat air for combustion) is not required in combined cycle operation, and all the boiler feed water is passed through the economisers. Therefore, the overall efficiency will improve. The steam turbine is the main electricity producer (80-85%) Fig 1.3, (Boissenin and Castanier, 1988). This re-powering of steam power plants leads to the following advantages (Gambini and Guizzi 1989):

- Simple lay out
- Very few modification to in the existing components
- Good improvements in performances and efficiency of the combined plant

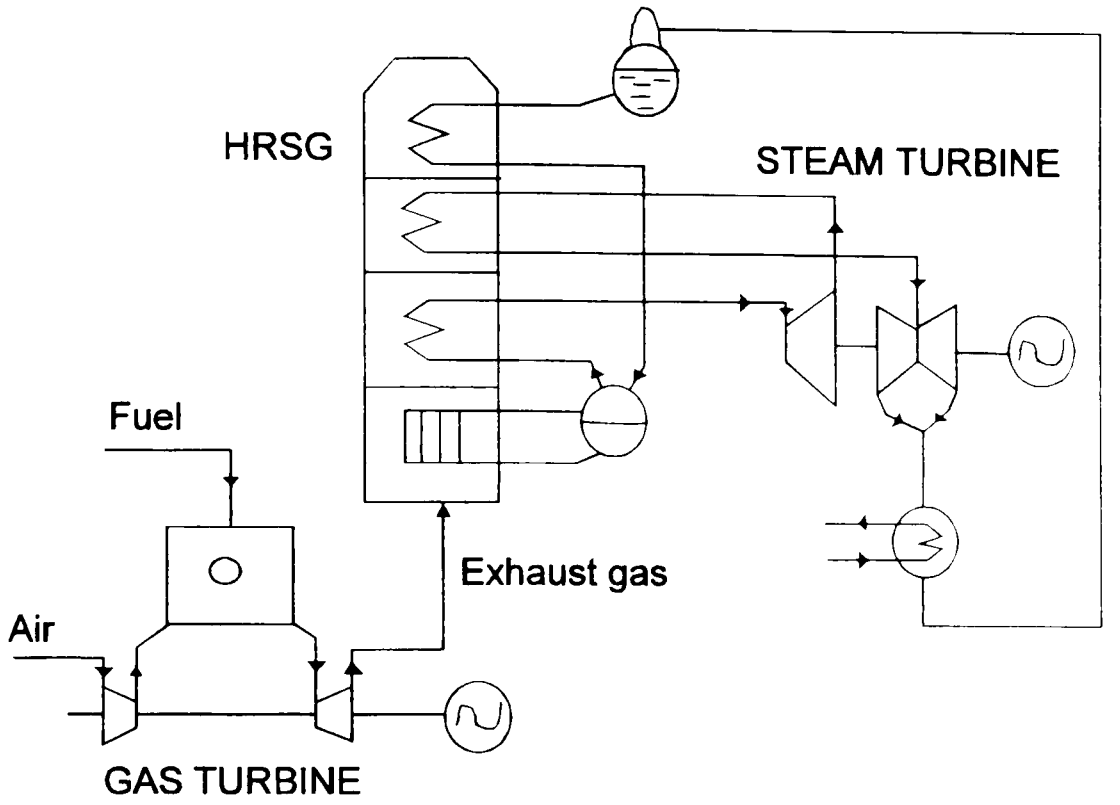

Fig 1.1: Unfired Heat Recovery Steam Generator.

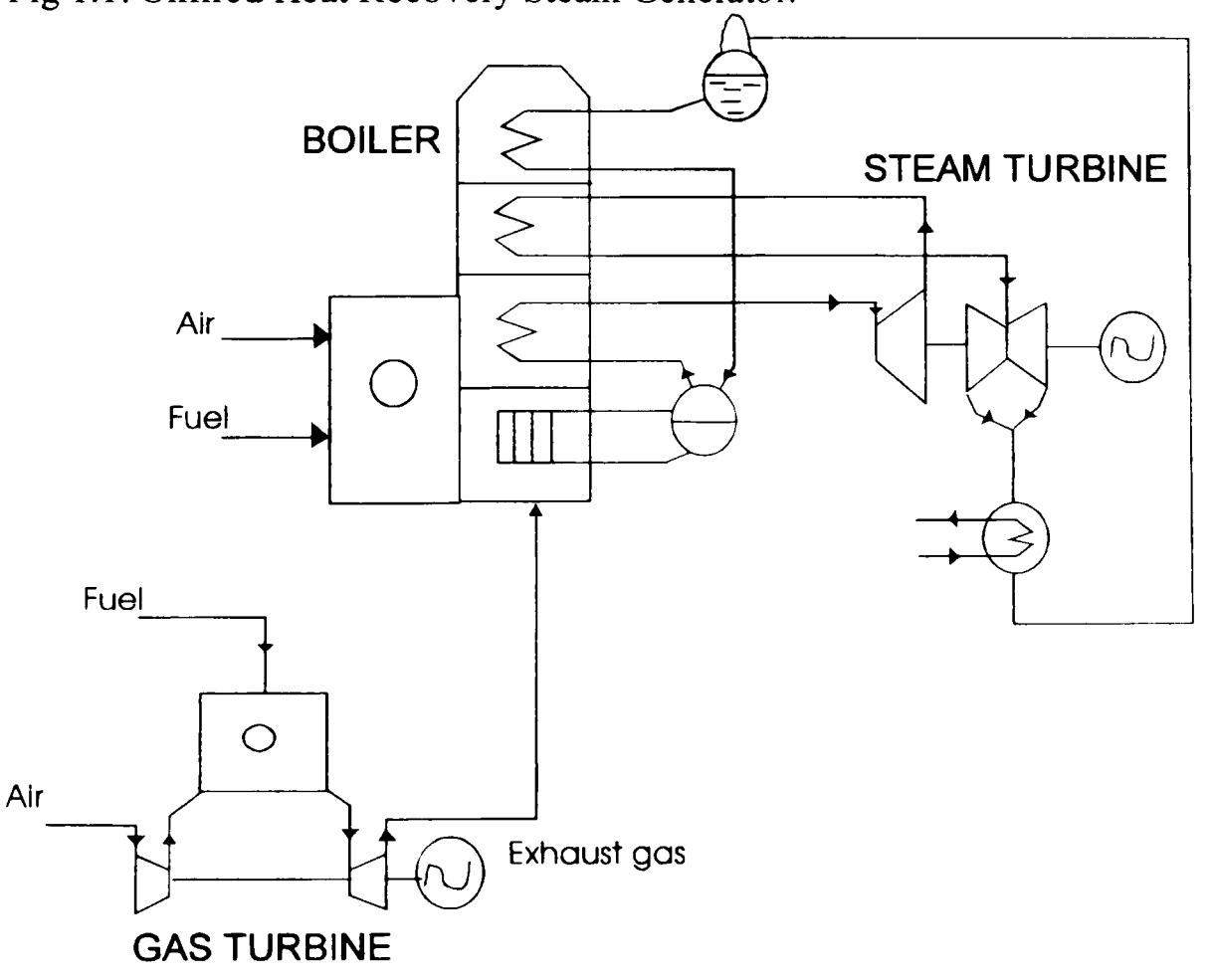

Fig 1.2: HRSG with Supplementary Fired Boiler.

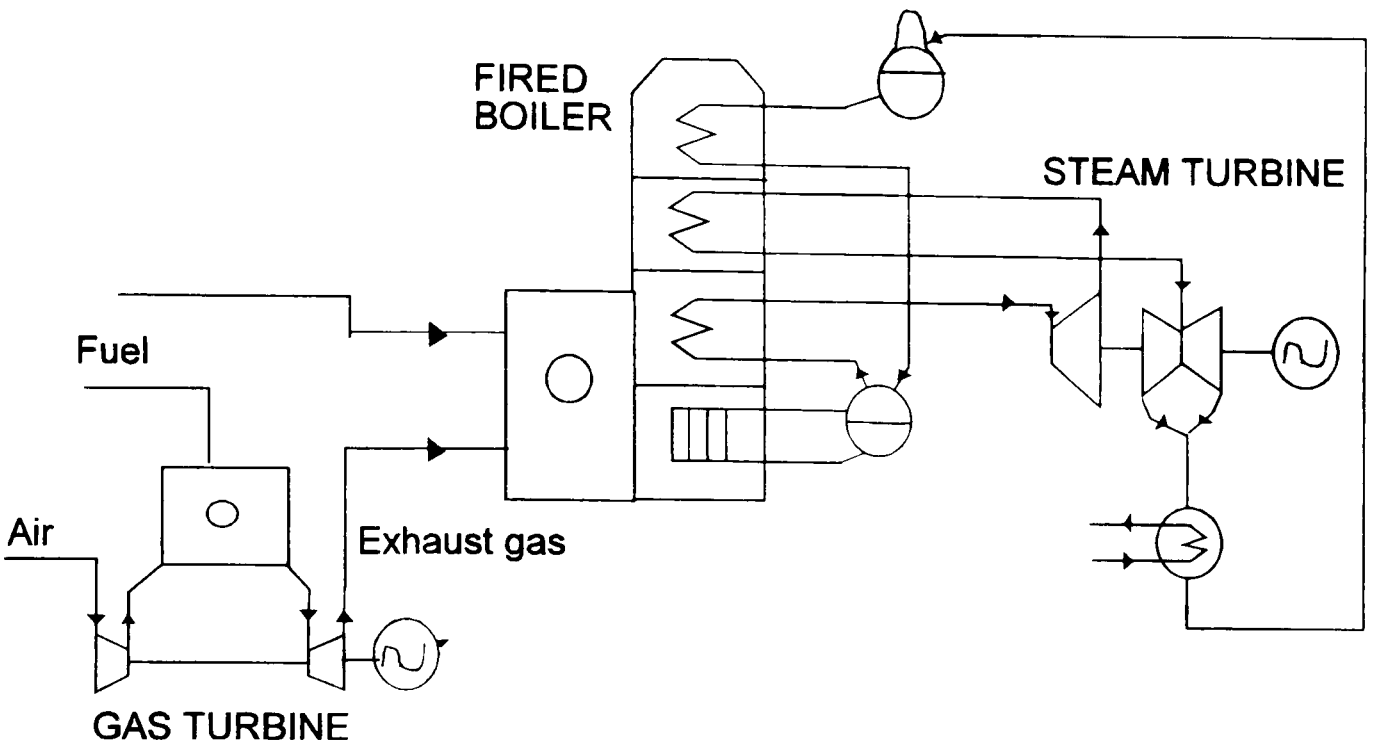

Fig 1.3: Low excess air (Fully Fired) CC configuration.

Integrated Gasifier Combined Cycle (IGCC)

In this configuration coal is used to produce necessary gas to the combined plant, this process reduces the subsequent combustion temperature and NO_x production (Zaporowski, 1996). The IGCC is a natural possibility for power plant construction, for countries, which are not be able, for economic reasons, to assign considerable quantities of natural gas for electric energy generation, Fig 1.4.

Steam Injection Gas Turbine (SIGT)

In SIGT, NO_x is controlled by injecting steam or water into the gas turbine inlet, Fig 1.5. To improve the performance of SIGT units, its thermodynamic characteristics have been analysed by many researchers (Larson and Williams, 1987; Noymer and Wilson, 1993; Rice, 1993a-c). In addition to the thermodynamic analysis, operational problems have been discussed for the purpose of the co-generation application, optimisation approaches have been adopted to improve the economic and energy saving properties for SIGT units (Ito *et al,* 1997).

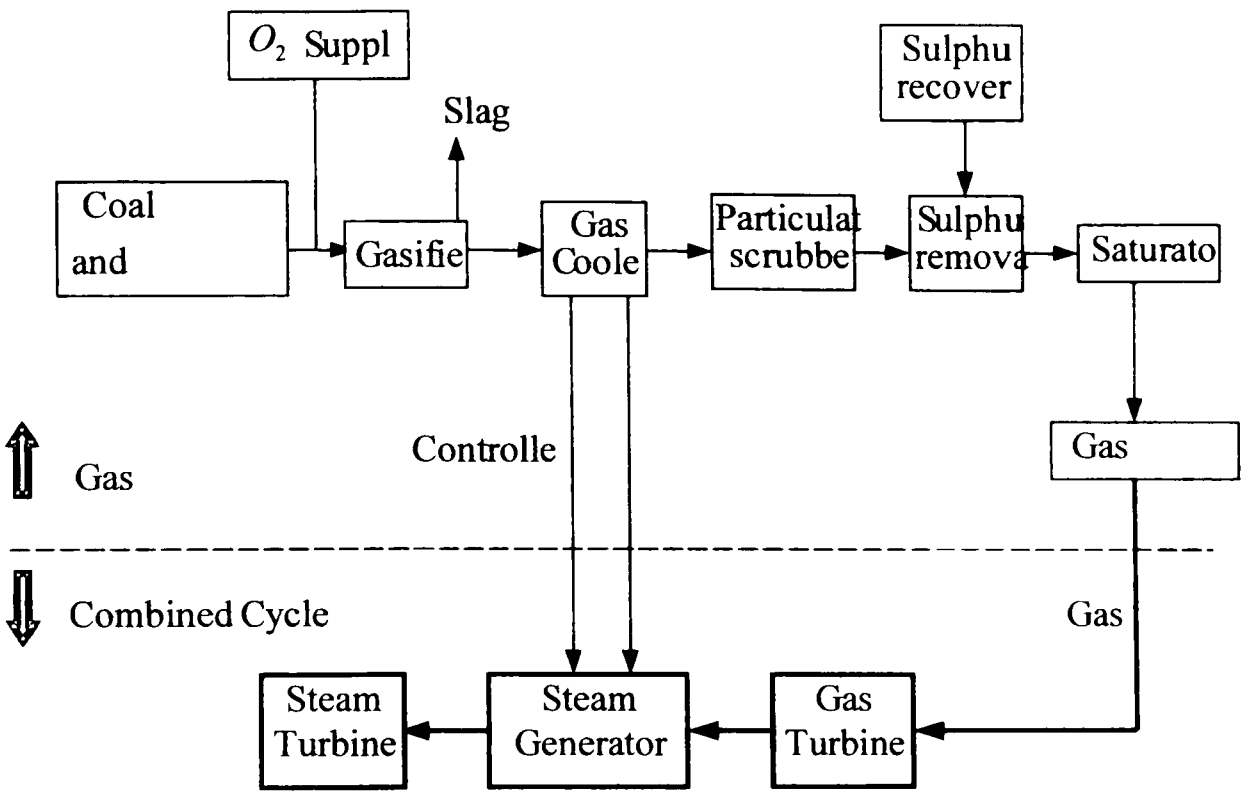

Fig 1.4: Integrated Gasifier Combined Cycle (IGCC)

E.G.

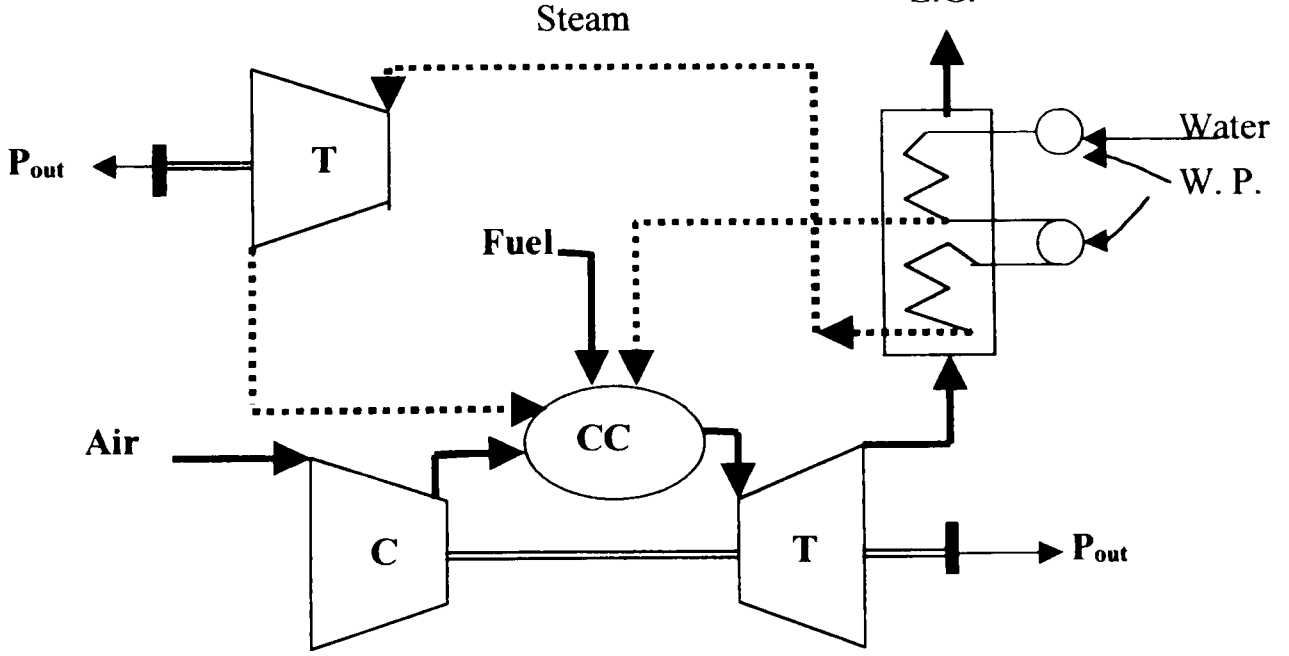

Key: ····· Steam Path —— Gas Path C: Compressor T: Turbine
CC: Combustion Chamber P_{out}: Output Power W. P.: Water Pump

Figure 1.5: Steam injection gas turbinesystem

1.3 Boiler

1.3.1 Boiler Description

The steam is produced in the boiler and superheated in the super-heater and re-heater. Then, the thermal energy of the steam is converted to mechanical energy in the various sections of the turbine. Boiler designs fall into two categories:

- *Drum Type Boilers*
- *Once Through Boilers*

Drum Type Boilers

A typical drum-type boiler is depicted in Fig 1.6. The feed-water is supplied to the drum. Then, the water flows into the down-comers, and then enters the risers. In the risers the heat from the furnace is used to increase the water temperature and eventually to cause evaporation. Thus the circulation of water, steam, and water and steam mixture takes place in the drum, the down-comers and the risers. Steam generated in the risers is separated in the drum from where it flows through the super-heater on to the high-pressure turbines. It may then be recycled to the boiler in the re-heater where its energy content is increased.

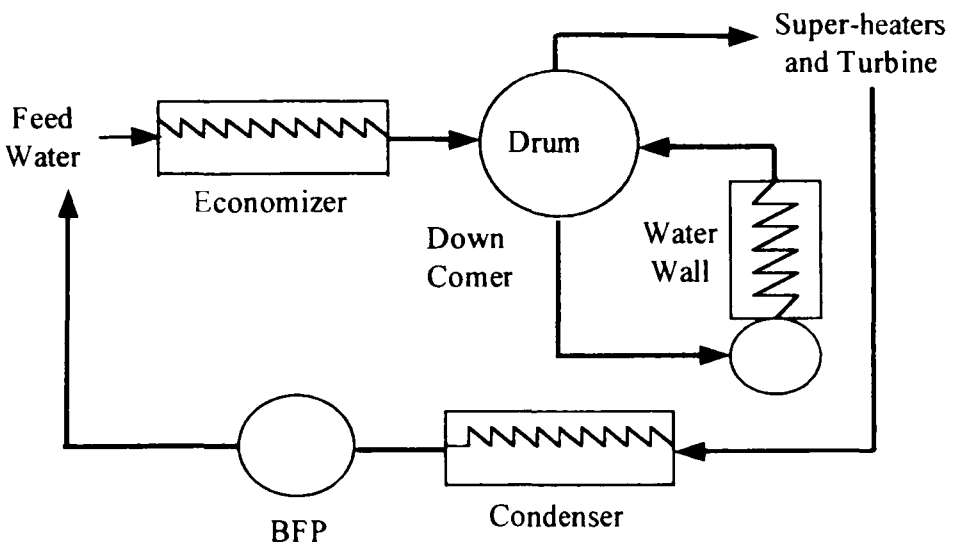

Fig 1.6: Drum type boiler

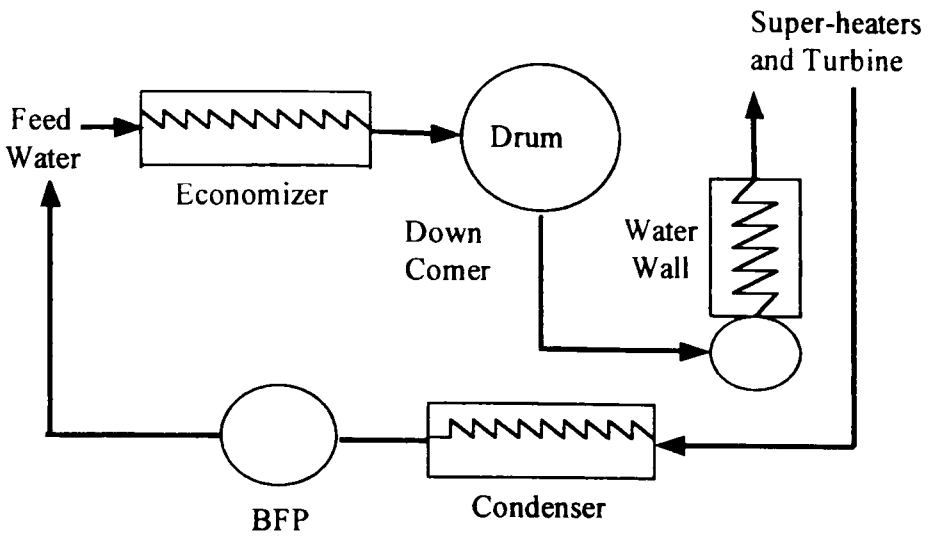

Fig 1.7: Once-through type boiler

Once Through Boilers

In a once-through boiler, Fig 1.7, there is no re-circulation of water within the furnace. Instead, feed-water, at high pressure, flows straight through the water-walls where it receives furnace heat and is converted to steam, which then passes through the super-heater and eventually enters the High Pressure (HP) turbine.

There are three major control loops involving power, throttle pressure, and steam temperature. These are controlled by manipulating the governor valve, feed-water valve, and firing rates either individually or in a co-ordinated mode by manipulating all three loops simultaneously. Unlike in a drum type boiler, there is no drum level to be controlled in a once-through boiler.

1.3.2 Boiler Modelling

One of the first steps in study of power plant is the development of a mathematical model of power plant. This model must not be over-simplified, or conclusions drawn from it will not be valid in the real world. The model should not be so complex as to complicate unnecessarily the analysis. Boiler models can be developed by two distinct methods:

- Physical modelling
- Black box modelling

The tree diagram of two methods and the associated literature has been shown in Fig 1.8.

Chapter 1

Physical Modelling

In the theoretical approach, a set of simultaneous partial differential equations is formulated to describe the dynamic balances of energy and mass within the process. This is then linearised under certain assumptions. The linear state equation is derived from the linearised model. However, because of the complexity of the process, this method tends to produce very high order models. Moreover, the validation of the model is cumbersome and time consuming (Appendix 1.1). The physical modelling of boiler can be divided to two categories:

I. High order physical models
II. Low order physical models

High Order Physical Models

The boiler models represented by 5^{th} order equation or more are called high order models.

A detailed non-linear boiler model is developed by McDonald *et al.* (1971) based on physical principles. The model is validated against plant tests. and it represents the dynamic relationships between the inputs and outputs are shown in Table 1.1. The model consists of 14 first order non-linear differential equations and 82 linear and non-linear algebraic equations. Harvey and Wall (1981) have used this model to design robust multivariable controllers in their investigations of boiler control.

Table 1.1: Input and Output for Boiler Model (McDonald *et al.* 1970)

Inputs	Outputs
1 Mill feeder stroke 2 Governor valve position 3 Feed-water valve position 4 Air flow 5 Super-heater and re-heater spray flows 6 Super-heater and re-heater burner tilts.	1. Electric power 2. Drum temperature and pressure 3. Drum water level 4. Throttle temperature and pressure 5. Re-heater outlet temp. and pressure 6. Steam flow

Dieck-Assad and Masada (1987) have used a 32nd order boiler- turbine model to solve optimal set-point scheduling problem for main and hot re-heat steam conditions in a 235 MW gas fired electric generating plant. The performance index minimises fuel consumption by rescheduling the set points of the main steam pressure and temperature and hot reheat steam temperature.

Manayathara and Bentsman (1994), developed a boiler model which is gas or oil-fired. The measurable outputs are steam pressure, excess oxygen in the stack and water level in drum. The input available for control consists of the fuel rate, airflow and Water flow. Pellegrinetti and Bentsman (1996) have presented control-oriented mathematical models with four measurable outputs, three controllable inputs. The effect of two disturbances, three constraints and model uncertainty is considered, Table 1.2. The model captures the major dynamics of a drum-boiler system like shrink and swell, non-linearity, and time delay. The model obtained can be directly used for the synthesis of the model based control algorithms as well as setting up a real-time simulator for testing of new boiler control systems and operator training. Cheung and Wang (1998) used this model to compare Fuzzy and PI controller for a benchmark drum boiler.

Saez and Cipriano (1998) have used physical models to determine the optimal set points for boiler. The measurable outputs is mass flow temperature and pressure to steam turbine, the controlled variables are drum water level, furnace gases pressure and superheated steam temperature, and the manipulated variables are feed-water flow, air flow and attemporizator water flow.

Table 1.2: Characteristics of Boiler Model (Pellegrinetti and Bentsmn 1996)

Inputs	**Outputs**	**Constraints**	**Disturbances**
Fuel flow rate Air flow rate Water flow rate	Drum pressure Excess oxygen level Drum water level Steam flow rate	Actuator Unidirectional flow rates Drum flooding	Steam demand Sensor noise

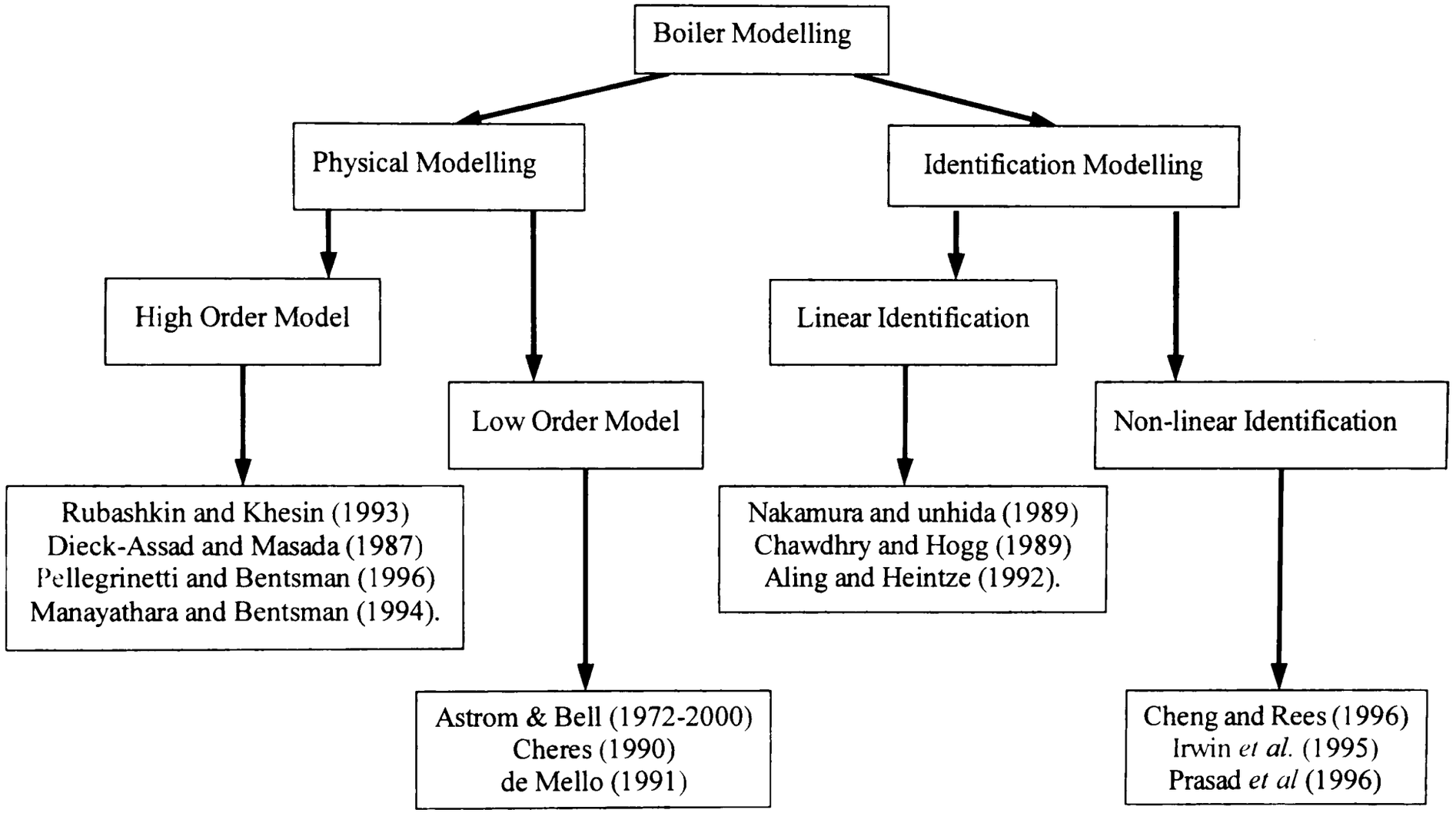

Fig 1.8: Different methods of boiler modelling

Low Order Physical Models

In some application, accurate low order boiler models are needed. These models are obtained from the simplification of high order models or by considering some part of the dynamics of system. Depend on application of model; dynamic behaviour of part of system is ignored. Low order boiler models were used in:

- Megawatt Response by IEEE Working Group (1973)
- Plant Control Schemes by Landis (1977)
- Long term Dynamic Simulation Programs (LTDS) by Undrill (1984)
- Dispatcher Training Simulators by Hemmaplardh and Lamont (1986)

A first order model was presented by Astrom and Eklund (1972). The model is obtained from the global energy balance for the total plant. The model has one state variable that is the drum pressure. The model is more widely used in control studies.

In existing simple models, level dynamics are usually neglected, which means that the shrink and swell affect is not modelled. Also, drum level is assumed to remain constant to simplify the modelling process. Bell and Astrom (1996) report a fourth order non-linear model that considers the dynamics of water level and captures shrink and swell affects. This model has steam quality in the riser, volume deviations of the steam below the liquid surface in the drum, water volume and drum pressure as state variables. Validation against plant data shows that the model captures the behaviour of real plants with high fidelity.

Astrom and Bell (2000) have presented a non-linear dynamic model for natural circulation drum boilers. The model describes the complicated dynamics of the drum, down comer and riser components. The model has four states; two account for storage of total energy and total mass, one characterizes steam distribution in the risers and another the steam distribution in the drum. The model can be characterized by steam tables and a few physical parameters. The model has been validated against data with very rich excitation that covers a wide operating range.

Data and control scheme for small and medium size boiler models have been presented by Cheres (1990). Methods and field tests for the data evaluation are included. The resulted error due to measurement inaccuracy, model simplification and the applied procedure for data evaluations are also presented. These partially solve the data problem. which limits the applicability of the low order models.

de Mello (1991) shows the validity of two simplified models by comparing their response characteristics against those obtained from more rigorous physical models. The first model requires nine boiler parameters to be derived, and for second needs six parameters. Scott and Russell (1994) used this model for the boiler with suitably chosen time constant for modelling of a combined cycle.

Black Box Modelling (Identification)

System Identification is an essential method to obtain the proper state equation to represent the relationship between output variables and the relevant input variables (Appendix 1.2). There are two methods for system identification:

- Linear method
- Non-linear method

Linear identification method

Chawdhry and Hogg (1989) obtained linear models of boilers directly from test data, using the methods of system identification that were proposed by Soderstrom and Stoica (1989). An autoregressive model has been fitted to the plant input and output data by Nakamura and Uchida (1989). The model has three inputs and two outputs. Steam temperature control is where attention is focused. To compensate for system non-linearities, the calculations for system identification and feedback gain are determined for two or three load levels.

MIMO system identification experiments on the boiler system of a 600 MW power plant have been reported by Aling and Heintze (1992). The aim of this research was to investigate the feasibility of closed loop identification for large-scale industrial processes. The conclusion was that closed loop system identification often requires

identification in parts, due to large response time difference in boiler control loops. The closed loop situation in combination with different time constants in different parts of boiler made the partitioning necessary.

Rubashkin and Khesin (1993) considered the problem of modelling a boiler outside the normal operating range, such as the start up regime. Such models are particularly well suited for operator training and fault monitoring.

Non-linear identification method

Cheng and Rees (1996) have presented an identification study for a non-linear steam generation drum-boiler system. The goal was to develop a simple non-linear dynamic model for the drum-boiler system by using a Fuzzy Dynamical Model (FDM), which can be interpreted qualitatively and quantitatively for the ease of control design.

Irwin *et al.* (1995) report on the application of a particular network paradigm (the multi-layer perceptron) to the off-line identification of a 200MW, oil-fired, drum-type boiler. Mathematical modelling of plant was undertaken to predict performance and responses, and for use in the design of controllers. The result showed significantly improved predictions of the plant outputs across the complete operating range.

Artificial neural networks (ANN) modelling techniques have been used for identifying global dynamic models of the boiler variable by Prasad *et al*, (1996). It was shown that the ANN model based non-linear predictive controller gives a superior performance in maintaining the main steam temperature and reheat steam temperature.

Conclusion:

In this section boiler modelling was discussed that could be divided to; parametric modelling and black box modelling. Parametric modelling can be considered as high order models which are complex and suitable for the detailed study of boiler behaviour, and low order models which are easy to understand and suitable for control studies. Black box modelling can be considered as linear identification in which theses models are suitable to apply classical controller and non-linear identification that is more suitable to study non-linear behaviour of boilers.

1.3.3 Control System for Boiler

The control systems associated with fossil-fuelled plants vary with the manufacturer and age of the unit. Usually the firing rate, pumping rate, and throttle valve settings are the manipulated variables. The controlled output variables of interest are temperature and pressure in boiler and electrical power and speed in generator. The main control concepts for the power production in fossil fired steam power plants are shown in Fig 1.9, these are:

- Normal operation range
- Boundary operation range
- Protected operation range

In each case the desired control variables must be governed in such a way that the generated power in the individual sub-units will be produced as economically as possible, while fulfilling the reliability condition that each process component must be run within its normal operation range.

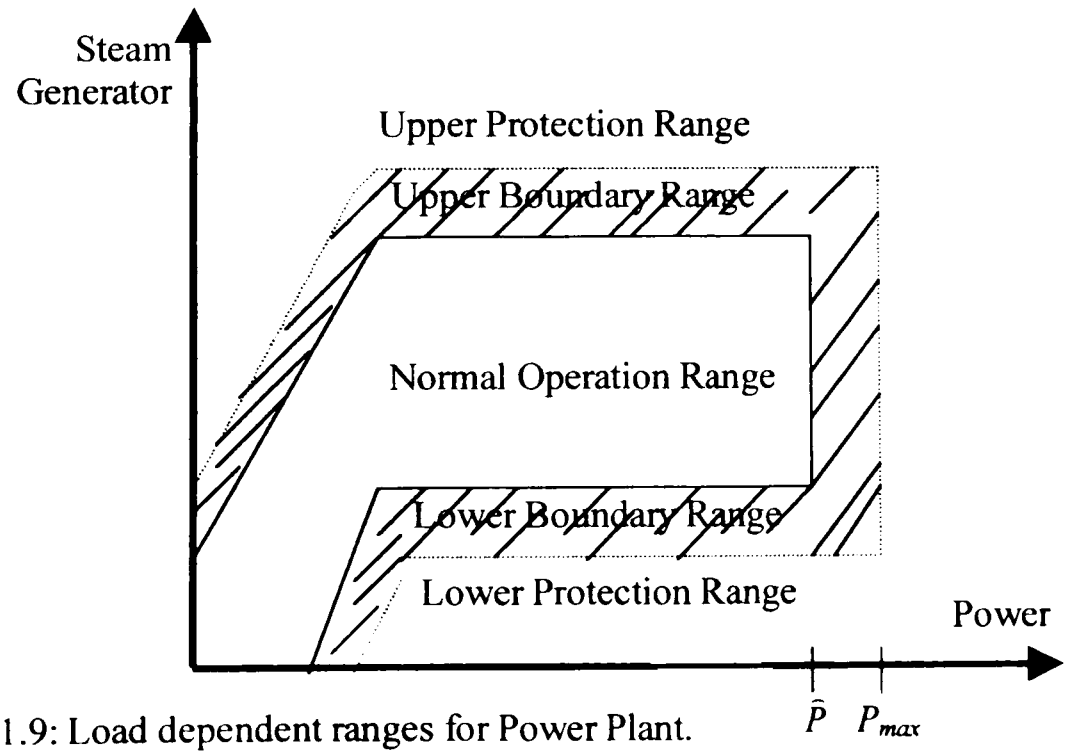

Fig 1.9: Load dependent ranges for Power Plant.

If the plant variables exceed safe limits, the protection system is designed to reduce the plant output or trip the unit. Traditionally, it was the task of the process operators to lead the process back to normal operation manually. With the increasing degree of automation, changeover equipment from the normal control concepts to special constrained control concepts have been introduced and applied to avoid critical process variables reaching the protection range. The switching back from the constrained to the normal control concept could be done automatically or manually.

The control system associated with a thermal plant can be classified into follow categories:

a) Overall unit control
b) Process set point control
c) Process parameter control
d) Actuator control

These control schemes are shown in Fig 1.10, and three high level controllers are described in the following sections.

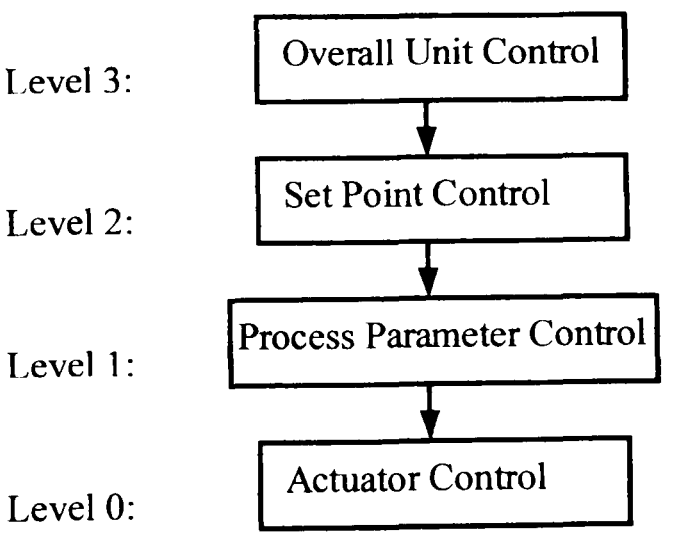

Fig 1.10: Control scheme for power plant

Chapter 1

A) Overall Unit Control

There are four overall unit control strategies or modes of operation:

- Boiler following (turbine leading)
- Turbine following (boiler leading)
- Integrated or co-ordinated boiler-turbine control
- Sliding pressure control

In the next section, each overall unit control will be explained.

I. Boiler following mode

Boiler following controller is more common in practice. In this control strategy, changes in generation are compensated by turbine control valve in first step and then, the boiler controls respond to the resulting changes in the steam flow and pressure by changing steam production (Fig 1.11). A difference between steam production and steam demand results in the change in boiler pressure. The throttle pressure deviation from its set-point value is used as an error signal by the combustion controls to regulate fuel and air input to the furnace.

With the boiler following mode of operation, the boiler-stored energy is initially used to meet the steam demand and initial response of MW output is rapid. The coupling between throttle pressure and MW output results in a "dip" in the MW output when the

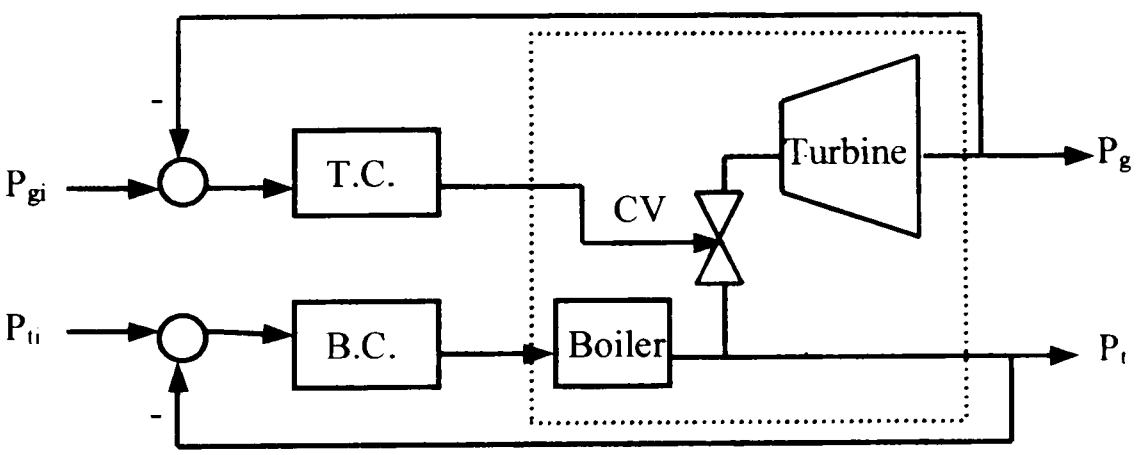

Key: P_g: Power Generator, P_{gi}: Set Point of power Generator, P_t: Throttle Pressure, P_{ti}: Set point of Throttle Pressure

Fig 1.11: Boiler following Mode

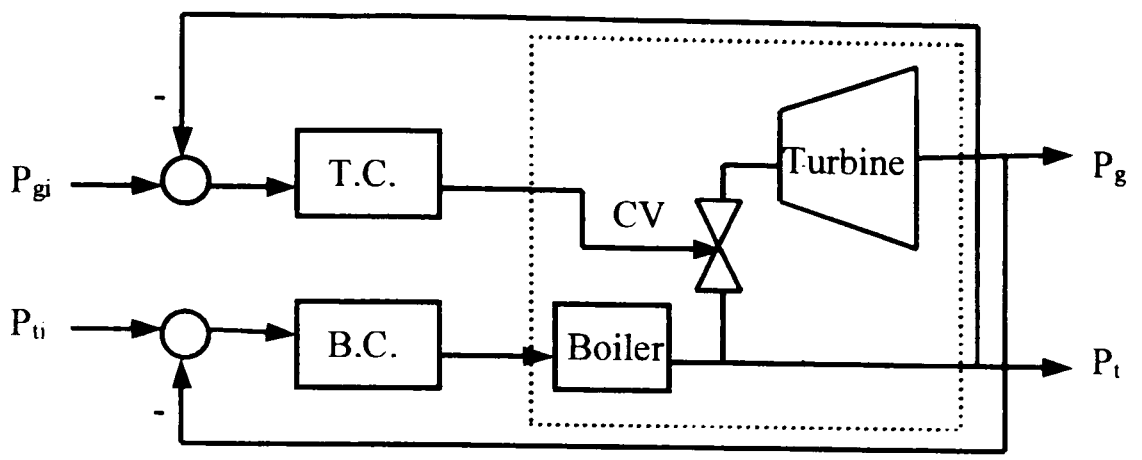

Key: P_g: Power Generator, P_{gi}: Set Point of power Generator,
P_t: Throttle Pressure, P_{ti}: Set point of Throttle Pressure

Fig 1.12: Turbine following Mode

boiler pressure is at a minimum. This coupling, along with boiler time lag, produces an oscillatory response. For large changes, the deviations in boiler variables may be excessive.

II. Turbine following mode

In this control strategy, changes in generation are compensated by changing input to the boiler. The MW demand signal is applied to the combustion controls. The turbine control valve regulates boiler pressure; fast action of the valves maintains essentially constant pressure (Fig 1.12).

With the turbine following mode, no use in made of stored energy in boiler; hence, steam flow and MW output closely follow steam production in the boiler. While the unit can be manoeuvred in a well-controlled manner, the response rate is limited by the slow response of the boiler.

III. Integrated or co-ordinated boiler-turbine control

This control provides an adjustable blend of both boiler following and turbine following modes of control. An improvement in unit response is achieved through integrated control. It is evident that the integrated control strikes a compromise between fast response and the boiler safety (Fig 1.13).

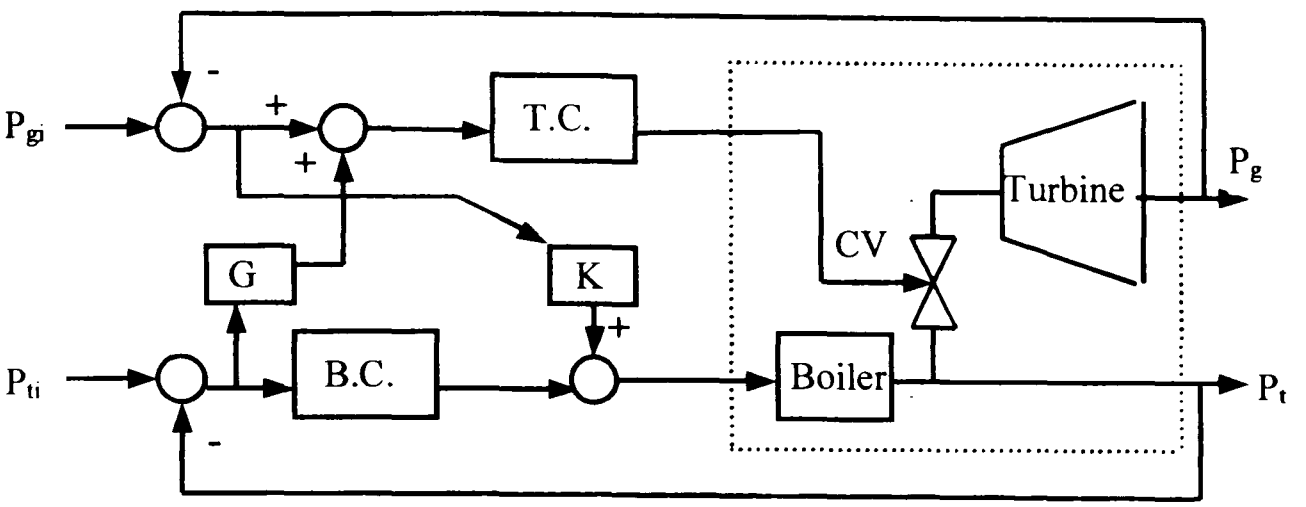

Key: P_g: Power Generator, P_{gi}: Set Point of power Generator,
P_t: Throttle Pressure, P_{ti}: Set point of Throttle Pressure

Fig 1.13: A Co-ordinated Control Mode

IV. Sliding pressure control

In the sliding pressure control, the throttle pressure set point is made a function of unit load rather a constant value (Fig 1.14). The control valves are left wide open (provided the drum pressure is above a minimum level) and the turbine power output is controlled by controlling the throttle pressure through manipulation of the boiler controls. A major advantage of this mode of control is that no change in throttling action occurs during load manoeuvring; therefore the temperature in the HP turbine remains nearly constant.

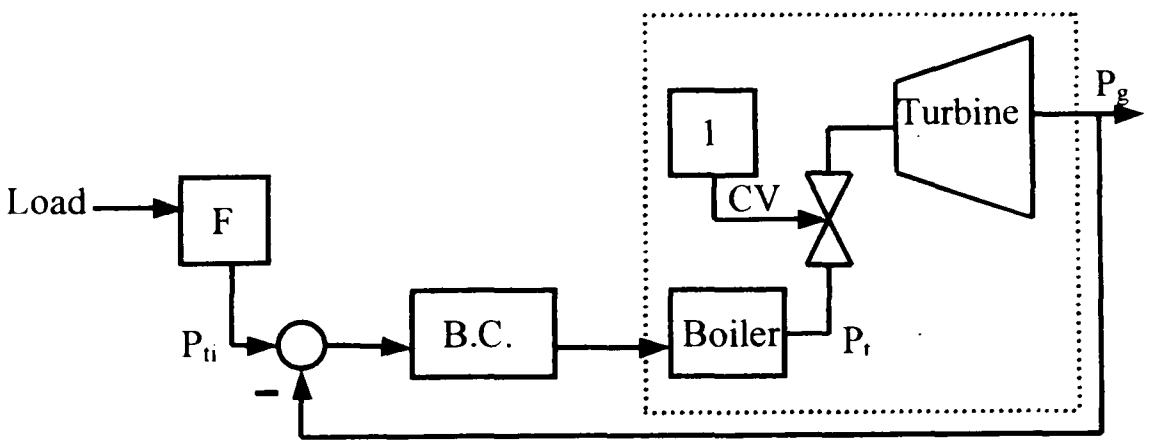

Key: P_g: Power Generator, P_{gi}: Set Point of power Generator,
P_t: Throttle Pressure, P_{ti}: Set point of Throttle Pressure

Fig 1.14: Sliding Pressure Mode

B) Process Set Point Control

The problem of optimising the economic operation and control of the boiler-turbine process has been studied with numerous strategies to minimise a cost functional or performance index function. Unfortunately, most solutions have not been applied to an actual plant due to the high cost of modifying the control system. There are two different architectures for combining a conventional control system with the multivariable controller in boiler to control process set point. These methods consist of:

I. Dynamic Set-point Manoeuvring (DSM)
II. Process Optimising Multivariable Control (POMC)

Dynamic Set-point Manoeuvring (DSM): In the DSM architecture, the multivariable controller does not replace the conventional control system but supplements it Fig 15. Ordys and Grimble (1995) used the DSM for optimising the control of a combined cycle gas turbine power plant. A realistic non-linear simulation model was used for the design and test of the final control scheme. As the optimising controller, a multivariable state-space LQGPC was chosen. The simulation showed the significant improvement in performance compared to the conventional control system with no optimising multivariable controller involved.

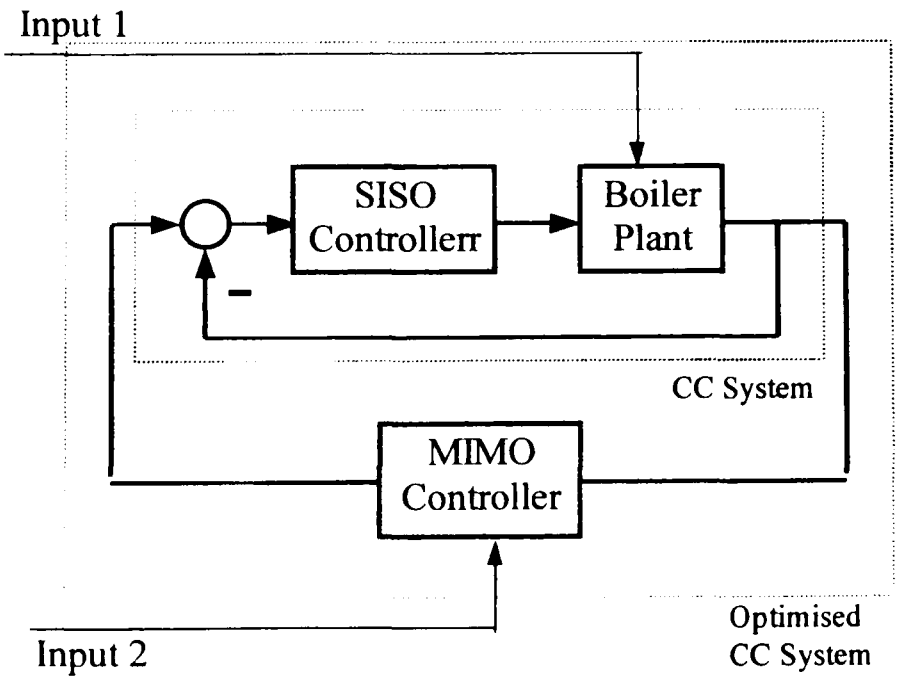

Fig 1.15: DSM architecture

Process Optimising Multivariable Control (POMC): The conventional control is the backbone in the POMC architecture. The SISO controllers in the CC system are the first level of control and POMC controller operates in parallel is the secondary level of control, Fig 1.16.

The POMC approach was suggested and applied for steam pressure and steam temperature control of an 85MW coal fired boiler simulator by Pidersen *et al.* (1996). The results showed that the introduction of POMC led to an improvement in the performance of the both the pressure and temperature control. A LQG controller was chosen as the optimising multivariable controller.

A non-linear control strategy to determine the optimal process set point is proposed by Saez and Cipriano (1998). The design includes economic and environmental criteria, and technical and operational constraints are considered. The control strategy proposed consists of a supervisor level to determine the optimal set points of regulation level. The supervisor level is based on an economic optimisation to minimize the power plant operation casts. The regulation level is based on proportional integral (PI) controller.

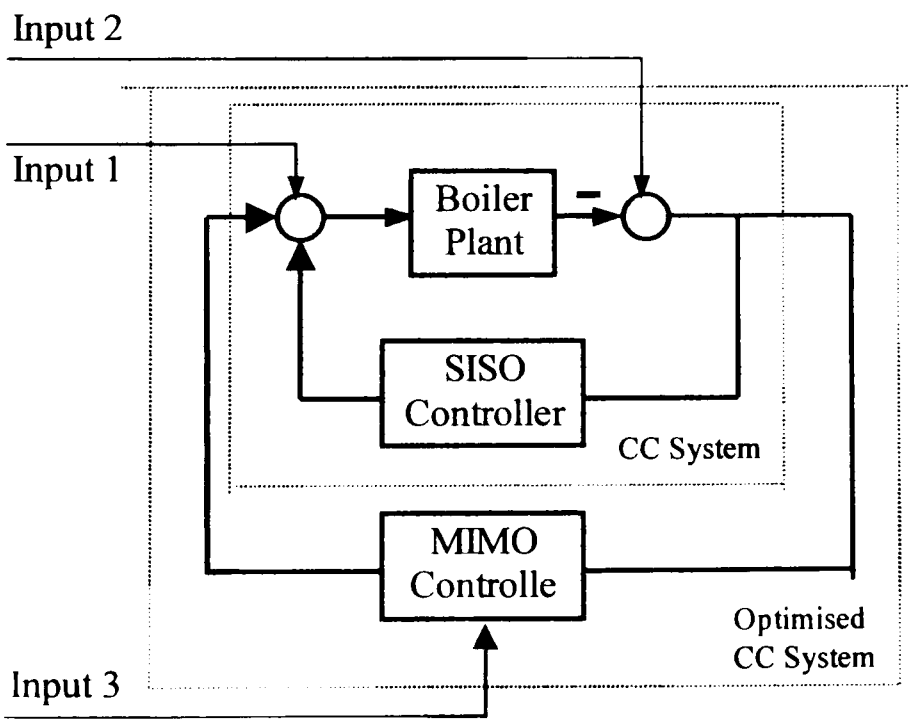

Key:
Input 1: Present set point for SISO controller

Input 2: Noise and Present operating point

Input 3: Present operating point, desired future operating point and future set points

Fig 1.16: POMC architecture

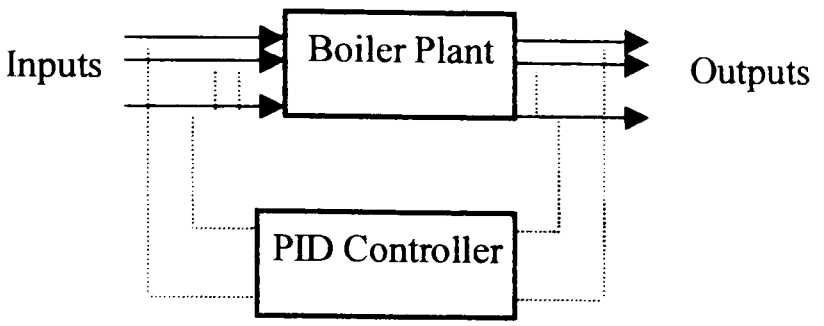

Fig 1.17: Scheme of Process Parameter Control

C) Process Parameter Control

This control level includes systems that regulate unit MW output, main steam pressure, feed-water, and air/fuel, Fig 1.17. The controller could be PID, LQR or GPC. In the following section, a comparison between these controllers is presented.

I. PID Control

Existing control schemes for drum-boiler systems are mainly PID controllers plus feed-forward compensation. In practice, single loop PID controllers are used to control these systems. Low order model and PI controller have been presented for five power plants by Cheres (1990). The normal procedure for the design of PI controllers is by constructing a linear system model with fixed parameters, obtained by linearizing the system around an operating point. Thus as the operating conditions change, the system performance will not be optimal. Hence a key problem in process control is to have a reliable, inexpensive method for tuning PID loops.

A method using an adaptive control scheme for enthalpy and electrical power control of a once-through boiler has been proposed and implemented by Unbehauen *et al.* (1991). An automatic tuning procedure, based on estimated plant parameters has been built into the control algorithm. Results of real time experiments show that the control strategy exhibits promising results under all operating conditions. It could be shown that adaptive boiler control saves fuel, increases efficiency and guarantees a uniform steam quality.

II. Modern Control

Ollat *et al.* (1989) has presented the design of a Linear Quadratic Gaussian Regulator (LQG) for a boiler furnace. With this approach the interaction between the four loops is taken into consideration. Therefore, this design guarantees the required tracking and robust performances.

Advanced digital control (ADC) methods have been presented by Nakamura and Uchida (1989). They used an optimal regulator designed with modern control theory. The plant consists of the boiler-turbine process with the conventional PID controller. The computer uses control algorithms to determine signals to fuel, spray, and gas-damper, which are added via digital-to-analogue (D/A) converters to control signals from the PID controller. It was found from experience in routine operation that ADC has a stabilising effect when the system is subjected to various disturbances.

III. GPC Control

Ding and Hogg (1991) have used a multivariable GPC algorithm to control a 160MW oil-fired boiler-turbine system with three inputs and three outputs. The results showed that the multivariable controller provides effective control over a wide range of operating conditions.

Hogg and El-Rabaie (1991) reported the application of GPC self-tuning control strategy to a 200 MW coal fired boiler. A multi-loop control scheme was used in controlling the boiler system. The super-heater steam pressure, super-heater steam temperature and reheat steam temperature were controlled using GPC. Results obtained with GPC showed a significant improvement in the performance over a wide range of operating conditions compared with conventional PI controllers.

The analysis of operational dynamics of the boiler along with economics and constraints of the operation indicates that the application of a model based multivariable predictive optimal control strategy can result in more economical operation of the boiler. Prasad *et al.* (1996) use this model to control steam temperature and pressure at their economic

optimum during the load-cycling operation of a 200 MW oil-fired drum-boiler. The main steam temperature is controlled by 1st and 2nd stage super heater spray flows and pressure by manipulating fuel flow. The re-heat steam temperature is controlled by manipulating flue gas re-circulation flow and reheat spray flow.

IV. Fuzzy Control

Since the dynamics of a boiler display non-linearity, non-minimum phase behaviour, instability and time delay, there is a potential to improve control performance by applying new non-linear control schemes like fuzzy control.

Cheng and Rees (1996) have used the FDM for the modelling of a boiler and they provides a simple way to deal with the control design by designing controls for each of the local linear models and then link them together by the membership functions.

The performance of fuzzy and PI controllers have been compared using a drum-boiler model by Cheung and Wang (1998). Their performance against set-point tracking and disturbance rejection has been compared. In conclusion for set point tracking the fuzzy controller gives better performance than the PI controller, and for disturbance rejection their performance is the same.

Conclusions

Boilers are non-linear, time varying MIMO and non-minimum phase systems. Boiler control contributes directly to operating efficiency, plant response, and plant life. Therefore, there is a potential to improve control performance by applying non-linear control schemes like fuzzy control. Such methods are interesting for the academic control community. On the other hand, the boiler behaviour around operation point can be considered and a linear model for the boiler established. Classical control design methods can then be applied to these linear models. Such methods are interesting for engineers in industry.

1.4 Steam Turbine

1.4.1 Modelling of Steam Turbine

The transfer function of a steam vessel and the expression for power developed by turbine has been explained in Appendix 1.3. The IEEE Working Group (1973; 1991) has presented basic models for speed governing and turbines in power system stability. A physical description of the equipment was given with one or more mathematical representation of the representations in block diagram form. It was assumed that all turbine control is accomplished by means of governor-controlled valves. This model can be used to represent any of the turbine configurations by neglecting appropriate time constants and setting some of the fractions to zero Fig 1.18. The time constant T_1 represents the main inlet volume and steam chest time constant. The time constants T_2 and T_3 represent re-heaters time constants and T_3, T_4 are IP and LP time constant respectively. $K_1 - \text{to} - K_8$ are power fractions. Appendix 1.4 shows the range of parameter for different configuration of steam turbine. The majority of the detailed analysis today utilises the standard IEEE models for representing steam turbine and governor response.

Anderson and Mirhidar (1990) have used low order System Frequency Response (SFR) model for turbine to estimate the frequency behaviour of a large power system to sudden load disturbance. The input to turbine is P_{des} and output from turbine is P_m. Data for an actual system separation is used to validate the SFR model. However, in spite of model simplicity, the comparison with actual system disturbances and detailed stability simulations are rather encouraging. Gibbs *et al* (1991) has reported the development of practical, multivariable, non-linear, model predictive control for fossil power plants. This model is used to predict the plant response to control inputs.

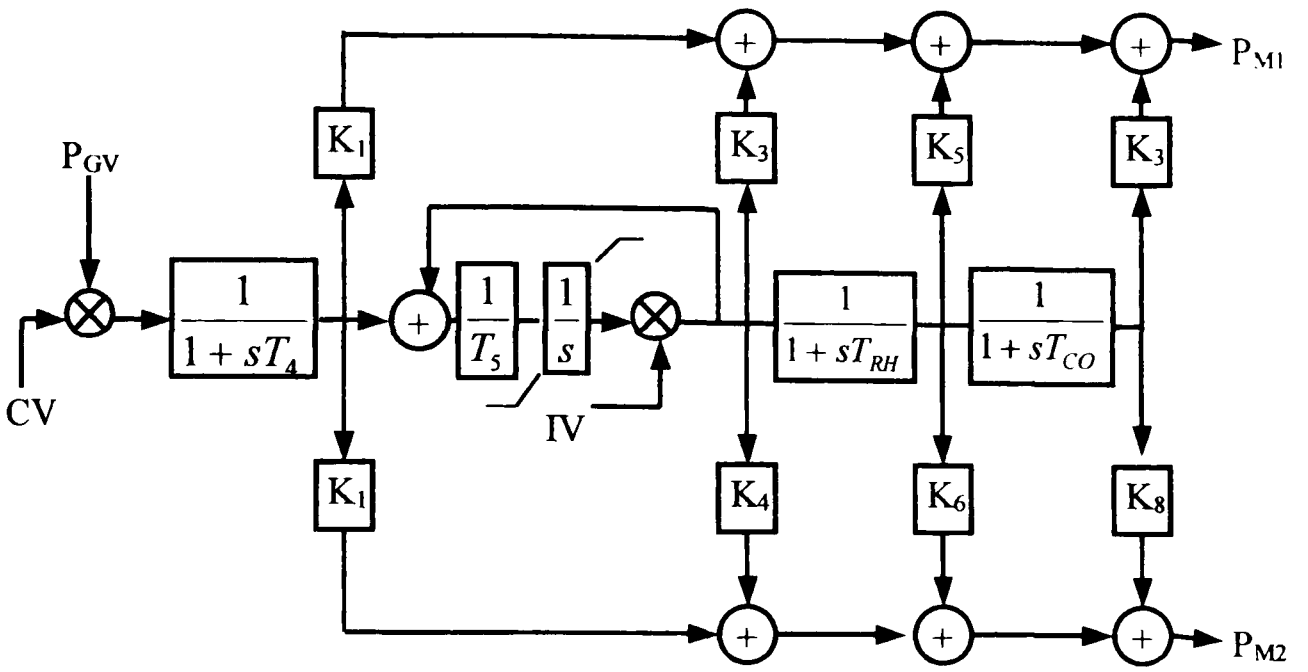

P_{M1} : HP Mechanical power,

P_{M2} : LP Mechanical Power

Fig 1.18: Generic Turbine Model including IV effects.

Several typical turbine and governor models according to IEEE recommendations have been implemented in the power system simulator by Wang *et al* (1991). The first order model along with position limits and dead band for governor and third order model for turbine has been used. Inputs to governor are deviation of frequency and load reference and output from turbine is mechanical power. The simulator can be used for dispatcher training and in addition for feasibility studies or development activities for possible future real time control functions thereby enhancing the supply reliability and operational efficiency.

The turbine/governor model based on the IEEE committee report (1973) has been used by Abdennour and Lee (1996) for designing a decentralised controller. The model is 5^{th} order represented by a number of first order lags. The only non-linearity comes from the actuator dynamics of the governor valve. The input to the governor is the mechanical power demand (P_o) and the output of the turbine is the mechanical power (P_m).The results show the output very closely follows the output demand.

An artificial neural network (ANN) based modelling has been proposed by Hiyama *et al* (1999) for the governor-turbine system. The proposed model consists of three blocks. The blocks are: governor, steam valve servo system and turbine-generator system. The input to turbine is the steam valve opening position, and the output is the real power output from the generator. The proposed model give quite accurate simulation results compared with the actual values.

1.4.2.Steam Turbine Controls

Older turbine governor designs used mechanical-hydraulic control but most governors supplied today are Electro-hydraulic. The following is brief descriptions of the functional characteristics of electro-hydraulic control systems, which offer more flexibility and adaptability, compare with mechanical systems.

Electro-hydraulic Control (EHC)

Fig 1.19 shows EHC speed-governing systems. The basic outputs to be defined are the CV and IV flow area. The inputs could be speed, acceleration, electrical power, etc. depending on the particular design.

An explanation of the block diagram of Fig 1.19 follows. S1 is equal to load reference signal (LR) less any contribution from speed deviation ($\Delta\omega$) and throttle pressure. The control valves flow area; a function of valve position is shown to follow S1 through a servo with a time constant T_{SM} subject to rate limits and positions limits. The intercept valves are controlled by a servo with constant T_{SI} subject to rate and position limits, following the sum of S1 and constant.

It should be noted that fast valving and over speed control have different, although related functions. The function of over speed control is turbine-generator protection. Fast valving is a stability aid; the function of fast valving is to assist in preventing loss of synchronism. Steam turbines (ratings of about 250 MW and greater) have extra circuitry for fast valving added to the Electro-Hydraulic control system. This circuitry is called the Early Valve Actuation (EVA) circuit, and a block diagram of EVA is shown

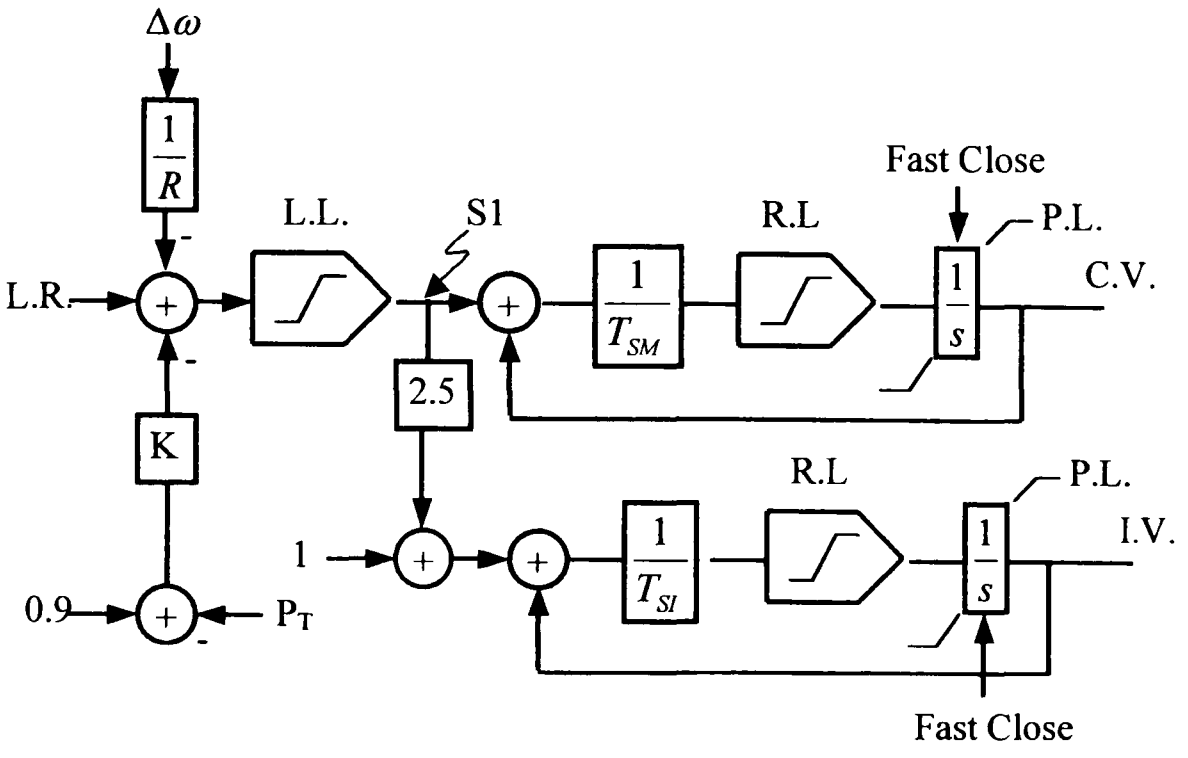

Key:L.L.: Load Limiter, R.L.: Rate Limits, P.L.: Position Limits, LR: Load Reference, P_T : Throttle Pressure. Typical value: R=0.05 pu, T_{SM} =0.1-0.2 sec, T_{SI} =0.1-0.2 sec, time of fast close=0.15 sec, Rate limits CV=-0.2-0.1,.Rate limits IV=-0.2-0.1.

Fig 1.19: EHC logic

in Fig 1.20. When the EVA circuit turns on, the only action is to fast close the IV completely in 0.1 to 0.2 seconds. When the EVA circuit clears, after one-second delay, the IV will reopen.

Kwak and Kim (1995) have been suggested a new fuzzy load scheduler as a top level of turbine control system Fig 1.21. It provides the load change rate for turbine, while assuring the thermal stresses always with in an allowable limit. A fuzzy inference engine

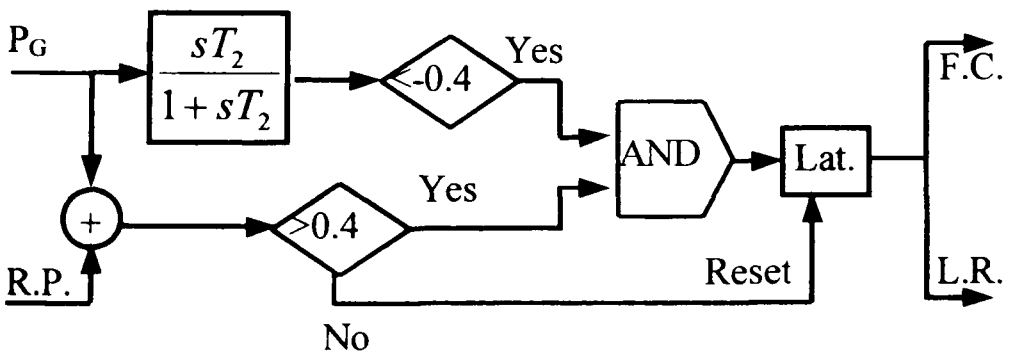

Key:
P_G: Generator Power
R.P.: Reheat Pressure
Lat: Latching Relay
C.V.: Control Valve
I.V.: Intercept valve
FC: Fast Close
L.R.: Load Reference

Fig 1.20: EVA Circuit Block Diagram

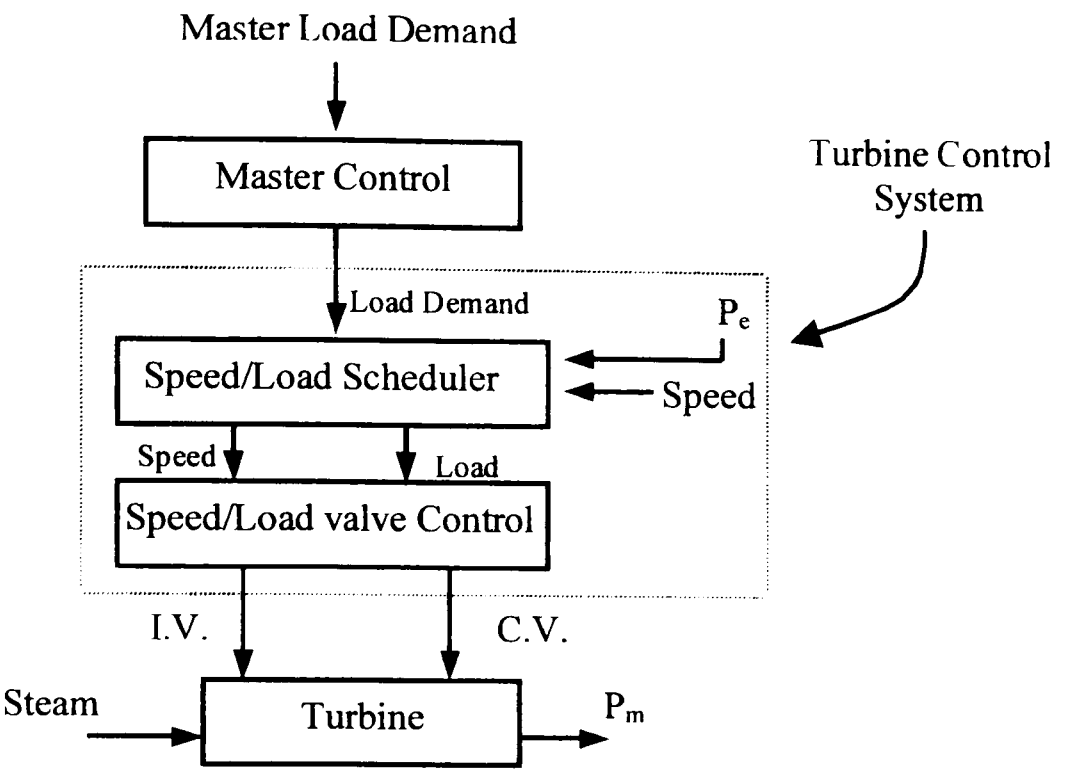

Fig 1.21: Turbine and Control System

is suggested to decide the load range change rate. Then, the boiler outlet steam is predicted, and thermal stresses of turbine rotors are computed. If the future thermal stresses are within limits, the load change rate is transferred to turbine controller. Otherwise, adjustment of the load variation rate of the turbine is performed by the supervisory inference engine according to the predicted thermal stresses. The results show that the fuzzy load scheduler is more effective than conventional method.

A hierarchical controller for optimal load cycling of steam turbines has been presented by Marcelle *et al.* (1994). The approach uses heuristic turbine control rules to implement the higher-level long term cost minimisation strategy. At the second level a model based optimal controller is used to calculate the optimal actuator positions needed to track the desired power demand at minimum cost. This hybrid controller produces good load tracking performance, as well as good long-term operation cost minimisation.

Recent situation of a global industrial competition and a growing big concern for environmental problem makes saving energy more important than ever. Genichi *et al.* (1998) has implemented an integrated multivariable control and real-time optimisation

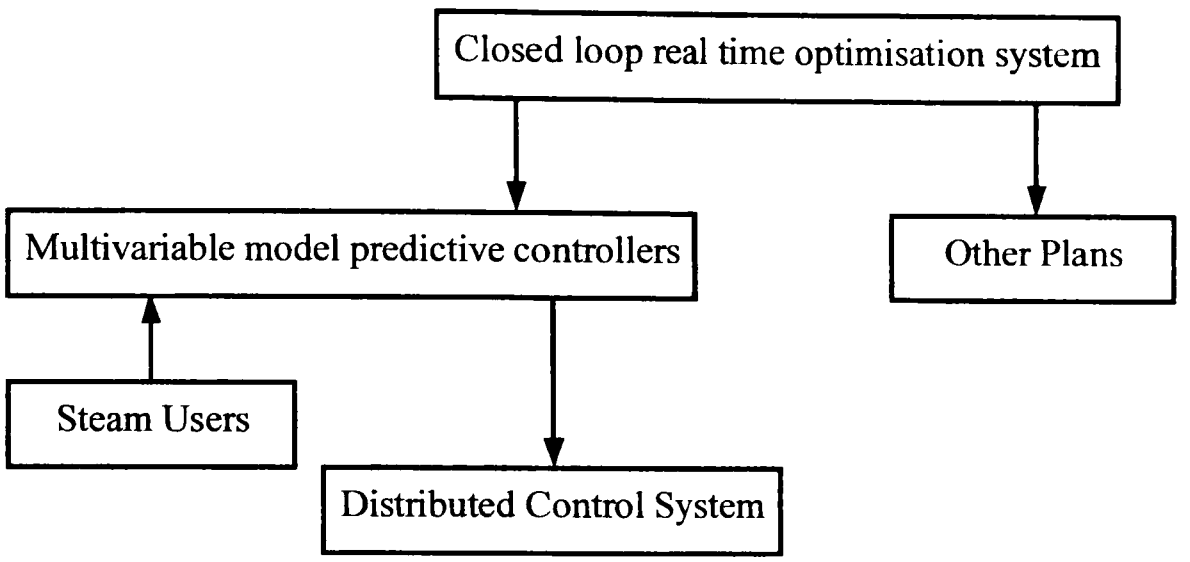

Fig 1.22: Overview of Integrated System

system on the power plant in order to achieve most efficient operation. The control system controls three boilers and five turbines. Turbines have been modelled in order to fit actual efficiency curves based on the manufacturer's design. Actual turbine efficiency is modelled as a polynomial equation that is a function of a turbine inlet steam rate based on the historical data. Dynamic matrix control (DMC) is used as a multivariable control system, which covers all boilers and turbines in the power plant. The real time optimisation (RTO) system optimises the loads of turbines in the power plant and the site-wide steam balance by adjusting the extraction or condense steam rate of the turbines in power plant Fig 1.22. As result, the integrated controllers (RTO+DMC) have reduced the fuel consumption and the operator's load in the power plant significantly.

Conclusions

Standard IEEE models for steam turbines are used by most researchers to model turbine behaviour. The parameters of model can be set to model different component of turbine. In this model, input to turbine is steam mass and output from turbine is P_m. Controls valve IV and CV is used to control the steam turbine.

1.5 Gas Turbine

1.5 1 Gas Turbine Description

The main components of an industrial power plant gas turbine are the compressor, the combustion chamber and the turbine, connected together as shown in Fig 1.23.
There are two main factors affecting the performance of the gas turbines; Component efficiencies and turbine working temperature, the overall efficiency of the gas turbine cycle depends also upon the pressure ratio of the compressor.
It is important to realize that in the gas turbine additional compressors and turbines can be added, with inter-coolers between the compressors, and reheat combustion chambers between the turbines. These refinements may be used to increase the power output and efficiency of the plant at the expense of added complexity, weight and cost. Based on three extra components, gas turbine system could be divided into two categories:

- Open cycle
- Close cycle

A comparison of open cycle and close cycle gas turbine is shown in Appendix 1.6.

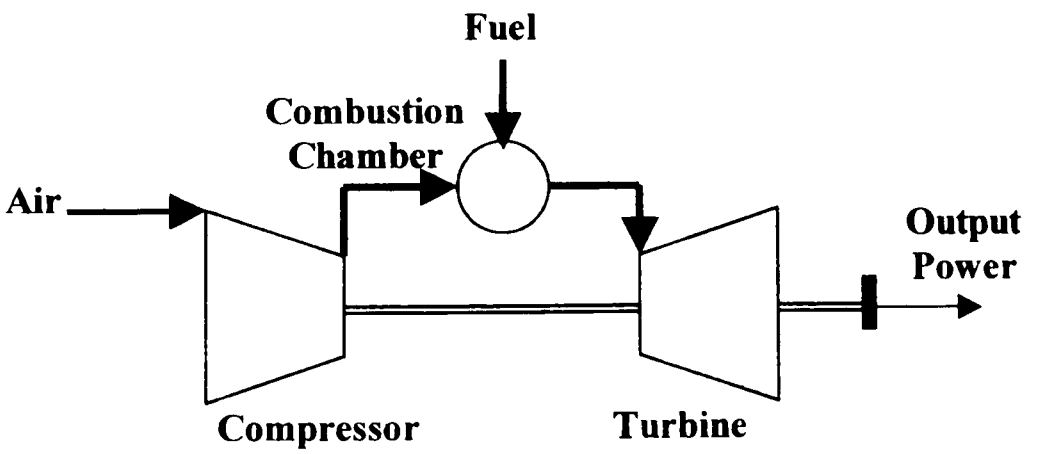

Fig 1.23: Simple gas turbine system

1.5.2 Gas Turbine Modelling

A thorough introduction to gas turbine theory is provided in the book of Cohen *et al.*, (1987). There also exists a large literature on the modelling of gas turbines. Model complexity varies according to the intended application. Gas turbine models can be developed by two distinct methods:

I. Physical Modelling

II. Black-Box Modelling

I. Physical Modelling

In theoretical approach, models are based on the physical description of the gas turbine components. These models are complex but able to provide a more comprehensive description of the gas turbine (Appendix 1.7).

Hussain and Seifi (1992) have presented a theoretical way of establishing the simple dynamic model of a single shaft gas turbine, especially for stability studies. The relation between input and output has been presented by a transfer function that with output as deviation of mechanical power and input as deviation of heat input rate.

Nern *et al.* (1994) uses the thermal model of the gas turbine to build the long-term model. The model constitutes the algebraic thermal model together with the disturbance free energy conversion model and the mass flow rate model. The complete sets of equations governing the pressure, temperature, mass flow and energy flow of the different sections within the gas turbine cycle are derived. The measurable output is mechanical power (P_m.) and exhaust gas mass flow rate ($\dot{m}_s$), Input available for control is airflow and gas flow.

An alternative method for providing comprehensive information about the dynamic behaviour of the engine under development is the use of a computational method capable of accurately predicting engine behaviour under various dynamic conditions.

A computational method with this capability with the corresponding modularly structured simulation code, called GETRAN, has been developed by Schobeiri *et al.* (1994). The code is capable of executing the simulation procedure at four levels, which increase with the degree of complexity of the system and dynamic event. As a result, a close agreement can be seen between the experimental measurements and the computation using the model.

A generic method for modelling the dynamic performance of gas turbines has been also developed based on a series of modular component models by Ricketts (1997). The user chooses inputs and outputs what gas flow and mechanical connections are to be made between the component models and can easily construct single shaft, twin shaft, recuperated, re-burner, inter-cooled or other arrangements. The model could be coded in software packages and analysed to assess transient performance and aided control design. The validation exercise demonstrates a good agreement between the measured and simulated data.

Another non-linear mathematical model is proposed by Camporeale *et al.* (1997) to provide a complete description of the gas turbine. The model and the consequent computer code have a modular form: each module is described by algebraic or differential equations that link one to the variables in the nodes, which the module is connected. The measurable outputs are the shaft rotational speed and the turbine inlet temperature. Inputs available for control are the fuel rate and the position of the compressor inlet guide vanes (IGV). The response of the system under a sudden variation of the electric load shows good performance in term of overshoot and oscillation of the controlled variables.

Crosa *et al.* (1998) have presented a physical simulator for predicting the off-design and dynamic behaviour of a single shaft heavy-duty gas turbine plant, suitable for gas steam combined cycles. The mathematical model, which is non-linear and based on the lumped parameter approach, is described by a set of first-order differential and algebraic equations. A code has been created in SIMULINK environment. The compression and expansion simulation takes into account the air bleeds and cooling effect; the

combustion chamber is complex and considers different combustion process, with different fuels, with and without steam and can determine the CO and NO_x emission.
Rowen, (1983) has reported a mathematical representation of a General Electric heavy-duty, simple cycle, single-shaft and fully open inlet guide vanes gas turbine. The model is used in dynamic power system studies and in dynamic analyses of connected equipment. Liquid and gas fuel systems, parallel and isolated operation, droop and isochronous governors, and the impact of both air and hydrogen-cooled generators are included in the model. The measurable outputs are P_m and the exhaust gas temperature (T_E). Inputs available for control are airflow and fuel flow signal (W_A, W_F). The control system includes speed control, temperature control, acceleration control, and upper and lower fuel limits. Rowen (1992) offers features, such as modulating IGV s, calculation of exhaust flow and accommodation of the variable ambient temperature. Using the information presented in this model, in combination with that in Rowen (1983), will allow simulating any heavy-duty single shaft gas turbine in any of the current or envisioned applications.

II. Black-Box Modelling

Doughty *et al.* (1989) has used the simple gas turbine model for electrical studies. The model is appropriate for simple-cycle single-shaft generator-drive gas turbines for a speed range of 95-107 percent of rated speed. Both droop and isochronous operating modes were modelled to permit evaluation of the co-generator when connected to the utility grid or operating in an isolated mode. The output of model is mechanical power and the input is fuel flow. The control system includes speed control only.
The test data was used to drive values for gas turbine model parameters by Hannett *et al.* (1995). In parallel with identifying values, the existing model structures were also examined and refinements were made to achieve better matches of simulation results

with field recordings of staged tests. The measurable outputs are the N_f (Free turbine speed), N (engine speed) and the exhaust gas temperature (T_E). Input available for control is Fuel Flow signal (W_F).

Sharma (1998) has developed an operating model of a small electric grid based on simple model for gas turbine. The measurable output is P_m. Input available for control is W_F. As result, there are some differences between actual measurement frequency deviation and the model predicted. This indicates that the time constants used were different from the actual value. The brief description of different black box modelling is given in Appendix 1.8.

1.5.3 Control of Gas Turbine

The control system for gas turbine includes

- Speed control
- Temperature control
- Acceleration control
- Upper and lower fuel limits
- *IGV* control

Models are used for dynamic study of gas turbine include some of these controller. Appendix 1.5 shows the models and related controller.

Speed control:

The speed controller (governor) operates on the speed error formed between a reference made up of speed plus the digital set-point, compared with actual system or rotor speed. Speed governor could be

I. Droop governor.
II. Isochronous governor

The digital set point is the normal means for controlling gas turbine output when operating in parallel and using the droop governor. The droop governor is a proportional

block, with typical gain value within 10 and 50 used to regulate the turbine power output during interconnected operation. Therefore, its output is proportional to the speed error. The isochronous governor is a proportional-integral block, which the rate of change of output is proportional to the speed error. Thus, the output of the isochronous governor will integrate in a corrective direction until the speed error is zero.

Temperature control

Exhaust temperature is the normal means of limiting gas turbine output at a predetermined firing temperature, independent of variation in ambient temperature of fuel characteristics. Since exhaust temperature is measured using a series of thermocouples incorporating radiation shields, there is a small transient error due to the time constants associated with the measuring system. Under normal systems conditions these time constants are of no significance to the load limiting function. However, where increasing gas turbine output is the result of a reduction of system frequency and therefore may occur quite rapidly, exhaust temperature measurement system time constants will result in some transient overshoot in load pickup. The design of the temperature controller is intended to compensate for this transient characteristic. For heat recovery applications, optimum part load cycle performance is obtained when the turbine exhaust temperature is at a maximum. This is achieved by closing the inlet guide vanes, within the operating range.

Acceleration control

Acceleration control is used primarily during gas turbine start-up to limit the rate of rotor acceleration prior to reaching governor speed. This control serves a secondary function, during normal operation, in that it acts to reduce fuel flow and limit the tendency to over speed in the event that the turbine generator separates from the system. The input to controller is speed and the output is rate of rotor acceleration, This controller act as limiters on the fuel request signal, its output must be ignored whenever its, input is positive.

Upper and lower fuel limits

Minimum and maximum fuel flow limits are established to ensure that the fuel is not reduced below the point of self-sustaining combustion, nor above the corresponding to the maximum turbine output at site minimum ambient temperature. Three control functions (speed, acceleration, and temperature) are all inputs to a low value selector. The output, is called fuel demand signal (F_D), is the lowest of the three inputs, whichever requires the least fuel. The output is compared with maximum and minimum limits, the max limit acts as a backup to temperature control and is not encountered in normal operation; the minimum limit is chosen to maintain adequate fuel flow to insure that flame is maintained within the gas turbine combustion system.

IGV **Control**

IGV orientation is controlled so that the firing temperature is always kept at an adequate level. This in order both to safeguard the turbine efficiency during all operating stages and to keep a high exhaust temperature evens at partial loads. This last condition is vital to preserve the efficiency of the downstream steam-cycle plant, especially when there is no post-combustion at the gas turbine exhaust.

IGV's are closed, within their operating range, to achieve the maximum allowable exhaust temperature even when the turbine is working at partial loads, thus reducing the air flow and not letting the ratio W_A/W_F to be raised too much. Reduced power output is obviously obtained by the reducing the fuel flow.

***NO*$_x$ Control**

The major atmospheric pollution issues involving combustion plant have been associated with the emissions of the acidic species nitrogen oxides (NO_x). Water injection for short periods of thrust augmentation was at one time common. Although fans commonly serve this propose today. It is now standard practice to inject water or steam into stationary gas turbines to control NO_x emissions.

Scott and Russell (1994) have used the PI controller to control fuel flow in their gas turbine model. The demand from the PI stage is fed to each gas turbine through a slew rate limiter. Raise and lower inhibits on the PI and GT set points can also be invoked if variable changes are too rapidly.

Rowen (1983) has reported a representation of fully open inlet guide vanes gas turbine. The model has three controllers in regulation level. Droop and isochronous governors, *P* for acceleration and PI controller for temperature has been considered in the model.

Rowen (1992) added the *IGV* controller to his model. The model has widely used in simulation and control studies in gas turbine. Bagnasco *et al.* (1998) have used this model including isochronous governor, *P* Controller for acceleration, PI controller for temperature and *IGV*.

Governor models can be an important variable affecting the dynamic performance of gas turbine. Detailed dynamic simulation models have been proposed for two types of governor controllers by Hannett and Khan, (1993). The governors are:

- GE Speed-tronic Governor control
- Wood-ward Governor Retrofit

The model structure for the GE speed-tronic control is based on that proposed by Rowen (1983). The wood-ward governor control consists of a PID controller for the speed/load error input signal. The measurable output is P_m. Input available is fuel flow signal (W_F).

As a result the model provided by Rowen for the speed-tronic governors was found to be adequate and with minor modification a similar model structure used for the wood-ward retrofit governors.

Saez and Cipriano (1998) have proposed a non-linear control strategy to determine the optimal process set points, where the design includes economic and environmental criteria. Also, the technical and operational constraints are considered. Figure 1.24 show the control strategy proposed.

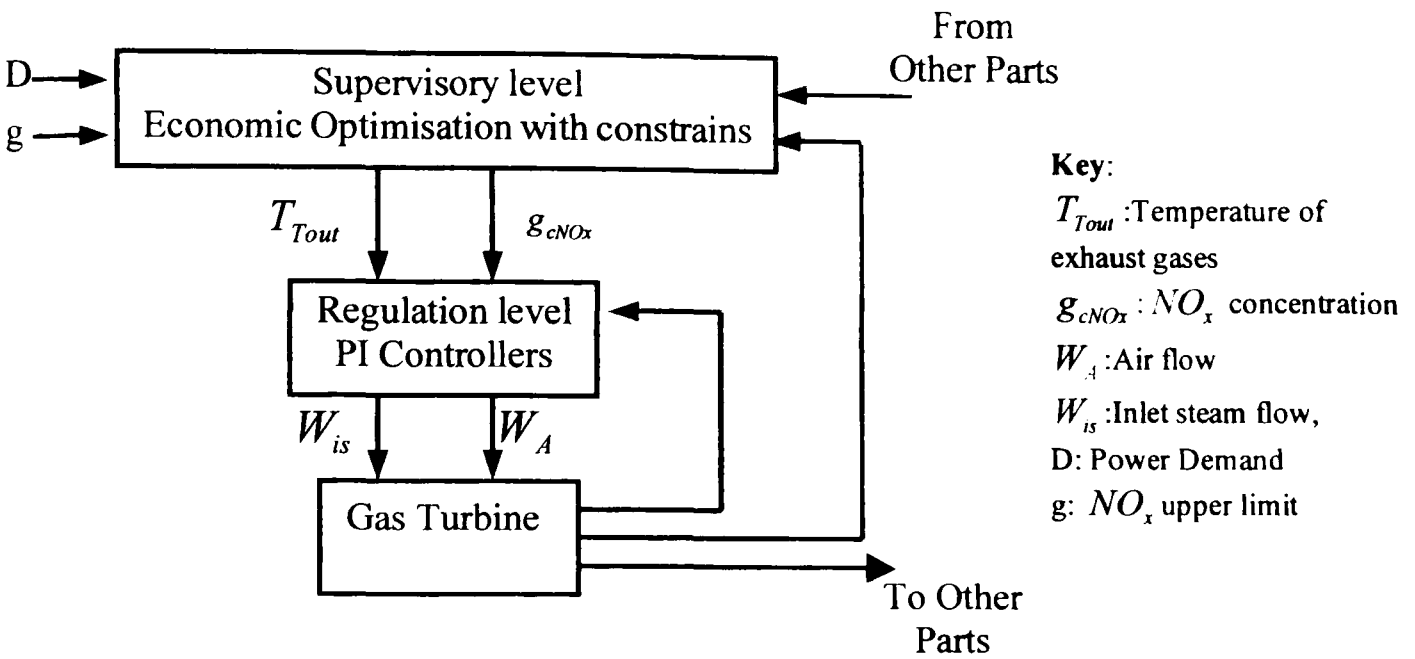

Fig 1.24: Control strategy proposed by Saez and Cipriano (1998)

The turbine dynamics in gas turbine are often complex and vary with operating point and ambient conditions; As a result there has been much recent research into the use of robust and adaptive controllers for gas turbines. Daley and Wang (1994) reported adaptive control of a simulated three-shaft gas turbine. A recently developed adaptive control scheme for SISO singular systems has been generalized to the MIMO case. It has been shown that this system is applicable to the three-shaft gas turbine, which can be written in singular system from by virtue of neglected high order dynamics. The estimation algorithm is based on an alternative regression model, which enables a one step ahead control algorithm to be constructed, which has clear advantages over the standard approach, which is unsuitable for this application.

Conclusions

Rowen model (1983; 1991) has been widely used by researchers to simulate the gas turbine behaviour. The model is parametric and is appropriate for most case of gas turbine behaviour.

1.6 Summary

In this chapter modelling of CCPP's was discussed. The kind of model of CCPP's depends on purpose of modelling. Simple models or complex models could be used to model the behaviour of CCPP's.

In complex models, the dynamic behaviour of each subsystem is considered in detail. These models, which are non-linear and high order, are difficult to understand and unsuitable for control studies. These models are used for designing of CCPP's or study the detailed dynamic behaviour of CCPP's.

On the other hand, simple models, which consider the main dynamic behaviour of CCPP's, are in per unit form and easy to understand, are used for control design of CCPP's. These models were used by many researchers to study power plant behaviour such as: Megawatt Response of power plants by de Mello *et al* (1974; 1991), Plant Control Schemes by Landis (1977), Long term Dynamic Simulation Programs (LTDS) by Undrill (1984) and Dispatcher Training Simulators by Hemmaplardh and Lamont, (1986).

Also, simulators, which are developed with these models, can be used in power system studies cause of other components of power systems such as transformer, transmission line and loads are considered as linear systems and their models are in per unit form, so, parametric low order model of CCPP's are suitable for control studies of power plants.

Chapter 2

Combined Cycle Power Plant Simulation Platform

2.1 Introduction

Combined Cycle Power Plants (CCPPs) are built in various configurations with varying number of processing units. The dynamic models of these plants are often required to ensure that the plants meet customer specification and are also useful in developing control strategies and commissioning procedures. This chapter presents a modular and hierarchical procedure to model these plants using SIMULINK. The chapter originates from an explanation of sub systems of the CCPP. In CCPP's, four main sub systems are considered. These subsystems are:

- Boiler
- Steam Turbine
- Gas Turbine
- Generator

For each sub system a suitable model, which is usually IEEE model, is chosen to develop generic and normalised sub system from published literature. After some model improvement the selected model is implemented in SIMULINK. Each subsystem consists of a number of blocks (components). Libraries of sub systems' blocks are created. These libraries allow the user to build different sub systems. Also, interface modules are provided to build a user defined configuration for the CCPP.
The chapter begins with a description of the equations that govern the dynamic of sub systems followed by the implementation of sub systems in SIMULINK. Steps of how the different configuration of CCPP can be build, is described. The simulator is validated using step responses analysis compared with published experimental data.

2.2 Boiler

In this section, de Mello *et al.* (1991) model for boiler is considered. The model is modified to include the drum level and steam temperature. The model was used by many researchers to study dynamic behaviour of boilers (IEEE Working Group, 1994; Bagnasco *et al.* 1998). The model is normalised and it is suitable for control studies and contains the non-minimum phase behaviour of the system.

2.2.1 Boiler Modelling

A boiler model based on first principles of mass, energy and volume balance is derived to lend insight into the parameters that figure in the proposed model (de Mello *et al.*, 1991). The boiler system blocks include:

- Fuel dynamic
- Water wall dynamic
- Drum and super-heater

Dominant energy storage in the boiler is during the saturation phase of water/steam. Storage in super-heater is considered from the mass, volume, and pressure effects of superheated steam assuming constant temperature. Throttle steam pressure is maintained through a fuel/air flow PID controller. The model has two inputs and two outputs. de Mello model has been extended in this thesis to include steam temperature and Drum level for use in CCPP configuration. The model is shown in Fig 2.1.

Fuel System Dynamics

The transfer function of fuel systems could be considered as a first order system with time delay for coal fuel power plants. The fuel system dynamics are characterized by a dead time of 20 seconds in series with a time constant of 30 seconds. Also fuel system can be consider as first order system for Oil/Gas fuel with time constant of 5 second. The model equations are as follows:

$$\dot{Q}(s) = T_F(s)U_f$$

where:

$$T_F(s) = \frac{e^{-20s}}{1+30s} \qquad \text{for Coal Fuel}$$

$$T_F(s) = \frac{1}{1+5s} \qquad \text{for Oil/Gas Fuel}$$

$\dot{Q}(s)$ Heat Flux from Furnace to Water walls

U_f Fuel Command Signal

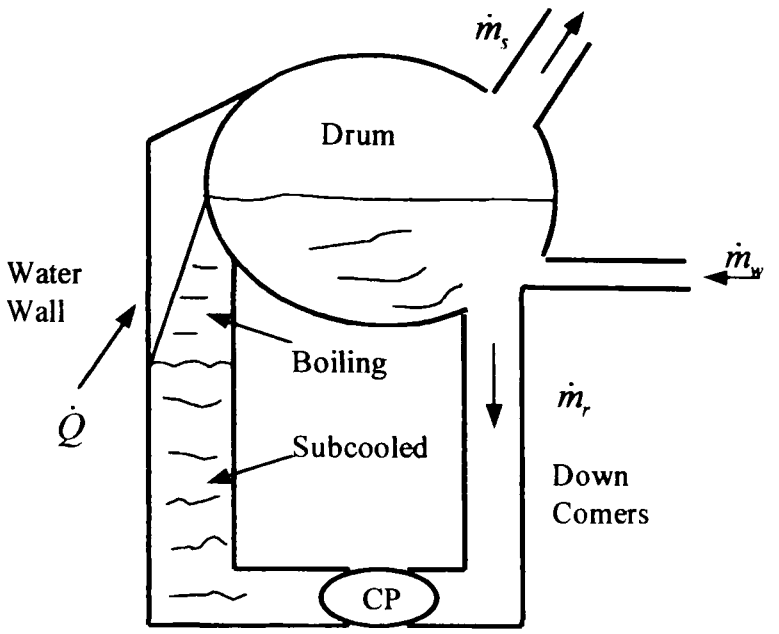

Fig 2.1: System defining steam generation and pressure

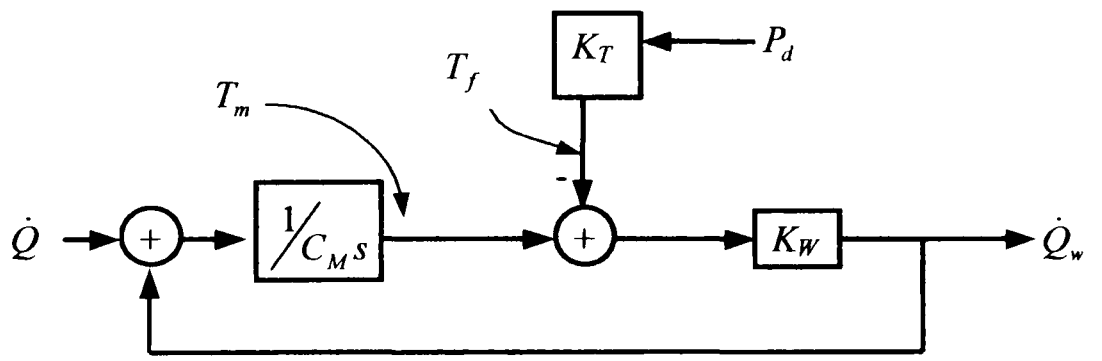

Fig 2.2: Computation of heat flux from tube metal to fluid

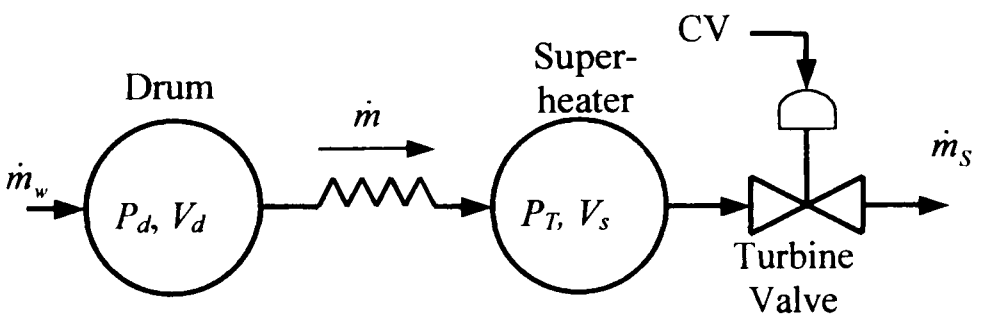

Fig 2.3: Lumped representation of drum and super-heater ($0 \leq CV \leq 1$)

Chapter 2

Water Wall Dynamics

The heat flux from tubes to fluid $\dot{Q}_w$ in water walls is assumed to be proportional to the temperature difference between metal and fluid. Temperature of the fluid is basically a function of drum pressure and metal temperature is a function of heat flux from furnace to water walls ($\dot{Q}$) and the heat flux from water walls to fluid ($\dot{Q}_w$). Fig 2.2 shows the relations in block diagram form.

The process of heat transfer from metal to inner fluid in the water walls is through temperature difference between metal and inner fluid. Metal temperature is obtained from integration of heat flux into and out of the tube walls divided by the tube heat capacitance (C_M).

The steam generated from a given amount of heat flux is influenced by the drum pressure through a multiplying effect as follows:

$$T_m(t) = T_m(0) + \int_0^t \{\frac{1}{C_M}(\dot{Q}(\xi) - \dot{Q}_w(\xi))d\xi\}$$

$$\dot{Q}_w(t) = K_W(T_m(t) - T_f(t))$$

where

C_M heat capacitance of water walls

K_W heat transfer coefficient between tubes and inner fluid

$\dot{Q}$ heat flux from furnace to water walls

T_m Metal temperature

T_f Fluid temperature

$$K_T = \frac{\partial T_{sat}}{\partial P_{sat}}$$

Drum and Super heater

The effect of super heater volume is considered assuming temperature is constant. The distributed nature of the process is approximated as in Fig 2.3 with one-lumped volumes. the pressure flow effects and flow rates between volumes are modelled by the following set of algebraic and differential equations:

$$P_D = P_T + K(\dot{m})^2$$
$$\dot{m}_s = K_v P_T = (CV)P_T$$
$$\dot{m} = \dot{m}_s + V_s \frac{\partial \rho_s}{\partial P_T}\frac{\partial P_T}{\partial t}$$
$$\dot{m}_w = \dot{m} + V_d \frac{\partial \rho_d}{\partial P_d}\frac{\partial P_d}{\partial t}$$

where:

K	is coefficients relating pressure drop to flow rate square
K_v	is proportional to turbine valve flow area
P	the symbol that denotes pressure at the volume denoted by the suffix.
V_d and V_s	volumes of the lumped drum and super heater
ρ_d, ρ_s	densities of steam in these volumes.

The steam generated from a given amount of heat flux is influenced by the drum pressure through a multiplying effect. After some straightforward algebra:

$$\dot{m}_W(t) = Q_w(t)(-P_D(t) + K_H(P_D(t) - P_{D0}))$$
$$P_D(t) = P_D(0) + \int_0^t \{\frac{1}{C_D}(\dot{m}_w(\theta) - \dot{m}(\theta))d\theta\}$$
$$P_T(t) = P_T(0) + \int_0^t \{\frac{1}{C_{SH}}(\dot{m}(\theta) - \dot{m}_S(\theta))d\theta\}$$
$$\dot{m}(t) = K(P_D(t) - P_T(t))^{1/2}$$
$$T_f(t) = K_T(P_D(t) - P_{D0})$$

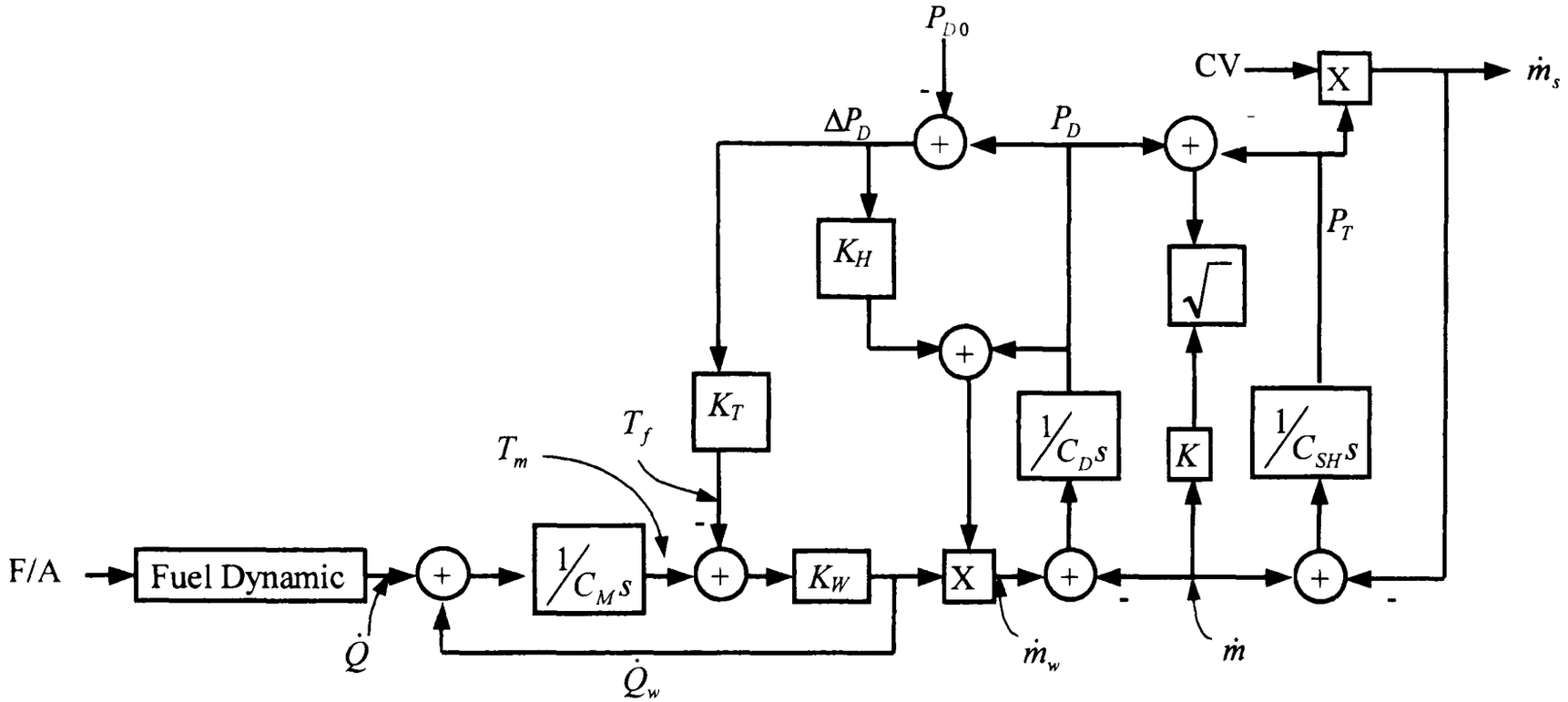

Fig 2.4: Boiler model

Inputs:
F/A: Signal to fuel and air
CV: Control valve

Outputs:
$\dot{m}_s$: Steam flow rate out of super heater
P_D : Drum pressure,
P_T : Throttle pressure

States:
$\dot{Q}$: Heat from furnace to tube
$\dot{Q}_w$: Heat transfer from tube to fluid
T_f : Temperature of inner fluid in water-wall
T_m : Metal temperature
$\dot{m}_w$: Steam generation
$\dot{m}$: Steam generation output of Drum
P_D : Drum pressure
P_T : Throttle pressure

Parameters:
C_M : Heat capacitance of water-wall
K_W : Heat transfer coefficient between tubes and inner fluid
K_T : The change in saturation temperature with pressure
K_H : The change in enthalpy with pressure
C_D : Boiler storage
K : Friction drop coefficient
C_{SH} : Storage constant

Calculation of Model Parameters

Fig 2.4 shows the boiler model and its 7 parameters, which should be calculated. The above equations were solved for a boiler with the following basic data defined for full load operating conditions of 480 lbs./sec steam output at 2400 psi, 1000'F.

$V_{ww} = 2850$ cu ft $\qquad V_D = 950$ cu ft $\qquad V_s \frac{d\rho_s}{dP_T} = 3.8, P_T = 2250$

$DA = 270$ sq. ft. $\qquad \dot{m_r} = 2000$ lbs./sec $\qquad P_D = 2640$

where:

V_s is the super-heater volume

$\frac{d\rho_s}{dP_T}$ is the partial density with respect to pressure at an average constant temperature super-heater.

The storage constant $(C_D + C_{SH})$ can be derived from the initial rate of change of drum pressure following a change in steam flow out of boiler. For instant if for a 2400 psi boiler, a step change in turbine valve position results in a %2 change in steam flow, and the initial rate of change of drum pressure is recorded as 16 psi/min, the constant is:

$$(C_D + C_{SH}) = \frac{\dot{m}_S(t)}{\Delta P_d} = \frac{0.02}{\frac{16}{60}\frac{1}{2400}} = 180 \text{ psi/lb (sec)}$$

with the variables, pressure and steam flow, expressed in per unit of rated. Experience has shown that splitting the total storage constant $(C_D + C_{SH})$ as 10% for C_{SH} and 90% for C_D yields a good approximation to the boiler pressure response.

The parameter K is obtained from a knowledge of the pressure drop between drum and admission to the turbine. For instant if at full load $(\dot{m}_S = 1\ pu)$ the drum and throttle pressures are 2640 and 2400 psi respectively, then:

$$K\sqrt{\frac{2640-2400}{2400}}=1 \quad \text{or } K=3.16$$

The parameter K_T relates the change in saturation temperature with pressure. Keeping the temperature as degree F and pressure in per unit:

$$K_T = 2400\frac{\partial T}{\partial P} = 2400\times 0.057 = 137$$

where:

$\frac{\partial T}{\partial P} = 0.057$ (for a 2400 psi unit from practical data)

Typically K_w can be estimated from the assumption of 25 F drop for full load steam generation. Hence:

$$K_W = \frac{1}{25} = 0.04$$

The value of heat capacitance CM can be obtained from the mass of water wall tubes multiplied by specific heat of metal. From experience with modelling of boilers it is found that the effective time constant of heat transfer for water walls to inner fluids is in the order of 7 seconds.

$$\frac{CM}{K_W} = 7 \text{ or } CM = 0.28$$

For a 2400 psi unit with enthalpy at the economizer outlet of 560 BTU/ lb;

$$K_H = \frac{\partial(h_g - h_{fw})}{\partial P} = -0.12 \quad BTU/lb/psi$$

In the per unit it is:

$$K_H = \frac{-0.12}{520}2400 = -0.55$$

where: $h_{go} - h_{fwo} = 520$

Using these parameters in the model of Fig 2.4 the boiler model is implemented in the SIMULINK in the next section.

2.2.2 Simulink Implementation of Boiler

These following equations have been used to implement the model in SIMULINK:

$$\dot{Q}(s) = T_F(s)U_f$$

$$T_m(t) = T_m(0) + \int_0^t \{\frac{1}{C_M}(\dot{Q}(\theta) - \dot{Q}_w(\theta))d\theta\}$$

$$\dot{Q}_w(t) = K_W(T_m(t) - T_f(t))$$

$$\dot{m}_W(t) = Q_w(t)(-P_D(t) + K_H(P_D(t) - P_{D0}))$$

$$P_D(t) = P_D(0) + \int_0^t \{\frac{1}{C_D}(\dot{m}_w(\theta) - \dot{m}(\theta))d\theta\}$$

$$P_T(t) = P_T(0) + \int_0^t \{\frac{1}{C_{SH}}(\dot{m}(\theta) - \dot{m}_S(\theta))d\theta\}$$

$$\dot{m}(t) = K(P_D(t) - P_T(t))^{1/2}$$

$$T_f(t) = K_T(P_D(t) - P_{D0})$$

$$\dot{m}_S(t) = (CV)P_T(t)$$

Model Improvement

To derive steam temperature and drum level, de Mello works has been improved to include the steam temperature and drum level using following equations:

$$T_s = a_1 P_T^{\,2} + a_2 P_T + a_3$$

$$DL = (V_w + a_m V_r)/A$$

Using steam table, the coefficient of equation a_1, a_2, a_3 and a_m can be derived (Appendix 2.1). The improvement model along with controllers has been shown in Fig 2.5. Using the implemented model in SIMULIK the step response of the model will be compared with the published experimental data in the next section.

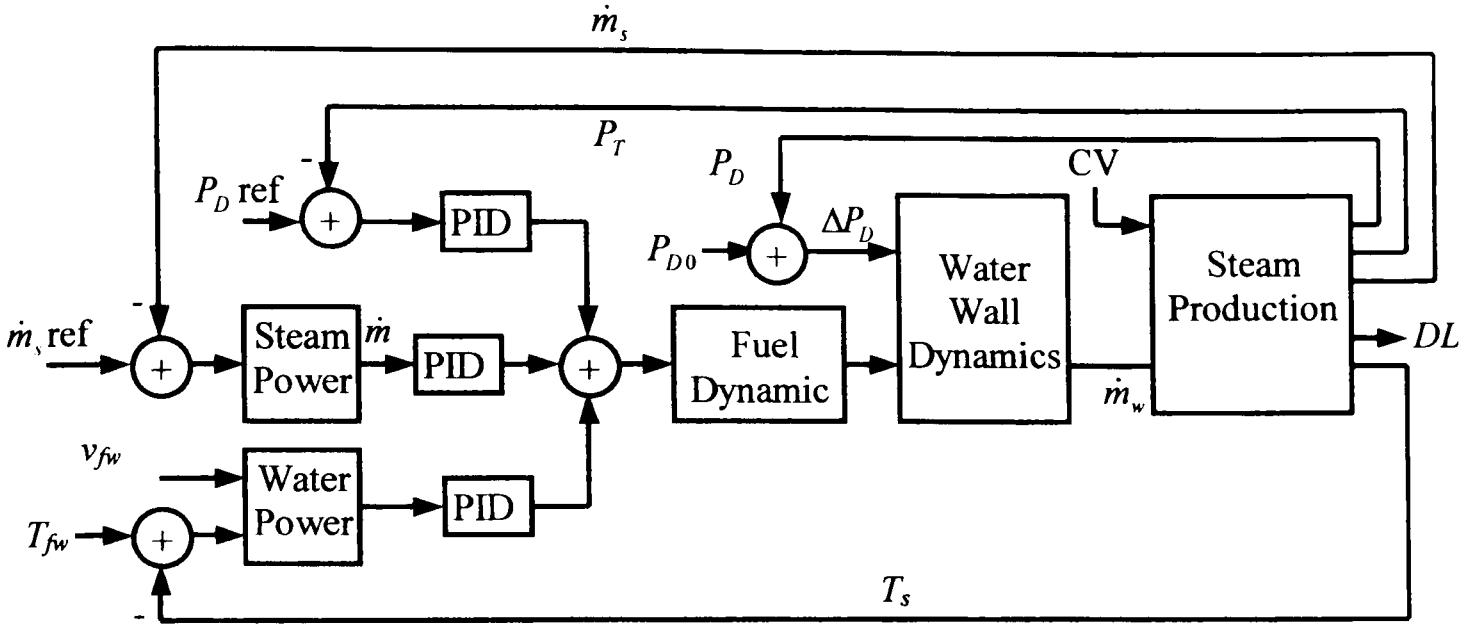

2.5a: The Block Diagram of boiler implementation in SIMULIK

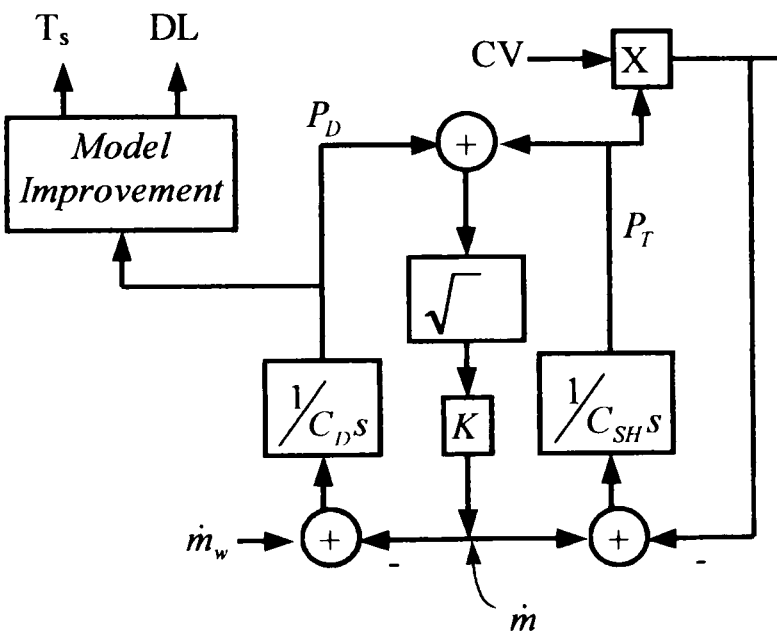

2.5b: Steam Production

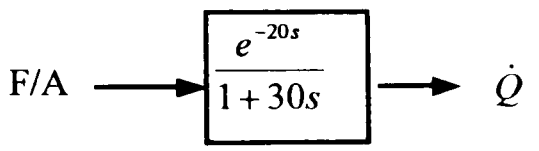

2.5c: Fuel Dynamic

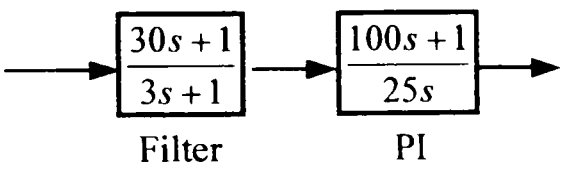

2.5d: PID Controller

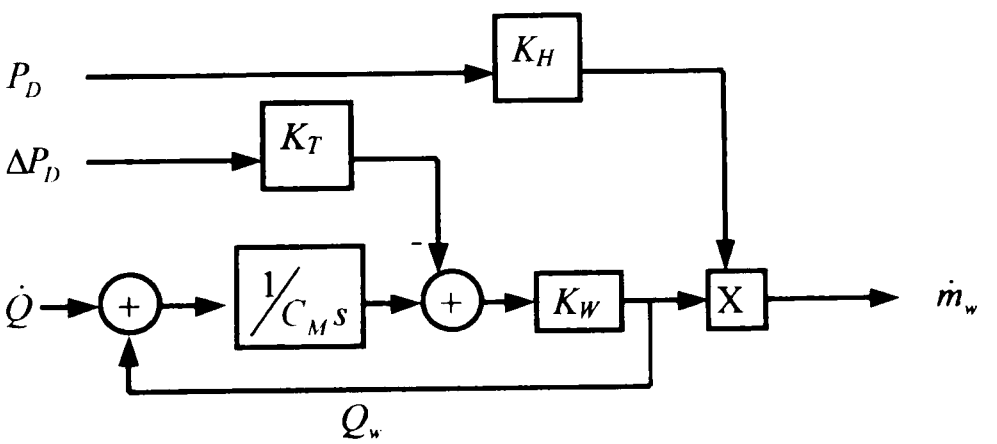

2.5e: Water Wall Dynamic

2.2.3 Simulation Results

In this section step response of boiler variables in two different configurations is considered:

- Without Pressure Control
- With Pressure Control

Boiler Response Without Pressure Control

Fig 2.6 and 2.7 show the response of Drum and Throttle pressure, heat flux, metal and fluid temperature, drum level, steam generation and steam flow rate out of drum of boiler to step change in inputs of boiler when there is no controller on throttle pressure.

Fig 2.6 shows the response of boiler's variables to 2% step increase in desired output around full load operating point, from an initial operating point of *Signal to fuel*=0.98 *pu* in $t=10^5$ to *Signal to Fuel*=1 *pu*. The step change in fuel causes a similar change in steam generation, drum and throttle pressure, temperatures and steam flow rate out of drum with delay due to fuel system's delay. It is clear that the steam generation is a non-linear function of heat flux and drum pressure in the boiler.

Fig 2.7 shows the effect of 2% step decrease in Control Valve Area (*CV*) around full load operating point, from an initial operating point of *CV*=0.98 *pu* in $t=10^5$ to *CV*=1 *pu* on different variables of boiler. Examination of the pressure response in Fig 2.7 reveals an interesting effect of pressure on steam generation. Basically this is a positive feedback effect, as constant BTU are needed to generate more steam with increases in pressure level. Steam generation and steam flow rate out of drum show non-minimum behaviour of boiler.

Boiler Response With Pressure Control

Fig 2.8 and 2.9 show the response of Drum and Throttle pressure, heat flux, metal and fluid temperature, drum level, steam generation and steam flow rate out of drum of boiler to step change in inputs of boiler when throttle pressure is controlled by a properly tuned PID controller.

Fig 2.8 shows the response of boiler's variables to 5% step decrease in set point around full load operating point, from an initial operating point of *Desired output*=1 *pu* in $t=10^5$ to *Desired output=0.95 pu*. The step change in throttle pressure reflects into a similar change in drum pressure, temperatures, steam generation and steam flow rate out of drum. There is almost no effect on fuel and heat flux.

Fig 2.9 shows the effect of 5% step decrease in Control Valve Area (*CV*) around full load operating point, from an initial operating point of *CV=0.95 pu* in $t=10^5$ to *CV*=1 *pu* on different variables of boiler.

With closing the *CV,* the steam flow rate out of drum starting to decrease, but cause the set point is constant, after a while steam flow rate out of drum reach to its previous value and because of steam flow rate out of drum is proportional to throttle pressure times CV, the throttle pressure will increase and then, heat flux, temperatures, steam generation and fuel signals increase.

Model Validation

These results have been compared with the published experimental data (IEEE Working Group, 1994). The differences between results and the experimental data are insignificant.

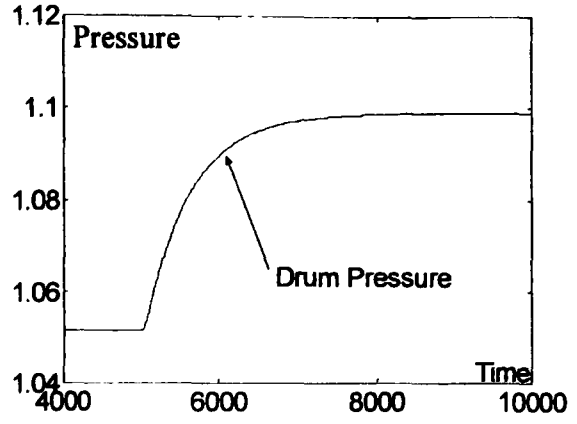

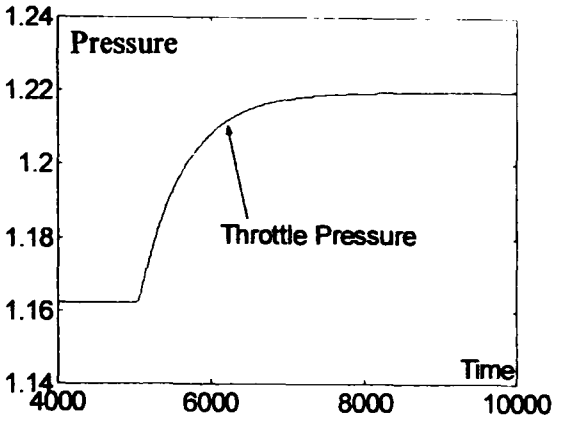

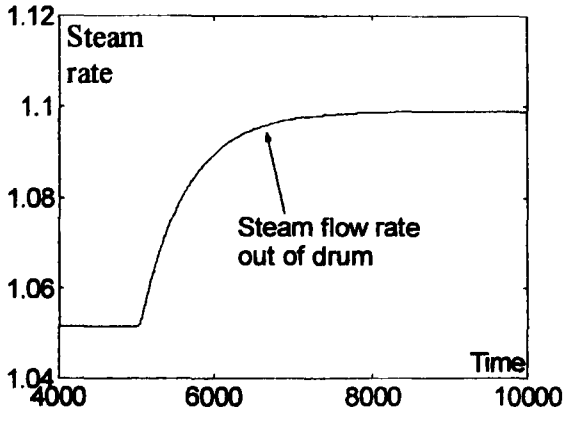

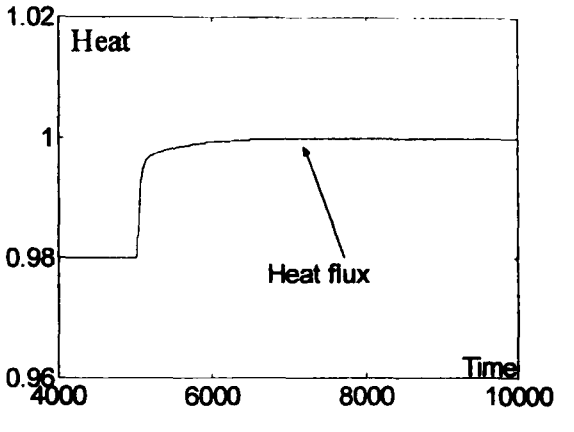

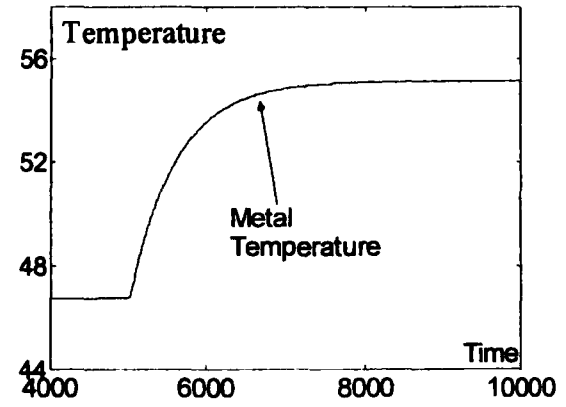

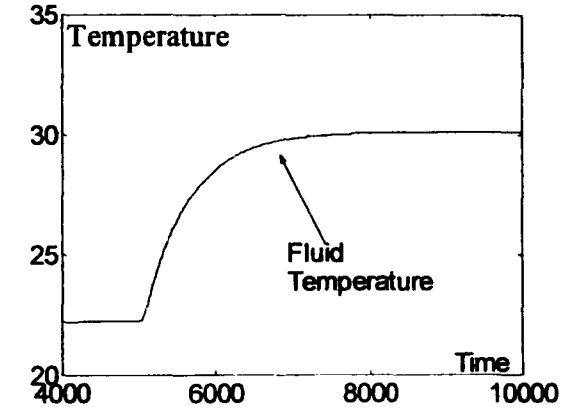

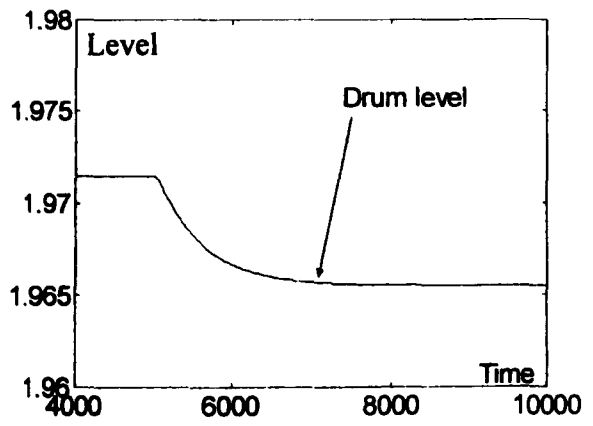

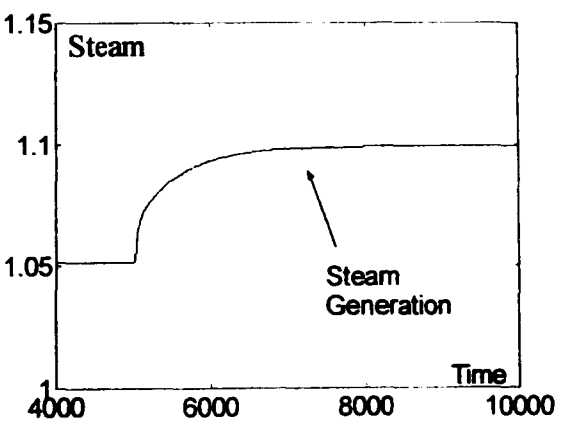

Fig 2.6: %2 Change in Set point when (CV=1) without control on the pressure

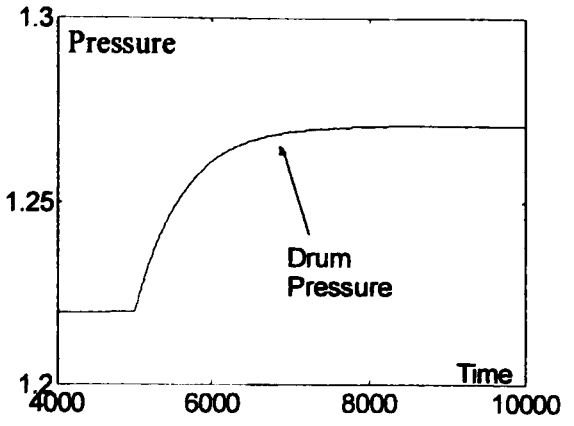

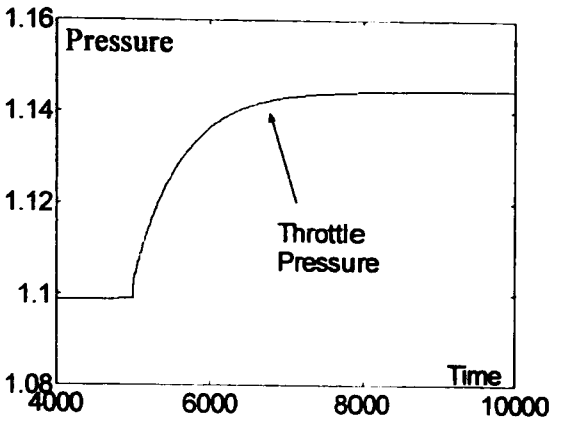

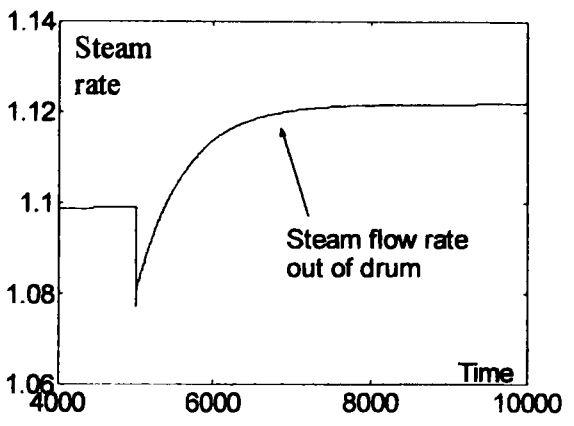

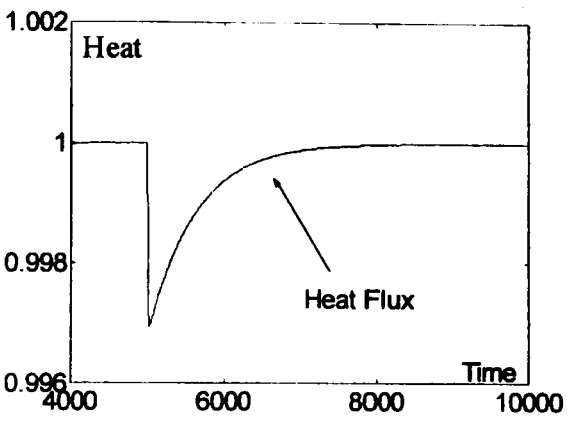

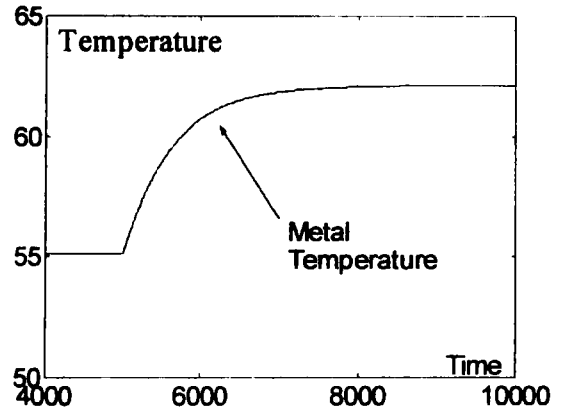

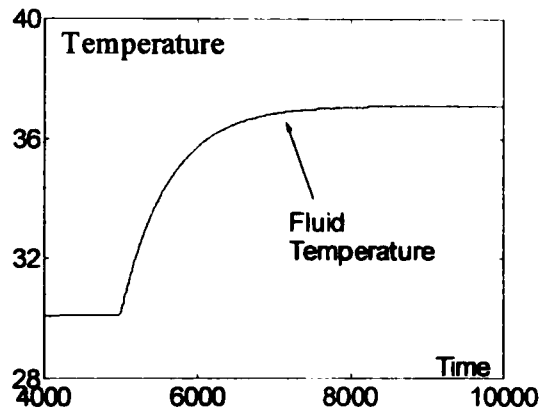

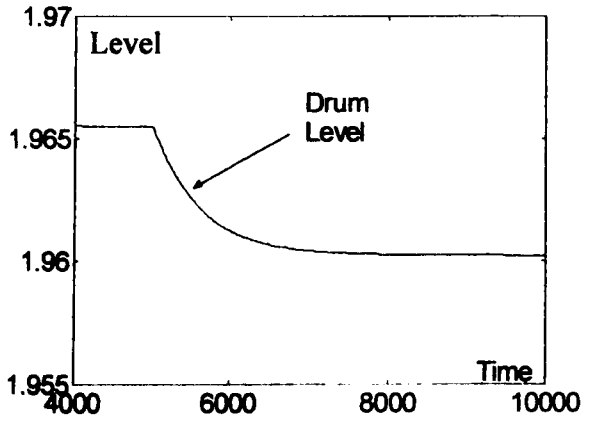

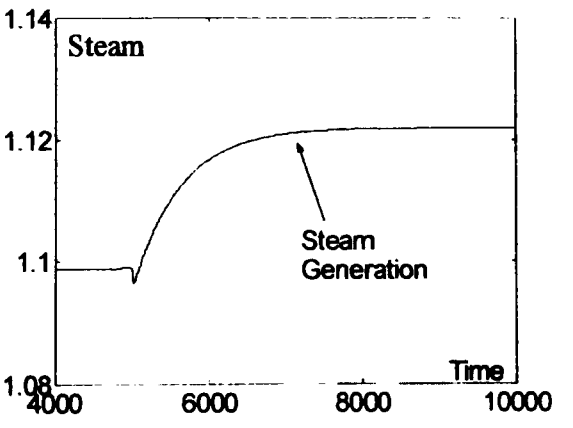

Fig 2.7: %2 change in CV when output is constant without control on pressure

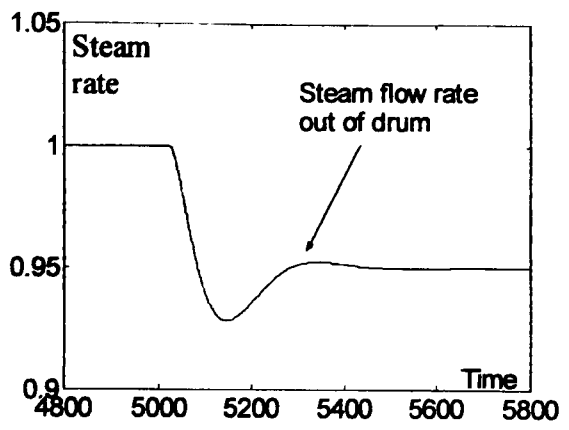

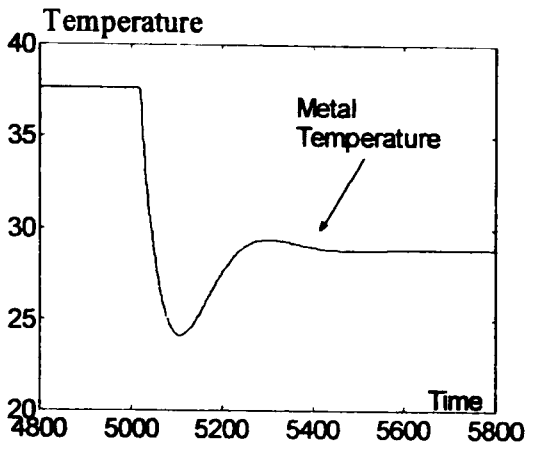

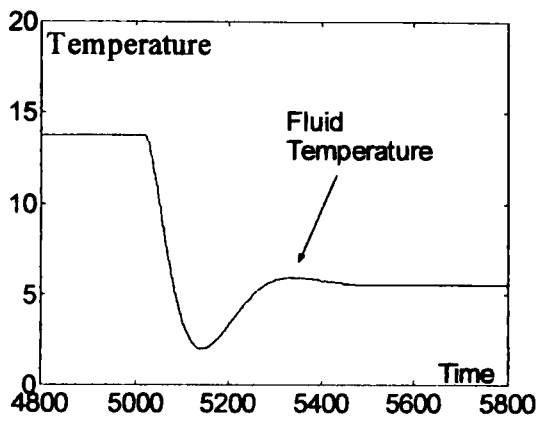

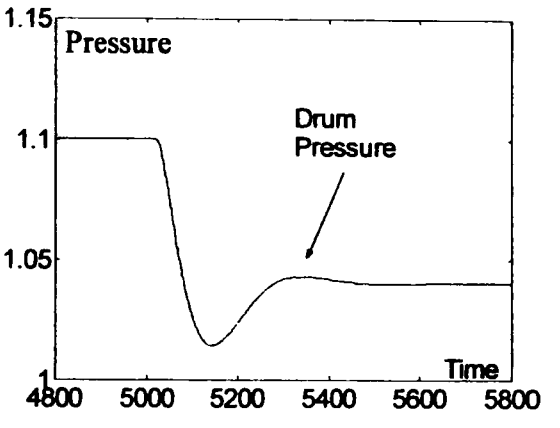

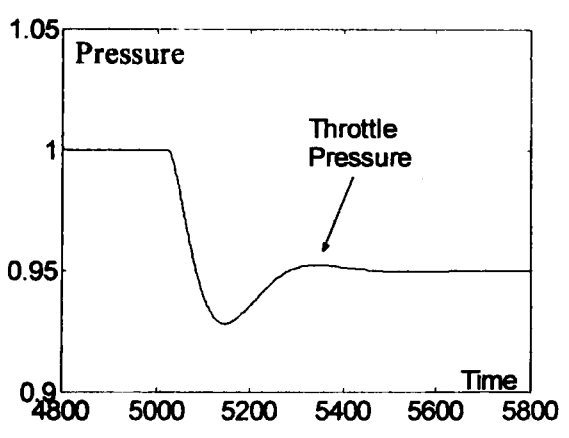

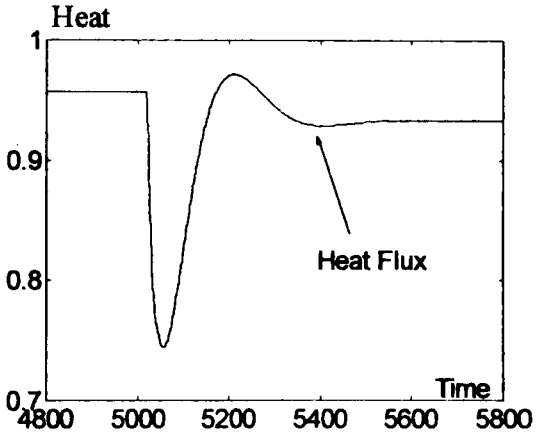

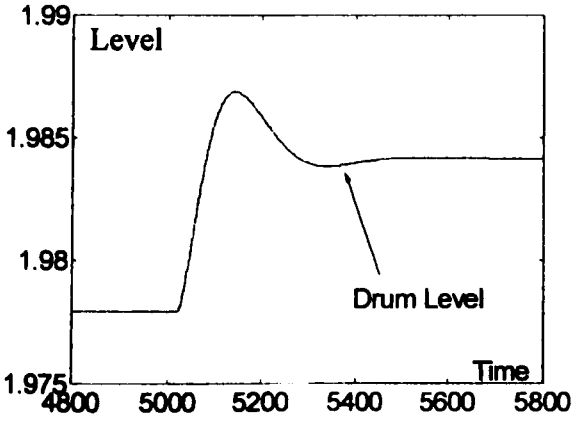

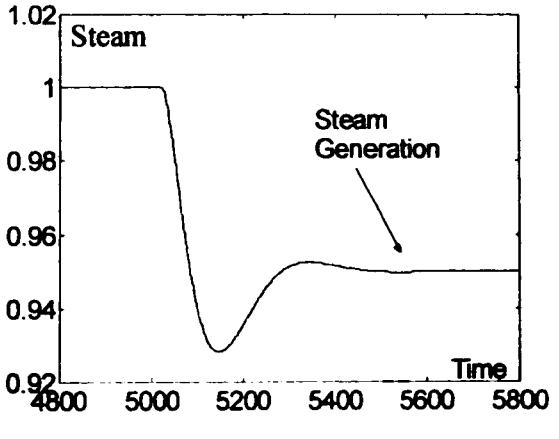

Fig 2.8: 5% change in set point (1 to.95) with control on the pressure and CV=1

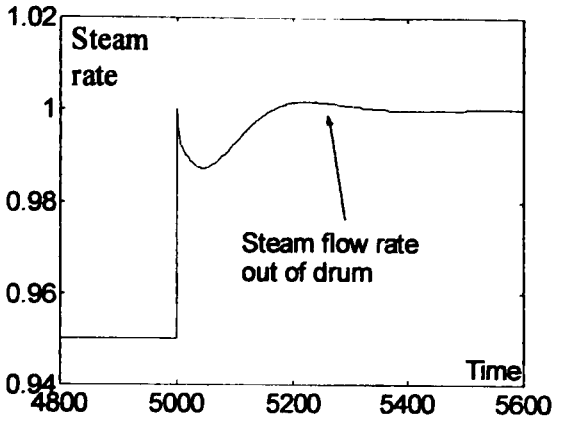

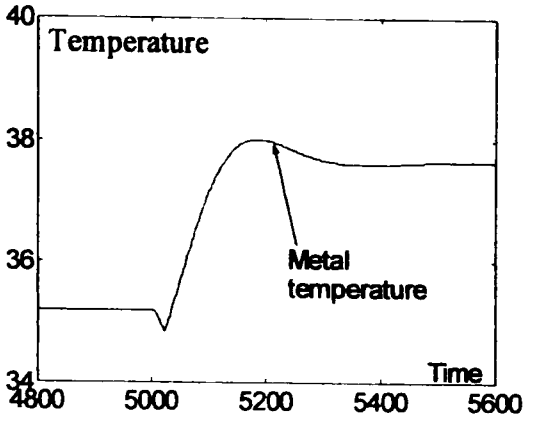

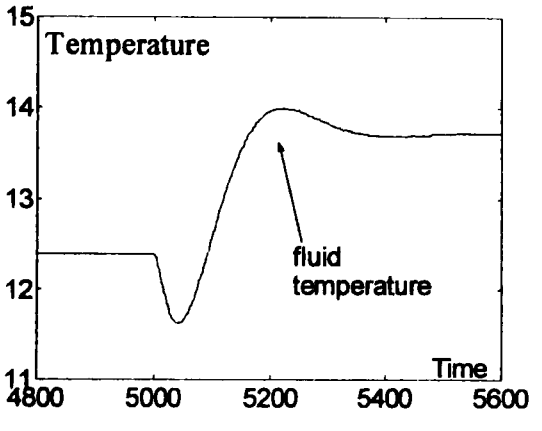

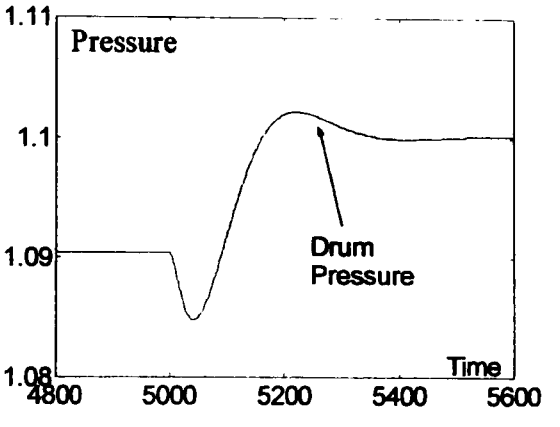

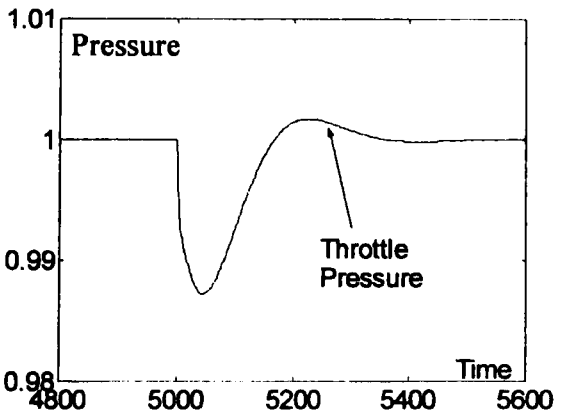

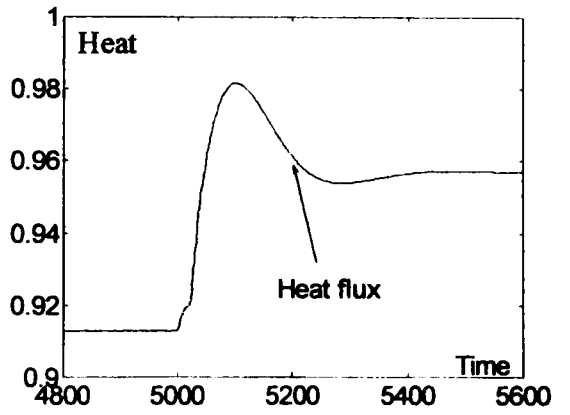

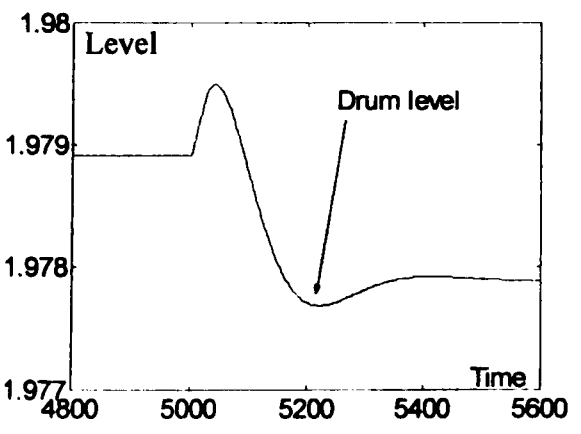

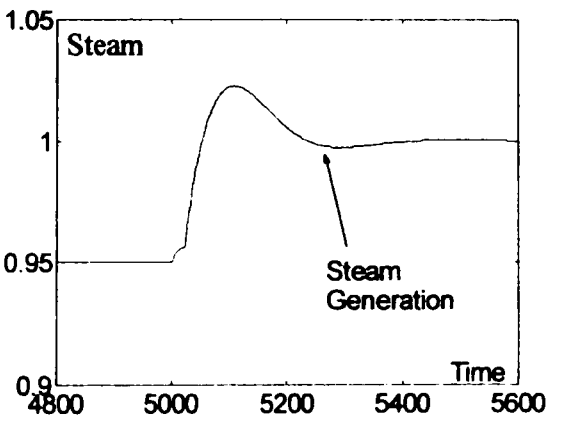

Fig 2.9: 5% change in CV with control of pressure and constant set point

2.3 Steam Turbine and Governor

First order transfer function (equation A1.3.4) is calculated to model each part of turbine assuming constant temperature and weight flow proportional to pressure in the vessel Fig A1.3.1. Also, Turbine control is accomplished by means of governor- controlled valves.

2.3.1 Steam Turbine and Governor Modelling

A generic model structure applicable to all commonly encountered steam turbine configurations was shown in Fig 1.18. This model can be used to represent any turbine by adjusting time constants and gains. The model has been implemented in SIMULINK. Older turbine governor designs used mechanical-hydraulic control, but new governors are Electro-Hydraulic Controller (EHC). This contributes to faster response and improved linearity. Fig 1.19 showed EHC speed-governing systems. The turbine speed/load control model can usually be generic when limited to normal primary speed control model and normal supplementary load control. The outputs are the CV and IV flow area. The inputs could be speed, acceleration or electrical power depending on the particular design. The EHC has been chosen as governor in CCPP simulator.

2.3.2 SIMULINK Implementation of Steam Turbine and Governor

A modular and hierarchical procedure to model steam turbine and governor turbine in SIMULINK has been used. The turbine that has been shown in Fig 2.10a consists of four subsystems including re-heater, high, intermediate and low-pressure stages. The electro-hydraulic governor has been implemented in SIMULINK Fig 2.10b. The Library of modules for turbine and governor has been shown in Fig 2.10c. The library consists of four blocks for steam turbine and one block for governor.

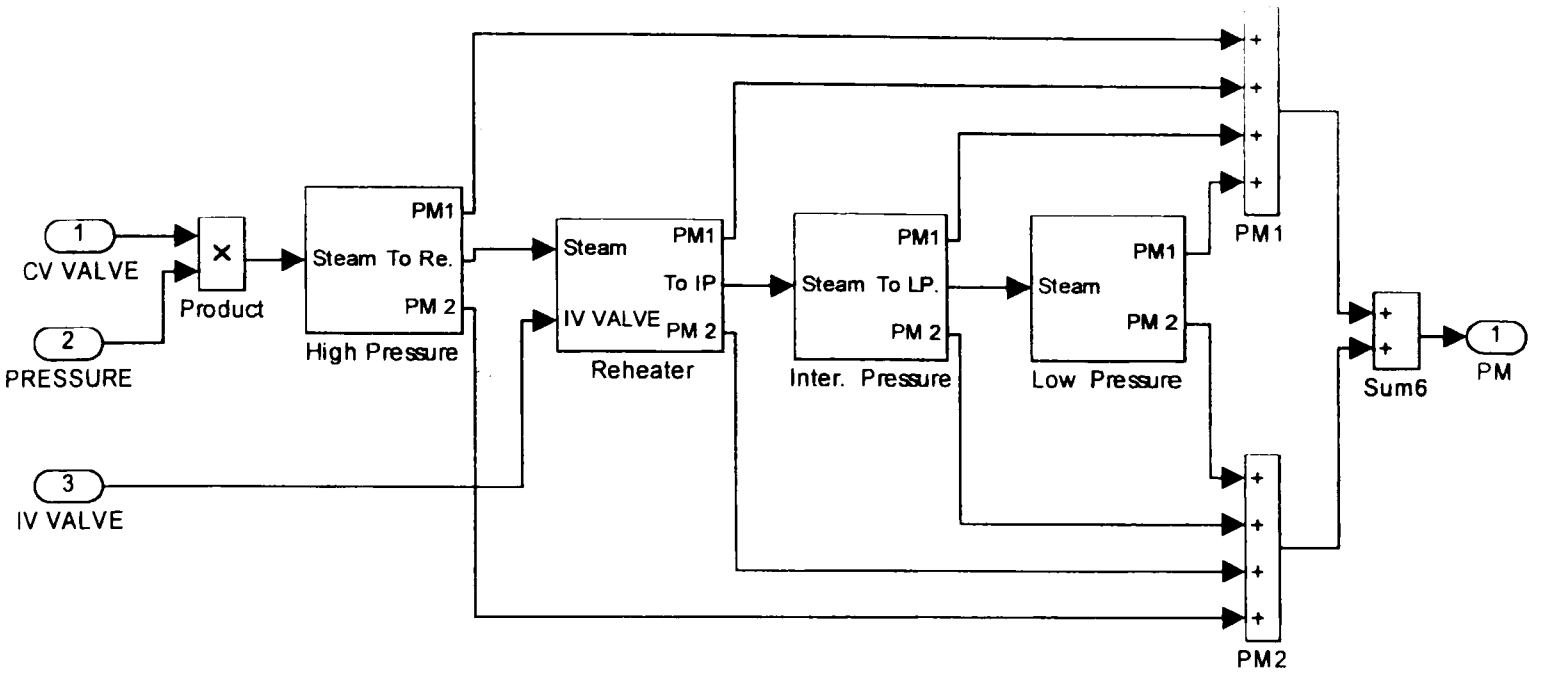

Fig 2.10a: Generic Turbine Model including IV effects

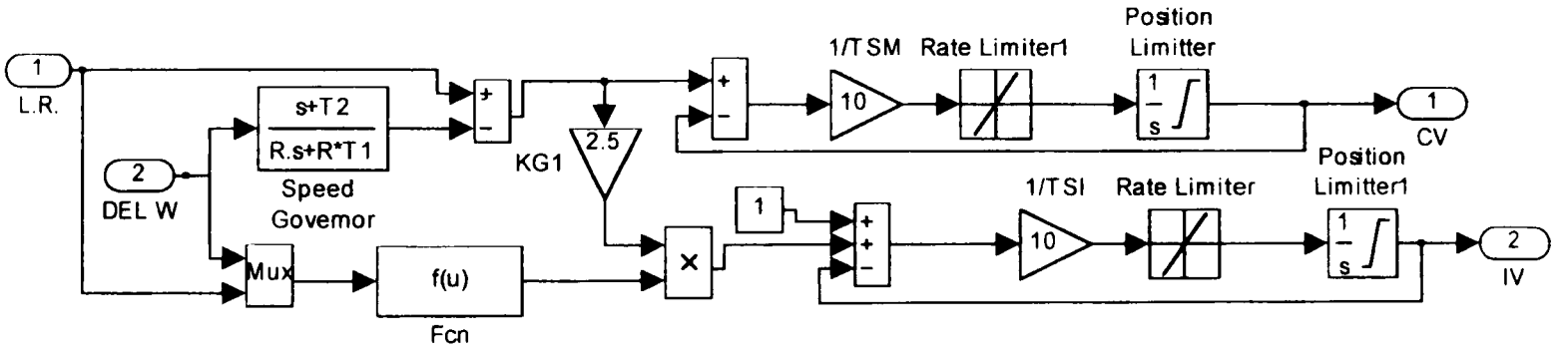

Fig 2.10b: Model of Electro-Hydraulic

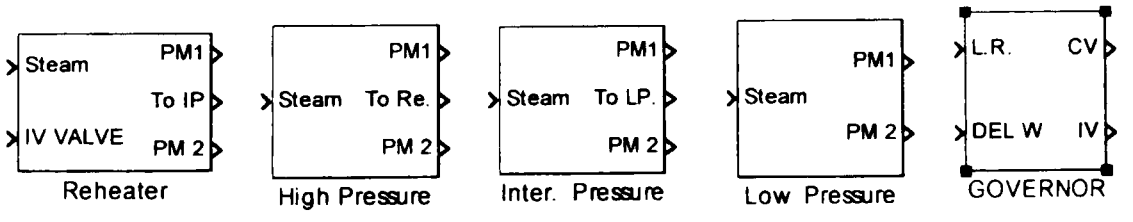

Fig 2.10c: Steam Turbine and Governor Library

2.4 Gas Turbine

Gas turbines are widely used as sources of power generation especially during peak load conditions. Some features such as ease of installation and maintenance, high reliability and quick response has made it an attractive means of producing mechanical energy. A fully dynamic model of gas turbine is not required especially for power system studies. Therefore, some simplifying assumptions need to be made to arrive at a simple dynamic model.

In this section, Rowen (1983; 1992) model for a general electric heavy-duty gas turbine is considered and then the model is implemented in SIMULINK. The model has been used by many authors to show dynamic behaviour of gas turbine (Hannett and Khan, 1993; IEEE Working Group, 1994; Bagnasco *et al.* 1998). Also the model is normalised and suitable for control studies.

2.4.1 Gas Turbine Modelling

A General electric heavy-duty, simple cycle, single-shaft gas turbine was modelled by Rowen (1983; 1992). The model includes the following subsystems:

- Liquid and gas fuel systems
- Parallel and isolated operation
- Droop and iso-chronous governors
- The impact of both air and hydrogen-cooled generators

The measurable outputs is mass flow, mechanical power and exhaust temperature. Input available for control is the fuel rate, mechanical speed. The proposed models were tested on a realistic industrial combined power plant (IEEE Working Group, 1994). The results highlight the differences between the various cases considered and provide useful information for the adoption of the more appropriate control mode, the calibration of the gas turbine regulators and the validation of load shedding procedures. The control systems considered are speed control, temperature control, acceleration control and *IGV* control. Fig 2.11a shows gas turbine along with its subsystems.

Chapter 2

Gas Turbine Dynamics

The gas turbine is essentially a linear, non-dynamic device with the exception of the rotor time constant. There is a small transport delay associated with the combustion reaction time, a time lag associated with the compressor discharge volume and transport delay to transport the gas from the combustion system through the turbine Fig 2.11b. In the context of the rotor and connected system time constants and the relatively slow set point ramp rates, these short term dynamic characteristics can be ignored.

Both the torque and exhaust temperature characteristics of the gas turbine are linear with respect to fuel flow and turbine speed over the 97-107% speed range to which these models are limited. The torque equation, $F_2(u)$, is accurate to within 5% at part load and is significantly more accurate at the 100% design rating. The exhaust temperature equation, $F_1(u)$, is somewhat less accurate at part load; however, since temperature control is only active at the design point, the impact of the part load inaccuracy is negligible to the overall simulation. The $F_1(u)$ and $F_2(u)$ are:

$$P_m = F_2(W_f, \omega) = 1.3(W_f - 0.23) + 0.5(1 - \omega) \ \ pu$$

$$T_E = F_1(W_f, \omega) = 540 - 390(1 - W_f) + 306(1 - \omega) \ \ ^\circ C$$

Fuel Dynamics

Gas turbine fuel systems are designed to provide energy input to the gas turbine in proportional to the product of the command signal (VCE) times the unit speed Fig 2.11c. This is analogous to the actual mode of operation of the fuel system, since liquid fuel pumps are driven at a speed proportional to turbine rotor speed and since gas fuel control is accomplished in two stages, with the output pressure of the first stage being proportional to rotor speed. The net effect is to reduce the turndown ratio of the primary fuel control from approximately 50:1 to 6:1. The gas turbine needs a significant fraction of rated fuel to support self-sustaining, no load conditions. This amounts to approximately 23% and is one of the economic driving forces to minimize operating time at fuel speed no load conditions. The relation between command signal (V_{CE}) and Fuel demand (F_D) is as follow:

$$F_D = 0.23 + 0.77\omega V_{CE}$$

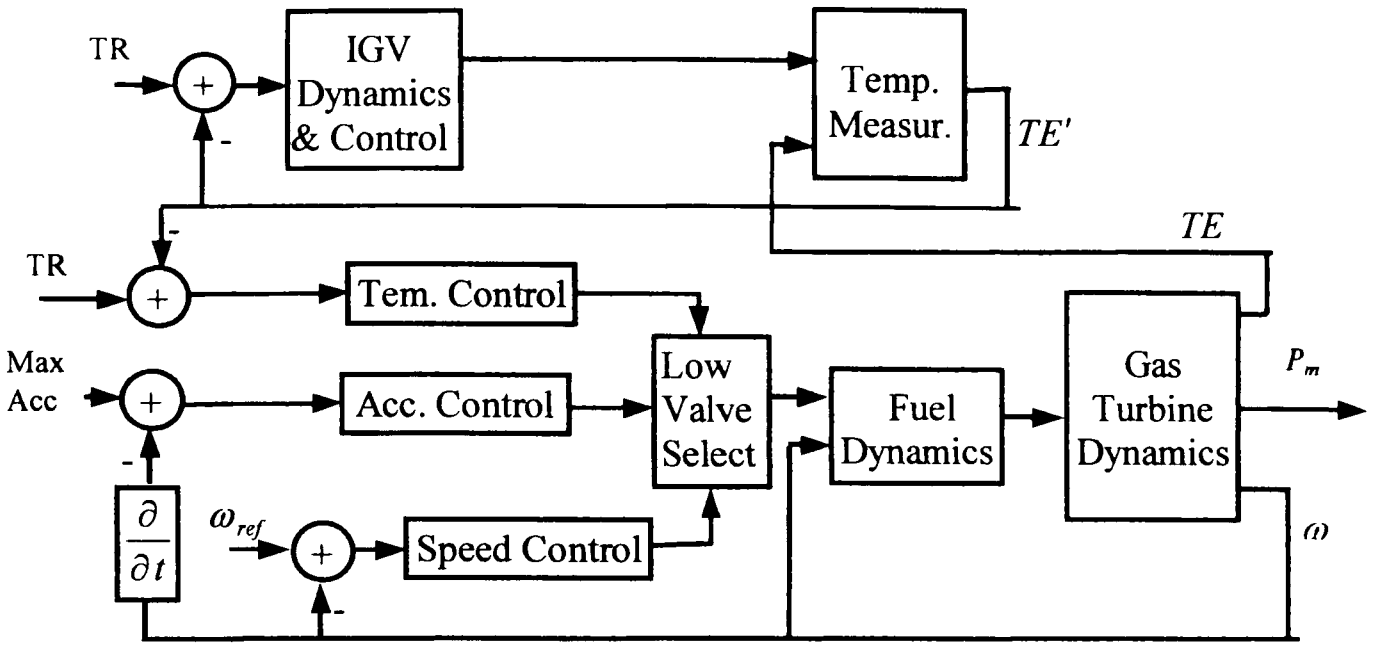

Fig 2.11a: The Block Diagram of Gas Turbine and its Controllers.

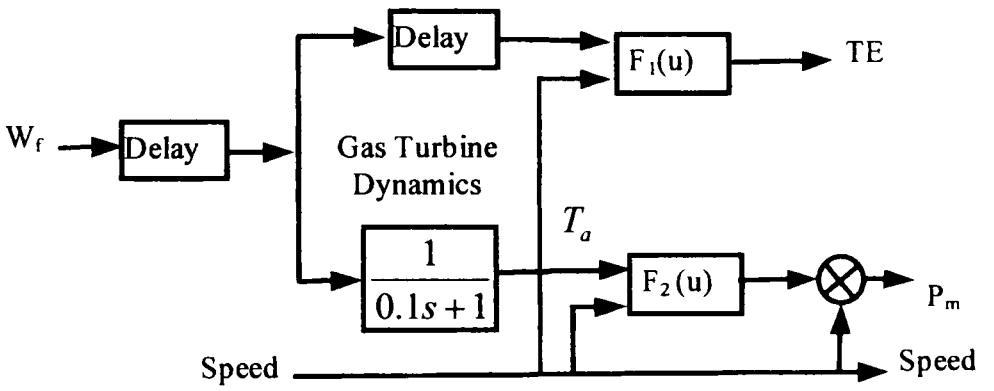

Fig 2.11b: Gas Turbine

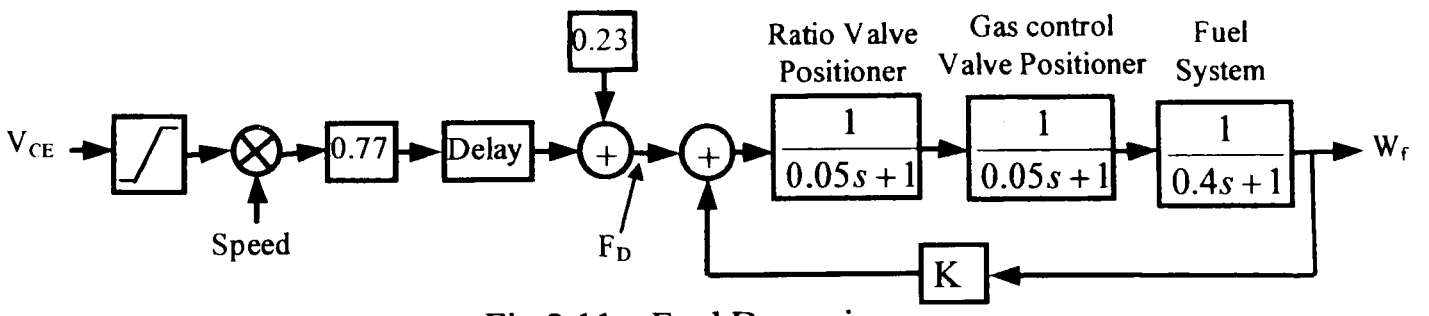

Fig 2.11c: Fuel Dynamics

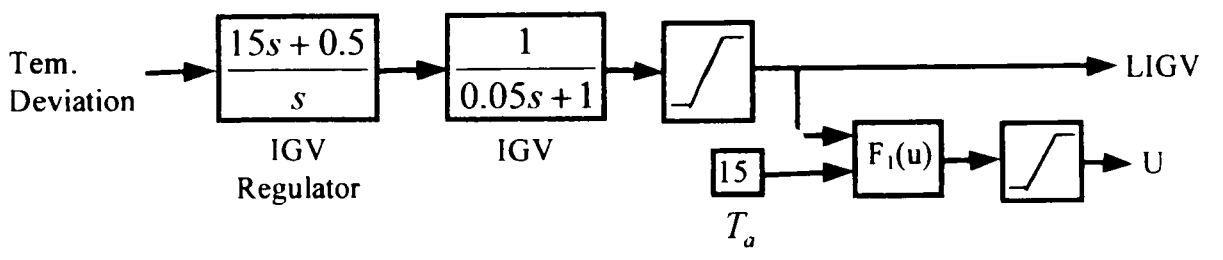

Fig 2.11d: IGV Control & Dynamics

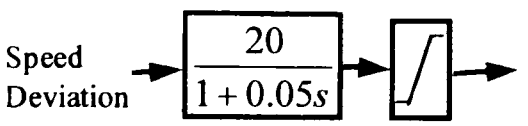

Fig 2.11e: Speed control

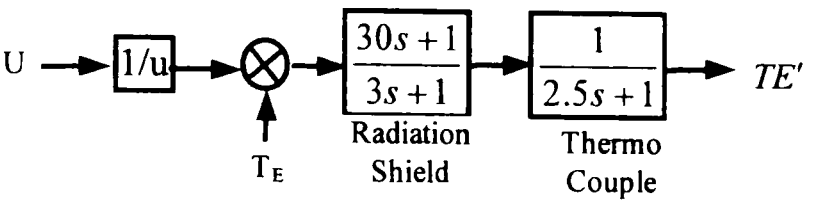

Fig 2.11f: Temperature Measurement

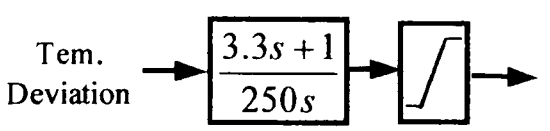

Fig 2.11g: Temperature control

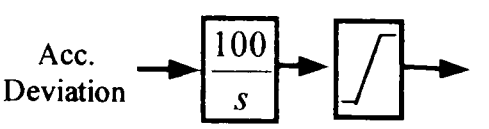

Fig 2.11h: Acceleration control

Fig 2.11: Gas Turbine Representation

IGV Controller and Dynamics

Part load optimisation of exhaust temperature is the primary function of the modulating inlet guide vane (IGV) control. For heat recovery applications, optimum part load cycle performance is obtained when the turbine exhaust temperature is at a maximum. This is achieved by closing the IGVs, within the operating range, at part loads, until the exhaust temperature is at its maximum allowable level.

A bias is provided at partially closed IGV angles to allow transient over firing, of up to 30F in turbine exhaust temperature. This permits the addition of fuel at part load causing the IGVs to open, increasing cycle airflow, and ultimately resulting in the turbine output increasing to meet the demands of the speed governor. The over firing has no impact on hot gas path thermal fatigue loading or part life since it is of relatively small magnitude, and has quite short time duration Fig 2.11d.

For simple cycle turbines, the IGVs are fully opened at the conclusion of start up, and are essentially fixed over the normal operating range.

Low Value Selector

Three control functions-speed governing under part load conditions, temperature control acting as an upper limit, and acceleration control to prevent over speeding- are all inputs to a low value selector Fig 2.11a. The output of the low value selector, which is called VCE, is the lowest of the three inputs. Transfer from one control to another is bumpless

and without any time lags. The output of the low value selector is compared with maximum and minimum limits. The maximum limit acts as a backup to temperature control and is not encountered in normal operation. The minimum limit is the more important dynamically, because the minimum limit is chosen to maintain adequate fuel flow to insure that flame is maintained within the gas turbine combustion system. This is typically set at a torque deficiency of approximately 10%, is a hard limit, and represents a maximum rate of deceleration or torque absorption from the system.

Controllers

The control system includes speed control, temperature control, axial flow compressor inlet guide vane control, acceleration control and upper and lower fuel limits.

The speed Governor representation is for an isochronous speed control, and operates on the speed error formed between references made up of one per unit speed, compared with actual rotor speed Fig 2.11e. The isochronous governor is a proportional plus reset speed controller in which the rate of change of output is proportional to the speed error. Thus the output of the isochronoous governor will integrate in a corrective direction until the speed error is zero.

The fuel gas control system consists of two valves in series, the first of which controls the pressure between the two valves as a function of turbine speed, and is used tc extend the controllable turndown ratio of the system during gas turbine start up Fig 2.11c. The second valve, the actual gas control valve, has a linear area versus lift characteristic and is aerodynamically designed so that sonic velocities are attained at the controlling area with flange to flange pressure ratios as low as 1.25. Since position of the second valve is held proportional to control system fuel command, the fuel flow rate is proportional to the product of fuel command and turbine speed.

The response of the pressure control portion of the system is dominated by the response of the first valve positioner since the volume between the valves is very small, and the pressure measurement transducer has a very small time constant. The gas control valve utilizes a positioner that is identical to the ratio valve, and therefore can be represented by an identical first order transfer function. The remaining time constant in the fuel

system is representative of the storage volume of the fuel gas piping between the gas control valve and the fuel nozzles at the gas turbine combustors, and is actually the largest time constant in the gas fuel control system.

Temperature control is the normal means of limiting gas turbine output at a predetermined firing temperature, independent of variation in ambient temperature or fuel characteristics. Since exhaust temperature is measured using a series of thermocouples incorporating radiation shields; there is a small transient error due to the time constants associated with the measuring system Fig 2.11f. Under normal system conditions these time constants are of no significance to the load timing function. However, where increasing gas turbine output is the result of a reduction of system frequency and therefore may occur quite rapidly, exhaust temperature measurement system time constants will results in some transient overshoot in load pickup. The design of the temperature controller is intended to compensate for this transient characteristic Fig 2.11g.

Acceleration control is used primarily during gas turbine start up to limit the rate of rotor acceleration prior to reaching minimum governor speed, thus ameliorating the thermal stresses encountered during start up. In the unlikely event of a rapid unloading of the driven compressor, this control would also act to reduce fuel flow to limit the rate of rise in speed l ig 2.11h. Minimum and maximum fuel flow limits are established to ensure that fuel flow is not reduced below the point of self-sustaining combustion, nor above that corresponding to the maximum turbine output at site minimum ambient temperature.

2.4.2 SIMULINK Implementation of Gas Turbine

The Gas turbine model has been shown in Fig 2.12. The model consists of subsystems and four controllers together. A modular and hierarchical procedure to model gas turbine in SIMULINK has been used. The modules are described in next section.

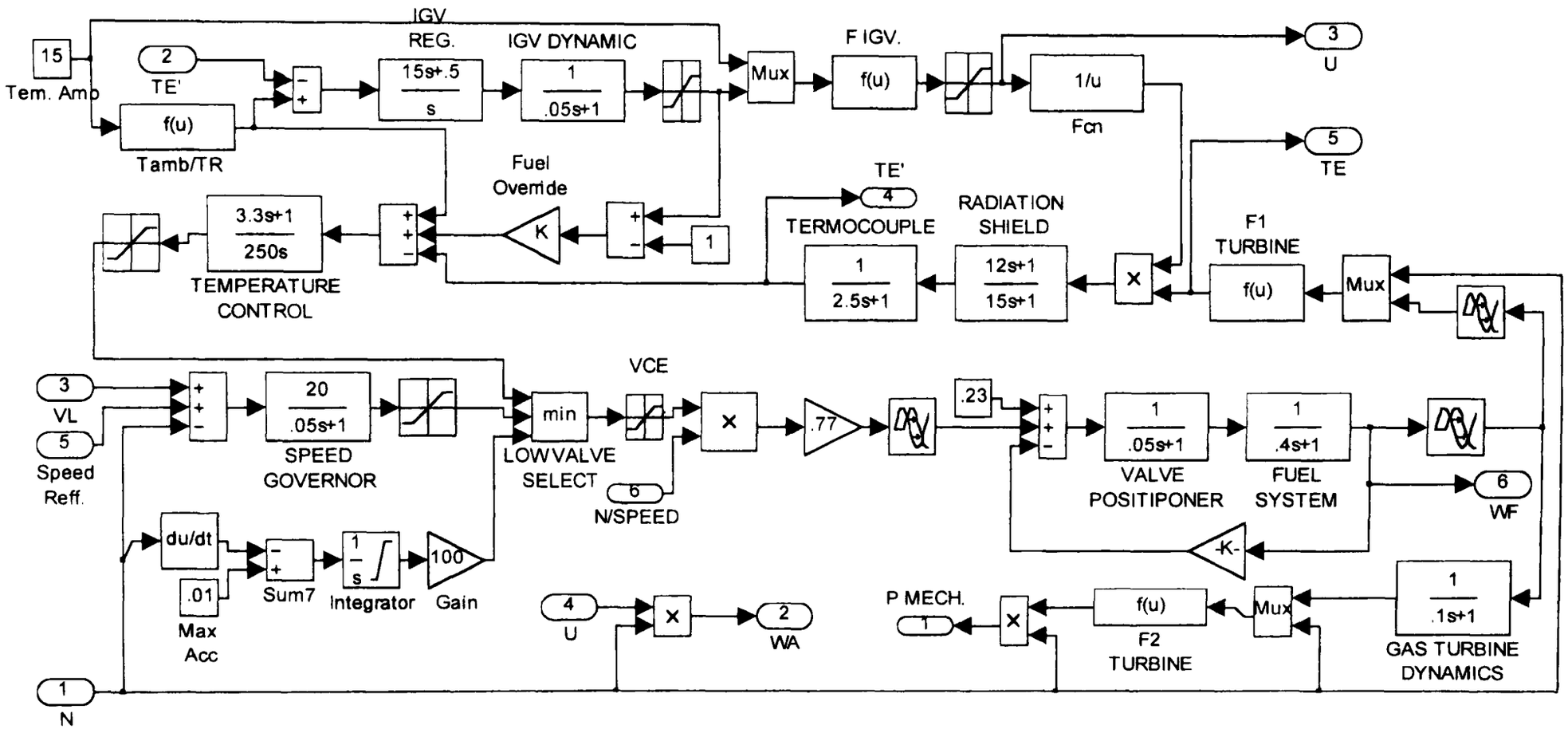

Fig 2.12:Gas Turbine Model in SIMULINK

SIMULINK Modules

The Library of modules for gas turbine has been shown in Fig 2.13a. The library consists of gas turbine.block along with five controllers subsystems, also temperature converter that is using to define different reference temperature for different gas turbines. Digital set point change from low speed stop (85%) to high speed (105%) occurs at a rate of 4% of rated speed per minute. The interface modules have been used between gas turbine subsystem and steam plan, also as power conversion in generator input to connect the gas turbine subsystem to other subsystems in the CCPP.

To change the parameters of model or input data to the simulator, the user just need to double click on the blocks and then he easily can enter his data. Fig 2.13b shows the example of Data input for Fuel/Air Controller. It makes the simulator user friendly.

Model Validation

The derived model is then tested by simulation studies and its performance checked against the published experimental data from the manufacturer's model and also against the published experimental data from the actual measured responses obtained during factory testing.

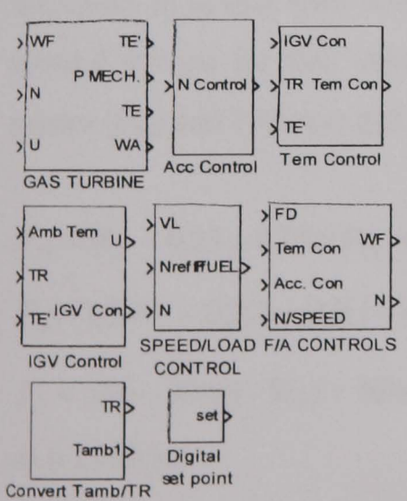

Fig 2.13a: Gas Turbine Library

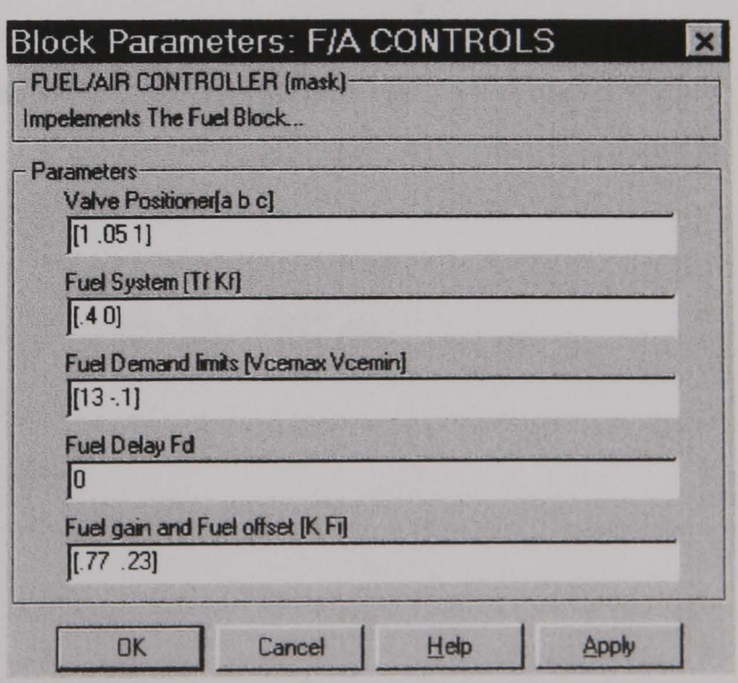

2.13b: Data input for Fuel/Air Controller

2.4.3 Simulation Results

The step response and ramp response of gas turbine has been considered. The model was connected to the simple model of generator and then the validation of model was tested using step and ramp, the reason for using ramp is because the gas turbine dynamic has fast dynamic behaviour and usually the change in set point is slow, also change in power demand is slow. The response of several variables of gas turbine to the following inputs changes are considered:

- Power demand (P_e) changes
- Load reference (LR) changes

The ramp response and step response of gas turbine are showed for each input changes.

Power demand changes

Fig 2.14 shows the ramp and step response of gas turbine to power demand changes. Before t=110 the system is in steady state with Load Reference (L.R)=1 *pu;* (the power that assume to produce) and P_e=0.9 *pu*. Difference between Load reference and electrical demand (0.1 *pu*) along with speed controller's coefficient (1/20) cause 0.1/20 *pu* increases in speed with respect to speed reference. Also, fuel demand signal (V_{CE}) is around 0.9 *pu* for this value of V_{CE}. Fuel demand (F_D), fuel flow (W_f), Mechanical power (P_m) and Exhaust gas temperature (TE) are:

$$F_D = W_f = 0.23 + 0.77\omega V_{CE} = 0.23 + 0.77 \times 1.005 \times 0.9 = 0.927\ pu$$

$$P_m = 1.3(W_f - 0.23) + 0.5(1 - \omega) = 0.91\ pu$$

$$T_E = 540 - 390(1 - W_f) + 306(1 - \omega) = 510^{\circ}C$$

$$\omega = 1.005\ pu$$

Increasing in P_e from 0.9-to-1 has the similar effects on V_{CE} and P_m. It also increases W_F and W_A. The variation of speed is decreasing to zero because the difference between Load reference and electrical demand goes zero Fig 2.14.

Load reference changes

Fig 2.15 shows the ramp and step response of gas turbine to Load reference changes. Before t=110 the system is in steady state with LR=0.95 *pu* (the power that assume to produce) and Pe=0.95 *pu*. Zero difference between Load reference and electrical demand cause almost zero *pu* variation of speed with respect to speed reference. Fuel demand signal (V_{CE}) is around 0.95 *pu* and for this value of V_{CE}, the fuel demand (F_D) the fuel flow (W_f), Mechanical power (P_m) and Exhaust gas temperature (TE) are:

$$F_D = W_f = 0.23 + 0.77\omega V_{CE} = 0.23 + 0.77 \times 1 \times 0.95 = 0.96\ pu$$

$$P_m = 1.3(W_f - 0.23) + 0.5(1 - \omega) = 0.95\ pu$$

$$T_E = 540 - 390(1 - W_f) + 306(1 - \omega) = 524^{\circ}C$$

$$\omega = 1\ pu$$

Increasing LR without changing P_e from 0.95-to-1 causes 0.05/20 *pu* changed in the speed Fig 2.15d. Because of no changes on electrical power demand (P_e) the changes of others variables are small. V_{CE}, P_m, W_f and W_a are increasing to 0.05/20 *pu*. At t=150s the LR decreases to its previous value, so all the variables settles down to their previous value Fig 2.15.

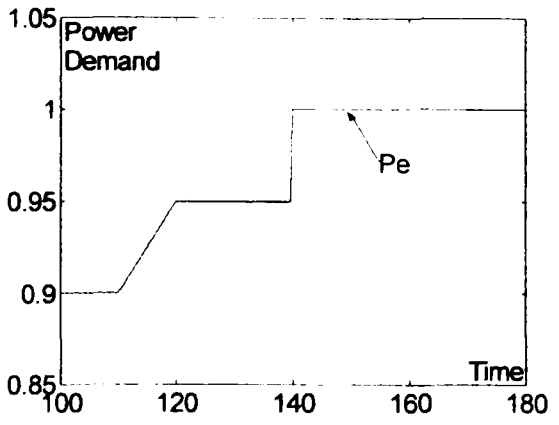

2.14a: Electrical power demand

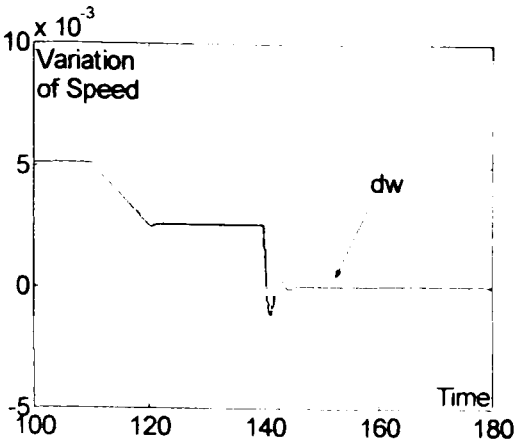

2.14b: Variation of Speed

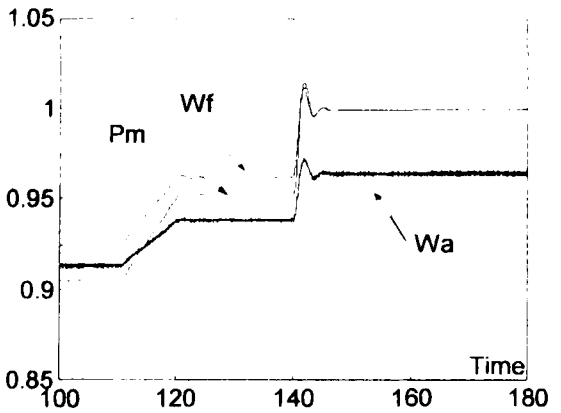

2.14c: Fuel flow (Wf), air flow (Wa) and Mechanical power (Pm).

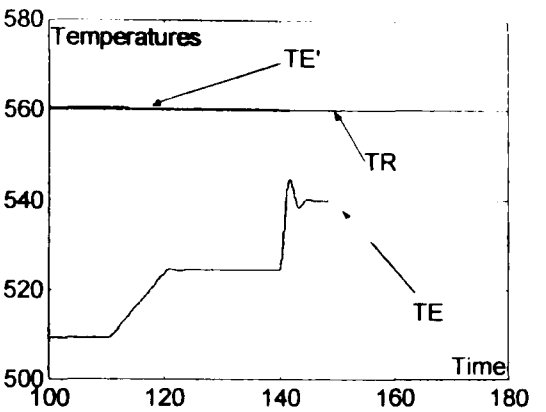

2.14d: Reference (TR), Exhaust (TE) Measured Exhaust (TE') temperatures

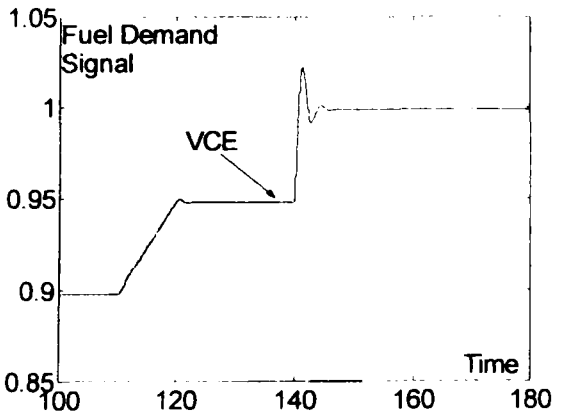

2.14e: Fuel Demand Signal

Fig.2.14: Ramp response of gas turbine to 5% change in Power demand during 10s along with Step response of gas turbine to 5% change to Power demand

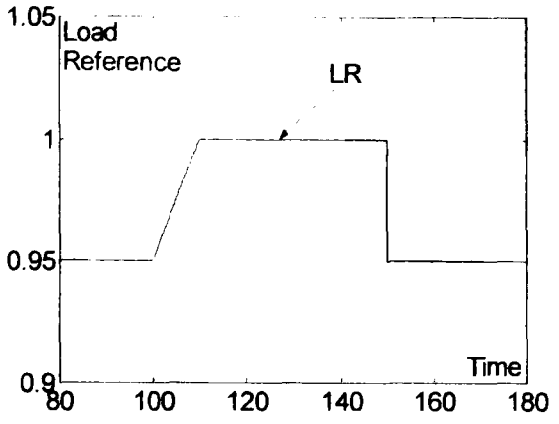

2.15a: Load Reference changes

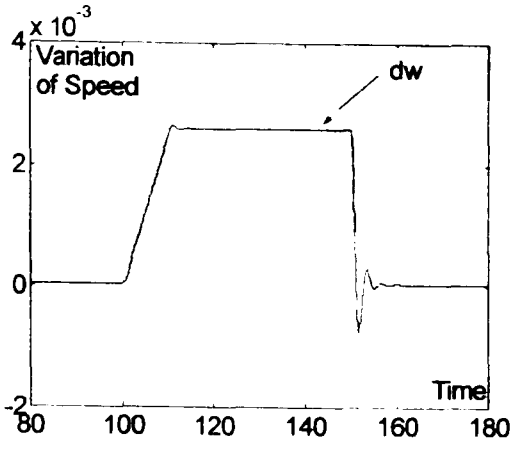

2.15b: Variation of Speed

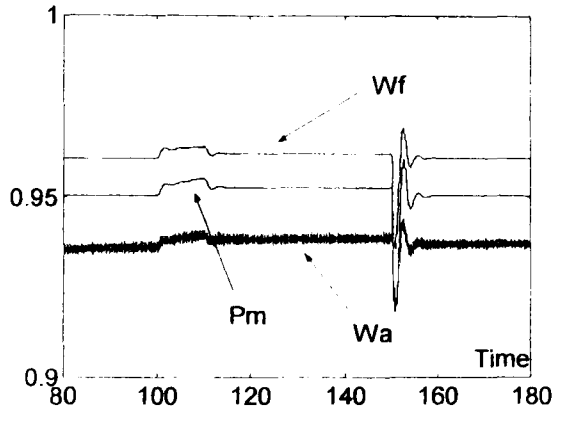

2.15c: Fuel flow (Wf), Air flow (Wa) and Mechanical power (Pm).

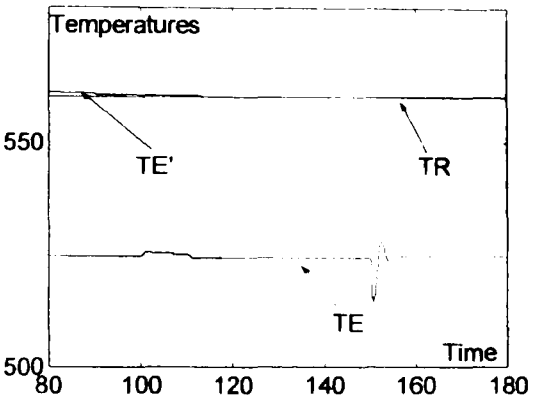

2.15d: Reference (TR), Exhaust (TE) Measured Exhaust (TE') temperatures

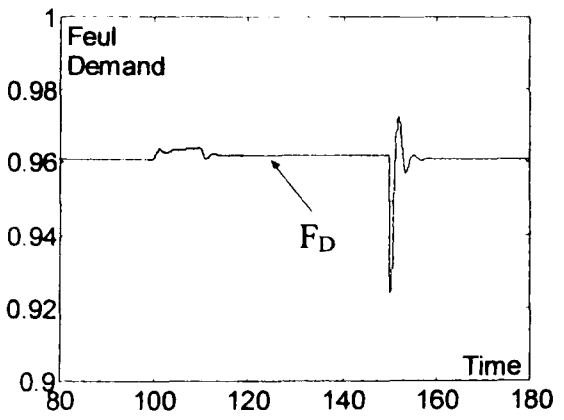

2.15e: Fuel Demand

Fig 2.15: Ramp response of gas turbine to 5% change in Load reference during 10s along with Step response of gas turbine to 5% change to Load reference

2.5 Generator and Excitation System

2.5.1 Generator and Excitation Modelling

Heffron and Phillips (1952), de Mello and Concordia (1969) described a simple linearized model, representing a synchronous generator, connected to an infinite bus through external impedance. This model has been used in CCPP simulator. When the behaviour of synchronous machines is to be simulated accurately in power system stability studies, it is essential that the excitation systems of the synchronous machines be modelled in sufficient detail. The desired models must be suitable for representing the actual excitation equipment performance for large, severe disturbance as well as for small perturbations. IEEE Committee reports (1992) on excitation system reference models. These models widely used for power system dynamic studies (Kundur, 1993).

2.5.2 SIMULINK Implementation of Generator and Exciter

Heffron and Phillips model has been implemented as generator subsystem along with type DC excitation system. Fig 2.16 shows the generator and excitation system. The exciter can also be found in power system toolbox of MATLAB.

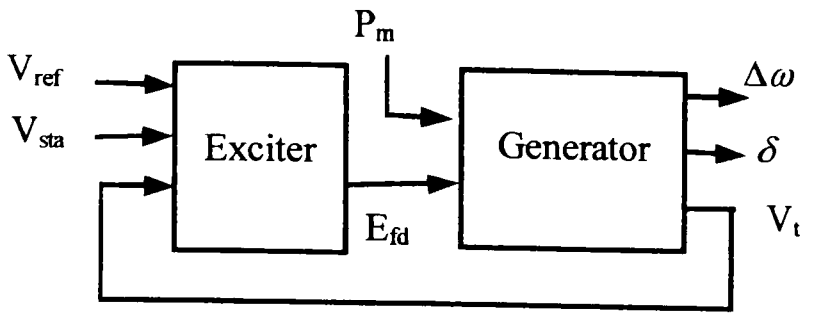

2.16a: The Block Diagram Exciter and Generator

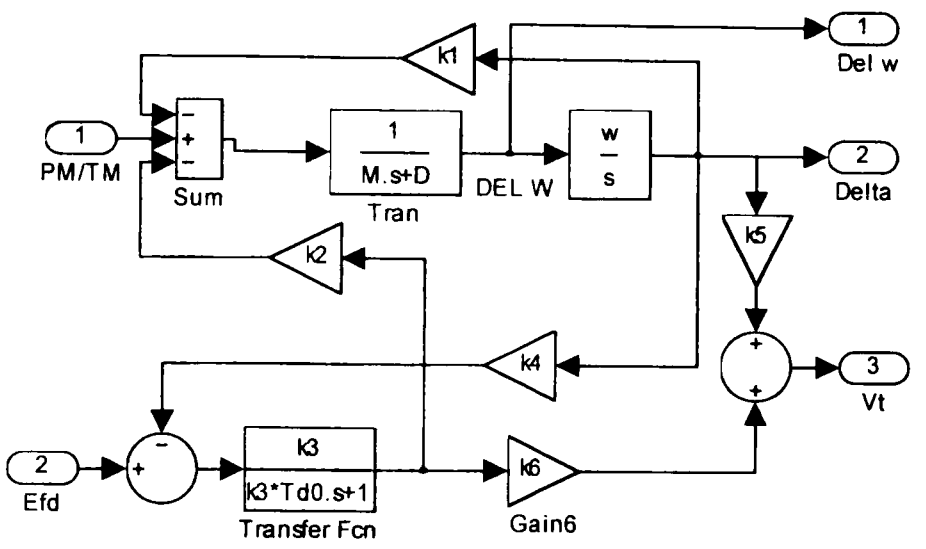

2.16b: The SIMULINK Implementation of Generator

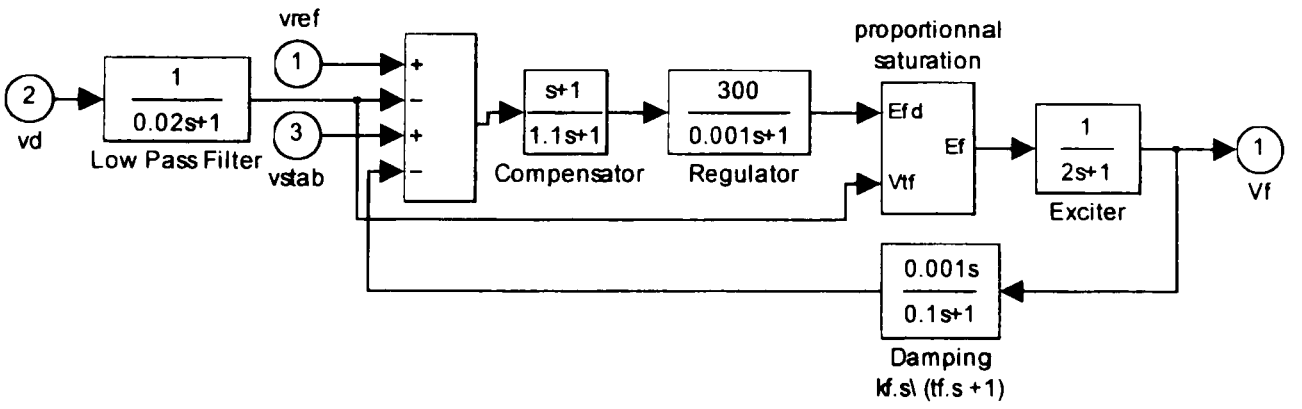

2.16c: The SIMULINK Implementation of Exciter

2.6 Combined Cycle Power Plant

Different subsystems of CCPP has been explained and implemented in SIMULINK in this Chapter. To build different configuration of CCPP of chapter one. it is needed to connect subsystems properly. Therefore, interface modules are introduced which link the subsystems together.

2.6.1 Interface Modules

To implement different CCPP configurations and to change the power base, two interface blocks were developed.

- Fuel reduction interface modules block
- Power base converter interface modules block

First block is located between gas turbine and boiler. The inputs to the block are temperature and mass of gas flow, HP Evaporator metal temperature of boiler and fuel and air supply Fig 2.17. The output shows how much energy is supplied to the boiler from gas turbine and it is presented as fuel reduction signal to the boiler.

The second interface block was implemented to match the base power of different blocks. Inputs to this block are new and old base power and old Per Unit powers, the output is new per unit power as shown in Fig 2.17. With setting this block the user can decide the power sharing between gas turbine and boiler that will be delivered to the system.

2.6.2 SIMULINK Implementation of Combined Cycle Power Plant

A modular and hierarchical procedure to model CCPP in SIMULINK has been used. Fig 2.17 shows the CCPP consists of four subsystems, Boiler and steam turbine in one block called steam plant, gas turbine and generator along with two interface blocks.

The Library of all modules of CCPP has been created. The library consists of different subsystems and blocks of CCPP. After implementation of all subsystems in SIMULINK, user can enter the parameters of blocks. The CCPP configuration can be implemented using the following steps:

- Suitable subsystem are chosen from the library of CCPP
- Using the interface module, the subsystems are linked together.
- With setting the interface modules the type of CCPP and power sharing between gas and steam turbine is selected.

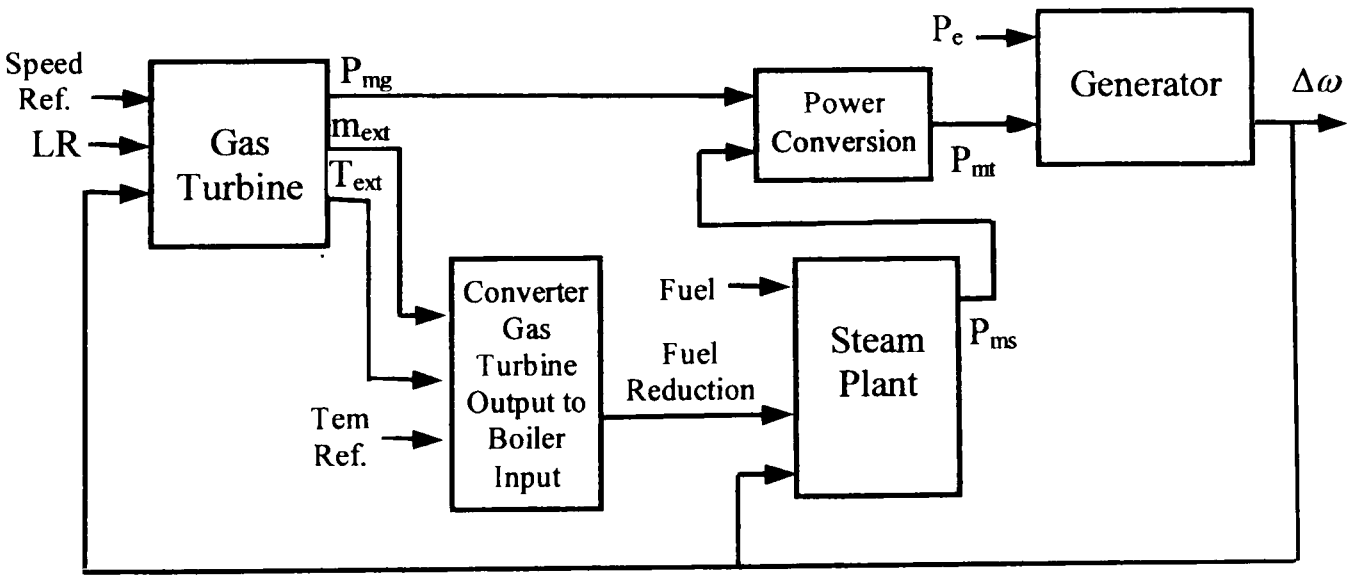

2.17: Block Diagram of CCPP

2.6.3 Simulation Results

In this section the step response of CCPP variables in two different configurations is presented:

- The CCPP without generator
- The CCPP connected to generator

The CCPP without generator

Fig 2.18 shows the response of several variables of CCPP to 10% step increase in Fuel Demand (F_D) from an initial operating point of 0.95 pu. The step change in F_D reflects into a similar change in fuel demand signal V_{CE}. The increase in firing causes an increase in the exhaust temperature beyond the exhaust temperature limit reference causing the temperature controller output (T_C) to come off its limit and override the F_D demand signal. This can be seen from VCE that trace following the T_C signal around one second after the step change. The response of the actual exhaust temperature (T_E) and measured temperature ($T_{E'}$) are also shown. The power is also shown. One can see that in the time frame of a few seconds there is no appreciable contribution from the steam turbine. In this operating region close to full load, the temperature controller quickly offsets increases in load demand.

The CCPP connected to generator

The second simulation test shows the response of CC connected to the simple generator model along with speed controller to:

- 5% step change in power demand
- 5% step change of steam turbine set point

Fig 2.19 shows the response of CCPP's variables to 5% step increase in power demand around full load operating point, from an initial operating point of Power Demand=0.95 *pu* to Power demand=1 *pu*. The step change in power demand reflects into a similar change in power generation from gas turbine and steam turbine. Fast dynamic behaviour of gas turbine cause the output of gas turbine is increasing to 1.09 *pu* (it is noticed that gas turbine is delivered only 30% of power generation) in few second after step. The output of steam turbine is gradually increasing and it causes the output of gas turbine gradually decreasing to around 1 *pu* after 100s. Because the LR does not change, the power generation and power demand would not be the same and the difference between these two powers is delivered by the speed deviation in generator Fig 19b.
Fig 2.20 shows the response of CCPP's variables to 5% step change in steam turbine set point from 0.95 *pu* to 1 *pu*. The step change in set point does not reflect into a similar change in power generation because the power demand is constant. This causes the speed deviation and therefore, the gas turbine and steam turbine power delivery are changing as it is shown in Fig 2.20b.
It is clear from transfer functions of subsystems and step responses of the CCPP that the gas turbine dynamic is faster than steam plant. It means the dominant pole in the CCPP belongs to steam plant and for control study it is better if this pole is considered. Also, the transfer function of boiler has a zero in right hand side of S plan that means non-minimum phase behaviour. These models are used in this thesis for control design studies.

Model Validation

These results have been compared with the published experimental data (de Mello, 1991; Bagnasco *et al.* 1998). The difference was insignificant and it is shows the model is suitable to simulate the response of the CCPP for use in system dynamic performance and control studies.

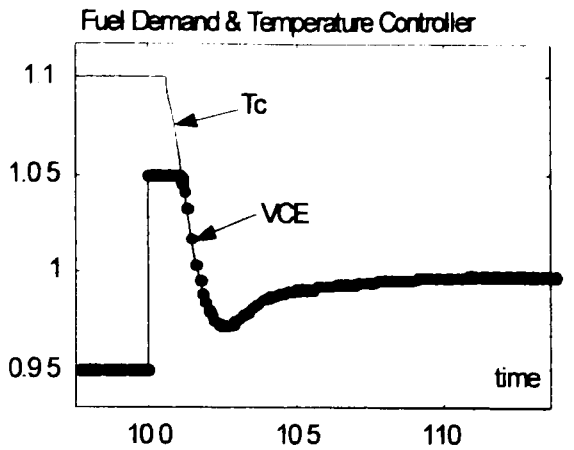

T_c: Temperature Controller output
Fig 2.18a: Fuel Demand and T_c

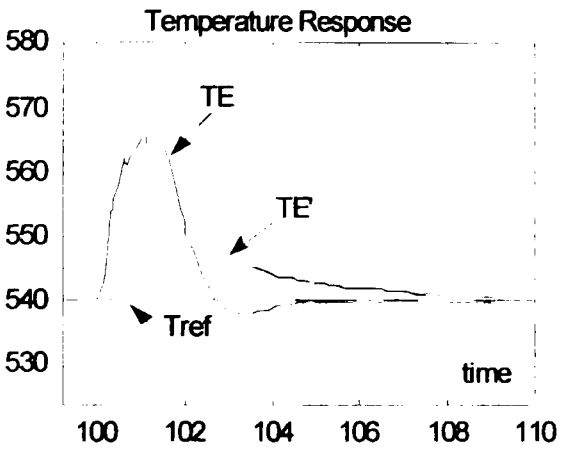

Fig 2.18b:Variation of Temperature

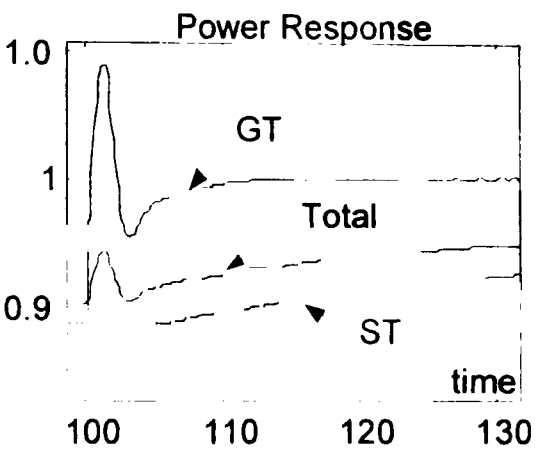

GT: Gas Turbine, ST: Steam Turbine
Fig 2.18c: Power Generation

Fig 2.18: Step response of CC to 10% change in Fuel demand (70% ST and 30% GT).

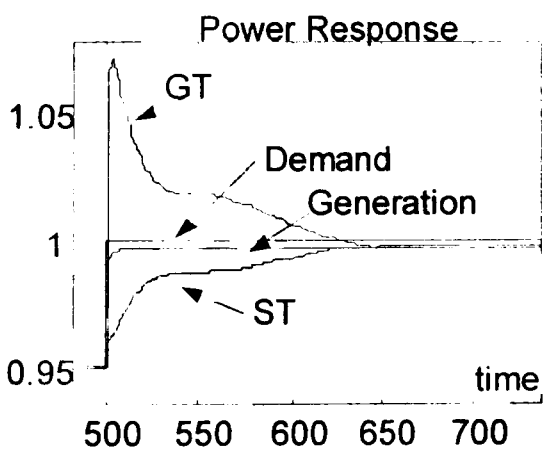

GT: Gas Turbine, ST: Steam Turbine
Fig 2.19a: Power Generation

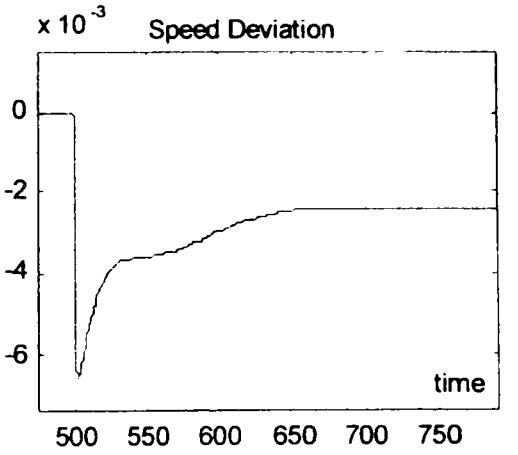

Fig 2.19b: Speed deviation

Fig 2.19: Step response of CC connected to generator to 5% change in power demand (70% steam and 30% gas).

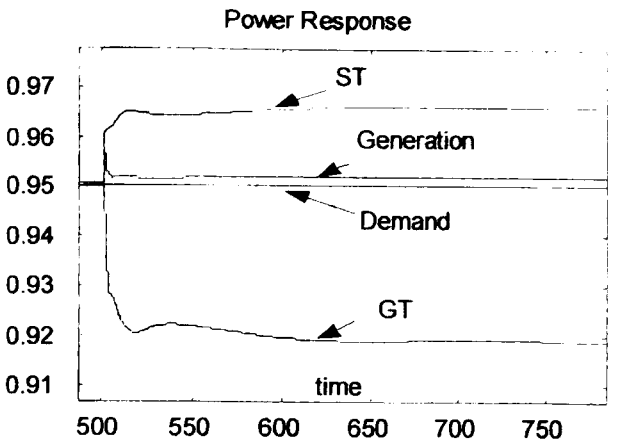

GT: Gas Turbine, ST: Steam Turbine
Fig 2.20a: Power Generation

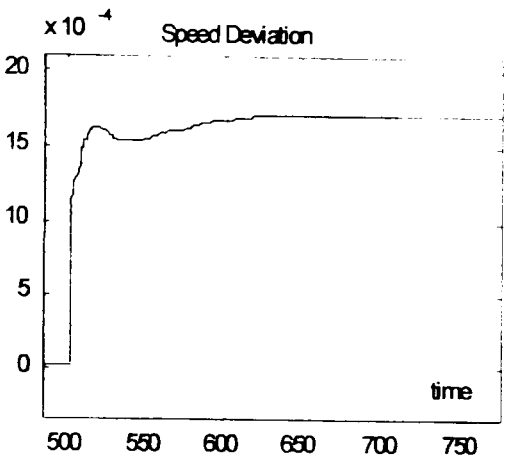

Fig 2.20b: Speed deviation

Fig 2.20: Step response of CC connected to generator to 5% change in steam turbine set point (70% steam and 30% gas).

2.7 Summary

The simulation of the CCPP's was described in this Chapter. In CCPP's, four main sub systems were considered; boiler, gas turbine, steam turbine and generator. For each sub system a suitable model was chosen from published literature. Then, the model of subsystem was implemented in SIMULINK. Each subsystem consists of some blocks (components). Libraries of sub systems' blocks were introduced. These libraries allow the user to create different configuration of the CCPP. Also, power-sharing block was introduced. This block allows the user to have different subsystems with different capacity in CCPP's. The CCPP model and sub systems models were validated by comparisons of predicted performance with published experimental data.

Chapter 3

Multivariable PID Tuning Methods

3.1 Introduction

Many industrial processes are inherently multivariable and need multivariable control methods to enhance their performance. This is a strong motivation to derive a simple and effective method for tuning multivariable PID controllers. PID control is one of most common control schemes for MIMO plants. These controllers are usually tuned using the prior knowledge of dynamics of system. But as the processes are non-linear, with changing the set point the dynamic of system is changing and the controller need to be retuned. Therefore the robustness of MIMO controller is desired to compensate for model uncertainties.

Depending on the application and requirement, either a fully cross-coupled or a multi-loop controller can be adopted for controlling MIMO processes. Multi-loop controllers, sometimes known as decentralised controllers, have a simpler structure and, accordingly, less tuning parameters than the fully cross-coupled ones. In addition, in the event of component failure, it is relatively easy to stabilise the system manually, since only one loop is directly affected by the failure (Halevi *et al.*, 1997; Skogestad and Morari 1989).

Hence for processes with modest interactions, multi-loop controllers are often more favourable than multivariable controllers. Design decisions made when closing the early loops may have undesirable effects on the behaviour of the remaining loops. The interactions are well taken care of only if the loops are of considerably different bandwidths and the closing sequence begins from the fastest loop. These assumptions can rarely be justified (Maciejowski, 1989). Generally, the closing of a new loop will bring about interaction to all the previously closed loops.

This chapter originates from a review of the multivariable PID tuning methods. The chapter begins with a description of two different groups of multivariable PID tuning methods. It continues with introducing new criteria to calculate the robust performance of multivariable processes. The proposed criterion is a modification of the criterion introduced by Gagnon, *et al,* (1999). Then, nominal performance, robust stability and robust performance of eight well known multivariable PID tuning methods are compared and discussed for the boiler model described in chapter 2.

3.2 Multivariable PID Tuning Methods

The tuning methods described in the literature can be classified under two groups, as shown in the Fig. 3.1:

1. Parametric model methods
2. Non-parametric model methods.

For the first group data is available by offline standard or online Identification. These methods require a linear model of the process, transfer function matrix or state space model, over the frequency range of interest. These methods are more suitable for off-line PID tuning.

The second group of methods uses only partial modelling information, usually steady state gains and critical frequency points. These methods are more suitable for online use. These methods can usually be applied without the need for extensive a priori plant information. Each group of method is discussed next.

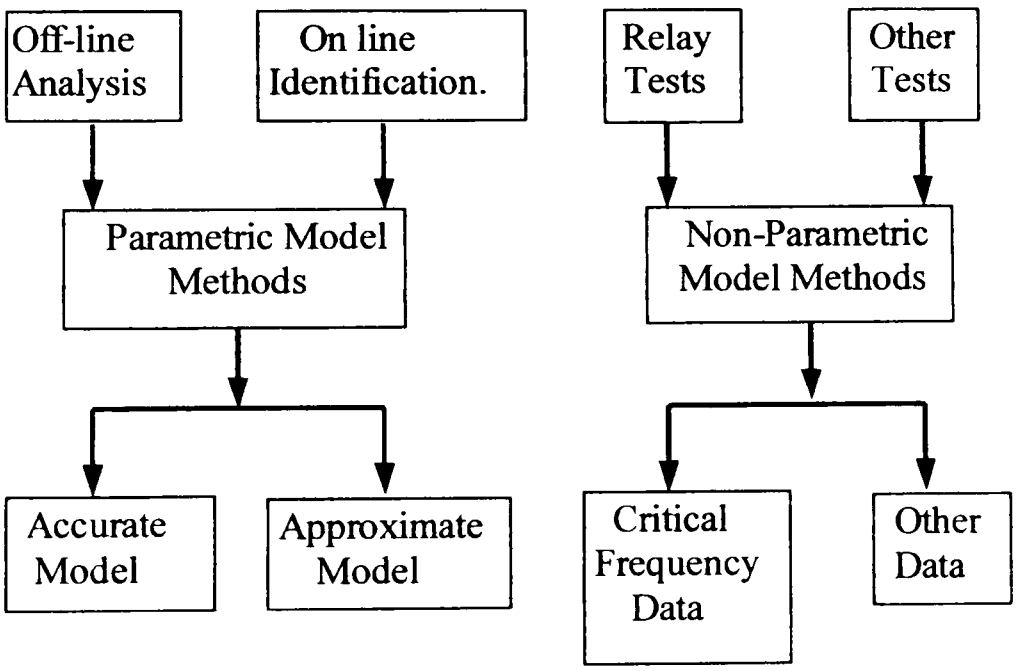

Fig.3.1:PID tuning Methods

3.2.1 Parametric Model Methods

Some important methods in this group are briefly described here.

Gain and Phase Margin Method

An analytical method of tuning multi-loop PID controllers based on gain and phase margins specifications were presented by Ho and Xu (1998). Conventionally in the Direct Nyquist Array (DNA) method (Rosenbrock 1970; 1974; Maciejowski, 1989) controller designs by shaping of the Gershgorin bands are performed off line using a trial and error graphical approach. This is often tedious and time consuming, and also requires much experience. Ho and Vasnani (1992); Ho and Xu (1998) have proposed a method of tuning multi-loop PID controllers based on gain and phase margins specifications. The method can tune the multi-loop controllers online and in real time using the Direct Nyquist Array Method to meet specified system robustness and performance. When interactions are significant, the multi-loop PID controller design method often fails to give acceptable response. Using feed-forward compensators or de-couplers, the interaction can be appropriately compensated so that effective non-interacting single SISO processes are obtained. This method, though tedious and having its limitations, has been successfully applied in many industrial application. The method is explained as follows:

Consider the multivariable process with $G(s)$ transfer function matrix. It is assumed that $G(s)$ is square and open loop stable:

$$G(s) = \begin{bmatrix} g_{11}(s) & \cdots & g_{1L}(s) \\ \vdots & \ddots & \vdots \\ g_{L1}(s) & \cdots & g_{LL}(s) \end{bmatrix} \tag{3.1}$$

where:

$$g_{ij}(s) = \frac{K_{ij}e^{-sL_{ij}}}{(s\tau_{ij}+1)(s\tau'_{ij}+1)} \qquad \tau'_{ij} \le \tau_{ij}$$

L_{ij} is the time delay of process ij $i = 1,\cdots,L$ $j = 1,\cdots,L$

$g_{ij}(s)$ is the commonly used second order plus dead time process.

To control the multivariable process G(s), L multi-loop diagonal PID controllers are used. The loop transfer function matrix is given by:

$$Q(s) = G(s)G_c(s) = \begin{bmatrix} q_{11}(s) & \cdots & q_{1L}(s) \\ \vdots & \ddots & \vdots \\ q_{L1}(s) & \cdots & q_{LL}(s) \end{bmatrix} \tag{3.2}$$

where

$$G_c(s) = diag[g_{c1}(s), g_{c2}(s)\cdots, g_{cL}(s)]$$

$$g_{ci}(s) = K_{ci}(1+\frac{1}{sT_{Ii}})(1+sT_{Di}) \quad i = 1,2,\cdots,L$$

In the proposed design method, A'_{mi} and φ'_{mi}, gain margin and phase margin of *i th* loop, are specified. The Design steps are as follows:

Algorithm1: PID controller for phase and gain margin method.

Step 1: Initialisation

1. Find a system model G(s)
2. Specify A'_{mi} and φ'_{mi} $1 \le i \le L$.

Step 2: Gain and phase margin calculation with interaction between loops

1. Calculation of gain margin

   a Using equation (3.1) calculate: $\omega_{pi} = \frac{\pi}{2L_{ii}}$ (3.3)

   b Using equation (3.1) calculate $A_{mi} = A'_{mi}(1+\frac{\sum_{j,j\neq i}|g_{ji}(i\omega_{pi})|}{2|g_{ii}(i\omega_{pi})|})$ (3.4)

2. Calculation of phase margin

a From equation (3.2) and (3-3) calculate: $\omega_{gi} = \dfrac{\omega_{pi}}{A_{mi}}$ (3.5)

b Using ω_{gi} and ϕ'_{mi} calculate: $\phi_{mi} = \phi'_{mi} + 2\arcsin\left(\dfrac{\sum_{j,j\neq i}\left|g_{ji}(i\omega_{gi})\right|}{2\left|g_{ii}(i\omega_{gi})\right|}\right)$ (3.6)

Step 3: PID gains calculation:

Using A_{mi} and ϕ_{mi}, equations (3.1) and (3.2) calculate the following gains:

$$\omega_{pi} = \frac{A_{mi}(\varphi_{mi} - \frac{\pi}{2}) + \frac{\pi}{2}A_{mi}^2}{(A_{mi}^2 - 1)L_{ii}} \qquad K_{ci} = \frac{\omega_{pi}\tau_{ii}}{A_{mi}K_{ii}}$$

$$T_{Ii} = (2\omega_{pi} - \frac{4\omega_{pi}^{\ 2}L_{ii}}{\pi} + \frac{1}{\tau_{ii}})^{-1} \qquad T_{Di} = \tau'_{ii} \tag{3.7}$$

Step 4: Repeat step 2 and 3 for $1 \le i \le L$ where L is number of inputs or outputs.

When large A'_{mi} and ϕ'_{mi} are used, the Gershgorin bands are shaped further from the point (-1+0i). The closed loop system is more robust but the response can be sluggish. The A'_{mi} and ϕ'_{mi} could be chosen as:

$2 \le A'_{mi} \le 5$ and $20^\circ \le \phi'_{mi} \le 60^\circ$ (3.8)

BLT Method

Luyben (1986; 1990) proposed the Biggest Log Modulus (BLT) tuning method. It is an iterative method to tune a set of multi-loop PI/PID controllers. The BLT method is a widely used method as it provides a standard tuning methodology for a multi loop controller. The BLT method is an off-line method that requires good knowledge of the process dynamics. Assume that the G(s) is the process transfer function. The steps of tuning method are:

Algorithm 2: BLT PID tuning method.

Step 1: Find the PID gains for the elements on diagonal of transfer function G(s).

a Calculate the ultimate gain and ultimate period of the elements on diagonal (K_{ci} *and* T_{ci}).

b Obtain the Ziegler-Nichols setting for each individual loop.

Step 2: Detune the controller

a Choose detune factor (F) $1.4 \le F \le 4$

b Change ultimate gains and ultimate period of each loop as follow:

$$K_{cid} = K_{ci} / F \qquad T_{id} = T_i F \tag{3.9}$$

Step 3: Calculate the biggest log modulus $L_{cm}^{\max}$;

a After controller setting as $G_C(s)$, calculate the multivariable Nyquist plot of the scalar function $W = -1 + \left| I + G(j\omega)G_C(j\omega) \right|$ (3.10)

b calculate a multivariable closed loop log modulus

$$L_{cm} = 20 \log_{10} \left| W / (W+1) \right| \tag{3.11}$$

c Define peak in the plot of L_{cm} over the entire frequency range as the biggest log modulus $L_{cm}^{\max}$

Step 4: PID gains calculation:

Change F factor until $L_{cm}^{\max}$ become equal to 2N, where N is the order of the system.

In this method, the larger the value of F, the more stable the system will be at the expense of a more sluggish set point and load response. This empirically determined criterion has been tested on a large number of systems and it gives reasonable performance, although slightly on the conservative side.

Chapter 3

Internal Model Control

Garcia and Morari (1982) introduced Internal Model Control (IMC). The general design methodology of IMC with PID structure was given by Rivera *et al*, 1986. They introduced the concept of obtaining PID controller parameters by approximating the simple feedback form of an IMC controller. As a straightforward approach, the control design is based on a process model and a low pass filter included for robustness. Lieslehto (1991), Dong and Brosilow (1997) have developed a multivariable tuning method based on IMC technique.

In the Lieslehto (1991) method, a SISO PID controller is designed for each element of transfer function G(s). Then a tuning matrix for the MIMO system is computed. The method can be summarised as follows:

Algorithm 3: IMC method for PID design

Step 1: Find the PID gains for the each elements of transfer function G(s).

a Consider $g_{ij}(s) = K_{ij}e^{-\theta s} / (T_{ij}s+1)$ and divide it to:

$$g_{ij}^{+}(s) = e^{-\theta s} \qquad g_{ij}^{-}(s) = K_{ij} / (T_{ij}s+1) \tag{3.12}$$

b Consider $g_{ij}^{imc}(s)$ as follow:

$$g_{ij}^{imc}(s) = (g_{ij}^{-}(s))^{-1} \times f(s) = (T_{ij}s+1) / (K_{ij}(\lambda_{ij}s+1)) \tag{3.13}$$

c Define the IMC controller transfer function as follow:

$$g_{cij}(s) = g_{ij}^{imc}(s) / (1 - g_{ij}^{imc}(s)g_{ij}^{+}(s)) \tag{3.14}$$

d Compare the IMC controller with the following PID and calculate the PID gains.

$$K_{ij}^{pid}(s) = k_{pij}(1 + 1/T_{Iij}s + T_{dij}s/(1+0.1T_{dij}s))$$
$$k_{Iij} = k_{pij} / T_{Iij} \qquad k_{dij} = k_{pij}T_{dij} \tag{3.15}$$

Step 2: Repeat Step one for all the elements of transfer function

$$1 \le i \le L \qquad 1 \le j \le L$$

Step 3: Tuning matrix for the MIMO system is computed as follows:

$$K_P = \begin{bmatrix} 1/k_{p11} & . & . & 1/k_{p1L} \\ . & . & . & . \\ . & . & . & . \\ 1/k_{pL1} & . & . & 1/k_{pLL} \end{bmatrix}^{-1} \qquad K_I = \begin{bmatrix} 1/k_{I11} & . & . & 1/k_{I1L} \\ . & . & . & . \\ . & . & . & . \\ 1/k_{IL1} & . & . & 1/k_{ILL} \end{bmatrix}^{-1} \tag{3.16}$$

The IMC controller includes implicit integral action and has a PID structure in cascade with a low pass filter $f(s)$. Morari and Zafiriou (1989) used the first order Pade approximation for the time delay in process model. By using a non-symmetric second order approximation, the simple second order form of the controller for the model can be presented. In addition significant improvements in model matching and controller tuning can be obtained for those processes that have significant dead time.

Dong and Brosilow (1997) generalised IMC approach by expanding the transfer function of the feedback form of the IMC controller in a Maclaurin series about zero, and dropping all terms higher than second order in the Laplace variable. For multivariable systems, the IMC structure Fig.3.2 reduces to the classical feedback structure Fig.3.3 with the controller C(s) as:

$$C(s) = Q(s)[I - M(s)Q(s)]]^{-1} \tag{3.17}$$

where

$$Q(s) = M_-^{-1}(s)F(s) \qquad M(s) = M_+(s)M_-(s)$$

$$M_+(s) = M(s)M_-^{-1}(s)\,;\; M_+(0) = I$$

$$F(s) = Diag\{1/(\varepsilon_i s + 1)^r\} \qquad F(0) = I$$

$M_-(s)$: the portion of the process model that we wish to invert

F(s) is a diagonal matrix of filters

Q(s) is the IMC controller,

M(s) is the process model

$C(s)$ can de rewritten as:

$$C(s) = s^{-1} f(s) \qquad \text{where} \qquad f(s) = sM_{-}^{-1}(s)F(s)\left[I - M_{+}(s)F(s)\right]^{-1}$$

$f(s)$ which does not have any pole at the origin can be expanded in a Maclaurin series expansion as shown below:

$$C(s) = s^{-1} f(s) = s^{-1}[f(0) + sf'(0) + s^2 f''(0)/2 + \ldots] = K + K_I s^{-1} + K_D s + \ldots \qquad (3.18)$$

where:

$$K = f'(0) \quad K_I = f(0) \quad K_D = f''(0)/2$$

Optimal Control Based Methods

Many different general approaches express the design objectives for a multi-loop PID controller design. The aim of most published articles in the control literature was focused on minimizing a single-objective function toward determining PID controller settings. Several different objective functions can be simultaneously considered in this study. A multi objective optimisation method is hence introduced to tune PID control system. Some possible design specifications are; nominal performance, minimum input energy, operational constrains, robust stability.

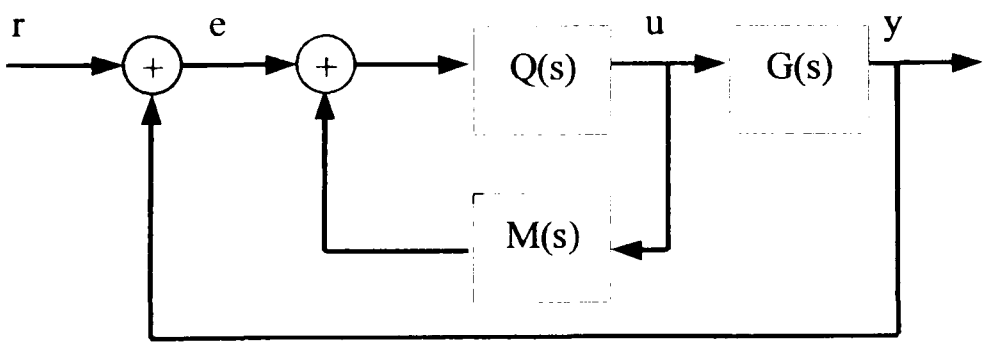

Fig.3.2: The Structure of IMC Controller

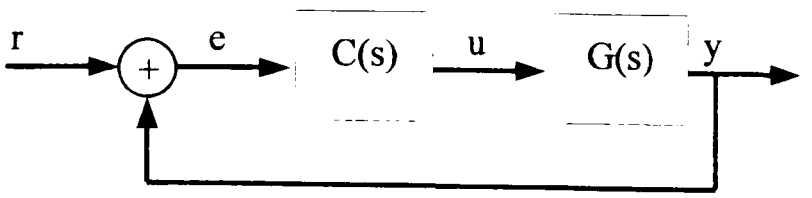

Fig.3.3: Classical Feedback Controller

Grimble (1991) employed H_∞ technique to drive the PID parameters. Yusof *et al.* (1994) presented a multivariable self-tuning PID. The objective of the controller was to minimize the variance of output.

Pegel and Engell (2001) presented a method to compute multivariable PID controllers based on the idea of the approximation of the optimal attainable closed loop performance computed by convex optimisation. The approximated controller can be compared directly to the attainable performance and therefore evaluated by an objective criterion. The efficiency of the method was demonstrated for the example of a fluidised catalytic cracker.

Wang and Wu (1995) have proposed a multi-objective optimisation method to calculate the parameters of the PID controller. A cost criterion for nominal plant performance is defined and minimised subject to input constraints. The one-parameter tuning PID controller was introduced in their work so that the number of the tuning parameters of the multi-loop controllers was reduced. The aim of method was to propose a trade-off design technique toward tuning multi-loop PID controllers that are capable of providing satisfactory control specifications. The set point and load disturbance could be changed simultaneously in the procedures for finding satisfactory parameters of PID controllers. Stability robustness as well as performance is also considered in the approach. In their study, the first order system model with time delay is considered and the optimal PID is expressed in the forms:

$$C(s) = K_{Cjj}\left(1 + \frac{1}{\tau_{Ijj}} + \tau_{Djj}s\right)\frac{1}{\tau_{Fjj}s + 1} \tag{3.19}$$

where the tuning modes of the optimal PID are denoted as:

$$K_{jj}K_{Cjj} = \frac{(1+\beta_j K_{jj})(\tau_{jj}+0.5d_{jj})}{\tau_{jj}+d_{jj}} \tag{3.20}$$

$$\tau_{Ijj} = \tau_{jj} + 0.5d_{jj}$$

$$\tau_{Djj} = \frac{0.5d_{jj}\tau_{jj}}{\tau_{jj}+0.5d_{jj}}$$

$$\tau_{Fjj} = \frac{0.5d_{jj}\tau_{jj}}{\tau_{jj}+d_{jj}}$$

K_{jj}, τ_{jj} and d_{jj} are the process gain, time constant and time delay of the principal diagonal of the transfer function matrix. Only the controllers K_{Cjj} are observed to be in terms of the tuneable parameters β_j which determine the desired performances, while the integral and derivative time constants, τ_{Ijj} and τ_{Djj}, of the controller and the time constant, τ_{Fjj}, of low pass filter are governed by the time constant and time delay of the principal diagonal of the transfer function matrix. The multi-objective PID control-tuning problem is therefore written in the following form:

$$\begin{cases} \min\limits_{x} f_1(x) \\ \min\limits_{x} f_2(x) \\ \quad \vdots \\ \min\limits_{x} f_n(x) \end{cases} \tag{3.21}$$

$$\textit{subject to:} \quad \begin{cases} g_j(x) \le 0 & j = n+1,\cdots,q \\ h_j(x) = 0 & j = q+1,\cdots,r \end{cases}$$

where $f_j(x)$ are the design specifications, $h_j(x)$ are equality constraints of the control system and $g_j(x)$ are inequality constraints of the problem. The tuning parameters of the multi-loop PID controllers were expressed by the vector $x = [\beta_1 \cdots \beta_m]^T$.

3.2.2. Non-Parametric Model Methods

The second group of tuning methods are based on the assumption that no dynamic model for the plant is available, only some particular points of process, such as critical points or steady-state gains are assumed to be known. The following assumptions are usually made (Davison, 1976):

1. The plant is linear and time invariant.
2. The uncontrolled plant is stable.
3. The controlled variables are measurable.
4. The class of input disturbance and reference inputs are known.

The main methods are discussed in the following sections.

Davison Method

Davison (1976) defined a robust multivariable PID controller as the one which stabilises the plant under first order perturbation in the plant state space matrices and asymptotically regulates the system to the desired set points.

The controller can be designed for different known input disturbances and reference signals. The control design aims at de-coupling the plant at low frequencies. Davison proposed the following tuning matrices for a multivariable controller:

$$K_p = \delta G^{-1}(0); K_I = \varepsilon G^{-1}(0) \tag{3.22}$$

where:

K_p K_I the proportional and integral gain matrices respectively

G the open-loop square matrix transfer function

δ and ε the fine tuning parameters

The values of δ and ε must be greater than zero for the closed-loop system to be stable. The tuning parameters for each loop is usually assumed are equal.

Penttinen-Koivo Method

The Pentittinen-Koivo (1980) method modified Davison method to achieve de-coupling also at high frequencies. Assuming the state space form of system is:

$$\begin{cases} \dot{x} = Ax + Bu \\ y = Cx \end{cases} \tag{3.23}$$

And then transfer function regarding to state space is:

$$G(s) = y(s) / u(s) = C(sI - A)^{-1} B \tag{3.24}$$

Transfer function matrix has the Laurent series expansion as below:

$$G(s) = \frac{CB}{s} + \frac{CAB}{s^2} + \frac{CA^2 B}{s^3} + \ldots \tag{3.25}$$

This means that at high frequencies, the system can be approximated by:

$$G(s) \Rightarrow \frac{CB}{s} \tag{3.26}$$

The tuning matrix for proportional part of the controller is selected to compensate this part and the integral part of the controller is selected as in the Davison method.

$$K_p = \delta(CB)^{-1} \tag{3.27}$$
$$K_I = \varepsilon(-CA^{-1}B)^{-1}$$

The fine-tuning parameters δ and ε are selected as in the Davison method.

The Maciejowski Tuning Method

The Davison method decouples the system at low frequencies and the Penttinen-Koivo method decouples the plant at high frequencies. Maciejowski suggested decoupling the system around the bandwidth, ω_b, of the system. This gives the following tuning matrices for the proportional and integral gains:

$$K_p = \delta\, G^{-1}(0) \qquad K_I = \varepsilon\, G^{-1}(j\omega_b) \tag{3.28}$$

K_p and K_I must be real, therefore a real approximation is performed using the ALIGN algorithm of Edmunds and Kouvaritakis (1979).

Modified Ziegler-Nichols (MZN) Method for SISO

This method may be classified under the more general frequency response-shaping framework, which is briefly described as follows. Given a point on the Nyquist curve of the process $G_p(s)$:

$$A = G_p(j\omega) = r_a e^{j(-\pi+\varphi_a)} \tag{3.29}$$

A controller $G_c(s)$ is to be computed to compensate for $G_p(s)$ such that this point is moved to B:

$$B = G_p(j\omega)G_c(j\omega) = r_b e^{j(-\pi+\varphi_b)} \tag{3.30}$$

When the controller is chosen as PID then:

$$
\begin{aligned}
K_C &= r_b \cos(\varphi_b - \varphi_a) / r_a \\
\omega T_d - 1/(\omega T_i) &= \tan(\varphi_b - \varphi_a) \\
T_d &= \alpha T_i
\end{aligned}
\tag{3.31}
$$

where α is recommended (Hagglund and Astrom, 1991) to be equal to 0.25. The parameter of PID are uniquely given by:

$$T_i = \beta / \omega \tag{3.32}$$

where

$$
\beta = \begin{cases} \dfrac{\tan(\varphi_b - \varphi_a) + \sqrt{4\alpha + \tan^2(\varphi_b - \varphi_a)}}{2\alpha} & \alpha > 0 \\ -\dfrac{1}{\tan(\varphi_b - \varphi_a)} & \alpha = 0 \end{cases}
\tag{3.33}
$$

$\alpha = 0$ is used for PI controller.

It should be noted that the performance achieved from these tuning methods might vary significantly, because the critical point is moved. Besides, some of these tuning methods may not produce satisfactory closed loop responses in certain circumstances. It is thus important to know where the critical point should be moved to for acceptable performance with some prior knowledge of the process.

Modified Ziegler-Nichols Method for MIMO

Consider a stable 2I2O process (Fig 3.4):

$$Y(s) = G_p(s)U(s) \tag{3.34}$$

where:

$$G_p(s)=\begin{bmatrix} g_{11}(s) & g_{12}(s) \\ g_{21}(s) & g_{22}(s) \end{bmatrix}$$

Assume that proper input-output pairing has been made to the process. If the process is inherently poorly paired, the RGA (Relative Gain Array) method (Maciejowski 1989) may be employed to make possible the necessary arrangement. The controller is:

$$G_C(s)=\begin{bmatrix} k_1(s) & 0 \\ 0 & k_2(s) \end{bmatrix} \tag{3.35}$$

In this case, In order to achieve good loop performance, $k_1(s)$ and $k_2(s)$ should be designed for $g_1(s)$ and $g_2(s)$ instead of process diagonal elements $g_{11}(s)$ and $g_{22}(s)$ which is the case in many other methods (Luyben 1986).

where:

$$g_1 = g_{11} - \frac{g_{12}g_{21}}{k_2^{-1}+g_{22}} \qquad g_2 = g_{22} - \frac{g_{21}g_{12}}{k_1^{-1}+g_{11}}$$

In the sequential loop closing method (Maciejowski 1989) $k_1(s)$ is first designed for $g_1(s)$ and then $k_2(s)$ is designed for the equivalent transfer function $g_2(s)$. In what follows, the MZN is applied to the equivalent transfer function $g_1(s)$ and $g_2(s)$. Let:

$$A_i = g_i(j\omega_i) = r_{ai}e^{j(-\pi+\varphi_{ai})} \qquad i=1,2 \tag{3.36}$$

$$B_i = g_i(j\omega_i)k_i(j\omega_i) = r_{bi}e^{j(-\pi+\varphi_{bi})} \quad i=1,2 \tag{3.37}$$

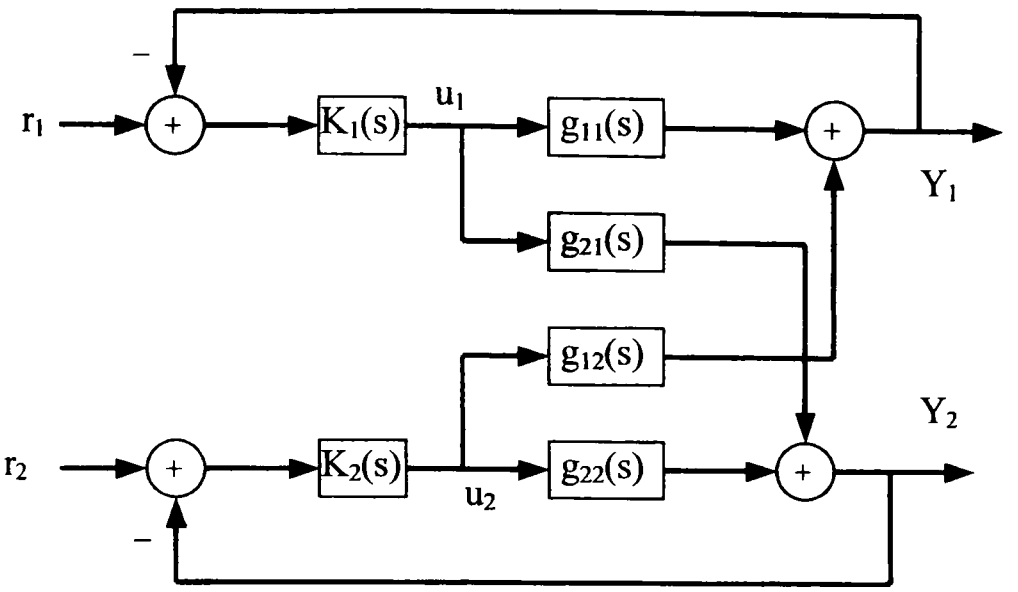

Fig 3.4: The TITO system with multi-loop controller

It should be pointed out that due to the dependence of g_1 (or g_2) on k_2 (or k_1), ω_1 and thus k_1 (or ω_2 and k_2) can not be determined until k_2 (or k_1) has been fixed. This results in a cause-effect loop and causes a major design difficulty. When the controller is chosen as PID and MZN method is applied to each $k_i(s)$, then:

$$k_i(s) = K_{Ci}(1 + \frac{1}{T_{Ii}s} + T_{Di}s) \qquad i = 1,2 \tag{3.38}$$

where:

$$K_{Ci} = r_{bi}\cos(\varphi_{bi} - \varphi_{ai}) / r_{ai}$$

$$\omega_i T_{di} - 1/(\omega_i T_{Ii}) = \tan(\varphi_{bi} - \varphi_{ai}) \qquad i = 1,2$$

$$T_{Di} = \alpha_i T_{Ii}$$

$$T_{Ii} = \beta_i / \omega_i$$

$$\beta_i = \begin{cases} \dfrac{\tan(\varphi_{bi} - \varphi_{ai}) + \sqrt{4\alpha_i + \tan^2(\varphi_{bi} - \varphi_{ai})}}{2\alpha_i} & \alpha_i > 0 \\ -\dfrac{1}{\tan(\varphi_{bi} - \varphi_{ai})} & \alpha_i = 0 \end{cases}$$

$\alpha_i > 0$ for full PID control, and $\alpha_i = 0$ for PI control. However, in equation (3.38) K_{CI} can not be calculated directly because is related to r_{aI} which depend on the unknown K_{C2}. To overcome to this problem, in equation (3.36) r_{ai} is substituted from equation (3.38) and after some straightforward algebra:

$$\frac{g_{11}(j\omega_1)}{[1+j(\alpha_2\frac{\beta_2\omega_1}{\omega_2}-\frac{\omega_2}{\beta_2\omega_1})]}K_{C1}+\cos(\varphi_{b1}-\varphi_{a1})r_{b1}e^{j(-\pi+\varphi_{a1})}g_{22}(j\omega_1)K_{C2}$$
$$+\Delta_1 K_{C1}K_{C2}=\frac{\cos(\varphi_{b1}-\varphi_{a1})r_{b1}e^{j(-\pi+\varphi_{a1})}}{[1+j(\alpha_2\frac{\beta_2\omega_1}{\omega_2}-\frac{\omega_2}{\beta_2\omega_1})]} \quad (3.39)$$

$$\frac{g_{22}(j\omega_2)}{[1+j(\alpha_1\frac{\beta_1\omega_2}{\omega_1}-\frac{\omega_1}{\beta_1\omega_2})]}K_{C2}+\cos(\varphi_{b2}-\varphi_{a2})r_{b2}e^{j(-\pi+\varphi_{a2})}g_{11}(j\omega_{12})K_{C2}$$
$$+\Delta_2 K_{C2}K_{C1}=\frac{\cos(\varphi_{b2}-\varphi_{a2})r_{b2}e^{j(-\pi+\varphi_{a2})}}{[1+j(\alpha_1\frac{\beta_1\omega_2}{\omega_1}-\frac{\omega_1}{\beta_1\omega_2})]} \quad (3.40)$$

where

$$\Delta_1 = g_{11}(j\omega_1)g_{22}(j\omega_1)-g_{12}(j\omega_1)g_{21}(j\omega_1)$$
$$\Delta_2 = g_{11}(j\omega_2)g_{22}(j\omega_2)-g_{12}(j\omega_2)g_{21}(j\omega_2)$$

Equations (3.39) and (3.40) are complex equations and these can be broken down to four real equations, and four unknown K_{C1}, K_{C2}, ω_1 and ω_2 will be specified. The main difficulty lies in the non-linearities of the equations that are further complicated by the coupling among them.

Generalised Ziegler-Nichols Method:

Niederlinski, (1971) proposed an extension of SISO Ziegler-Nichols method to MIMO system. A critical point is selected by closing the loops with P-controller and bringing the system under stable oscillation. The method is however difficult to use for auto tuning. Zhuang and Atherton (1994) have used this method for auto-tuning PID controllers.

The ZN method for obtaining the ultimate gain and frequency is also discussed and the disadvantage, however that is not mentioned is that there is no control of the resulting oscillation. Even in ideal world simulation it is almost impossible to adjust the gain so that it reaches exactly the correct value to maintain the loop oscillation. In practice, of course, the plant will have non-linear effect and these hopefully, if the gain is set too high, will limit the amplitude of any oscillations but also in practice dead zone may exist which then cause the person carrying out the tuning to increase the gain too rapidly.

Relay Feedback Tuning Methods

The next group of tuning methods are using relay feedback method to identify the model of system. The advantage for the relay feedback auto tuning approach proposed by Astrom and Hagglund (1984; 1988) is that setting of the relay levels allows the amplitude of the oscillation to be controlled and with the large gain the limit cycle builds up quickly (Wang *et al.*, 1997). When the relay technique is extended to a MIMO system there are three possible relay feedback schemes, which are explained in following section.

Independent Single Relay Feedback (IRF)

Only one loop at a time is closed subject to relay feedback, while all others are kept open. The IRF does not excite multivariable interaction directly. and it is difficult to tune a fully cross-coupled multivariable PID tuning with IRF.

Sequential Relay Feedback (SRF)

The main idea of sequential relay tuning is to tune the multivariable system loop-by-loop, closing each Loop once it is tuned, until all the loops are tuned. To tune each loop, a relay feedback configuration is set up to determine the ultimate gain and frequency of the corresponding loop. The PI/PID setting are then computed on the basis of this information.

Loh, *et al.*, (1993) have presented an auto-tuning method for multi-loop PID controllers using a combination of relay auto-tuning and sequential loop closing. The method has several advantages:

1. Overall closed loop stability is guaranteed
2. Very little knowledge of the process is required
3. It is an auto-tuning procedure

The process of calculating the ultimate gain and frequency is based on the relay feedback method of scalar case. It is recommended (Loh *et al.*, 1993) that the sequential tuning should be started with the faster loops. This improves the set point tracking of the controller. Set point weighting is also recommended to reduce overshoots and interactions without changing settling time. The closed loop transfer function relating the set points, R(s), and the plant outputs, Y(s), is:

$$G_c(s) = (I + G(s)K(s))^{-1} G(s)K_p(\beta + K_I(s)) \tag{3.41}$$

where:

$$K(s) = K_p(I + K_I(s))$$

$$K_p = diag(k_{p1}, k_{p2}, \ldots, k_{pL})$$

$$K_I(s) = diag(\frac{1}{T_{i1}s}, \frac{1}{T_{i2}s}, \ldots, \frac{1}{T_{iL}s})$$

$$\beta = diag(\beta_1, \beta_2, \ldots, \beta_L)$$

Decentralized Relay Feedback (DRF)

Decentralized relay feedback (DRF) is a complete closed loop test while independent single relay feedback (IRF) and sequential relay feedback (SRF) are only partial closed loop tests. Closed loop testing is preferred to open loop one (Astrom *et al.* 1988; 1995) since a closed loop test keeps outputs close to the set-points so that it causes less perturbation to the process and makes a linear model valid. In addition, DRF can be employed to effectively excite and identify multivariable process interaction, while IRF and SRF may not excite multivariable interaction directly. In DRF, It is shown that for a stable MIMO process the oscillation frequencies will remain almost unchanged under relatively large relay amplitude variations. The oscillations with a common frequency are the mode, which is most likely to occur (Atherton, 1975) when the process has significant interaction (Halevi *et al.*, 1997).

Palmor *et al.*, (1995a) have proposed an algorithm for automatic tuning of decentralized control for two-input and two-output (2I2O) plants. The main objective of the auto-tuner is to identify the desired critical point (DCP). This method will be discussed in details in next chapter.

A fundamental problem associated with relays in feedback control systems is the determination of limit-cycle frequencies and stability. Relays in these applications are used mainly for identification of points on the process Nyquist curve, from which essential information for tuning industrial process controllers, such as the PID controller and the smith dead-time compensator, is extracted. Atherton (1975), Wadey and Atherton (1984) developed an exact method for evaluating limit-cycle periods in multivariable systems with decentralised relays. This method involves infinite series, though special summation tables were presented for common cases. An exact method for determining limit cycles in decentralized relay systems has been reported by Palmor *et al.*, (1995b).

All the existing works using DRF (Plamor *et al.*, 1995a; Zhuang and Atherton 1994) can be used to tune only a multi loop PID controller, and thus they are suitable for

processes with modest interactions. A method for auto-tuning fully cross-coupled multivariable PID controllers is proposed for processes with significant interactions by Wang *et al.*, (1997). The method has the following advantages:

1 Closed loop tuning
2 Low order transfer function model of a multivariable process are used.
3 Designed controllers achieve approximate de-coupling near the critical and zero performance.

The PID steps design is:

Algorithm 4: Multivariable PID controllers from decentralized relay method (Wang *et al.*, 1997)

Step 1: Identify the gains of system in critical points $G(j\omega_c)$ and steady state $G(0)$.

Step 2: Approximate the process model using two gains from step 1 by first order plus delay. (Ho *et al.*,1995)

Consider $g_{ii}(s) = K_{ii}e^{-L_{ii}s}/(T_{ii}s+1)$ is *i th* diagonal element of process where Its parameters are given by:

$$K_{ii} = g_{ii}(0)$$

$$T_{ii} = \frac{1}{\omega_c}\left(\frac{K_{ii}^2}{|g_{ii}(j\omega_c)|^2} - 1\right)^{-1/2}$$

$$L_{ii} = \frac{1}{\omega_c}\{-\arg[g_{ii}(j\omega_c)] - \tan^{-1}(\omega_c T_{ii})\}$$

Step 3: Calculation of diagonal elements of the PID controller matrix

a Consider $g_{ii}(s) = K_{ii}e^{-L_{ii}s}/(T_{ii}s+1)$, *i th* diagonal element of process from step 2.

b Assume the *i th* diagonal element of controller as below:

$$k_{ii}(s) = k_{pii}(1 + 1/T_{Iii}s) \tag{3.42}$$

Its parameters are given by:

$$k_{pii} = \frac{\omega_{pii}\tau_{ii}}{A_m k_{ii}}$$

$$T_{Iii} = (2\omega_{pii} - \frac{4\omega^2_{pii}L_{ii}}{\pi} + \frac{1}{\tau_{ii}})^{-1}$$

$$\omega_{pii} = \frac{A_m\phi_m + 0.5\pi A_m(A_m - 1)}{(A_m{}^2 - 1)L_{ii}}$$

A_m and ϕ_m are the specified gain and phase margins

c Repeat step 2 for $1 \le i \le L$

Step 4: Calculation of off diagonal elements of the controller

a Assume the *ij th* off diagonal element of controller as below:

$$k_{ij}(s) = k_{pij}(1 + \frac{1}{T_{Iij}s} + T_{Dij}s) \tag{3.43}$$

Parameters of $k_{ij}(s)$ are given by:

$$k_{pij} = \gamma_{ij}\cos\varphi_{ij}$$

$$T_{Iij} = \frac{k_{pij}L_{ij}}{k_{pjj}f_{ij}(0)}$$

$$T_{Dij} = \frac{1}{\omega_c}(\tan\varphi_{ij} - \frac{1}{\omega_c T_{Iij}})$$

b Repeat step 4 for $1 \le i \le L$ and $1 \le j \le L$ where $i \ne j$

3.3 Robustness Test

The main purpose of using feedback is to reduce the effects of uncertainty. Some uncertainty is always present, both in the environment of the system (such as disturbance and noise signals) and in the behaviour of the system itself (the model of system is not perfect).

It is needed to some extent to separate out the assessment of how well a feedback system deals with unwanted or unexpected signals- its performance- from the assessment of how resilient it is in the face of internal changes in behaviour-its robustness. It has been shown that the same tools are used to evaluate these two aspects of a feedback system's behaviour (Maciejowski, 1989).

In this section, criteria to assess the nominal performance, robust stability and robust performance of the closed loop system are reviewed. Also, a new criterion to achieve robust performance for closed loop system is introduced.

Assuming a nominal model of system and controller denoted by G(s) and K(s), respectively and assume the closed loop system is internally stable. The closed loop system may be built by Fig.3.5.

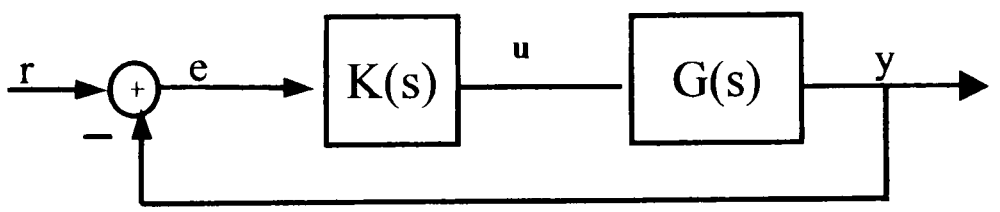

Fig 3.5: The closed loop block diagram of system and controller

Also, for input multiplicative uncertainty defined in Fig.3.6, the standard closed loop system is defined as:

$$y(s) = M(s)u(s) \tag{3.44}$$

where:

$$M(s) = \begin{bmatrix} -W_1(s)T(s) & W_1(s)T(s)G^{-1}(s) \\ -W_2(s)S(s)G(s) & W_2(s)S(s) \end{bmatrix} \qquad \begin{aligned} y(s) &= \begin{bmatrix} y_1(s) & e(s)^T \end{bmatrix}^T \\ u(s) &= \begin{bmatrix} u_1(s) & r(s)^T \end{bmatrix}^T \end{aligned}$$

$T(s) = G(s)K(s)[I + G(s)K(s)]^{-1}$	The complementary sensitivity function
$S(s) = [I + G(s)K(s)]^{-1}$	The sensitivity function.
$G_c(s) = [I + W_1(s)\Delta G(s)]G(s)$	The plant model with uncertainty.
$G_c(s) \in \hat{G}(s)$	$\hat{G}(s)$ is all possible plant models.
$W_1(s)$	Multiplicative uncertainty weighting function
$W_2(s)$	Performance weighting function

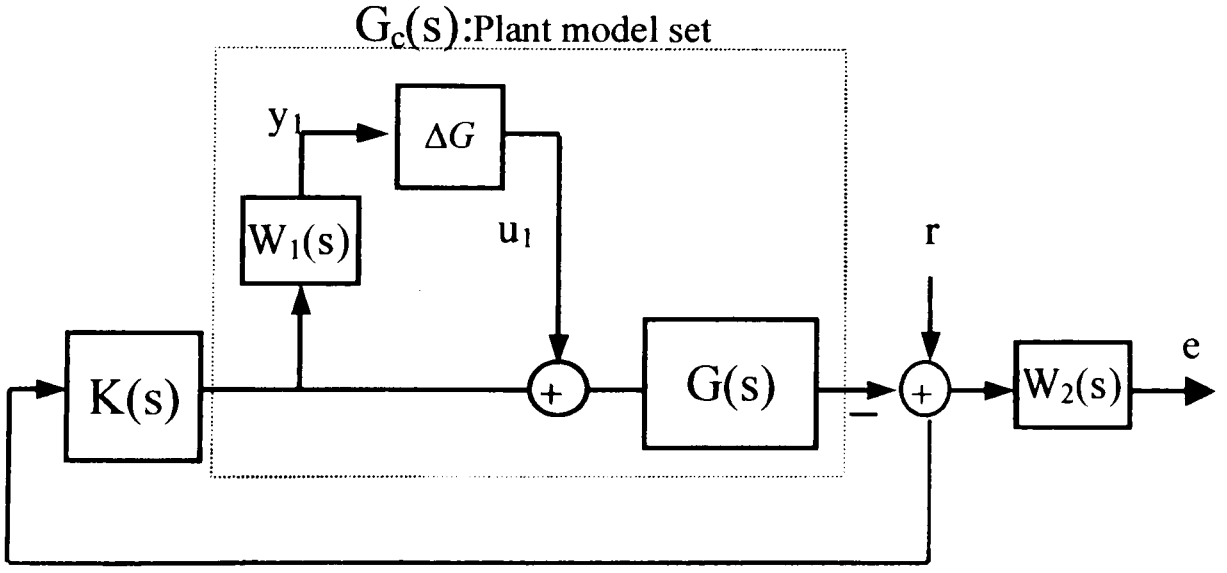

Fig 3.6: The Input Multiplicative Uncertainty

Other type of perturbation may also be considered but for comparison purposes the analysis is restricted to input multiplicative uncertainty. To achieve better performance, the weighted sensitivity function should be minimised.

$$\min \left\| W_2(j\omega) S(j\omega) \right\|_\infty \qquad \forall \omega \tag{3.45}$$

To achieve better robustness, the weighted complementary sensitivity function should be minimised (Maciejowski, 1989).

$$\min \left\| W_1(j\omega) T(j\omega) \right\|_\infty \qquad \forall \omega \tag{3.46}$$

The smallest and largest principal gains of multivariable sensitivity and complementary sensitivity have been shown in Fig 3.7. To minimise $\left\| W_2(j\omega) S(j\omega) \right\|_\infty$ and $\left\| W_1(j\omega) T(j\omega) \right\|_\infty$ at all frequencies, $W_2(s)$ and $W_1(s)$ should be chosen as inverse of $S(j\omega)$ and $T(j\omega)$, respectively. The frequency responses of $W_1(s)$ and $W_2(s)$ have been shown in Fig 3.8 and Fig 3.9, respectively.

3.3.1 Nominal Performance

Closed-loop system achieves nominal performance if and only if (Maciejowski, 1989):

$$\left\| W_2(s) \left[I + G(s) K(s) \right]^{-1} \right\|_\infty < 1 \tag{3.47}$$

Weighting function $W_2(s)$ is used to reflect the relative importance of various frequency ranges for which performance is desired. Since $W_2(s)$ is a scalar, the maximum singular value plot of the sensitivity transfer function $[I + G(s)K(s)]^{-1}$ must lie below the plot of $1/|W_2(s)|$, at every frequency. i.e.:

$$\sigma\left[(I + GK)^{-1}(j\omega) \right] < \left| 1/W_2(j\omega) \right| \qquad \forall\, \omega \tag{3.48}$$

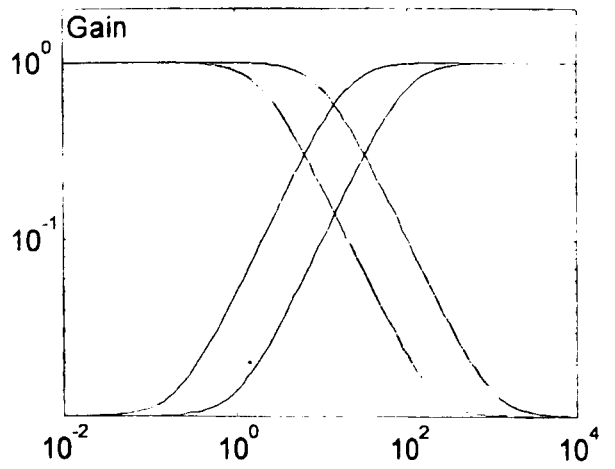

Fig 3.7: Smallest and largest principal gains of multivariable sensitivity function S and complementary sensitivity function T where horizontal axis is frequency.

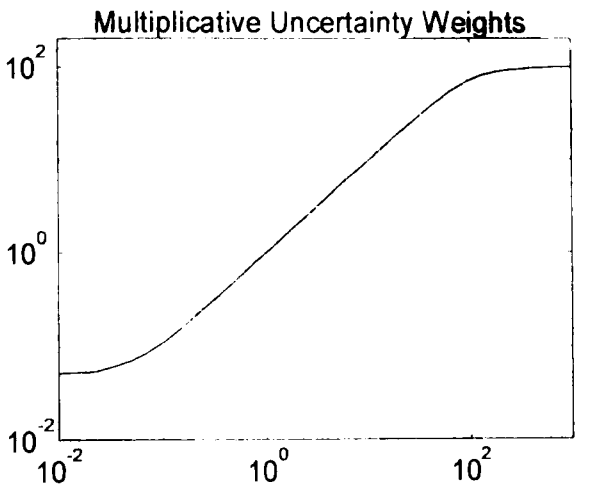

Fig 3.8:Multiplicative Uncertainty Weighting Function

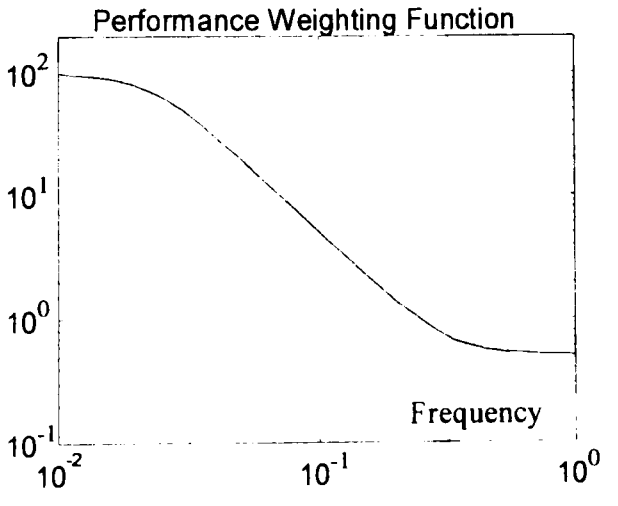

Fig 3.9: Performance weighting function (Vertical axis is amplitude)

3.3.2 Robust Stability

Closed-loop system achieves robust stability if the closed loop system is internally stable for all of the possible plant models $G \in \hat{G}$. This is equivalent to a norm test on a nominal closed loop transfer function (Doyle *et al*, 1982).

$$\left\| W_1(s)G(s)K(s)[I + G(s)K(s)]^{-1} \right\|_\infty < 1 \tag{3.49}$$

$W_1(s)$ is the weighting on multiplicative uncertainly of the system.

Since $W_1(s)$ is a scalar, the maximum singular value plot of the complementary sensitivity function $G(s)K(s)[I + G(s)K(s)]^{-1}$ must lie below the plot of $1/|W_1(s)|$ at every frequency. i.e.:

$$\sigma\left[GK(I + GK)^{-1}(j\omega)\right] < |1/W_1(j\omega)| \qquad \forall\, \omega \tag{3.50}$$

3.3.3 Robust Performance

Closed-loop system achieves robust performance if the closed loop system is internally stable for all $G \in \hat{G}$, and in addition, the performance objective, is satisfied for every $G \in \hat{G}$ (Safonov, 1982; Doyle, 1982).

$$\left\| W_2(j\omega)\left[I + G_c(j\omega)K(j\omega)\right]^{-1} \right\| < 1 \qquad \forall\, \omega \tag{3.51}$$

where

$G_c(j\omega) = \left[I + W_1(j\omega)\Delta G(j\omega)\right]G(j\omega)$

3.3.4 Proposed Criteria for Robust Performance

The robust performance is guaranteed if $\mu(M) < 1$ (Maciejowski, 1989). An interesting criterion proposed by Gagnon, *et al*, (1999) to assess the robust performance of multi-loop PID controller is given by:

$$J = \min_{K(s)} \{ \sum_{i=1}^{m} \left| \mu_{\Delta G(s)} [M(s)] - 1 \right|^{n} \} \tag{3.52}$$

where:

n is an integer penalty weighting

m represents the number of frequency points at which the criteria is evaluated.

This criterion does not however penalise the actuator variations, which is often important in terms of control energy cost and actuator saturation, wear and tear and hence plant availability. The criterion is therefore modified to include the control sensitivity.

$$J = \min_{K(s)} \{ \sum_{i=1}^{m} W_p \left| \mu_{\Delta G(s)} [M(s)] - 1 \right|^{2} + W_u \mu_{\Delta G(s)} [C(s)] \} \tag{3.53}$$

where

$C(s) = K(s)(I + G(s)K(s))^{-1}$

W_p and W_u are appropriate weightings.

3.4 Case Studies

In this section, nine different PID tuning methods, which were introduced in section 3.2, will be used to calculate the PID parameters for two systems. Methods are:

1. Davison Method *(1976)*
2. Penttinen-Koivo method *(1980)*
3. Maciejowski method *(1989)*
4. The BLT method *(Luyben, 1986)*
5. Optimal control *(Wang and Wu, 1995)*
6. Ho *et al* (1998)
7. IMC method *(Dong and Brosilow, 1997)*
8. Loh *et al* (1993)
9. Wang *et al* (1997)

Systems to be controlled are as follows:

- The eight tray Wood and Berry (1973) distillation column for separating methanol and water
- Boiler model from chapter 2

To compare nominal performance, stability robustness and performance robustness of nine PID tuning methods, the criteria that were defined in Section 3.3, will be applied to closed loop feedback systems.

Example 1

The example used for testing the tuning methods is the tray Wood and Berry (Luyben, 1990) distillation column for separating methanol and water. The system is a 2I2O system with the following open loop transfer function:

$$G(s)=\begin{bmatrix} \dfrac{12.8e^{-s}}{16.7s+1} & \dfrac{-18.9e^{-3s}}{21s+1} \\ \dfrac{6.6e^{-7s}}{10.9s+1} & \dfrac{-19.6e^{-3s}}{14.4s+1} \end{bmatrix} \tag{3.54}$$

The outputs of the model are the reflux and steam flow and the inputs are the distillate and bottoms compositions. Eight methods have been used to design a PI controller for the above system.

The Frequency and Time domain indices achieved for each method are shown in Table 3.1 and Table 3.2.

Frequency domain specifications: using Table 3.1 the frequency domain indices show that the method 2 has maximum peak sensitivity and control sensitivity. Method 2 also gives the largest bandwidth.

Time domain specifications: The step response specification of the methods has been shown in Table 3.2. The methods are compared for the performance characteristics as follow:

Settling time: the methods 5 and 3 have minimum settling time and methods 1 and 6 have the maximum settling time.

Overshoot: the methods 6 and 5 have minimum overshooting and method 2 and 9 have the maximum overshoot.

Rising time: the methods 2, 3 and 8 have minimum rising time and method 4 has the maximum rising time.

Maximum actuator excursion: The method 2 has the biggest and 6 has the smallest respectively. This is confirmed by the facts that the method 2 has the most bandwidths in open loop and therefore lowest disturbance rejection. In the other words method 6 has narrower bandwidths and consequently more disturbance rejection.

Robustness tests: Nominal Performance, Robust Stability and Robust Performance Comparison of methods according to equations (3.47), (3.49), (3.51) and (3.53) have been shown in Figs. 3.11, 3.12, 3.13 and 3.14 respectively.

Nominal performance: Fig 3.11 shows that the controlled system has achieved nominal performance for all methods. This conclusion follows from the fact that maximum singular values are less than one.

Stability robustness: The methods 1,2,8 have not achieved robust stability, and method 3 has best stability robustness as shown in Fig 3.12.

Performance robustness: Fig 3.13 shows the maximum value of upper bound of $\mu(M)$. The robust performance is achieved if $\mu(M)<1$. Therefore the methods of 1,2,6,8,9 did not achieve robust performance. This is also confirmed by the proposed criterion of equation (3.53), Fig 3.14.

A qualitative comparison of the methods shows that methods 1, 2, 8, 9 require the least computation and coding requirements. Methods 3, 6 and 7 require a simple dynamic model of the system. The 4 and 5 methods require the most design effort and often used in off-line applications (Katebi *et al*, 2000a).

Example 2

As a second example, the boiler model from Chapter 2 has been considered (Moradi *et al*, 2000b). The model has two inputs and four outputs. After Linearisation the model around Inputs = [1 1] and Outputs = [1 1 1 1] the transfer function on model is:

$$G(s)=\begin{bmatrix} g1 & g2 \\ g3 & g4 \\ g5 & g6 \\ g7 & g8 \end{bmatrix}=\begin{bmatrix} \dfrac{.0031s-.00034}{s^2+.0178s+.00055} & \dfrac{.0023s-3e-5}{s^2+.017s+.0004} \\ \dfrac{-.0067s+.00062}{s^2+.017s+.00053} & \dfrac{s^2+.043s+.00065}{s^2+.067s+.0006} \\ \dfrac{-.007s+.00078}{s^2+.0178s+.00055} & \dfrac{-.005s+7e-5}{s^2+.017s+.0004} \\ \dfrac{-.0067s+.00062}{s^2+.017s+.00053} & \dfrac{-.024s+5e-5}{s^2+.067s+.0006} \end{bmatrix}$$

where inputs and outputs are, Fig 3.10:

- Inputs
  I. Fuel and Air demand
  II. Control Valve
- Outputs
  I. Drum Level
  II. Steam Flow
  III. Drum Pressure
  IV. Throttle Pressure

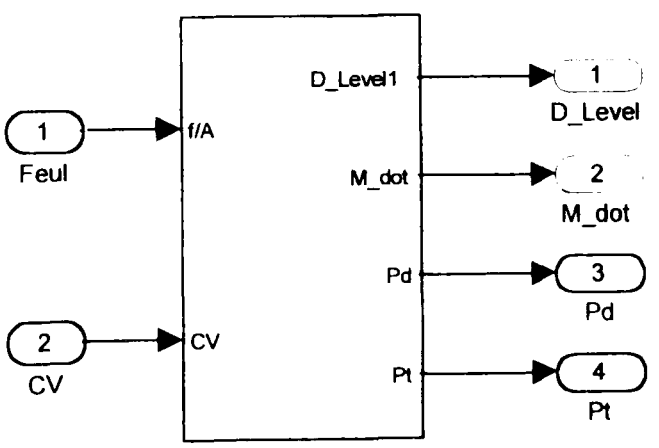

Fig 3.10: Boiler's Inputs and Outputs

RGA was used to find out which pairing between inputs and outputs is suitable. The results showed the suitable pairing is:

$$G(s)=\begin{bmatrix} g7 & g8 \\ g3 & g4 \end{bmatrix}=\begin{bmatrix} \dfrac{-.007s+.00078}{s^2+.0178s+.00055} & \dfrac{-.005s+7e-5}{s^2+.017s+.0004} \\ \dfrac{-.0067s+.00062}{s^2+.017s+.00053} & \dfrac{s^2+.043s+.00065}{s^2+.067s+.0006} \end{bmatrix} \tag{3.55}$$

With following RGA at steady state and ω_c:

$$RGA(0)=\begin{bmatrix} 1.1517 & -0.1517 \\ -0.1517 & 1.1517 \end{bmatrix}$$

$$RGA(\omega_c=0.0314)=\begin{bmatrix} 1.2751 & -0.2751 \\ -0.2751 & 1.2751 \end{bmatrix}$$

where the manipulated variable $u_1(s)$ and $u_2(s)$ are the feed/air demand and the control valve position respectively. The control variables $Y_1(s)$ and $Y_2(s)$ are throttle pressure and the steam flow respectively. Eight methods have been used to design a PI controller for the above system.

The boiler model is second order. In channel one, second order model with a 20 sec time delay is used to calculate the controller parameters for methods 1, 2, 3, 4 and 5. Methods 6 and 7 only applicable to systems with first order dynamic. A first order approximation is made for the sake of comparison. The controller designed based on this model is not reliable it can be observed from Tables 3.3.

Step response specifications: The controllers are designed to give similar rise time and settling time as shown in Table 3.4. This is achieved by adjusting a tuning parameter.

Robustness tests: The nominal performance, the stability robustness criterion, the performance robustness criterion and the proposed criterion are calculated for each method and shown in Figs. 3.15, 3.16, 3.17 and 3.18 respectively.

Nominal performance: Fig 3.15 shows method 5 has the best nominal performance and method 6 has the worst nominal performance.

Stability robustness: From Fig 3.16, methods 8, 3 and 5 have the best stability robustness and methods 1,2 and 7 have not achieved robust stability.
Performance robustness: Using equation (3.51), Fig 3.17 shows that methods 5, 4 and 3 have the best robustness performance. But the proposed method shows that methods 3, 1 and 4 have the best performance robustness and methods 6 and 7 have the worst Fig 3.18.

All methods can, in principle, be implemented on-line, but methods 1, 2 and 5 require the least computation and coding requirements. Methods 3, 4 and 6 require a simple dynamic model of the system. The BLT method requires the most design effort and often used in off-line applications. Method 3 requires the solution of a least square minimisation problem and this may cause numerical difficulties if the system is ill conditioned.

3.5 Summary

Nine PID tuning methods for multivariable systems were compared for their robustness properties in this chapter. The results for well-known Wood and Berry distillation column system showed that the Maciejowski method outperforms other methods. The Optimal Control Method was next. This method achieved the nominal performance and robust stability and showed improved time domain indices. The Penttinen-Kiovo method showed the poorest stability and performance robustness. Davison, Penttinen-Koivo, Ho *et al.*, Loh *et al.* and Wang *et al.* methods do not achieve the robust performance and Davison, Penttinen-Koivo and Loh *et al.* methods do not achieve the robust stability.
Also these nine PID tuning methods were compared for their robustness for application to non-minimum phase industrial boilers. Method 5 was shown to outperform other methods in robustness properties. Method 2 has poor performance and stability robustness to additive perturbations. The feedback relay method 8 performed well in stability robustness and performance robustness. The study shows that some of the methods such as IMC method are only applicable to slow systems with first order dynamics.

Table 3.1 The Frequency Domain Specifications

Method	S_m	S(j.01)	ω_m	BW	M_m
1	11.4	-31.5	3.6	0.29-0.65	2.6
2	18.4	-25.9	10	1.2-1.3	13.7
3	4.7	-25.4	0.9	0.18-0.18	-8.97
4	6.4	-9.3	2.3	0.4-0.12	0.395
5	4.5	-19.3	2.4	0.47-0.25	-7.1
6	8.4	-16.2	2.5	0.6-0.21	-12.4
7	12.3	-4.6	3.4	0.75-0.03	1.183
8	9.9	-17.1	2.8	1-0.17	0.9235
9	9.4	-21.8	1.1	0.35-0.18	0.33

S_m: Maximum Sensitivity, ω_m: Frequency of Maximum Sensitivity, BW: Bandwidth, M_m: Maximum Control Sensitivity

Table 3.2 The Time Domain Specification

Method	OS%	RT(s)	ST(s)
1	35-31	9-2.5	43-42.5
2	54-56	8-2	31-41
3	12-3.5	9-5	30-9.4
4	10-0	4.2-84	20-130
5	2.3-4	10-5	12-26
6	0-0	3-32	34-48
7	6-0	2.5-51	25-85
8	53-0	2-25	19-38
9	39-11	4-8	24-37

OS: Over Shoot, RT: Rise Time, ST: Settling Time (Loop one-Loop two)

Table 3.3: PI parameters of methods for Boiler model

Method	Kp_{11}, KI_{11}	Kp_{12}, KI_{12}	Kp_{21}, KI_{21}	Kp_{22}, KI_{22}
1	0.023, 0.0003	-0.903, -0.013	0.571, 0.008	1.02, 0.015
2	-0.474, -0.003	-8.91, -0.055	-34.32, -0.69	-115, -2.34
3	-.0, 0.0004	0.023, -0.0145	0.0005, 0.009	0.0002, 0.016
4	3.86, 0.056	0, 0	0, 0	2.49, 0.0067
5	3.958, 0.031	0, 0	0, 0	2.593, 0.035
6	0.5, 0.0008	0, 0	0, 0	2006.8, 5.35
7	0, 0.0002	-0.4, -0.0068	1104.8, 8.63	620.9, 15.36
8	0.992, 0.002	0, 0	0, 0	1, 0.026

K_{pij}, KI_{ij} ij th elements of proportional and integral gain matrices, respectively.

Table 3.4 The Time Domain Specification of Closed Loop System for Boiler Model

Method	OS%	RT(s)	ST(s)
1	1-0	400-280	620-680
2	25-3	10-240	160-680
3	3-4	260-120	660-640
4	57-0	20-820	260-1800
5	43-16	20-80	420-420
6	42-7	44-4	700-108
7	0-0	10-500	200-720
8	21-8	80-100	560-500

OS: Over Shoot, RT: Rise Time, ST: Settling Time (Loop one-Loop two)

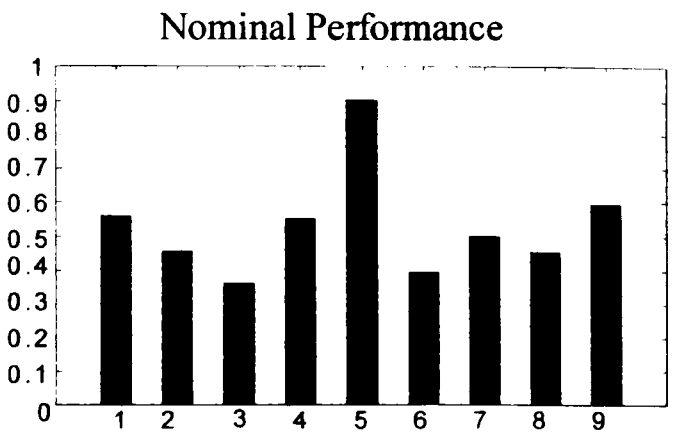

Fig 3.11: Nominal Performance Comparison

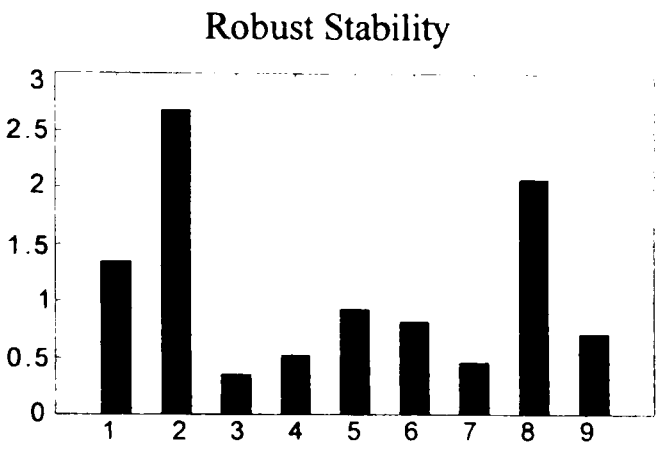

Fig 3.12: Robust Stability Comparison

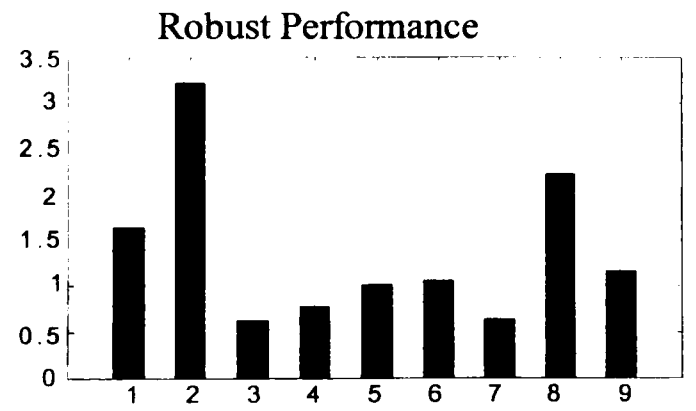

Fig 3.13: Robust Performance Comparison

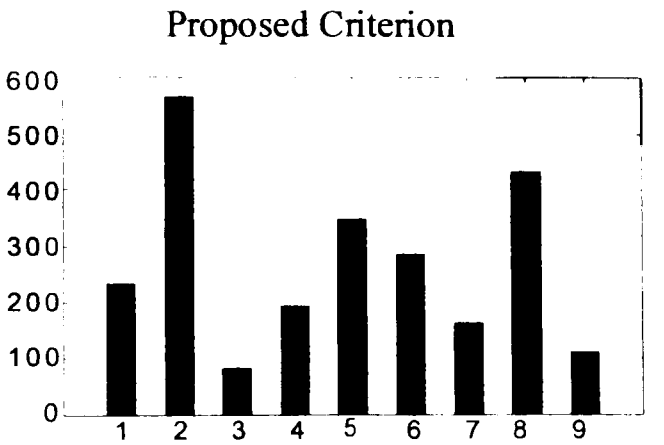

Fig 3.14: Robust Performance the proposed criterion

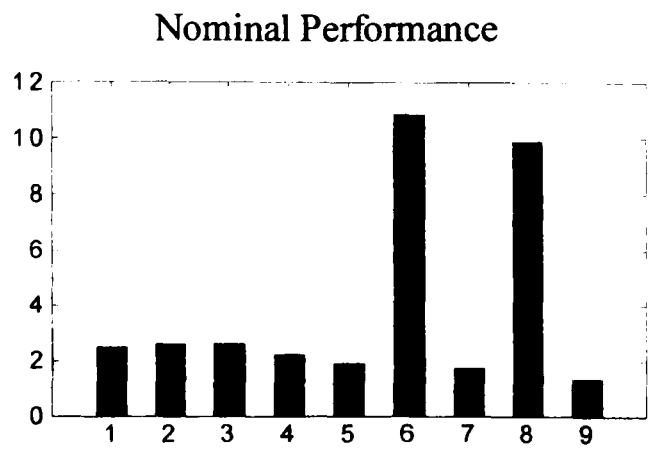

Fig 3.15: Nominal Performance Comparison

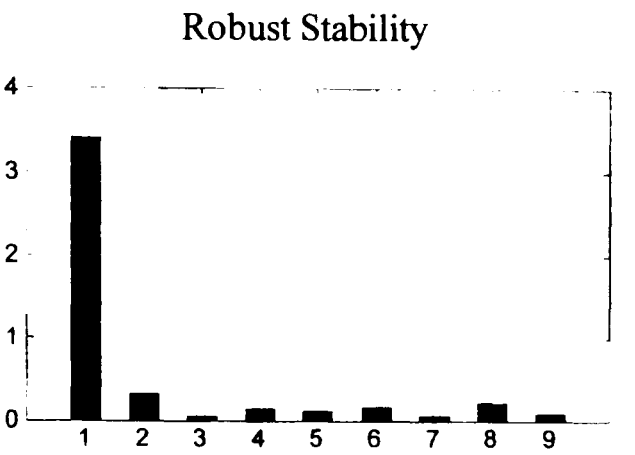

Fig 3.16: Robust Stability Comparison

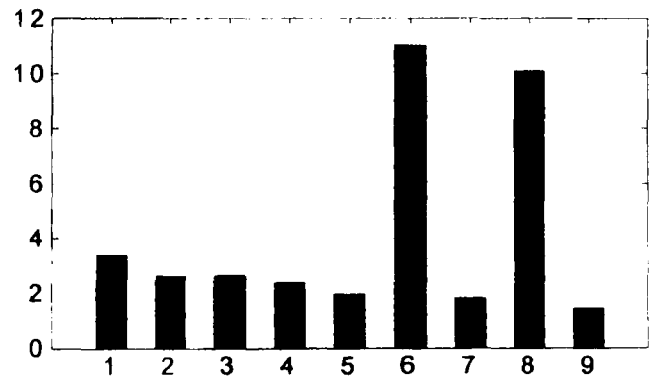

Fig 3.17: Robust Performance Comparison

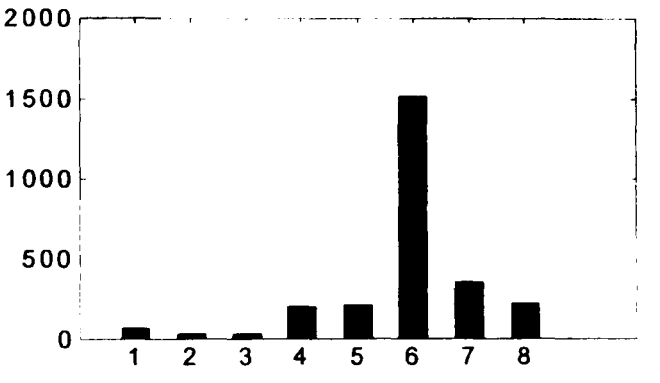

Fig 3.18: Robust Performance the proposed criterion

Chapter 4

Robust Multi-Input and Multi-Output PID Control

4.1 Introduction

A fundamental problem associated with relays in feedback control systems is the determination of limit cycle frequencies and gains. In recent years the existence of various automatic-tuning techniques for industrial SISO controllers has led to renewed interest in relay control and particularly in the limit cycles associated with such control (Astrom and Hagglund, 1984; 1988, Palmor and Blau, 1994). Relays in these applications are used mainly for the identification of points on the process Nyquist curve, from which essential information for tuning industrial process controllers, such as the PID controller can be obtained.

When the relay technique is extended to MIMO systems, there are three possible schemes (Wang *et al*, 1997):

1-Independent single Relay Feedback (IRF)

2-Sequential Relay Feedback (SRF)

3-Decentrelised Relay Feedback (DRF)

Chapter 4

Using the result from relay experiments, either a fully cross-coupled or a multi-loop controller can be adopted for MIMO processes (Wang *et al*, 1997). Multi-loop controllers, sometimes known as decentralised controllers, have a simpler structure and, accordingly, less tuning parameters than the fully cross-coupled ones. In addition, in the event of component failure, it is relatively easy to stabilise the system manually, since only one loop is directly affected by the failure (Skogestad and Morari, 1989).

An algorithm for automatic tuning of decentralized controllers for two-input and two-output (2I2O) plants has been proposed (Palmor *et al*, 1995a). The main objective of the auto-tuner is to identify a Desired Critical Point (DCP). The Palmor method identifies the DCP with almost no a priori information about the process.

The aim of this chapter is to introduce a new relay identification method for multivariable PID tuning. The chapter originates from a review of the critical points for MIMO processes. Calculations of process gains at bandwidth frequency and zero frequency is described. Then, Palmor *et al*, (1995a) 2I2O PID auto-tuning method is extended for MIMO processes. In section 4.7, a new relay identification method for PID tuning at bandwidth frequency is introduced. Comparison between Palmor tuning method and proposed method will discuss at the end of this chapter.

4.2 Critical Points of Systems

The knowledge of desired critical point is essential to the tuning procedure. Critical points of a system depend on the specification and the complexity of the system. The relay experiment is one method, which can be used to identify the critical points of processes. During the identification phase with relay experiment, all the controllers are replaced by relays, thus generating limit cycle oscillations. Many of PID tuning methods then use the critical point information to tune the PID controller. For this, the ultimate gain and ultimate period of process are measured. The critical points of different systems are explained in the next sections.

4.2.1 Critical Points for 2I2O Systems

In Fig 4.1 a block diagram of decentralized control systems for a 2I2O process is depicted, where $y(t) \in R^2$ is the vector of process outputs, $u(t) \in R^2$ is the vector of manipulated variables (or control signals) and $r(t) \in R^2$ is the vector of the reference signals. Similarly, $e(t) \in R^2$ is the vector of loop errors.

In SISO systems there are only a finite number of critical gains that bring the system to the verge of instability. In most cases there is only one such gain. Unlike SISO plants, for 2I2O systems there are many critical points (Palmor *et al.*, 1995a). There are many gains (K_1, K_2) that, when replacing $K_1(s)$ and $K_2(s)$ in Fig 4.1a, lead to neutral stability, i.e. poles on the imaginary axis. The collection of all these gains is called the stability limits of the system as shown in Fig 4.2a. In Fig 4.2a each point on the curves corresponds to a pair of gains (K_{c1},K_{c2}) and a critical frequency, which together are referred to as a critical point. The points on the axes represent the situation where one loop is open (K_i=0). If the system does not have full interaction, i.e. either $g_{12}(s)$, $g_{21}(s)$ or both are zero, the stability limits take the rectangular form (curve 1 in Fig 4.2a). In this case the two critical gains are independent of each other, and the system becomes

unstable when either one of the gains exceeds its SISO critical value. The curve 2 represents system with interactions. The deviation from rectangular shape may be regarded as a measure of interaction. Clearly, different critical points lead to different settings, and hence different performance. Therefore it is necessary to specify on which critical point the tuning should be based. This critical point will be referred as the desired critical point (DCP). The choice of the DCP depends on the relative importance of loops, which is commonly expressed through a weighting factor (Luyben, 1986). The weighting factor can be express by different criteria such as; relationship between loops gain in steady state (Palmor *et al.*, 1995a) or relationship between loops gain in bandwidth frequency that it will be introduced in this chapter.

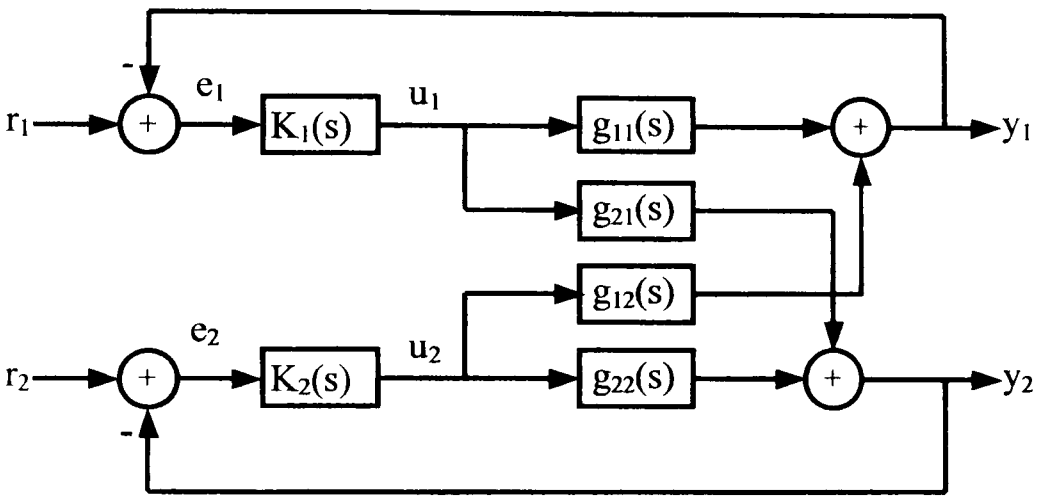

Fig 4.1a: The 2I2O system with multi-loop controller

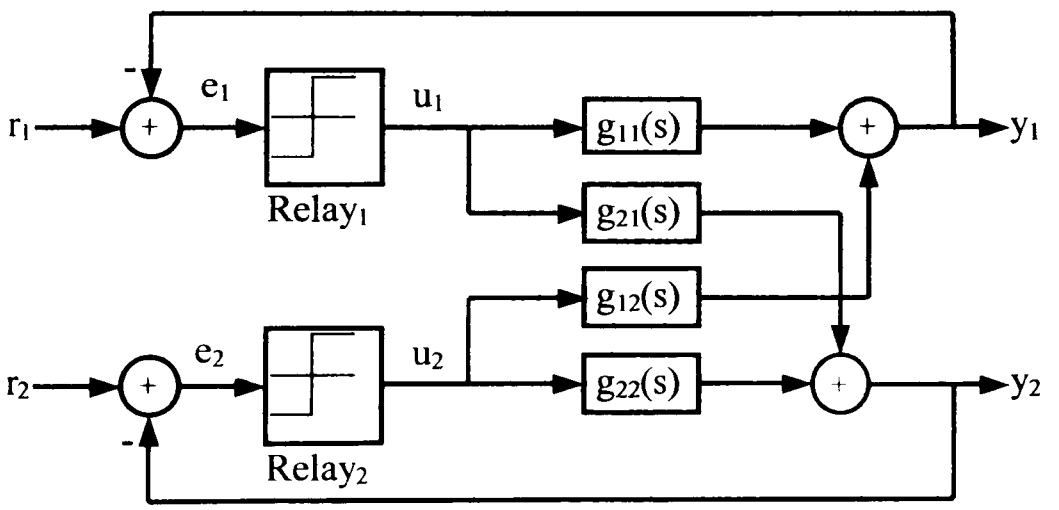

Fig.4.1b: A 2I2O decentralized relay system

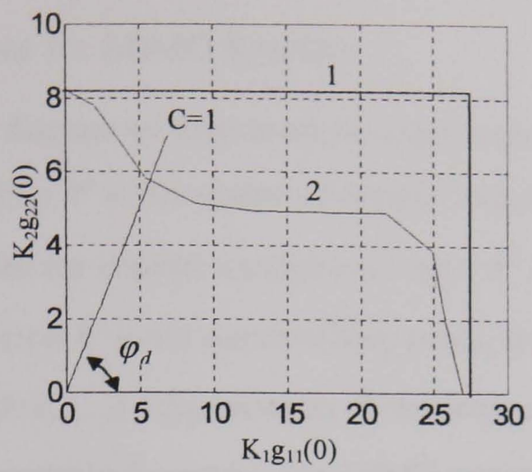

Fig 4.2a Critical Point of example 2 (after Palmor *et al.*, 1995a)

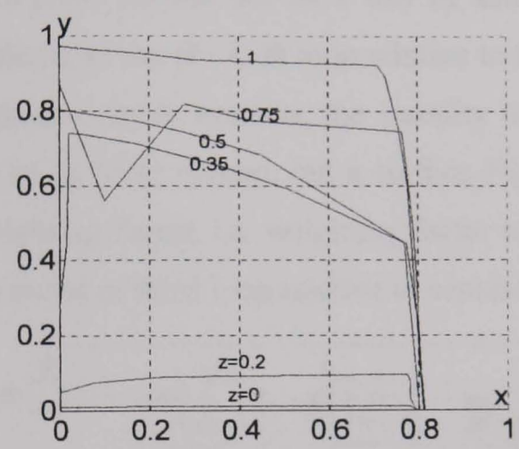

Fig 4.2b: Critical Points of 3I3O Systems. $x = K_{c1}g_{11}(0), y = K_{c2}g_{22}(0), z = K_{c3}g_{33}(0)$

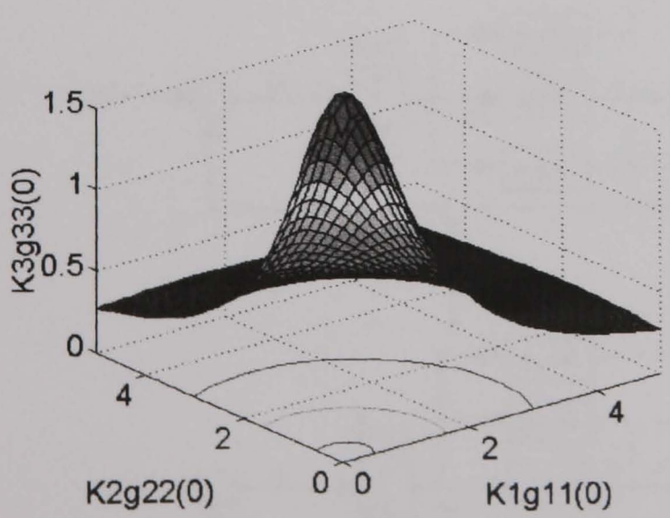

Fig 4.2c Critical Points of 3I3O Systems

4.2.2 Critical Points for MIMO Systems

In Fig 4.3 a block diagram of decentralized control systems for a MIMO process is depicted, where $y(t) \in R^L$ is the vector of process outputs, $u(t) \in R^L$ is the vector of manipulated variables (or control signals) and $r(t) \in R^L$ is the vector of the reference signals. Similarly, $e(t) \in R^L$ is the vector of loop errors. It is clearly seen that the control signal u_i in loop i (i=1,2,...,L) depends just on the error $e_i(t)$ in the same loop. This is the structure of decentralized control. For MIMO systems, the stability limits form a space of dimensions of *(L-1)* so that the DCP can be selected using *(L-1)* weighting factors, i.e. weighting factor of the *(k+1) th* loop relative to the *k th* loop *(k=1,2,...,L-1)*. For three inputs and three outputs systems, the stability limits do not form a point as SISO system or curve as in 2I2O system, but a surface Fig 4.2(b-c). The DCP can be selected using two weighting factor, i.e. weighting factor of the second loop relative to the first and weighting factor of third loop relative to second.

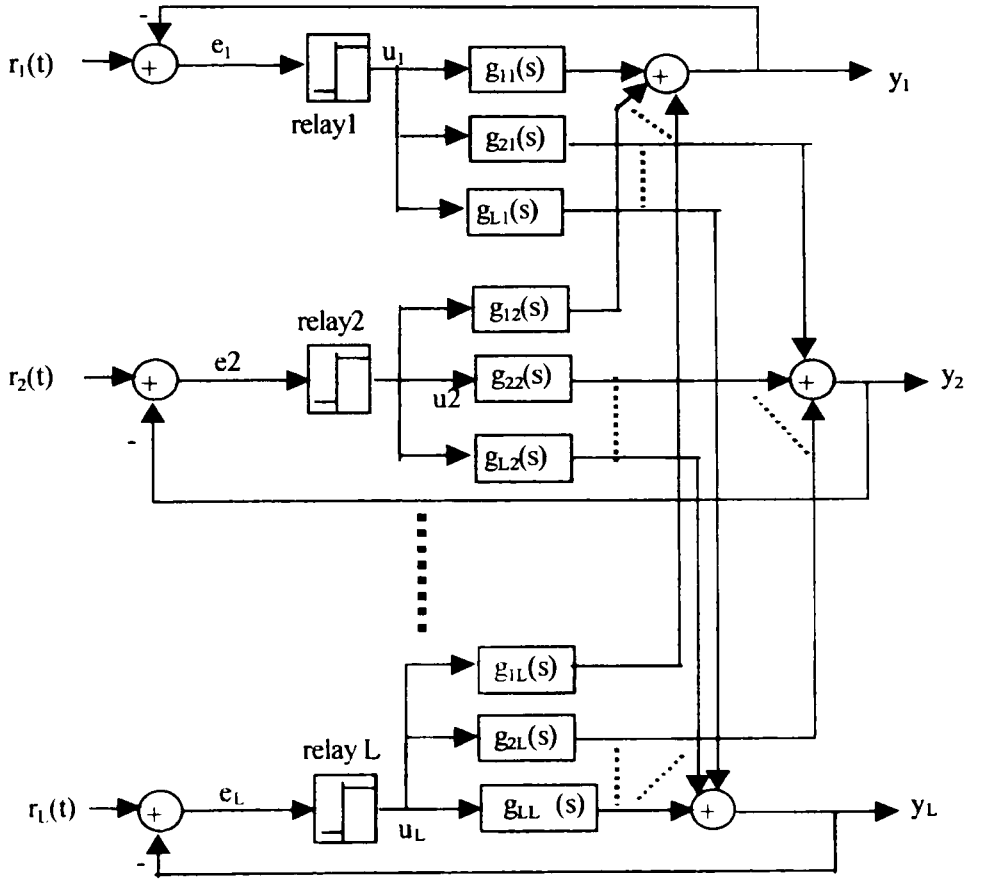

Fig 4.3: A MIMO decentralized relay system

4.3 Determination of Gains at Bandwidth and Zero Frequency

To identify the process frequency response $G(j\omega)$ at the critical oscillation frequency $\omega_c \approx \omega_b$, the relay method as shown in Fig 4.3 is used. In relay test the stationary process inputs $u_i(t)$ and outputs $y_i(t)$ are all periodic, and they can be expanded in Fourier series. The first harmonics of these periodic waves are extracted (Ramirez, 1985) as:

$$y(j\omega_b) = G(j\omega_b)u(j\omega_b) \tag{4.1}$$

where:

$$y(j\omega_b) = \begin{bmatrix} y_1(j\omega_b) \\ y_2(j\omega_b) \\ \vdots \\ y_L(j\omega_b) \end{bmatrix} = \begin{bmatrix} \frac{1}{T}\int_0^T y_1(t)e^{-j\omega_b t}dt \\ \frac{1}{T}\int_0^T y_2(t)e^{-j\omega_b t}dt \\ \vdots \\ \frac{1}{T}\int_0^T y_L(t)e^{-j\omega_b t}dt \end{bmatrix} \quad u(j\omega_b) = \begin{bmatrix} u_1(j\omega_b) \\ u_2(j\omega_b) \\ \vdots \\ u_L(j\omega_b) \end{bmatrix} = \begin{bmatrix} \frac{1}{T}\int_0^T u_1(t)e^{-j\omega_b t}dt \\ \frac{1}{T}\int_0^T u_2(t)e^{-j\omega_b t}dt \\ \vdots \\ \frac{1}{T}\int_0^T u_L(t)e^{-j\omega_b t}dt \end{bmatrix}$$

Since (4.1) is vector equation, it is not sufficient to determine $G(j\omega_b)$. Consequently, the relay experiments must be repeated L times, the relay amplitude of the dominant loop is slightly increased or the relay amplitude of other loops is decreased. The oscillation frequencies for each experiment remain close to that of the previous experiment. Now, equation (4.1) can be written for L relay experiments as:

$$Y(j\omega_b) = G(j\omega_b)U(j\omega_b) \tag{4.2}$$

where:

$$G(j\omega_b)=\begin{bmatrix} g_{11}(j\omega_b) & g_{12}(j\omega_b) & \cdots & g_{1L}(j\omega_b) \\ g_{21}(j\omega_b) & g_{22}(j\omega_b) & \cdots & g_{2L}(j\omega_b) \\ \vdots & \vdots & \ddots & \vdots \\ g_{L1}(j\omega_b) & g_{L2}(j\omega_b) & \cdots & g_{LL}(j\omega_b) \end{bmatrix}$$

$$Y(j\omega_b)=\begin{bmatrix} Y^1(j\omega_b) & Y^2(j\omega_b) & \cdots & Y^L(j\omega_b) \end{bmatrix}$$

$$Y^i(j\omega_b)=\begin{bmatrix} y_1^i(j\omega_b) & y_2^i(j\omega_b) & \cdots & y_L^i(j\omega_b) \end{bmatrix}^T$$

$$U(j\omega_b)=\begin{bmatrix} U^1(j\omega_b) & U^2(j\omega_b) & \cdots & U^L(j\omega_b) \end{bmatrix}$$

$$U^i(j\omega_b)=\begin{bmatrix} u_1^i(j\omega_b) & u_2^i(j\omega_b) & \cdots & u_L^i(j\omega_b) \end{bmatrix}^T$$

where the superscript indicate the experiment number. A solution can easily be found for the $G(j\omega_b)$ as:

$$G(j\omega_b)=Y(j\omega_b)U^{-1}(j\omega_b) \tag{4.3}$$

This means that from inputs and outputs signal the values of outputs and inputs at fundamental frequency $\omega_c \approx \omega_b$ are extracted in each relay experiments, Fig 4.4 shows the procedure, then after L relay experiments these values are inserted into equation (4.3) to determine the process gains at bandwidth frequency.

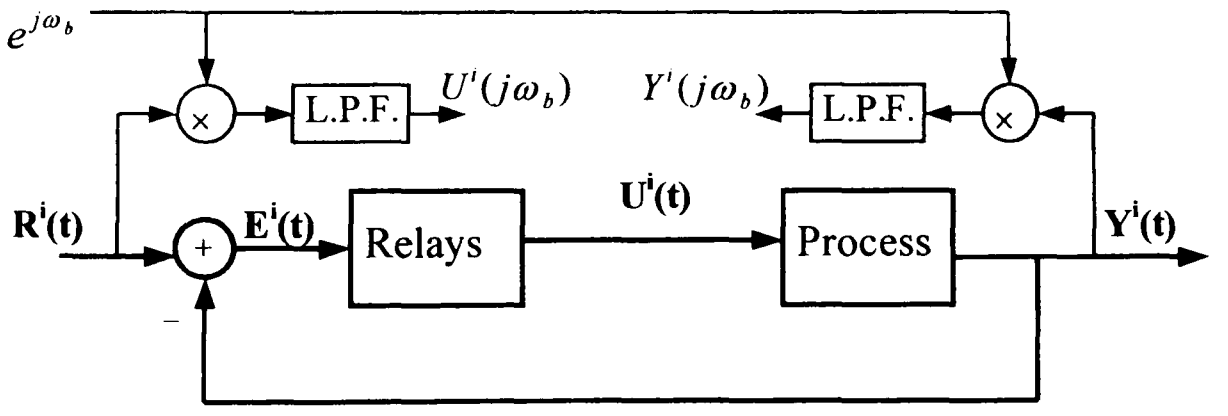

Fig 4.4: Calculation of outputs and inputs at ω_b in *i th* relay test

To calculate steady state gains of system, set $\omega_b = 0$ in equations (4.1)-(4.3) and the result is:

$$G(0) = Y(0)U^{-1}(0) \tag{4.4}$$

This means that the average values of outputs and inputs, using low pass filter, are extracted during each relay test. Using these values the steady state gains are simply calculated by equation (4.4). Fig 4.4 shows the block diagram of procedure (set $\omega_b = 0$).

4.4 Decentralized Relay Control System

Theorem 1: Consider the decentralized relay feedback system of Fig 4.4. If a limit cycle exists then its period T and the time shifts h remain the same for all M_k, b_k and Δ_k satisfying:

$$M_1(i) : M_2(i) : \cdots : M_L(i) = \delta_1 : \delta_2 : \cdots : \delta_L$$

$$M_k(i) : b_k(i) : \Delta_k(i) = 1 : \beta_k : \gamma_k \quad (k = 1,2,\cdots,L)$$

where:

δ_k, β_k and γ_k are nonnegative constants.

$b_k(i)$ hysterisis of relay k at i *th* experiments

$\Delta_k(i)$ dead zone of relay k at i *th* experiments

$M_k(i)$ Output of the relay k in i *th* experiment.

Proof: (Palmor *et al.* ,1995b)

A special case of theorem 1 has been used to develop a new automatic-tuning algorithm for a decentralised 2I2O PID controller (Krasney, 1991. Palmor *et al.*, 1995b)

Corollary 1: Consider the system as shown in Fig 4.1b, All pairs $[M_1(i), M_2(i)]$ such that $\frac{M_1(i)}{M_2(i)}$ = constant, lead to limit cycles with the same period T, the same time shift and the same ratio of amplitudes $\frac{a_1(i)}{a_2(i)}$.

where:

$a_k(i)$ Output of the relay k in i *th* experiment $(k = 1,2,\cdots,L)$

Proof: (Krasney, 1991)

From the theorem 1 it follows that in the relay set-up, the critical points depend only on the ratio $\frac{M_{(k+1)}(i)}{M_k(i)}$, though theoretically the results are independent of the absolute magnitudes $M_k(i)$ and $M_{(k+1)}(i)$, these values do have practical significance. To reduce the effect of noise and to cause noticeable changes in y, $M_k(i)$ $k = 1,2,\cdots,L$ must be large. Hence there is lower bound on M_k, denoted by $\underline{M_k}$. On the other hand, too large M_k cannot be used due to actuator constraints or because the allowed change in y may be restricted. Hence there is an upper bound on M_k, denoted by $\overline{M_k}$. The theorem 1 and the preceding discussion indicate that:

(a) By using L relays tests, a critical point for L-inputs and L-outputs system is identified.

(b) In practice, the amplitude of $k\ th$ relay is $\underline{M_k} \le M_k \le \overline{M_k}$ because of constrained on manipulated variables.

(c) All sets $(M_1, M_2, \cdots, M_L)$ such that $\frac{M_k(i)}{M_{k+1}(i)}$= constant correspond to one critical point.

(d) It is possible to 'move' along the stability boundary by varying the ratios $\frac{M_k(i)}{M_{k+1}(i)}$.

From parts (c) and (d) for all sets $(M_1, M_2, \cdots, M_L)$ such that:

$M_1(i): M_2(i): \cdots : M_L(i) = \delta_1 : \delta_2 : \cdots : \delta_L$ lead to limit cycle with the same period T and same time shift and same ratio of $a_1(i): a_2(i): \cdots : a_L(i) = \nu_1 : \nu_2 : \cdots : \nu_L$

where:

$a_k(i)$:	Input to relay k in $i\ th$ experiment
ν_k	Constant.

In other word, a relationship between ratios of $k\ th$ relays input and the ratios of relays amplitude could be defined by following function:

$$\frac{a_{k+1}(i)}{a_k(i)} = f_k\left[\frac{M_2(i)}{M_1(i)}, \frac{M_3(i)}{M_2(i)}, \cdots, \frac{M_L(i)}{M_{(L-1)}(i)}\right] \tag{4.5}$$

In next section equation (4.5) is used along with Linear Interpolation to calculate the next set of relay ratios.

4.5 Palmor Relay Identification Method for PID Tuning

The Palmor relay identification method is for 2I2O plants Fig 4.1a. The method can be summarized as follows:

Choosing Desired Critical Point

Select criteria C to choose desired critical point (4.6):

$$\tan \varphi_d = \frac{C}{1} = \frac{K_{2cr} g_{22}(0)}{K_{1cr} g_{11}(0)} \tag{4.6}$$

Where C is the weighting factor of the second loop relative to the first. Selecting $C > 1$ means that loop 2 is required to be under tighter control relative to loop 1 in steady state. The relative weightings can be alternatively expressed via the angle, defined in the above formula, φ is the angle connecting a critical point to the origin in the loop-gain plane. The subscript 'd' denotes a desired quantity as shown Fig 4.2.

Determination of Steady State Gains

Consider the 2I2O system shown in Fig 4.1b with at least one input with non-zero mean. Then the error signals $e_i(t)$ and the control $u_i(t)$ are also of non-zero mean. A DC balance, or mathematically, comparing the constant terms of the Fourier series of outputs and controls signal in *i th* experiment, would be calculated by equation (4.4):

$$G(0) = Y(0)U^{-1}(0)$$

where:

$$Y(0)=\begin{bmatrix}\bar{y}_1^1 & \bar{y}_1^2\\ \bar{y}_2^1 & \bar{y}_2^2\end{bmatrix} \qquad U(0)=\begin{bmatrix}\bar{u}_1^1 & \bar{u}_1^2\\ \bar{u}_2^1 & \bar{u}_2^2\end{bmatrix} \qquad G(0)=\begin{bmatrix}g_{11}(0) & g_{12}(0)\\ g_{21}(0) & g_{22}(0)\end{bmatrix}$$

$$\bar{y}^i=\begin{bmatrix}\frac{1}{T}\int_0^T y_1^i(t)dt\\ \frac{1}{T}\int_0^T y_2^i(t)dt\end{bmatrix} \qquad \bar{u}^i=\begin{bmatrix}\frac{1}{T}\int_0^T u_1^i(t)dt\\ \frac{1}{T}\int_0^T u_2^i(t)dt\end{bmatrix}$$

Reference inputs r_1 and r_2 are chosen to ensure that the matrix $\bar{u}$ is non-singular, e.g. $r_1^1(t)\neq 0, r_2^1(t)=0$ and $r_1^2(t)=0, r_2^2(t)\neq 0$. Steady state gains of system are identified from this equation after just two relay experiments.

Initialisations of First Two Relays Outputs

After just two limit cycle experiments in 2I2O systems, all steady state gains are identified and two critical points can be found. It is recommended to use in the first experiments the largest allowed relay ratio namely $\frac{\bar{M}_1}{M_2}$ and in the second $\frac{M_1}{M_2}$. These relay ratios will lead to two critical points, each on a different side of the DCP. These first two critical points provide two good starting points for the next step, and are also close to the two independent single-loop critical points. A good approximation of a critical point is given by:

$$K_{icr}=\frac{4M_i}{\pi a_i}, \quad \omega_{cr}=\frac{2\pi}{T} \quad (i=1,2) \tag{4.7}$$

Having identified two critical points, the question now is how to determine the relay ratio for the next experiments in a systematic fashion that will lead to a rapid convergence to the DCP.

Identification of the DCP

Substituting equation (4.7) in equation (4.6) the relation between desired relay ratio and input to relays are:

$$\frac{M_1}{M_2} = \frac{1}{C_d}\frac{a_1}{a_2}\left|\frac{g_{22}(0)}{g_{11}(0)}\right| \tag{4.8}$$

Recalling from Corollary 1 that, along the stability limits, a_1/a_2 =f (M_1/M_2) via some unknown implicit function f, the problem becomes that the finding M_1/M_2 such that (4.6) holds-in other words, M_1/M_2 that leads to the desired angle φ_d. To this end, the straight line is used to approximate the function, *f*:

$$\frac{a_1}{a_2} = \frac{M_1}{M_2}b_1 + b_2 \tag{4.9}$$

and from the results of the two experiments, the constants b_1 and b_2 are found as:

$$b_1 = \frac{(\frac{a_1}{a_2})_1 - (\frac{a_1}{a_2})_2}{(\frac{M_1}{M_2})_1 - (\frac{M_1}{M_2})_2} \tag{4.10}$$

$$b_2 = (\frac{a_1}{a_2})_1 - b_1(\frac{M_1}{M_2})_1$$

Substituting (4.9) into the desired relation (4.8) yields:

$$\left(\frac{M_1}{M_2}\right)_3 = \left| \frac{b_2}{C_d \left| \frac{g_{11}(0)}{g_{22}(0)} \right| - b_1} \right| \tag{4.11}$$

If the approximation (4.7) is perfectly accurate then (4.11) leads exactly to the desired critical point. Since it is not, there will be some error. A tolerance ε is defined, and algorithm is stopped when $|\varphi - \varphi_d| < \varepsilon$. Otherwise, the procedure is continued in the same fashion where the best two experiments, i.e. those that are closer to φ_d play the role of experiments 1 and 2 in (4.7)- (4.10). This simple algorithm shows excellent convergence properties.

PID Tuning

Once the DCP has been found, the setting of the PID controllers can be determined in a straightforward manner. A simple choice is to use the Ziegler and Nichols (1942) rules.

Discussion

In Palmor method the relative importance of the loops corresponding to a particular point has been described in (4.6). So the method does not consider the interaction between two loops and the steady state gains was used to identify the DCP. For PID tuning, it has been shown that de-coupling the system around bandwidth frequency has the best robustness (Katebi *et al.* 2000a). In the proposed extension the process gains at bandwidth frequency are used and new weighting factors are introduced.

4.6 Extension of Palmor Method for MIMO Relay Identification

In this section Palmor method will be extended for MIMO systems and an algorithm for MIMO PID tuning method will be introduce.

4.6.1 Choosing the Desired Critical Point

To choose the critical point the following criteria was used:

$$\tan\varphi_{dk} = \frac{K_{(k+1)}}{K_k}\frac{g_{(k+1)(k+1)}(0)}{g_{kk}(0)} \qquad k = 1,2,\cdots,L-1 \tag{4.12}$$

where:

$\tan\varphi_{dk}$ is the weighting factor of the *(k+1) th* loop relative to loop k Selecting $\tan\varphi_{dk}>1$ means that loop *(k+1)* is required to be under tighter control relative to loop k in steady state.

4.6.2 Steady State Gains Calculation

The steady state gains of process are identified simultaneously with the critical points, after L limit cycle experiments, as follow:

$$G(0)=\begin{bmatrix} g_{11}(0) & g_{12}(0) & \cdots & g_{1L}(0) \\ g_{21}(0) & g_{22}(0) & \cdots & g_{2L}(0) \\ \vdots & \vdots & \ddots & \vdots \\ g_{L1}(0) & g_{L2}(0) & \cdots & g_{LL}(0) \end{bmatrix} = \begin{bmatrix} \bar{y}_1^1 & \bar{y}_1^2 & \cdots & \bar{y}_1^L \\ \bar{y}_2^1 & \bar{y}_2^2 & \cdots & \bar{y}_2^L \\ \vdots & \vdots & \ddots & \vdots \\ \bar{y}_L^1 & \bar{y}_L^2 & \cdots & \bar{y}_L^L \end{bmatrix} \begin{bmatrix} \bar{u}_1^1 & \bar{u}_1^2 & \cdots & \bar{u}_1^L \\ \bar{u}_2^1 & \bar{u}_2^2 & \cdots & \bar{u}_2^L \\ \vdots & \vdots & \ddots & \vdots \\ \bar{u}_L^1 & \bar{u}_L^2 & \cdots & \bar{u}_L^L \end{bmatrix}^{-1} \tag{4.13}$$

where:

$\bar{y}_i^j$ is average of *i th* output during in *j th* experiment.

$\bar{u}_i^j$ is average of *i th* output during in *j th* experiment.

Proof: See appendix 4.1.

4.6.3 Initialisation of Relay Ratio

To identify the first L critical points, as explained in Palmor method, it is recommended to use following ratios for first L relay experiments:

$$M_{Rk}(h)=\frac{M_k(h)}{M_{k+1}(h)} \qquad h=1,2,\cdots,L \qquad k=1,2,\cdots,L-1 \tag{4.14}$$

where:

$$M_k(h)=\begin{cases} \overline{M}_k & if \quad k=h \\ \underline{M}_k & if \quad k\neq h \end{cases}$$

These relay ratios will lead to L critical points each on a different side of the DCP.

4.6.4 Linear Interpolation

From L relay experiments, L critical points will be identified as follow:

h *th* Experiment

$M_1(h),\ M_2(h),\cdots,M_L(h) \qquad h=(i-L+1),(i-L+2),\cdots,i$

$a_1(h),a_2(h),\cdots,a_L(h)$

$$\therefore K_1(h)=\frac{4M_1(h)}{\pi a_1(h)} \qquad K_2(h)=\frac{4M_2(h)}{\pi a_2(h)} \quad \cdots \quad K_L(h)=\frac{4M_L(h)}{\pi a_L(h)} \tag{4.15}$$

The question now is how to determine the relay ratio for the next experiment in a systematic fashion that will lead to a rapid convergence to the DCP.

Condition:
$$\tan\varphi_{dk}=\frac{K_{(k+1)}(i+1)}{K_k(i+1)}\frac{g_{(k+1)(k+1)}(0)}{g_{kk}(0)} \qquad k=1,2,\cdots,L-1$$
$$=\frac{4M_{(k+1)}(i+1)}{\pi a_{(k+1)}(i+1)}\frac{\pi a_k(i+1)}{4M_k(i+1)}\frac{g_{(k+1)(k+1)}(0)}{g_{kk}(0)} \qquad k=1,2,\cdots,L-1$$

Introduce:
$$a_{Rk}(i+1)=\frac{a_k(i+1)}{a_{k+1}(i+1)} \qquad k=1,2,\cdots,L-1$$
$$M_{Rk}(i+1)=\frac{M_k(i+1)}{M_{k+1}(i+1)}$$

$$\therefore \tan\varphi_{dk}=\frac{a_{Rk}(i+1)}{M_{Rk}(i+1)}\frac{g_{(k+1)(k+1)}(0)}{g_{kk}(0)} \qquad k=1,2,\cdots,L-1 \tag{4.16}$$

Recalling from Theorem 1 that, along the stability limits and using equation (4.5) the relay ratio for the next experiment could be:

$$a_{Rk}(i+1) = f_k[M_{R1}(i+1), M_{R2}(i+1), \cdots, M_{R(L-1)}(i+1)] \quad k = 1,2,\cdots, L-1$$

Via some unknown implicit function f, the problems becomes that the finding $[M_{Rk}(i+1) \quad k = 1,2,\cdots, L-1]$ such that (4.16) holds; in other words, the value of $[M_{Rk}(i+1)]$ that leads to the desired angle $[\varphi_{dk} \quad k = 1,2,\cdots, L-1]$. To this end, a linear approximation to the function f is used:

Assumption:

$$\begin{cases} a_{R1}(i+1) = b_{i11} M_{R1}(i+1) + b_{i12} M_{R2}(i+1) + \cdots + b_{i1(L-1)} M_{R(L-1)}(i+1) + b_{i1L} \\ \vdots \\ a_{R(L-1)}(i+1) = b_{i(L-1)1} M_{R1}(i+1) + b_{i(L-1)2} M_{R2}(i+1) + \cdots + b_{i(L-1)(L-1)} M_{R(L-1)}(i+1) + b_{i(L-1)L} \end{cases} \tag{4.17}$$

Use $[i-(L-1)]th$, $[i-(L-2)]th, \cdots$ and $i\,th$ experiments and find the coefficients of equation (4.17) by solving:

$$A_R = B\hat{M}_R \rightarrow B = A_R \hat{M}_R^{-1} \tag{4.18}$$

where:

$$A_R = \begin{bmatrix} a_{R1}(i) & a_{R1}(i-1) & \cdots & a_{R1}[i-(L-1)] \\ a_{R2}(i) & a_{R2}(i-1) & \cdots & a_{R2}[i-(L-1)] \\ \vdots & \vdots & \ddots & \vdots \\ a_{R(L-1)}(i) & a_{R(L-1)}(i-1) & \cdots & a_{R(L-1)}[i-(L-1)] \end{bmatrix}$$

$$\hat{M}_R = \begin{bmatrix} M_{R1}(i) & M_{R1}(i-1) & \cdots & M_{R1}[i-(L-1)] \\ \vdots & \vdots & \ddots & \vdots \\ M_{R(L-1)}(i) & M_{R(L-1)}(i-1) & \cdots & M_{R(L-1)}[i-(L-1)] \\ 1 & 1 & \cdots & 1 \end{bmatrix}$$

$$B = \begin{bmatrix} b_{i11} & b_{i12} & \cdots & b_{i1L} \\ b_{i21} & b_{i22} & \cdots & b_{i2L} \\ \vdots & \vdots & \ddots & \vdots \\ b_{i(L-1)1} & b_{i(L-1)2} & \cdots & b_{i(L-1)L} \end{bmatrix}$$

After calculating the matrix B from equation (4.18), the equation (4.17) can be rewritten for *(i+1)* experiment as:

$$A_R(i+1) = B_1 M_R(i+1) + B_2 \tag{4.19}$$

where:

$$A_R(i+1) = \begin{bmatrix} a_{R1}(i+1) \\ a_{R2}(i+1) \\ \vdots \\ a_{R(L-1)}(i+1) \end{bmatrix} \quad B_1 = \begin{bmatrix} b_{i11} & b_{i12} & \cdots & b_{i1(L-1)} \\ b_{i21} & b_{i22} & \cdots & b_{i2(L-1)} \\ \vdots & \vdots & \ddots & \vdots \\ b_{i(L-1)1} & b_{i(L-1)2} & \cdots & b_{i(L-1)(L-1)} \end{bmatrix}$$

$$M_R(i+1) = \begin{bmatrix} M_{R1}(i+1) \\ M_{R2}(i+1) \\ \vdots \\ M_{R(L-1)}(i+1) \end{bmatrix} \quad B_2 = \begin{bmatrix} b_{i1L} \\ b_{i1L} \\ \vdots \\ b_{i(L-1)L} \end{bmatrix}$$

4.6.5 Relay Ratios for the Next Experiment

The equation (4.16) shows the relation between relay ratios and DCP. This equation can be written as:

$$A_R(i+1) = B_t M_R(i+1) \tag{4.20}$$

where:

$$B_t = \begin{bmatrix} b_{t1} & 0 & \cdots & 0 \\ 0 & b_{t2} & \cdots & 0 \\ \vdots & \vdots & \ddots & \vdots \\ 0 & 0 & \cdots & b_{t(L-1)} \end{bmatrix} \qquad b_{tk} = [\tan\varphi_{dk} \frac{g_{kk}(0)}{g_{(k+1)(k+1)}(0)}] \quad k = 1,2,\cdots,L-1$$

Substitute for $A_R(i+1)$ in equation (4.19) from equation (4.20) and after some straightforward algebra the new relay ratios in compact form will be:

$$M_R(i+1) = [B_t - B_1]^{-1} B_2 \tag{4.21}$$

If the approximation (4.17) is perfectly accurate then $M_R(i+1)$ leads exactly to the desired critical point. Since it is not, there will be some error. A tolerance ε_k is defined, and algorithm is stopped when $|\varphi - \varphi_{dk}| < \varepsilon_k$ for each *(k=1,2,...,L-1)*. Otherwise, the procedure is continued in the same fashion as in experiment *(i+1)*. Where the best L experiments, i.e. those that are closer to φ_{dk} play the role of experiments $[i-(L-1)],[i-(L-2)],\cdots,i$ in equations (4.16)- (4.19). This simple algorithm shows excellent convergence properties. The details of this method for 3I3O systems have been shown in appendix 4.2.

Chapter 4

Decentralized PID controller tuning procedure for MIMO process

Algorithm 1: Decentralized PID tuning procedure for L-inputs and L-outputs process.

Step 1: Select *(L-1)* weighting factor for DCP from equation (4.12)

Step 2: Initialise the relay ratios for first L relay experiments:

For h *th* $(h = 1,2,\cdots,L)$ relay experiments

Select the relay ratio as equation (4.14)

Step 3: Determination of steady state gains

(a) Do first L relay experiments using initial relays ratios

(b) Calculate steady state gains from equation (4.13)

Step 4: Checking initial relays ratio for DCP

(a) Start with $h=1$ and calculate the following ratios:

$$\tan\varphi_k^h = \frac{a_{Rk}(h)}{M_{Rk}(h)}\frac{g_{(k+1)(k+1)}(0)}{g_{kk}(0)} \qquad k = 1,2,\cdots,L-1$$

(b) if $\left|\varphi_k^h - \varphi_{kd}\right| < \varepsilon_k$ choose h *th* critical point as DCP and Stop.

(c) $h = h+1$ if $h \le L$ $\rightarrow$ Go to Step 4 otherwise $i=L$

Step 5: Find new relays ratio:

(a) Find matrix B using equation (4.18)

(b) Find matrix $B1$,$B2$ and Bt using equation (4.19) and (4.20)

(c) Calculate $M_R(i+1)$ using equation (4.21)

Step 6: Checking new relays ratio for DCP

Form $(i+1)$ *th* relay experiment calculate the following ratios:

$$\tan\varphi_k^{i+1} = \frac{a_{Rk}(i+1)}{M_{Rk}(i+1)}\frac{g_{(k+1)(k+1)}(0)}{g_{kk}(0)} \qquad k = 1,2,\cdots,L-1$$

if $\left|\varphi_k^{i+1} - \varphi_{kd}\right| < \varepsilon_k$ choose $(i+1)$ *th* experiment critical point as DCP and stop

Step 7: Select the best L experiments from *(L+1)* available experiments, those that are closer to φ_{dk}. These experiments play the role of experiments $(h = 1,2,\cdots,L)$ in step 5.

Step 8: $i \rightarrow i+1$ and Go to Step 5.

4.7 PID Design at Bandwidth Frequency

The closed loop bandwidth, ω_b, (Fig 4.5) is the lowest frequency such that:

$$|T(j\omega_b)| = |T(0)|/\sqrt{2}$$

where:

$$T(s) = \frac{G(s)K(s)}{1+G(s)K(s)}$$

The loop bandwidth ω_b is usually very close to the 'gain cross-over' frequency ω_c, at which $|G(j\omega_c)K(j\omega_c)| = 1$. It has been illustrated that for typical, acceptable designs the loop bandwidth in terms of the crossover frequency could be estimated by: $\omega_c \le \omega_b \le 2\omega_c$ (Maciejowski, 1989).

4.7.1 Selecting the Range of Oscillation Frequency

If a $L \times L$ process is controlled by decentralized relay feedback, its outputs usually oscillate in the form of limit cycles after an initial transient. It was found by Atherton (1975) that for typical coupled multivariable processes, L outputs normally have the same oscillation frequencies, that is, $\omega_c = \omega_{c1} = \omega_{c2} \cdots = \omega_{cm}$, will be called common frequency, but different phases.

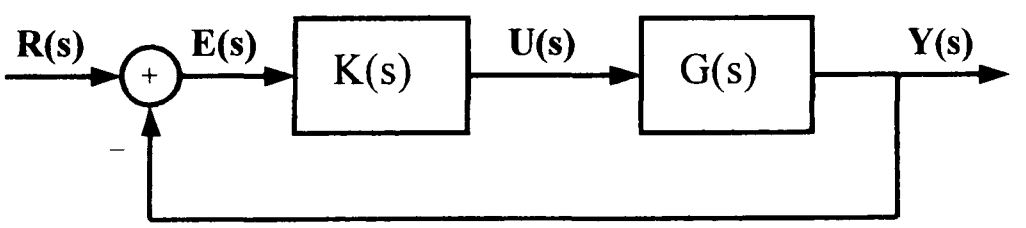

Fig 4.5: The closed loop block diagram of process and controller

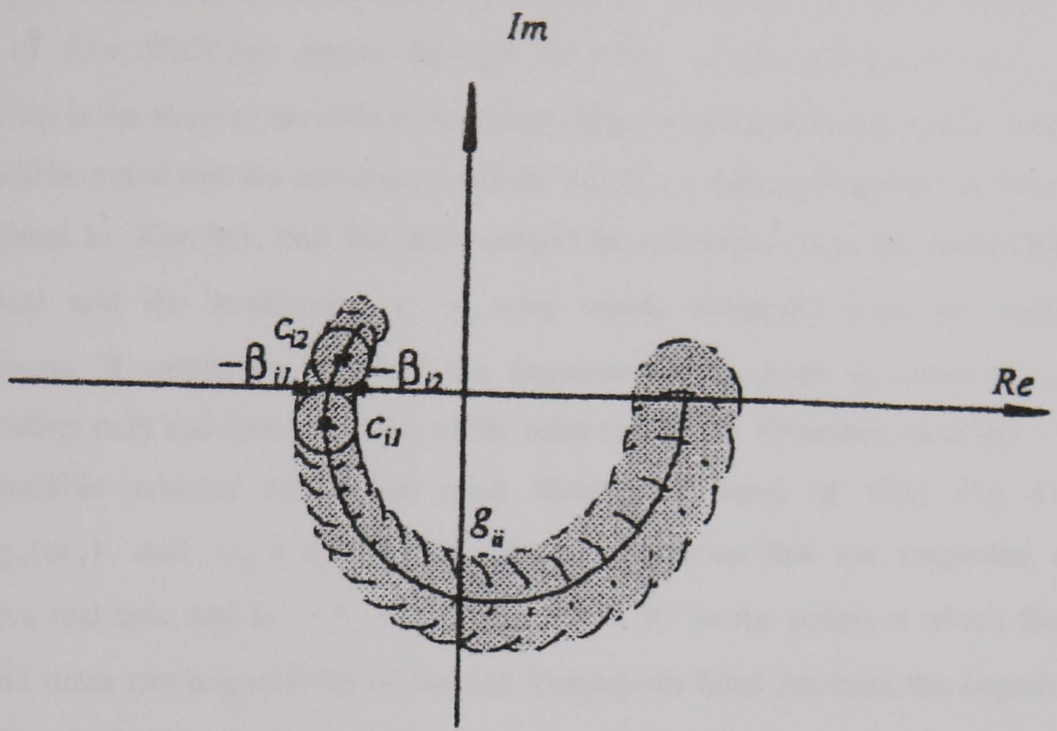

Fig 4.6:Gershgorin band

The describing function method was extended by Loh and Vasnani (1994) to analyse multivariable oscillations under decentralized relay feedback. In this context, it is assumed that the L-inputs, L-outputs process has low pass transfer function in each element of its transfer function matrix and one of its characteristic loci has at least 180° phase lag. Let the relay output amplitudes be M_i, the inputs of the relays have amplitudes a_i, and $K(a, M) = diag\{4M_i/\pi a_i\}$ be the describing-function matrix of the decentralized relay controller.

Theorem 2: (Loh and Vasnani, 1994) If the decentralized relay feedback system oscillates at a common frequency then at least one of the characteristic loci of $K(a, M)G(j\omega)$ crosses the point $-1+0j$ on the complex plane, and the oscillation frequency corresponds to the frequency at which the crossing occurs. Further, if the

process is stable then the limit cycle oscillation is stable, the outermost characteristic locus of $K(a, M)G(j\omega)$ passes through the point $-1+0j$ and the process critical frequency is the same as the critical frequency of the outermost characteristic locus.

It should be noted that the crossing condition and the oscillation frequency in Theorem 2 are related to $K(a, M)$, and the latter cannot be calculated until the oscillations are observed and the amplitudes a_i of relay inputs measured from the oscillation waveforms. It would be useful if the frequency were given in terms of process information only and independently of the relay controller. Therefore, consider a $L \times L$ multivariable process $G(s)$. For each Gershgorin band of $G(s)$ Fig 4.6, let $c_{i1} = g_{ii}(\omega_{i1})$ *and* $c_{i2} = g_{ii}(\omega_{i2})$ be centres of circles that are tangential to the negative real axis, and let $-\beta_{i1} + j0$ *and* $\beta_{i2} + j0$ be the points at which the outer rim and inner rim respectively of the *i th* Gershgorin band intersect the negative real axis. If *i th* Gershgorin band does not intersect the negative real axis, $[\omega_{i1}, \omega_{i2}]$ is defined to be empty. The following result gives an estimate of ω_c in terms of ω_{i1} *and* ω_{i2}.

Theorem 3: If the decentralized relay feedback system oscillates at a common frequency ω_c, then there exists $k \in \{1,2,\cdots, L\}$ such that $\omega_c \in [\omega_{k1}, \omega_{k2}]$.

Proof: (Wang *et al.*, 1997)

In view of Theorems 2 and 3, the oscillation frequency ω_c for a stable process depends on which characteristic locus of $G(s)$ is moved outermost by the multiplication of the corresponding relay element describing function $K_i = 4M_i/\pi a_i$. In general, one can enlarge the gain K_i by increasing the ratios of the relay amplitudes in the *i th* loop to those loops. This outermost loop is called the *dominant* loop. It should be noted that the dominant loop remains dominant and the critical frequency varies little with a fairly large change of relay amplitude ratios unless an inner characteristic locus becomes a new outermost.

Theorem 4: If the decentralized relay feedback system for a stable process oscillates at a common frequency and for some k, $K_k > \frac{K_i \beta_{i1}}{\beta_{k2}}, i = 1,2,\cdots,L,\ i \neq k$, then only $k\,th$ characteristic locus of $K(a,M)G(j\omega)$ crosses the point $-1+0j$ and the oscillation frequency satisfies $\omega_c \in [\omega_{k1}, \omega_{k2}]$.

Proof: (Wang *et al.*, 1997)

By Theorem 4, if the relay amplitudes is varied such that the resulting describing function gain matrix $K'(a,M)$ still satisfy $K_k' > \frac{K_i' \beta_{i1}}{\beta_{k2}}, i = 1,2,\cdots,L, i \neq k$, then the resulting limit-cycle oscillation frequency is expected to be in the range $[\omega_{k1}, \omega_{k2}]$, and thus close to the previous value if the interval $[\omega_{k1}, \omega_{k2}]$ is small. In general the conditions $K_k > \frac{K_i \beta_{i1}}{\beta_{k2}}, i = 1,2,\cdots,L, i \neq k$, remain true if one increases the amplitude of the dominant loop or decreases one or more relay amplitudes among other loops.

The preceding discussion indicates that by increasing the amplitude of the dominant loop or decreasing one or more relay amplitudes among other loops, the limit-cycle oscillation frequency is expected to remain constant. This means choosing the *dominant* loop has the effect of choosing the range of frequency

4.7.2 Desired Critical Points Criteria

To determine the DCP, it is necessary that relative importance of the loops corresponding to a particular point should be described. Since the significant performance parameter is the loop gain at bandwidth frequency, the proposed method selects criteria (4.22) to choose desired critical point:

$$\tan\varphi_{dk} = \frac{C_{(k+1)k}}{1} = \frac{K_{(k+1)cr}\, g_{(k+1)(k+1)}(\omega_b)}{K_{kcr}\, g_{kk}(\omega_b)} \qquad k = 1,2\cdots,(L-1) \tag{4.22}$$

where:

$C_{(k+1)k}$ is the weighting factor of the $(k+1)\,th$ loop relative to the $k\,th$ loop. Selecting $C_{(k+1)k}$ >1 means that loop $(k+1)$ is required to be under tighter control relative to loop k at bandwidth frequency. The relative weightings can be alternatively expressed via the angle φ_{dk}, defined in the above formula. The angle φ_{dk} connects a critical point to the origin in the loop-gain plane. The subscript 'd' denotes a desired quantity as shown.

$g_{kk}(\omega_b)$: is as constant real approximation to $g_{kk}(s)$ at particular point $s = j\omega_b$ using the ALIGN algorithm (Kouvaritakis, 1974).

$$\begin{bmatrix} g_{11}(\omega_b) & g_{12}(\omega_b) & \cdots & g_{1L}(\omega_b) \\ g_{21}(\omega_b) & g_{22}(\omega_b) & \cdots & g_{2L}(\omega_b) \\ \vdots & \vdots & \ddots & \vdots \\ g_{L1}(\omega_b) & g_{L2}(\omega_b) & \cdots & g_{LL}(\omega_b) \end{bmatrix} = ALIGN\left(\begin{bmatrix} g_{11}(j\omega_b) & g_{12}(j\omega_b) & \cdots & g_{1L}(j\omega_b) \\ g_{21}(j\omega_b) & g_{22}(j\omega_b) & \cdots & g_{2L}(j\omega_b) \\ \vdots & \vdots & \ddots & \vdots \\ g_{L1}(j\omega_b) & g_{L2}(j\omega_b) & \cdots & g_{LL}(j\omega_b) \end{bmatrix}\right)$$

ω_b is bandwidth of the transfer function matrix. Therefore the weighting factors $C_{(k+1)k}$ are calculated at bandwidth frequency compare with the Palmor method where $C_{(k+1)k}$ was calculated at zero frequency.

4.7.3 Determination of Gains at Bandwidth Frequency

To identify the process frequency response $G(j\omega)$ at the critical oscillation frequency $\omega_c \approx \omega_b$, the equation (4.3) can be used.

Decentralized PID controller for MIMO process at bandwidth frequency

Algorithm 2: Decentralized PID controller tuning procedure for MIMO process at bandwidth frequency:

Step 1: Select *(L-1)* weighting factors for DCP:

$$\tan\varphi_{dk} = \frac{C_{(k+1)k}}{1} = \frac{K_{(k+1)cr}\, g_{(k+1)(k+1)}(\omega_b)}{K_{kcr}\, g_{kk}(\omega_b)} \qquad k = 1,2\cdots,(L-1)$$

Step 2: Determine the process gain at ω_c: $G(j\omega_b) = Y(j\omega_b)U^{-1}(j\omega_b)$ from (4.3)

Step 3: Initialise the relay ratios for first L relay experiments:

For h *th* $(h = 1,2,\cdots,L)$ relay experiments select the relay ratio as:

$$M_{R_{max}k}(h) = \frac{\overline{M}_h(h)}{\underline{M}_k(h)}, \quad [k = 1,2,\cdots,(L-1)]$$

Step 4: Start with $h=1$ and for h *th* relay experiment, calculate the following ratios:

$$\tan\varphi_k^h = \frac{a_{Rk}(h)}{M_{Rk}(h)} \frac{g_{(k+1)(k+1)}(\omega_b)}{g_{kk}(\omega_b)} \qquad k = 1,2,\cdots,L-1$$

if $\left|\varphi_k^h - \varphi_{kd}\right| < \varepsilon_k$ → Stop.

$h = h+1$ if $h \le L$ → Go to Step 4 Otherwise: $i=L$

Step 5: Find new relay ratio: $M_R(i+1) = [B_t - B_1]^{-1} B_2$

The same as, algorithm 1 with considering gains in bandwidth frequency.

Step 6: Form $(i+1)$ *th* relay experiment, calculate the following ratios:

$$\tan\varphi_k^{i+1} = \frac{a_{Rk}(i+1)}{M_{Rk}(i+1)} \frac{g_{(k+1)(k+1)}(\omega_b)}{g_{kk}(\omega_b)} \qquad k = 1,2,\cdots,L-1$$

if $\left|\varphi_k^{i+1} - \varphi_{kd}\right| < \varepsilon_k$ → Stop

Step 7: Select the best L experiments from *(L+1)* available experiments, those that are closer to φ_{dk}. These experiments play the role of experiments $(h = 1,2,\cdots,L)$.

Step 8: i → $i+1$ and Go to Step 5.

4.8 Case Studies

In this section three systems are considered. PID controller parameters using Palmor (called method 1) and proposed (called method 2) tuning methods for these systems will be calculated. Then nominal performance and robustness stability and robustness performance of closed loop systems of Palmor method will be compared with proposed method. The criteria previously introduced in section 3.3 will be used to compare the two methods. This means the closed loop system should satisfy the following conditions:

For nominal performance:

$$\left\|\omega_2(s)[I+G(s)K(s)]^{-1}\right\| < 1$$

For robust stability:

$$\left\|\omega_1(s)G(s)K(s)[I+G(s)K(s)]^{-1}\right\|_\infty < 1$$

For robust performance:

$$J = \min_{K(s)} \{\sum_{i=1}^{m} \omega_p \left| \mu_{\Delta G(s)} [M(s)] - 1 \right|^2 + \omega_u \mu_{\Delta G(s)} [C(s)]\}$$

Example1: Consider the process (Wood and Berry, 1973)

$$G(s)=\begin{bmatrix}\dfrac{12.8e^{-s}}{16.7s+1} & \dfrac{-18.9e^{-3s}}{21s+1}\\ \dfrac{6.6e^{-7s}}{10.9s+1} & \dfrac{-19.6e^{-3s}}{14.4s+1}\end{bmatrix} \tag{4.23}$$

The data collected for Palmor method (method 1) and the proposed method (method 2) are summarised in Table 4.1. Both methods converged in 4 iterations. The DCP are K_{c1}=0.402, K_{c2}=-0.261 and K_{c1}=0.1682, K_{c2}=-0.3223 in Palmor and proposed method, respectively. Fig 4.8 shows that the controlled system has achieved nominal performance for both methods. Also, the comparison of robustness stability and performance of the two methods show Palmor method has poor robustness performance and robustness stability compared to proposed method Fig 4.8. The step response of the methods has been shown in Fig 4.9.

Table 4.1:The data collected for Palmor the proposed method during tuning session

Exp. No.		M_1	M_2	a_1	a_2	K_{1cr}	K_{2cr}	ω_{cr}	$\lvert\phi-\phi_d\rvert$
1	Method1	0.3	0.03	0.224	0.154	1.7	-0.248	1.56	32.5
	Method2	0.3	0.03	0.224	0.154	1.7	-0.248	1.56	41
2	Method1	0.02	0.08	0.212	0.307	0.12	-0.331	0.529	31.5
	Method2	0.02	0.08	0.212	0.307	0.12	-0.331	0.529	12
3	Method1	.092	0.08	0.138	0.441	0.853	-0.23	0.498	22.7
	Method2	0.0312	0.08	0.217	0.3445	0.1831	-0.2957	0.5216	3
4	Method1	0.059	0.08	0.186	0.389	0.402	-0.261	0.491	0.44
	Method2	0.0286	0.08	0.2165	0.3165	0.1682	-0.3223	0.5271	1.7

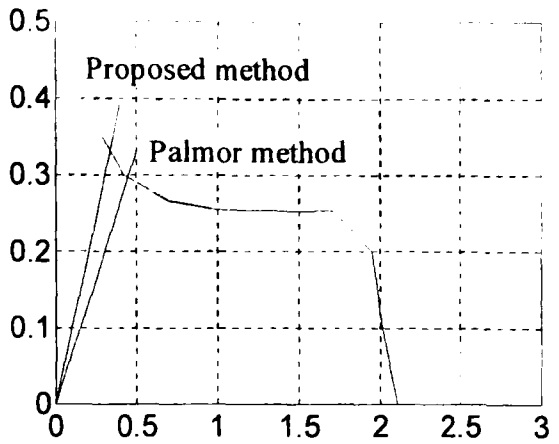

Fig 4.7: Critical point of example 1

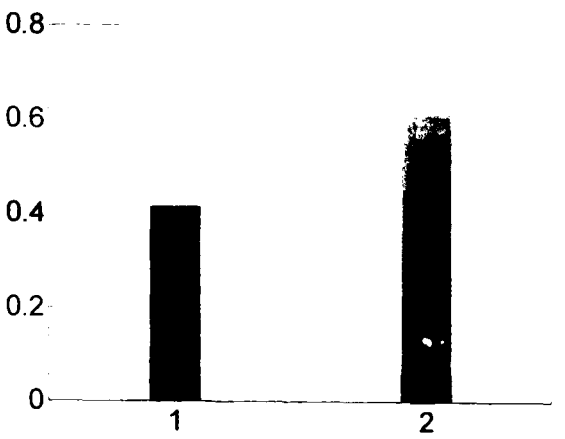

Fig 4.8a: Nominal performance

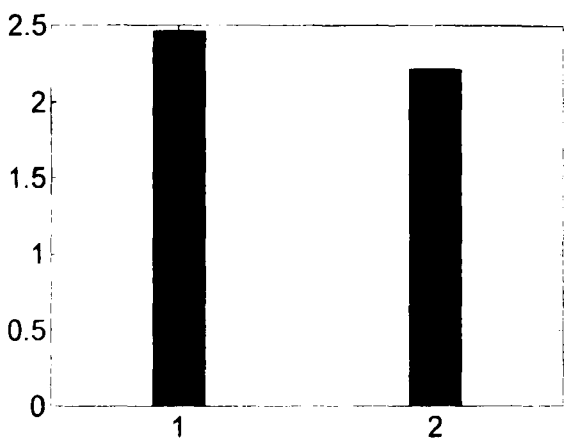

Fig 4.8b: Robustness Stability

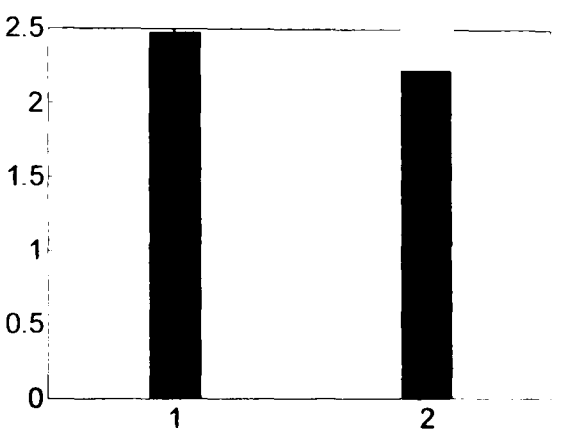

Fig 4.8c:Robustness Performance

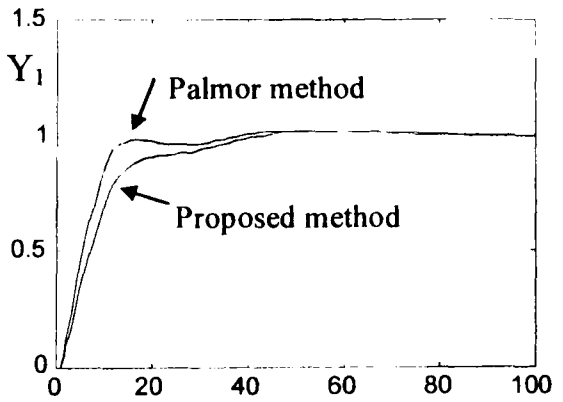

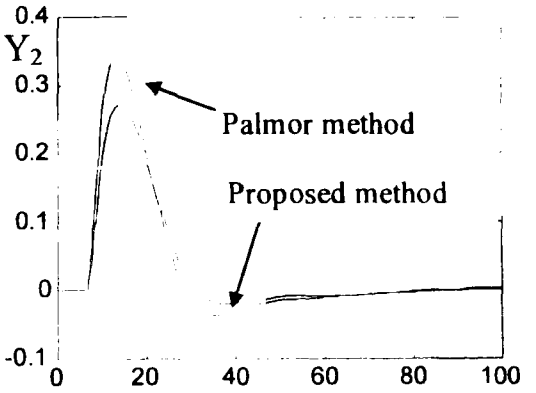

Fig 4.9a: Outputs Response (Y_1 and Y_2) to step changes in r1

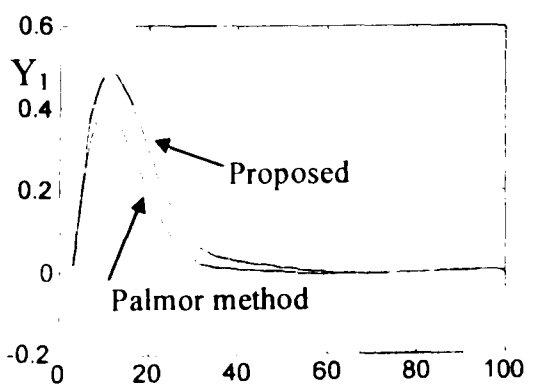

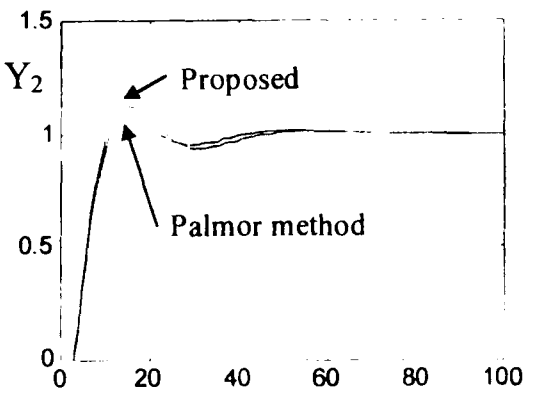

Fig 4.9b: Outputs response (Y_1 and Y_2) to step changes in r2

Example2:

As a second example, the boiler model from Chapter 3, equation (3.55) has been considered.

$$G(s)=\begin{bmatrix} g7 & g8 \\ g3 & g4 \end{bmatrix}=\begin{bmatrix} \dfrac{-.007s+.00078}{s^2+.0178s+.00055} & \dfrac{-.005s+7e-5}{s^2+.017s+.0004} \\ \dfrac{-.0067s+.00062}{s^2+.017s+.00053} & \dfrac{s^2+.043s+.00065}{s^2+.067s+.0006} \end{bmatrix} \tag{4.24}$$

where the manipulated variable $u_1(s)$ and $u_2(s)$ are the feed/air demand and the control valve position respectively. The control variables $y_1(s)$ and $y_2(s)$ are throttle pressure and the steam flow respectively. The boiler model has been used to calculate the best DCP. The data collected for Palmor method and the proposed method are summarised in Table 4.2. Both two methods were converged in 4 iterations. The DCP are K_{c1}=2.02, K_{c2}=1.96 and K_{c1}=1.97, K_{c2}=1.68 in the Palmor and proposed method, respectively.

Fig 4.10 shows that the controlled system has achieved nominal performance for both methods. The comparison of robustness stability and robustness performance of two methods show proposed method has better robustness performance and robustness stability compared to Palmor method Fig 4.11. The step response of the methods has been shown in Fig 4.12. From step responses it is clear that both two methods almost show the same performance.

Table 4.2: The data collected for Palmor the proposed method during tuning session

Exp. No.		M_1	M_2	a_1	a_2	K_{1cr}	K_{2cr}	ω_{cr}	$\lvert\phi - \phi_d\rvert$
1	Method1	0.9	0.5	0.513	0.235	2.234	2.71	0.033	6.34
	Method2	0.9	0.5	0.513	0.235	2.234	2.71	0.033	10.14
2	Method1	1.716	0.5	1.122	0.422	1.95	1.51	0.035	6
	Method2	1.716	0.5	1.122	0.422	1.95	1.51	0.035	2.5
3	Method1	1.23	0.5	0.77	0.317	2.03	2.01	0.036	0.65
	Method2	1.49	0.5	0.962	0.375	1.975	1.698	0.037	0.39
4	Method1	1.264	0.5	0.798	0.325	2.02	1.96	0.037	0.1
	Method2	1.518	0.5	0.981	0.38	1.97	1.68	0.037	0.04

Remarks:

For the Boiler example the following result are obtained:

1-As the Boiler model in non-linear, the oscillation frequency has wide range variation.

2-The critical points not only depend on the ratio M_1/M_2, but also depend on the absolute magnitudes M_1 and M_2.

3-variation of M_i that produce the oscillation is small, in the other word $(\overline{M_i} - \underline{M_i})$ is small.

- 1: Palmor Method
- 2: Proposed Method

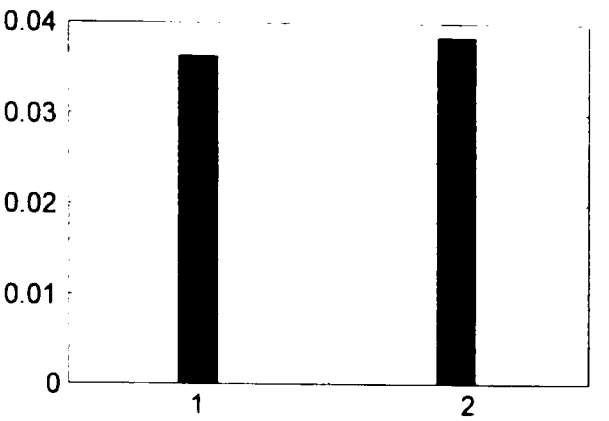

Fig 4.10: Nominal performance

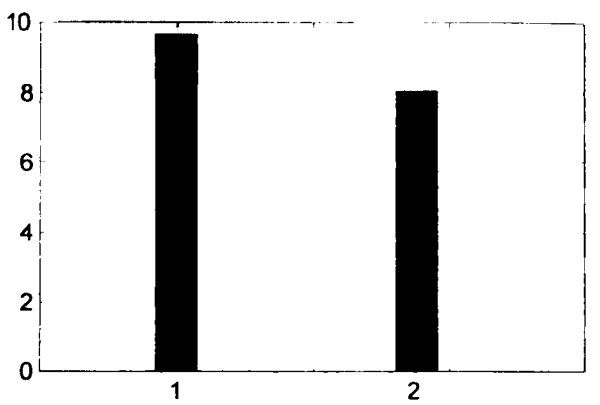

Fig 4.11a: Robustness Stability

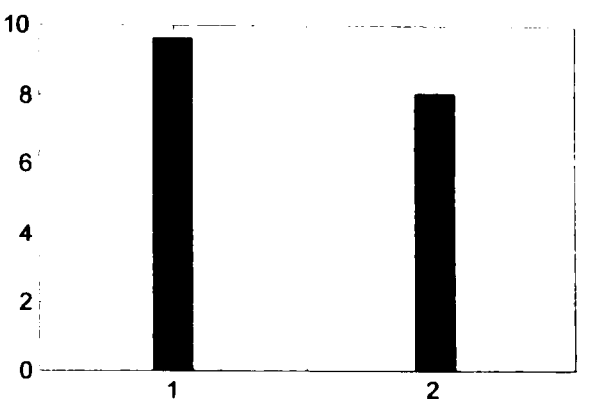

Fig 4.11b:Robustness Performance

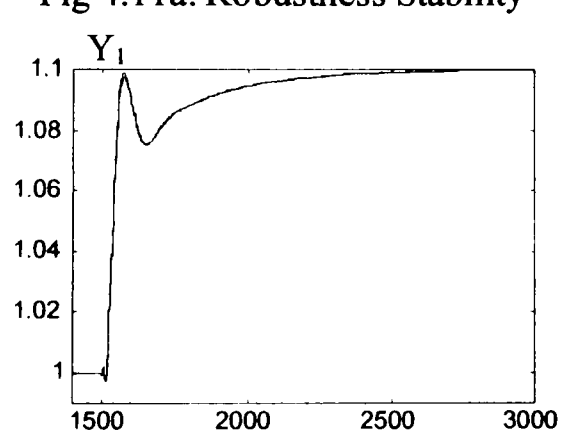

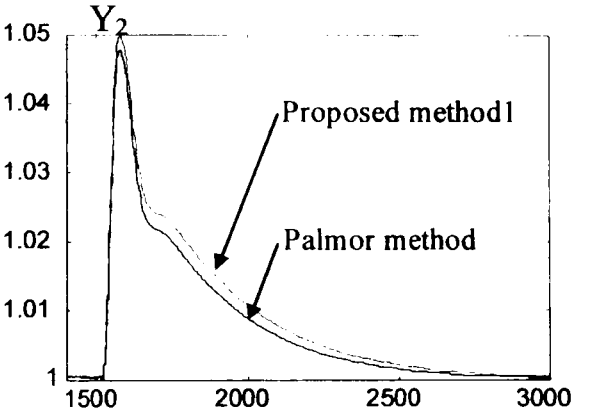

Fig 4.12a: Outputs response (Y_1 and Y_2) to step changes in r1

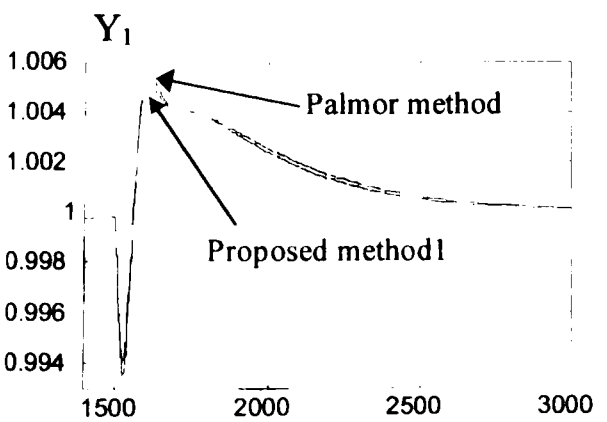

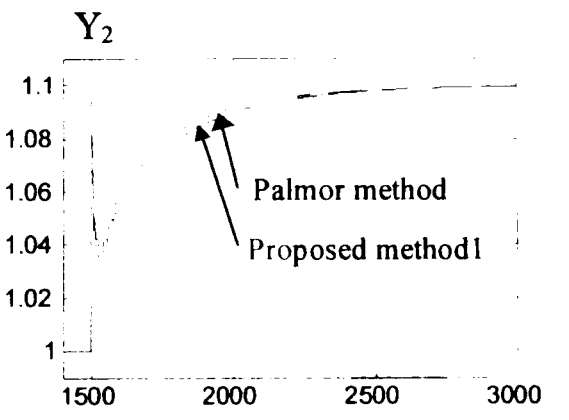

Fig 4.12b: Outputs Response (Y_1 and Y_2) to step changes in r2

Table.4.3: The data collected for 3I3O system, Palmor method during tuning session

Exp. No.		M_1	M_2	M_3	a_1	a_2	a_2	K_{1cr}	K_{2cr}	K_{3cr}	ω_{cr}	φ_1	φ_2
1	Method1	-7	0.7	-0.7	1.04	0.656	0.24	8.57	1.36	3.71	1.73	4.53	85
2	Method1	-1.25	2.5	-0.7	0.498	1.254	1.787	3.2	2.54	0.5	0.683	21.7	38.2
3	Method1	-0.446	2.5	-0.738	0.583	1.165	1.787	0.974	2.73	0.526	0.712	54.5	37.6
4	Method1	-0.944	2.5	-0.862	0.55	1.21	1.86	2.19	2.63	0.59	0.7	31	41.9
5	Method1	-0.633	2.5	-1.024	0.585	1.338	1.993	1.38	2.38	0.654	0.728	40.8	47.7
6	Method1	-0.553	2.5	-0.936	0.59	1.293	1.969	1.193	2.46	0.605	0.725	45.9	44.5
7	Method1	-0.564	2.5	-0.948	0.594	1.31	1.95	1.21	2.43	0.619	0.726	45.1	45.2

Example3: As last example, a 3I3O process plants is considered as follows:

$$\begin{bmatrix} \frac{-1}{6s+1}e^{-s} & \frac{1.5}{15s+1}e^{-s} & \frac{0.5}{10s+1}e^{-s} \\ \frac{0.5}{s^2+4s+1}e^{-2s} & \frac{0.5}{s^2+4s+1}e^{-3s} & \frac{0.513}{s+1}e^{-2s} \\ \frac{0.375}{10s+1}e^{-3s} & \frac{-2}{10s+1}e^{-2s} & \frac{-2}{3s+1}e^{-3s} \end{bmatrix}$$

The data collected for the Palmor method is summarised in Table 4.3. The results show that the extended Palmor method for 3I3O is converged to DCP in 7 iterations.

4.9 Summary

In this chapter, first the Palmor decentralized relay identification method for PID tuning for 2I2O systems was extended for MIMO systems. The tuning procedure consists of two stages. In the first stage, the desired critical point, which consists of the steady state gains of L loops and a critical frequency, is identified. In the second stage, the data of the desired critical point is used to tune the PID controller by the Ziegler-Nichols rule or its modifications.

Then, a new criterion for tuning of decentralized PID controller for MIMO plants was introduced. In the proposed method the bandwidth frequency of the system was used to calculate the DCP. The process gains at crossovers frequency, which are required for the appropriate DCP choice of the, are determined using L relays experiments.

The robustness and performance of method was compared with the Palmor method. The results showed that the method is more robust and converges faster than Palmor method.

Chapter 5

The SISO Predictive PID Controller Design Problem

5.1 Introduction

Proportional-Integral-Derivative (PID) controllers and Generalised Predictive Controllers (GPC) are the two control algorithms commonly found in industrial applications. PID controllers are used extensively in the process industries because of their robust performance and simplicity. The three parameters of a PID controller must be tuned to the process to obtain a satisfactory closed-loop process performance.

Over the years, numerous techniques have been suggested for tuning of the PID parameters. Explicit relations for tuning PID controllers were proposed in (Ziegler and Nichols, 1942); (Cohen and Coon 1953). These tuning methods have practical value but also suffer from some limitations. The Ziegler-Nichols paper (1942) had two procedures, one a closed loop sustained oscillation method that extracts the critical point of a plant by driving the plant to the stability boundary. For some processes this can be risky.

Second, the open loop reaction curve method which was modified later by Cohen and Coon. The Cohen-Coon method requires an open loop test on the process and is inconvenient to apply. Astrom and Hagglund (1988) developed a relay feedback technique for auto tuning of PID controllers. For many years, because of its simplicity and efficiency, relay based auto-tuning methods have been integrated into commercial controllers, which have been successful in many process control applications (Astrom and Hagglund, 1995). The structure of PID controllers is discussed in (He and Garvey, 1996) with respect to self-tuning algorithms and automatic selection of structures. There is a wealth of literature on PID tuning for scalar systems. Good reviews of tuning PID methods are given in Astrom *et al.*, 1993; Astrom *et al* 1995; Gorez and Calcev (1997), Tan *et al.* (1999) and Yu (1999).

On the other hand, the GPC method was proposed by Clarke *et al.* (1987) and this has become one of the most popular Model Based Predictive Control (MPC) methods both in industry and academia (Maciejowski, 2001). It has been successfully implemented in many industrial applications (Clarke, 1988) showing good performance and a certain degree of robustness. It can handle many different control problems for a wide range of plants with a reasonable number of design variables, which have to be specified by the user depending upon prior knowledge of the plant and control objectives. The GPC provides an analytical solution; it can deal with unstable and non-minimum phase plants. The GPC is an optimal method, which incorporates the concept of a control horizon as well as the consideration of weighting of control increments in the cost function.

Because of wide application of the PID controllers, many researchers have attempted to use advanced control techniques such as optimal control and GPC to restrict the structure of these controllers to retrieve the PID controller. Rivera *et al.* (1986) introduced an IMC based PID controller design for a first order process model and Chien (1988) extended IMC-PID controller design to cover the second order process model. The limitation of these works is that the tuning rules are derived for the delay

free system. A first order Pade approximation or a first order Taylor series expansion was used to remove the delay from the system. Morari and Zafiriou (1989); Morari (1994) have shown that IMC leads to PID controllers for virtually all models common in industrial practice. In Wang *et al.* (2000) a least square algorithm was used to compute the closest equivalent PID controller to an IMC design and a frequency response approach is adopted. However, the design is still ineffective when applied to time-delay and unstable systems. Marques and Fliess (2000) have developed a simple approach for PID control of linear continuous systems based on flat output trajectory generation. Important characteristics of model predictive control methods have been combined with PID control properties by considering flatness based predicted trajectories. In Rusnak's works (1999; 2000) the linear quadratic regulator (LQR) theory has been used to formulate tracking problems and to show those cases when the solution gives PID controllers. This avoided heuristics and gives a systematic approach to the explanation of the good performance of the PID controllers. In Rusnak (2000) the generalised PID structure had been introduced and applied up to a fifth order system. Tan *et al.* (2000) have also presented a PID control design based on a GPC approach. The real time application results showed that their method is applicable and efficient.

This Chapter presents a predictive PID controller, which has important characteristics of the MPC. The PID controller is defined by using a bank of M parallel conventional PID controllers where M is the prediction horizon. The Chapter has been organised as follow: Section 2 defines the predictive PID controller. The optimal values of gains are calculated in Section 3. The stability of the closed loop system is studied in Section 4. The controller for low order systems is calculated in Section 5. The constraint handling is discussed in Section 6. Simulation results are presented in Section 7 and the conclusion is drawn in Section 8.

5.2 PID Type Predictor

5.2.1 Introduction

In conventional PID the control actions are taken based on past and present error of the output with respect to set point. But in Predictive PID controller, that will be introduced later, the output of controller depends on past, present and predicted future error. Predicted future output of system, like MPC, will be used to estimate the future error. The prediction horizon of predictive PID, called M, is the most important parameter of the controller that should be tuned. It is clear that without prediction (M=0) the predictive PID is like conventional PID.

5.2.2 General form of PID

A discrete PID controller has the following form:

$$\tilde{u}(k) = k_P e(k) + k_I \sum_{j=1}^{k} e(j) + k_D[e(k) - e(k-1)] \tag{5.1}$$

where:

k_P, k_I and k_D are the proportional, integral and derivates gains, respectively.

Taking the difference on both sides of equation (5.1) at step (k) and (k-1) leads to:

$$\begin{aligned} \Delta\tilde{u}(k) &= \tilde{u}(k) - \tilde{u}(k-1) \\ &= k_P[e(k) - e(k-1)] + k_I e(k) + k_D[e(k) - 2e(k-1) + e(k-2)] \end{aligned} \tag{5.2}$$

Transforming equation (5.2) into z domain gives:

$$\widetilde{U}(z) = \frac{[q_0 + q_1 z^{-1} + q_2 z^{-2}]}{1 - z^{-1}} E(z) \tag{5.3}$$

where:

$q_0 = (k_P + k_I + k_D), \quad q_1 = -(k_P + 2k_D) \quad q_2 = k_D$

5.2.3 Predictive form of PID

A type of predictive PID controller is defined as follows:

$$u(k) = \sum_{i=0}^{M} \left(k_P e(k+i) + k_I \sum_{j=1}^{k} e(j+i) + k_D [e(k+i) - e(k+i-1)] \right) \tag{5.4}$$

The controller consists of M parallel PID controllers as shown in Fig 5.1a. For M=0, the controller is identical to the conventional PID in equation (5.1). For M>0 the proposed controller has predictive capability similar to MPC where M is prediction horizon of PID controller. The horizon, M will be selected to find the best approximation to GPC solution. Using (5.1), equation (5.4) can be decomposed into M control signal as follows:

$$u(k) = \widetilde{u}(k) + \widetilde{u}(k+1) + \cdots + \widetilde{u}(k+M) \tag{5.5}$$

where:

$$\widetilde{u}(k+i) = \left(k_P e(k+i) + k_I \sum_{j=1}^{k} e(j+i) + k_D (e(k+i) - e(k+i-1)) \right) \qquad (i = 0, \cdots, M)$$

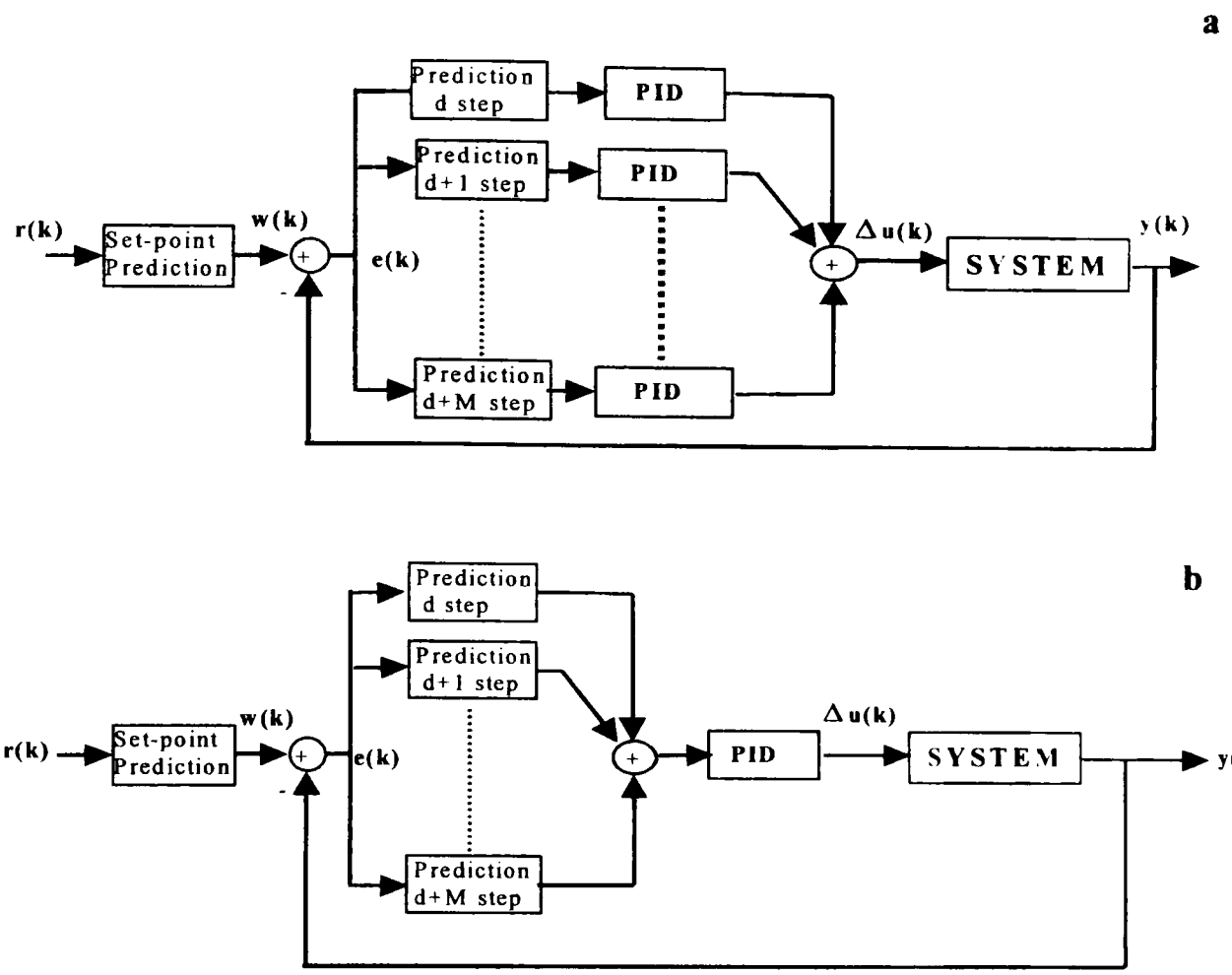

Fig 5.1: The block diagram of proposed method

a) *M* level of PID b) *M* horizon prediction c) Structure of controller.

It is assumed that $e=r-y=-y$ $(r=0)$ and if incremental form of control signal is considered, $\Delta u(k)=u(k)-u(k-1)$, and after some straightforward algebra, the control signal can be written as:

$$\Delta u(k) = \Delta \tilde{u}(k) + \Delta \tilde{u}(k+1) + \cdots + \Delta \tilde{u}(k+M) \tag{5.6}$$

where:

$$\Delta \tilde{u}(k+i) = -\{k_P[y(k+i)-y(k+i-1)] + k_I y(k+i) + k_D[y(k+i)-2y(k+i-1)+y(k+i-2)]\}$$

In compact form $\Delta \tilde{u}(k+i)$ can be written as:

$$\Delta \tilde{u}(k+i) = -KY(k+i) \tag{5.7}$$

where:

$$K = [k_D \quad -k_P - 2k_D \quad k_P + k_I + k_D]$$
$$Y(k+i) = [y(k+i-2) \quad y(k+i-1) \quad y(k+i)]^T$$

Using equation (5.7) in equation (5.5):

$$\begin{aligned}\Delta u(k) &= \Delta \tilde{u}(k) + \Delta \tilde{u}(k+1) + \cdots + \Delta \tilde{u}(k+M) \\ &= -K\{Y(k) + Y(k+1) + \cdots + Y(k+M)\}\end{aligned} \tag{5.8}$$

This implies that the current control signal value is a linear combination of the future predicted outputs. So, the future output should be predicted.

Future Output Predictor for Predictive PID

A CARIMA model for SISO process can be expressed as:

$$A(z^{-1})y(k) = B(z^{-1})\Delta u(k-1) \tag{5.9}$$

where:

$$A(z^{-1}) = 1 + a_1 z^{-1} + \cdots + a_{n_a} z^{-n_a}$$

$$B(z^{-1}) = b_0 + b_1 z^{-1} + \cdots + b_{n_b} z^{-n_b}$$

The i th step ahead prediction of output can be obtained from the following equation (Camacho and Bordons, 1999):

$$\begin{aligned} y(k+i) = &\begin{bmatrix} g_{i-1} & g_{i-2} & \cdots & g_0 \end{bmatrix} \begin{bmatrix} \Delta u(t) \\ \Delta u(t+1) \\ \vdots \\ \Delta u(t+i-1) \end{bmatrix} \\ &+ \begin{bmatrix} f_{i1} & f_{i2} & \cdots & f_{i(n_a+1)} \end{bmatrix} \begin{bmatrix} y(t) \\ y(t-1) \\ \vdots \\ y(t-n_a) \end{bmatrix} + \begin{bmatrix} g_{i1}^{'} & g_{i2}^{'} & \cdots & g_{in_b}^{'} \end{bmatrix} \begin{bmatrix} \Delta u(t-1) \\ \Delta u(t-2) \\ \vdots \\ \Delta u(t-n_b) \end{bmatrix} \end{aligned} \tag{5.10}$$

Therefore, from equation (5.7) the output prediction for i th PID will be:

$$Y(k+i) = G_i \Delta \hat{u}(k) + F_i y_0(k) + G_i^{'} \Delta u_0(k) \tag{5.11}$$

where:

$$G_i = \begin{bmatrix} g_{i-3} & \cdots & g_0 & 0 & 0 \\ g_{i-2} & g_{i-3} & \cdots & g_0 & 0 \\ g_{i-1} & g_{i-2} & g_{i-3} & \cdots & g_0 \end{bmatrix}_{3 \times Nu} \qquad F_i = \begin{bmatrix} f_{(i-2)1} & f_{(i-2)2} & \cdots & f_{(i-2)(n_a+1)} \\ f_{(i-1)1} & f_{(i-1)2} & \cdots & f_{(i-1)(n_a+1)} \\ f_{i1} & f_{i2} & \cdots & f_{i(n_a+1)} \end{bmatrix}$$

$$G_i^{'} = \begin{bmatrix} g_{(i-2)1}^{'} & g_{(i-2)2}^{'} & \cdots & g_{(i-2)n_b}^{'} \\ g_{(i-1)1}^{'} & g_{(i-1)2}^{'} & \cdots & g_{(i-1)n_b}^{'} \\ g_{i1}^{'} & g_{i2}^{'} & \cdots & g_{in_b}^{'} \end{bmatrix}$$

$$\Delta\hat{u}(k) = \begin{bmatrix} \Delta u(k) & \Delta u(k+1) & \cdots & \Delta u(k+N_u-1) \end{bmatrix}^T$$

$$\Delta u_0(k) = \begin{bmatrix} \Delta u(k-1) & \Delta u(k-2) & \cdots & \Delta u(k-n_b) \end{bmatrix}^T$$

$$y_0(k) = \begin{bmatrix} y(k) & y(k-1) & \cdots & y(k-n_a) \end{bmatrix}^T$$

In equation (5.11), future control inputs$\{\Delta u(k+i) \quad i = 1{:}(N_u - 1)\}$ are needed to calculate the present control signal. Substituting equation (5.11) in equation (5.8):

$$\Delta u(k) = -K\sum_{i=0}^{M} Y(k+1) = -K\left\{\sum_{i=0}^{M} G_i \Delta\hat{u}(k) + \sum_{i=0}^{M} F_i y_0(k) + \sum_{i=0}^{M} G_i^{'} \Delta u_0(k)\right\} \tag{5.12}$$

Rewriting the control signal in compact form for PID type predictive control gives:

$$\Delta u(k) = -K\left\{\alpha\Delta\hat{u}(k) + F_f y_0(k) + G_g \Delta u_0(k)\right\} \tag{5.13}$$

where:

$$\alpha = \sum_{i=0}^{M} G_i \qquad F_f = \sum_{i=0}^{M} F_i \qquad G_g = \sum_{i=0}^{M} G_i^{'}$$

In real world where systems are causal, the control signal could not depend on future control signal, so the $\{\Delta u(k+i) = 0 \quad i = 1{:}(N_u - 1)\}$ and the equation (5.13) can be written as:

$$\Delta u(k) = -(1 + K\alpha)^{-1} K\left\{F_f y_0(k) + G_g \Delta u_0(k)\right\} \tag{5.14}$$

In equation (5.14) the output of predictive PID controller is defined as function of process specification (α, F_f, G_g) and PID gains.

5.2.4 System with Time Delay

For system with time delay, d, the output of the process will not be affected by $\Delta u(k)$ until the time instant *(k+d+1)*, the previous outputs will be a part of the free response and there is no point in considering them as part of the objective function. In this case the first PID predicts d step ahead and last PID predicts *(d+M)* step ahead Fig 5.1. The control signal can be written as:

$$\Delta u(k-d) = -(1+K\alpha)^{-1} K\left\{F_f y_0(k) + G_g \Delta u_0(k)\right\}$$

Shifting the control signal for d step ahead gives:

$$\Delta u(k) = -(1+K\alpha_d)^{-1} K\left\{F_{fd} y_0(k) + G_{gd} \Delta u_0(k)\right\} \tag{5.15}$$

where coefficient matrices are:

$$\alpha_d = \sum_{i=d}^{d+M} G_i \qquad F_{fd} = \sum_{i=d}^{d+M} F_i \qquad G_{gd} = \sum_{i=d}^{d+M} G_i$$

5.3 Optimal Values of PID-type Predictive Gains

To obtain the optimal values of the gains, the Generalised Predictive Control (GPC) algorithm is used. For process control, default settings of output cost horizon $\{N_1 : N_2\} = \{1:N\}$, and the control cost horizon $N_u = 1$ can be used in GPC to give reasonable performance (Clarke *et al.*,1987). GPC consists of applying a control sequence that minimises the following cost function:

$$J(1,N)=\sum_{i=1}^{N}[y(k+d+i)-w(k+d+i)]^2+\lambda\Delta u(k)\Delta u(k) \tag{5.16}$$

The minimum of J (assuming there are no constraints on the control signals) is found using the usual gradient analysis, which leads to (Camacho and Bordons, 1999):

$$\Delta u(k)=(G^TG+\lambda I)^{-1}G^T[w-Fy_0(k)-G'\Delta u_0(k)] \tag{5.17}$$

which can summarised (assuming the future set point $w(t+i)$=0):

$$\Delta u(k)=-K_{GPC}[F \quad G']\begin{bmatrix}y_0(k)\\ \Delta u_0(k)\end{bmatrix}=-K_0\begin{bmatrix}y_0(k)\\ \Delta u_0(k)\end{bmatrix} \tag{5.18}$$

where:

$$K_0=K_{GPC}[F \quad G'] \qquad \Delta u_0(k)=\begin{bmatrix}\Delta u(k-1) & \Delta u(k-2) & \cdots & \Delta u(k-n_b)\end{bmatrix}^T$$

$$y_0(k)=\begin{bmatrix}y(k) & y(k-1) & \cdots & y(k-n_a)\end{bmatrix}^T \qquad K_{GPC}=(G^TG+\lambda I)^{-1}G^T$$

To compute the optimal values of predictive control PID gains, the PID control signals should be made the same as GPC controller. This means using equation (5.13) and (5.18), the following optimal problem should be solved:

$$Min_{K\in K^S_{PID},M}J(K,K_0) \tag{5.19}$$

K^S_{PID} = Set of stability gain for PID

where:

$$J(K,K_0)=\left\|-(1+K\alpha)^{-1}K\begin{bmatrix}F_f & G_g\end{bmatrix}Z(K)+K_0Z(K_0)\right\|_2$$

$Z=\begin{pmatrix}y_0(k)\\ \Delta u_0(k)\end{pmatrix}$ depends on the controls gains used. Write $Z(k)=Z(k_0)+\Delta Z$

Inserting $N_u=1$ in equation (5.13), then the optimisation problem will be:

$$\begin{aligned}J(K,K_0)&=\left\|-(1+K\alpha)^{-1}K\begin{bmatrix}F_f & G_g\end{bmatrix}(Z(K_0)+\Delta Z)+K_0Z(K_0)\right\|_2\\ &\le\left\|(-(1+K\alpha)^{-1}K\begin{bmatrix}F_f & G_g\end{bmatrix}-K_0)Z(K_0)\right\|_2+\left\|-(1+K\alpha)^{-1}K\begin{bmatrix}F_f & G_g\end{bmatrix}\Delta Z\right\|_2\\ &\le\left\|(-(1+K\alpha)^{-1}K\begin{bmatrix}F_f & G_g\end{bmatrix}-K_0)\right\|_2\|Z(K_0)\|_2+\left\|-(1+K\alpha)^{-1}K\begin{bmatrix}F_f & G_g\end{bmatrix}\right\|_2\|\Delta Z\|_2\end{aligned}$$

Thus:

(i) A minimum norm solution is sought from:

$$\left\|-(1+K\alpha)^{-1}K\begin{bmatrix}F_f & G_g\end{bmatrix}+K_0\right\|_2$$

This is found as, $(1+K\alpha)^{-1}K\begin{bmatrix}F_f & G_g\end{bmatrix}=K_0$

(ii) It is assumed that it is possible to find suitable gain K close to K_0 so that $\|\Delta Z\|_2$ is suitably small.

The solution for K can be found in terms of K_0 as:

$$K_0=(1+K\alpha)^{-1}K\begin{bmatrix}F_f & G_g\end{bmatrix}\rightarrow K_0=(1+K\alpha)^{-1}KS_0$$

$$K_0(1+K\alpha)=KS_0\rightarrow K(S_0-\alpha K_0)=K_0 \qquad (5.20)$$

where

$$S_0=\begin{bmatrix}F_f & G_g\end{bmatrix}$$

A unique solution to equation (5.20) always exists and takes the form:

$$K = K_0(S_0 - \alpha K_0)^T[(S_0 - \alpha K_0)(S_0 - \alpha K_0)^T]^{-1} \tag{5.21}$$

After calculation K from (5.21) the PID gains will be calculated using equation (5.7) as:

$k_D = K(1)$

$k_P = -[K(2) - 2K(1)]$

$k_I = K(1) + K(2) + K(3)$

Set Point Rebuilt

In GPC algorithm the information about N horizon of set point are used to calculate the control sequence. In the proposed method the new set point is generated to save the information about the future set point. The new set point, r(k), is calculated from previous set point, w(k),as:

$$\begin{aligned} r(1) &= \sum_{i=1}^{N} w(i)/N \\ r(i) &= r(i-1) + w(i+N-1) - w(i-1) \qquad i = 2\cdots n \end{aligned} \tag{5.22}$$

The rebuilt set point is average of set point in N next steps. The Proposed method uses these generated set points to achieve the GPC performance.

Another alternative to rebuild new set point is:

$$r(k) = K_{GPC}W(k) \qquad k = 1,\cdots,n$$

where

$W(k) = [w(k) \quad w(k+1) \quad \cdots \quad w(k+N)]$

K_{GPC} is the GPC gains calculated from (5.19)

$W(k)$ is future set point of system.

Predictive PID Control Algorithm

The predictive PID controller can be implemented using the following procedure.

Algorithm 1: Predictive PID controller for SISO process.

Step 1: Initialisation

1. Find a system model and calculate the discrete polynomials A and B
2. Choose the value of prediction horizon, M, and formulate the future set point vectors r(k)

Step 2: Off line Calculation

1. Calculate the matrices α, F_f, G_g from equations (5.13) or (5.15).
2. Calculate the GPC gain, K_{GPC}, using equation (5.18)
3. Calculate the optimal value of predictive PID gains using equation (5.21)
4. Iterate over the value of M to minimize the cost function.

Step 3: On line Calculation

1. Calculate the following signals
   a. $\begin{bmatrix} F_f & G_g \end{bmatrix} Z(K)$
   b. $R(k) = \begin{bmatrix} r(k-2) & r(k-1) & r(k) \end{bmatrix}$ using equation (5.22)
2. Calculate the control increment

$$u(k) = u(k-1) + (I + K\alpha)^{-1} K[R(k) - \begin{bmatrix} F_f & G_g \end{bmatrix} Z(K)]$$

Step 4: Fine Tuning

1. Apply the control signal and check closed loop performance.
2. Fine tune the PID gains if necessary.

5.4 Stability Study for Proposed Method

To study the stability of proposed method the closed loop transfer function of system is calculated Fig 5.1. Writing control law equation (5.12) in matrix form with set point gives:

$$\Delta u(k) = -K\left\{\alpha\Delta u(k) + F_f\theta(k) + G_g\Delta U(k)\right\} \tag{5.23}$$

where:

$$G_i = \begin{bmatrix} g_{i-3} \\ g_{i-2} \\ g_{i-1} \end{bmatrix} \quad G_i^{'} = \begin{bmatrix} g^{'}_{(i-2)1} & g^{'}_{(i-2)2} & \cdots & g^{'}_{(i-2)n_b} \\ g^{'}_{(i-1)1} & g^{'}_{(i-1)2} & \cdots & g^{'}_{(i-1)n_b} \\ g^{'}_{i1} & g^{'}_{i2} & \cdots & g^{'}_{in_b} \end{bmatrix}$$

$$F_i = \begin{bmatrix} f_{(i-2)1} & f_{(i-2)2} & \cdots & f_{(i-2)(n_a+1)} \\ f_{(i-1)1} & f_{(i-1)2} & \cdots & f_{(i-1)(n_a+1)} \\ f_{i1} & f_{i2} & \cdots & f_{i(n_a+1)} \end{bmatrix}$$

$$\alpha = \sum_{i=0}^{M} G_i \qquad F_f = \sum_{i=0}^{M} F_i \qquad G_g = \sum_{i=0}^{M} G_i^{'}$$

$$\theta(k) = \begin{bmatrix} -e(k) & -e(k-1) & \cdots & -e(k-n_a) \end{bmatrix}^T$$

$$\Delta U(k) = \begin{bmatrix} \Delta u(k-1) & \Delta u(k-2) & \cdots & \Delta u(k-n_b) \end{bmatrix}^T$$

$$e(k-i) = w(k-i) - y(k-i) \qquad i = (0,\cdots,n_a)$$

Rewriting control law in compact form and after some straightforward algebra gives:

$$A_c(z^{-1})y = w^{*} - B_c(z^{-1})\Delta u \tag{5.24}$$

where:

$$A_c(z^{-1}) = KF_f Z_y \qquad B_c(z^{-1}) = G^* Z_u$$
$$w^* = k_{ref} w \qquad k_{ref} = KF_f$$
$$Z_y = [1 \quad z^{-1} \quad \cdots \quad z^{-na}]^T$$
$$G^* = [1 + K\alpha \quad KG_g]$$
$$Z_u = [1 \quad z^{-1} \quad \cdots \quad z^{-nb}]^T$$

A CARIMA model for system is given by:

$$\widetilde{A}(z^{-1})y(k) = z^{-d}B(z^{-1})\Delta u(k-1) = z^{-d-1}B(z^{-1})\Delta u(k) \tag{5.25}$$

where:

$$\widetilde{A}(z^{-1}) = D(z^{-1})A(z^{-1}) = (1 - z^{-1})A(z^{-1})$$

$d \geq 0$ is the time delay of system

Inserting equation (5.25) in equation (5.24), gives the closed loop transfer function of system as:

$$y = \frac{B(z^{-1})z^{-d-1}}{A_c(z^{-1})B(z^{-1})z^{-d-1} + B_c(z^{-1})\widetilde{A}(z^{-1})} w^* \tag{5.26}$$

So the closed loop poles are the roots of characteristic equation:

$$A_c(z^{-1})B(z^{-1})z^{-d-1} + B_c(z^{-1})\widetilde{A}(z^{-1}) = 0 \tag{5.27}$$

Equations (5.23-5.27) show that poles of closed loop system, which are the roots of characteristic equation, depend on PID gains. On other hand, the PID gains are affected by selection of prediction horizon of proposed method (M).

5.5 Proposed Method for Second Order Systems

A CARIMA model for second order system is given by:

$$\tilde{A}(z^{-1})y(k) = z^{-d}B(z^{-1})\Delta u(k-1) + C(z^{-1})\frac{e(k)}{D(z^{-1})} \tag{5.28}$$

where:

$D(z^{-1}) = 1 - z^{-1}$

$A(z^{-1}) = 1 + a_1 z^{-1} + a_2 z^{-2}$

$B(z^{-1}) = b_1 + b_2 z^{-1}$

$\tilde{A}(z^{-1}) = 1 + (a_1 - 1)z^{-1} + (a_2 - a_1)z^{-2} - a_2 z^{-3}$

$d \geq 1$ is the time delay of system

The equivalent time domain difference equation is (with C=0):

$$y(k+1) = -a_1' y(k) - a_2' y(k-1) - a_3' y(k-2) + b_1 \Delta u(k-1-d) + b_2 \Delta u(k-2-d) \tag{5.29}$$

where:

$a_1' = a_1 - 1, \quad a_2' = a_2 - a_1, \quad a_3' = -a_2$

Using the transformation, $v(k-1) = u(k-1) + \frac{b_2}{b_1}u(k-2)$, the equation (5.29) can be written:

$$y(k+1) = -a_1' y(k) - a_2' y(k-1) - a_3' y(k-2) + b_1 \Delta v(k-1-d) \tag{5.30}$$

If the PID controller design procedure apply to system that is defined by equation (5.30), in this case the optimisation is respect to the new manipulated signal $v(k)$ but there is no

need to use the least square optimisation and approximate the control signal since the result is exact. When $\Delta v(k)$ was calculated then $\Delta u(k)$ could be calculated as:

$$\Delta u(k) = \Delta v(k) - \Delta u(k-1) \qquad or$$
$$\Delta u(k) = \sum_{i=0}^{k-1}\left((-\frac{b_2}{b_1})^i \Delta v(k-i)\right) \qquad k = 1,2,\cdots \tag{5.31}$$

Using equation (5.19) with N_u=1 and N output prediction horizon, the control signal for GPC method is:

$$\Delta v(k) = -K_0\begin{bmatrix} y(k) \\ y(k-1) \\ y(k-2) \end{bmatrix} \tag{5.32}$$

For the proposed method, from equation (5.8) with M=0 the control signal is:

$$\Delta v(k-d) = KY(k) \tag{5.33}$$
$$K = [k_P + k_I + k_D \quad -k_P - 2k_D \quad k_D]$$

To achieve GPC performance the control signal in (5.33) should be equal to (5.32), after some algebra with d=0, leads to:

$$\begin{aligned} K &= K_{GPC}F = K_0 \\ k_P &= -K_0(2) - 2K_0(3) \\ k_I &= K_0(1) + K_0(2) + K_0(3) \\ k_D &= K_0(3) \end{aligned} \tag{5.34}$$

Therefore, GPC for second order system is equal to a PID controller when PID coefficients are calculated using equation (5.34). For second order system with delay according to equation (5.33), the control signal will be:

$$\Delta v(k) = KY(k+d) \tag{5.35}$$

After some straightforward algebra, equation (5.33) can written as:

$$\Delta v(k) = -(1+K\alpha)^{-1} K\left[\widetilde{F}\right][Y(k)] \tag{5.36}$$

where:

$$\widetilde{F} = \begin{bmatrix} f_{d1} & f_{d2} & f_{d3} \\ f_{(d-1)1} & f_{(d-1)2} & f_{(d-1)3} \\ f_{(d-2)1} & f_{(d-2)2} & f_{(d-2)3} \end{bmatrix} \qquad \alpha = \begin{bmatrix} g_{d-1} & g_{d-2} & g_{d-3} \end{bmatrix}^T$$

To achieve the same result as GPC the equation (5.36) and (5.33) should be equal so:

$$K_0(1+K\alpha) = K\widetilde{F} \rightarrow K(\widetilde{F} - \alpha K_0) = K_0 \tag{5.37}$$

A unique solution for K in equation (5.37) exists. The required PID gain will be:

$$k_P = -K(2) - 2K(3)$$
$$k_I = K(1) + K(2) + K(3)$$
$$k_D = K(3)$$

where:

$$K = K_0(\widetilde{F}_k - \alpha_k K_0)^{-1} \qquad k < d$$
$$K = K_0(\widetilde{F} - \alpha K_0)^{-1} \qquad k > d$$

$$\widetilde{F}_k = \begin{bmatrix} f_{d(k-d+1)} & f_{d(k-d+2)} & f_{d(k-d+3)} \\ f_{(d-1)(k-d+1)} & f_{(d-1)(k-d+2)} & f_{(d-1)(k-d+3)} \\ f_{(d-2)(k-d+1)} & f_{(d-2)(k-d+2)} & f_{(d-2)(k-d+3)} \end{bmatrix} \qquad \alpha = \begin{bmatrix} g_{k-1} & g_{k-2} & g_{k-3} \end{bmatrix}^T$$
$$f_{ij=0} \quad for \quad i<0 \, or \, j<0$$

Remark 1: For second order system one level of PID (M=0) is enough to achieve the GPC performance. For higher order systems, M will be selected to find the best approximation to GPC solution.

5.6 Constrained Predictive PID Method

5.6.1 Introduction

All real world control systems must deal with constrains. The constraints acting on a process can originate from amplitude limits in the control signal, slew rate limits of the actuator and limits on the output signals. As a result of constrains, the actual plant input will be different from the output of the controller. When this happens, the controller output does not drive the plant and as a result, the states of the controller are wrongly updated. The constraints can be expressed in condensed form as (Camacho and Bordons 1999):

$$Ru \leq c \tag{5.38}$$

To consider constraints, in Predictive PID proposed method two ways have been suggested.

- Using anti-windup integrator
- Calculation optimal values of constrained Predictive PID gains

5.6.2 Anti-windup Integrator

Windup problems were originally encountered when using PI/PID controllers for controlling linear systems with control input saturations. To implement the anti-windup in proposed method the following changes in calculation of control signal should be apply:

Using Anti windup integrator Fig 5.2. The constrained control signal in equation (5.6) will be:

$$\begin{aligned}\Delta u(k) &= \Delta\tilde{u}(k) + \Delta\tilde{u}(k+1) + \cdots + \Delta\tilde{u}(k+M) + \frac{u^*(k) - u(k)}{T_t} \\ &= \Delta u(k)_{un} + \frac{u^*(k) - u(k)}{T_t}\end{aligned} \tag{5.39}$$

where:

$u^*(k) = f[u(k)]$ f is a non-linear function

$\Delta u(k)_{un}$: Unconstrained control signal

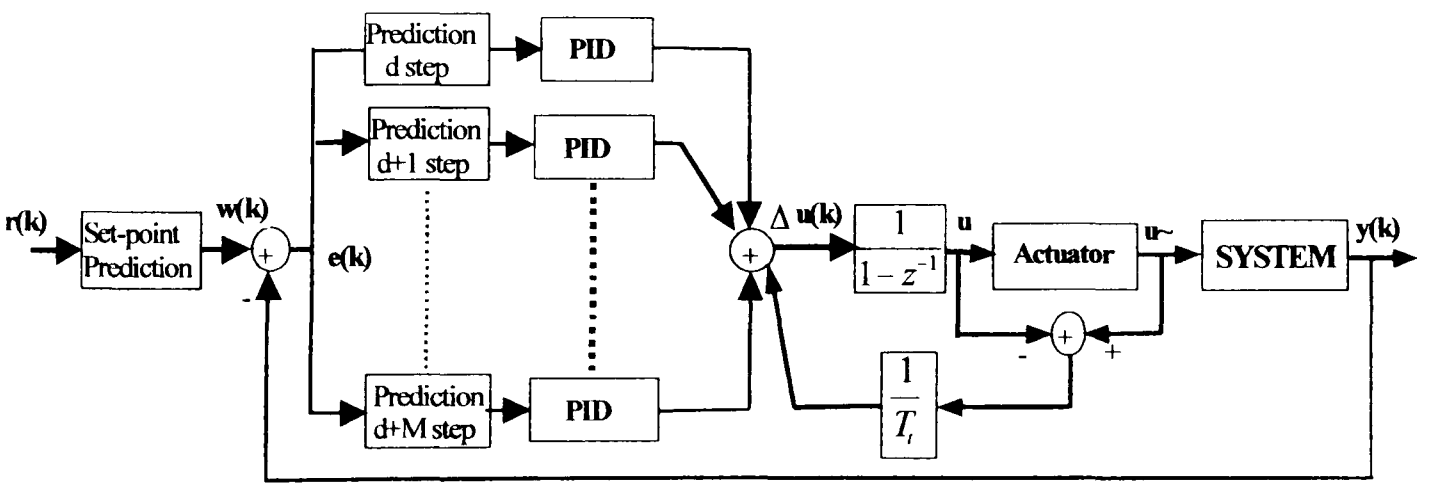

Fig 5.2: The Predictive PID along with and integral anti windup.

After some straight forward algebra:

$$u(k) = \frac{T_i}{1+T_i}[u(k-1) + \Delta u(k)_{un} + \frac{u^*(k)}{T_i}] = \frac{T_i}{1+T_i}[u(k-1) + \Delta u(k)_{un}] + \frac{u^*(k)}{T_i+1} \qquad (5.40)$$

It is clear that for unconstraint systems where $u^*(k) = u(k)$, equations (5.39) and (5.40) are equal to equations (5.6) and (5.5) respectively.

5.6.3 Optimal Values for Constrained Predictive PID

PID type predictive control when constraints are taken into account consists of minimising expression (5.19) subject to a set of linear constraint (5.38). That is, the optimisation of a quadratic function with linear constraints, what is usually known as a quadratic programming (QP) problem. (Kuznetsov and Clarke 1994)

To obtain the optimal values of the gains, the GPC algorithm with constrains is used. GPC with constrains consists of applying a control sequence that minimises the following cost function:

$$\begin{aligned} &\min \quad J(u) = \frac{1}{2}u^T Hu + b^T u + f_0 \\ &\textit{subject to} \quad Ru \le c \end{aligned} \qquad (5.41)$$

It is clear that the implementation of GPC for processes with bounded signals requires the solution of a QP problem. There are a lot of QP techniques to compute the optimal values of GPC control signal $[\Delta u(k)_{opt}]$ from equation (5.41). After computing $\Delta u(k)_{opt}$, to compute the optimal values of predictive PID gains, the predictive PID

control signals should be made the same as GPC controller. This means the equation (5.14) should be equal to $\Delta u(k)_{opt}$. After some straightforward algebra:

$$\Delta u(k)_{opt} = -(1+K\alpha_d)^{-1}K\begin{bmatrix}F_f & G_g\end{bmatrix}\begin{bmatrix}y_0\\ \Delta u_0\end{bmatrix} \rightarrow \Delta u(k)_{opt} = K(1+K\alpha)^{-1}M_m$$

$$\Delta u(k)_{opt}(1+K\alpha) = KM_m \rightarrow K[M_m - \alpha\Delta u(k)_{opt}] = \Delta u(k)_{opt} \qquad (5.42)$$

where:

$$M_m = -\begin{bmatrix}F_f & G_g\end{bmatrix}\begin{bmatrix}y_0\\ \Delta u_0\end{bmatrix}$$

The value of PID gains can then be calculated as:

$$K = K_0(M_m - \alpha\Delta u(k)_{opt})^T[(M_m - \alpha\Delta u(k)_{opt})(M_m - \alpha\Delta u(k)_{opt})^T]^{-1}\Delta u(k)_{opt} \quad (5.43)$$

The values of the PID gains found in equation (5.43) ensure that constrains are not violated. The gains are, however, time varying since the control signal calculated from MPC algorithm changes with time. Hence, an adaptive PID controller as described later can be formulated to handle the system input constraints. The approach requires one to solve the constrained MPC control problem at each instant of time in order to find the PID gains, and as such the question may arise as to why the MPC solution is not used directly. This is of course true, but this technique can be used in a supervisory role or can even be employed to replace the integral wind up scheme in order to obtain a better solution. Furthermore, the algorithm can be used with existing industrial PID controllers without the need for major refurbishment of the control system. The adaptive PID algorithms can be stated as follows:

Adaptive Predictive PID Controller

Algorithm 2: Adaptive predictive PID controller for systems with input constraints

Step 1: Initialisation

Set t=0 and follow steps 1 and 2 of algorithm one in section 5.3.

Step 2: On line Calculation

1 If $Ru > c$ (i.e. the constrains are violated), calculate the PID gains, using equation (5.43).

2 Follow step 3 of the unconstrained algorithm

Step 3: Set t=t+1 and go to step 2.

5.7. Case Studies:

In this section, the stability and performance of different systems for predictive PID design method will be discussed.

5.7.1 Stability Study

The effect of M on PID parameters and variation of PID parameters on stability region for three types of systems has been considered; the systems are:

1- Non-minimum phase second order system $g_1(s) = \dfrac{-10s+1}{40s^2+10s+1}$

2- Stable second order system with time delay $g_2(s) = \dfrac{1}{40s^2+10s+1}e^{-3s}$

3- Unstable second order system $g_3(s) = \dfrac{1}{40s^2-10s+1}$

The results showed that for non-minimum phase system the stability region is closed and bigger M causes the smaller stability region. For Stable systems the regions are not

closed, but like non-minimum phase increasing the level of PID controller decreases the stability regions. For g3 the regions are not closed and bigger M cause bigger stability regions Fig 5.3.

Remark 1:

Bigger M decreases the PID coefficient and for stable system increases the possibility of stability. For nun minimum phase bigger M decrease the possibility of stability. And for unstable system increasing M increases the possibility of stability.

5.7.2 Performance Study

In this section 5 different systems are considered. The systems are:

1 2^{nd} order system

2 2^{nd} order system with time delay

3 Non-minimum phase 2^{nd} order system

4 Third order system

5 Boiler system (loop one)

6 Boiler system (loop two)

GPC and Proposed PID methods were used to design the controller for each system when there is zero mean with noise in system. For GPC, the horizon prediction of output N=25, control input horizon N_u=1, $\lambda = 80$ were assumed. The GPC gain and Proposed PID gains are shown in Table 5.1.

For stable second order system the PID gains is calculated using equation (5.34) where the solution of predictive PID is exact. Therefore, step response of proposed and GPC methods are the same (Fig. 5.4a).

For second order system with delay the PID gains are calculated by (5.37). The closed loop response of system to step input for proposed and GPC method are the same. It should be reminded that the PID gains, in this case, for k<d has been considered constant (Fig. 5.4a).

For g_3 the PID gains are calculated using equation (5.21), which gives an approximation of GPC gains. From Fig 5.4b it is clear that the step response of closed loop system obtained using equation (5.21) is very close to the step response of GPC.

The step responses of closed loop third order system for proposed and GPC methods are shown in Fig 5.4c. For third order system, Fig 5.4c shows that closed loop system with predictive PID controller is unstable, that means calculated PID gains are not suitable approximation of GPC gain. Increasing M up to 1, the step response shows reasonable approximation of GPC gains.

As last example, the predictive PID controller design method has been applied to boiler model. The step response of closed loop system for loop one and loop two of boiler model has been shown in Fig 5.4d. The results show that the method is applicable for industrial boiler model with one and two level of PID for loop one and loop two, respectively.

A comparison of disturbance rejection properties of the PID predictive controller with MPC and conventional PID for second order system (g_2) is shown in Fig 5.5a for. For the value of M=1, the proposed controller rejects the disturbance much faster than the conventional PID at the expense of a larger overshoot. Fig 5.5b shows the simulation result for the case where the future set point is not known. The predictive PID response for M=1 is almost critically damped compared to the PID where the response is over damped. Fig 5.5c demonstrates the simulation for case where the known set-point changes are applied in advance for d steps, the period of the dead time. Again, a better performance can be achieved using the proposed predictive PID controller.

Remark 2:

For any order of system, with changing the level of PID (M) it is usually possible to achieve to GPC performance, for second order system one level of PID (M=0) is enough to achieve the GPC performance. For higher order systems M will be selected to find the best approximation to GPC solution.

5.8 Summary

A new PID controller structure based on GPC approach has been developed which is widely applicable to many practical problems. It will yield an optimum control performance according to a performance index specified. In the proposed configuration, the system transient behaviour is managed by the predicted trajectories and closed loop stability was assured by PID structure of controller. The controller reduces to the same structure as a PI or PID controller for first and second order systems, respectively. It was shown that the optimal values of PID gains might found using a scheme similar to a MPC. Various benchmark processes were employed to illustrate the stability and performance of the proposed method. One of the main advantages of the proposed controller is that it can be used with systems of any order and the PID tuning can be used to adjust the controller performance.

System	Level of PID (M)	GPC Gain	Proposed PID Gain	Description
$g_1(z) = \frac{0.3457}{z^2 - 0.8952z + 0.3679}$	0	[0.4128 –0.3696 0.1502]	[0.0692 0.1934 0.1502]	Stable second order system
$g_2(z) = \frac{0.3457}{z^2 - 0.8952z + 0.3679} z^{-4}$	1	[0.408 0.365 0.15]	[0.081 0.225 0.175]	Second order system with time delay
$g_3(z) = \frac{0.09628z - 0.688}{z^2 - 0.8952z + 0.3679}$	1	[-0.536 0.483 -0.198 0.37]	[-0.087 -0.251 -0.198]	Non-minimum phase second order system
$g_4(z) = \frac{0.1121z^2 - 0.3007z + 0.05282}{z^3 - 1.501z^2 + 0.9104z - 0.2231}$	2 3	[1.383 -2.07 1.251 -0.305 0.482 0.072]	[-0.049 0.234 0.544] [0.041 0.156 0.393]	Stable third order system
$g_5(z) = \frac{-.007z + 0.007}{z^2 - 1.98z + .98}$	0	[.1658 .078 0.0287 0.1487]	[-0.029 0.1004 0.0037]	Boiler model; transfer function between Throttle pressure and fuel/air.
$g_6(z) = \frac{z^2 - 1.96z + 0.96}{z^2 - 1.93z + .93}$	1	[.374 –.129 0.0005 –.11 0.069]	[0.128 0.25 0.0005]	Boiler model; transfer function between flow rate and Control Valve.

Table 1: GPC and Proposed PID control design for 5 different systems.

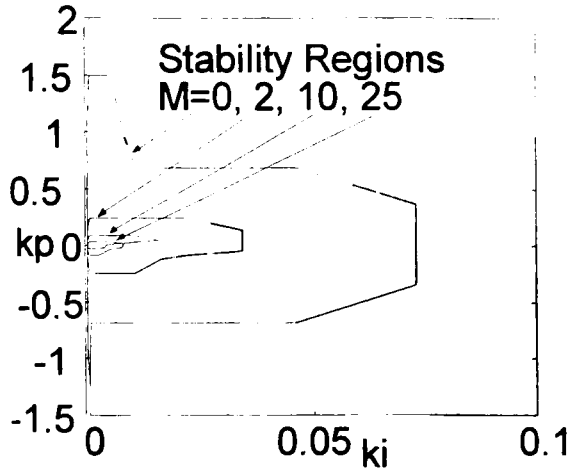

g1 (kd=constant)

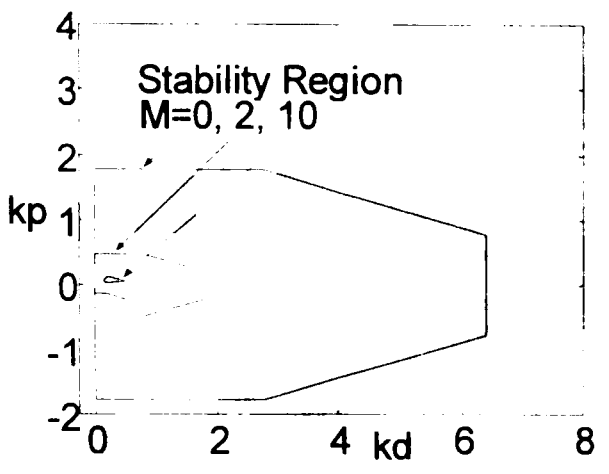

g1 (ki=constant)

Fig 5.3a: The stability region for closed loop second order non-minimum phase system.

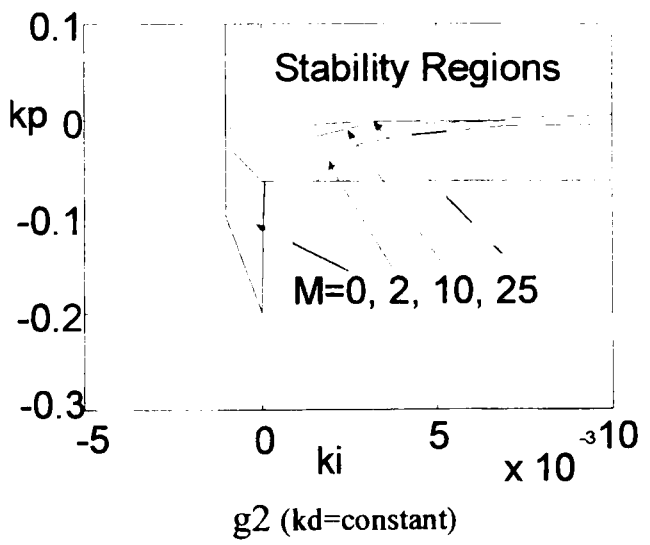

g2 (kd=constant)

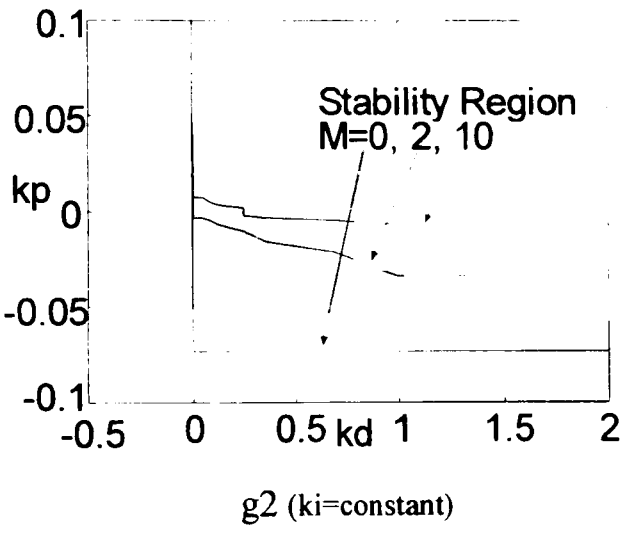

g2 (ki=constant)

Fig 5.3b: The stability region for closed loop second order system.

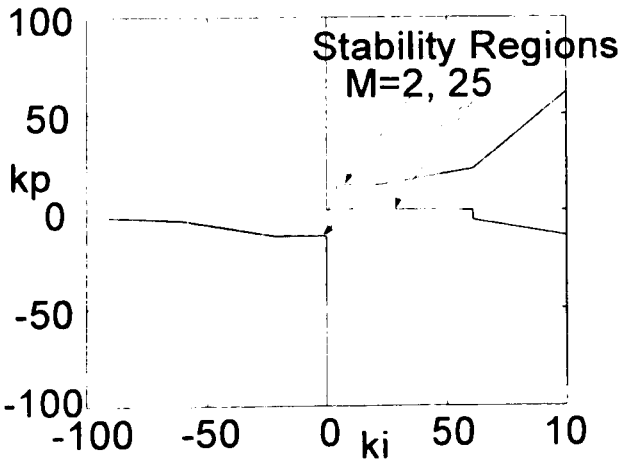

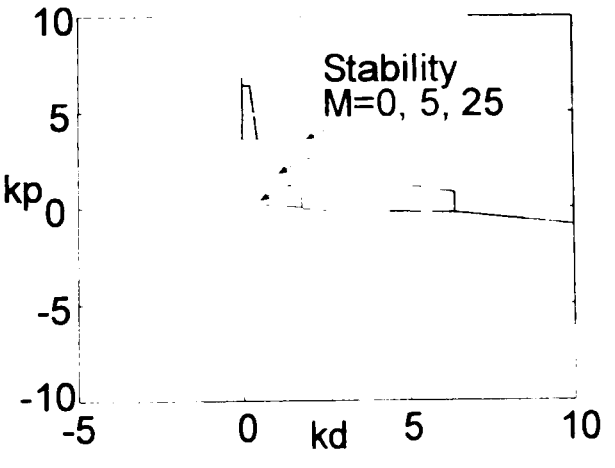

Fig 5.3c: The stability region for closed loop unstable second order phase system.

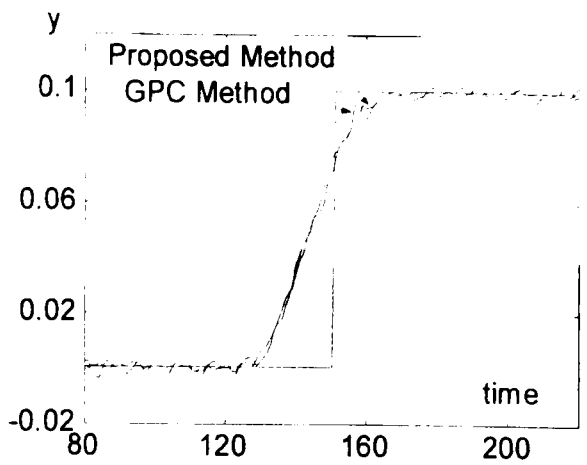

g1

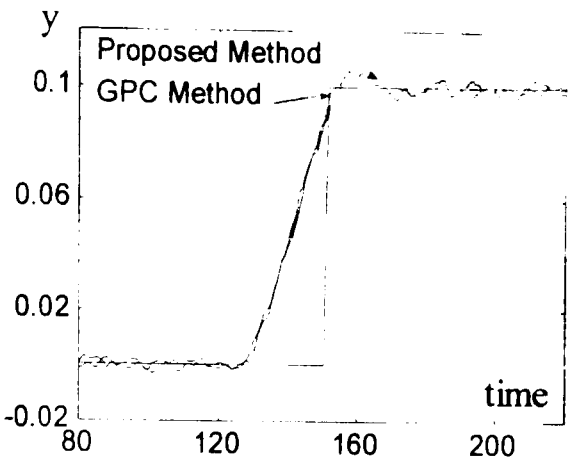

g2

Fig 5.4a: The comparison of GPC and Proposed Method for second order system.

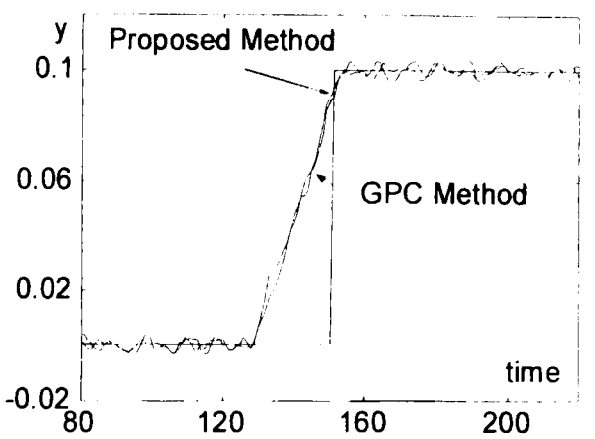

g3

Fig 5.4b: The output of GPC method and Proposed method for example 3 with M=1.

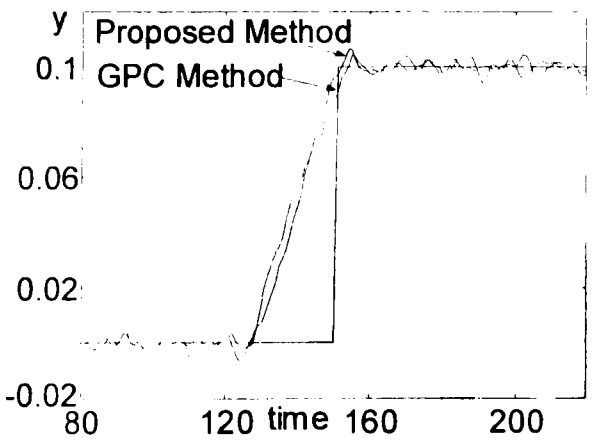

M=1

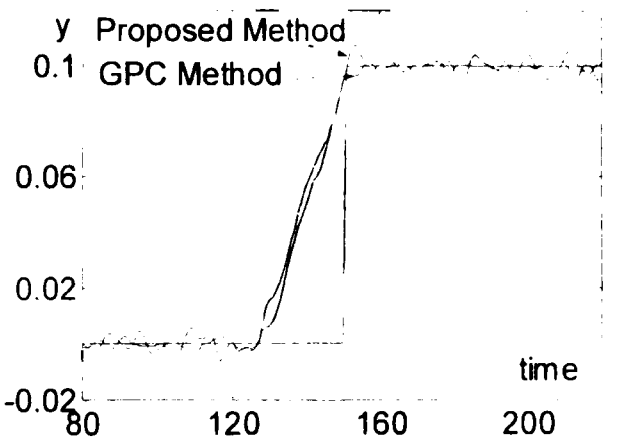

M=2

Fig 5.4c: The output of GPC method and Proposed method for example 4 with M= 1 and 2.

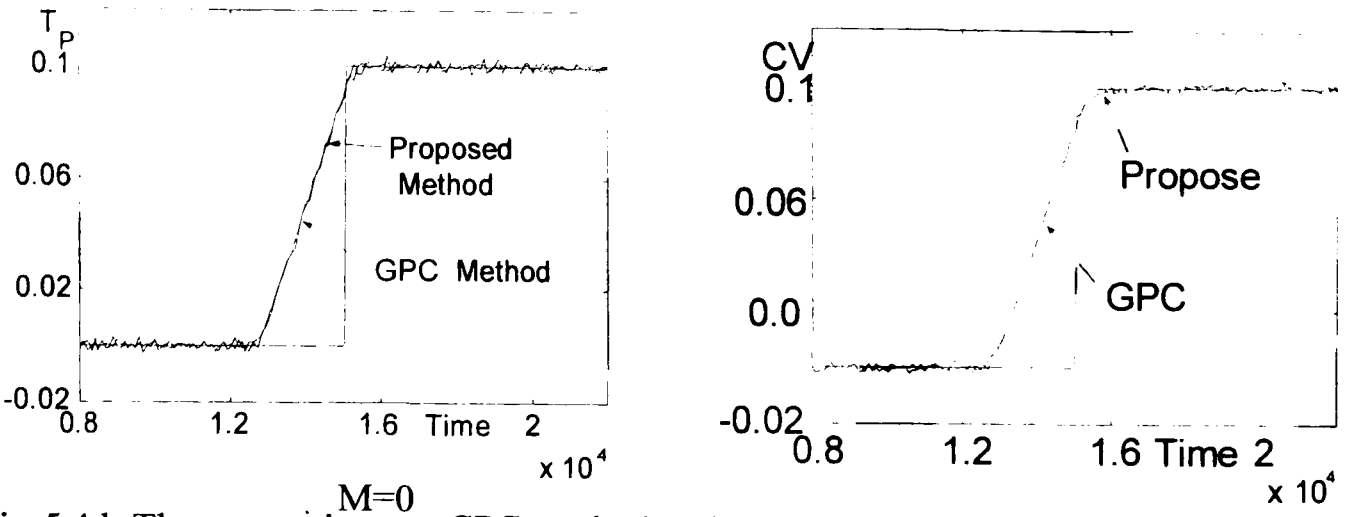

M=0

Fig 5.4d: The comparison of GPC method and proposed method for De_Mello Boiler model; A: Input: Fuel & output and Output: Throttle Pressure. B: Input Control valve and output Mass flow

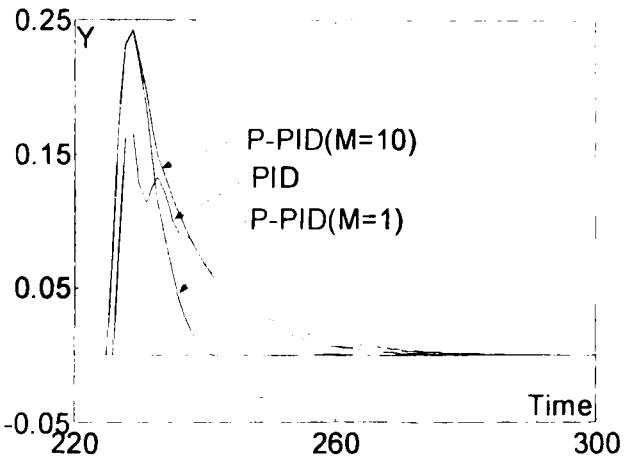

5.5a: Comparison of disturbance rejection of the conventional PID with Proposed Method

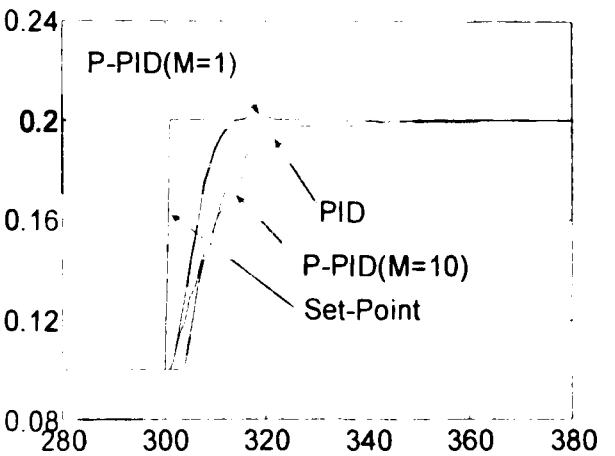

5.5b: The comparison of conventional PID with Proposed Method without future set point information.

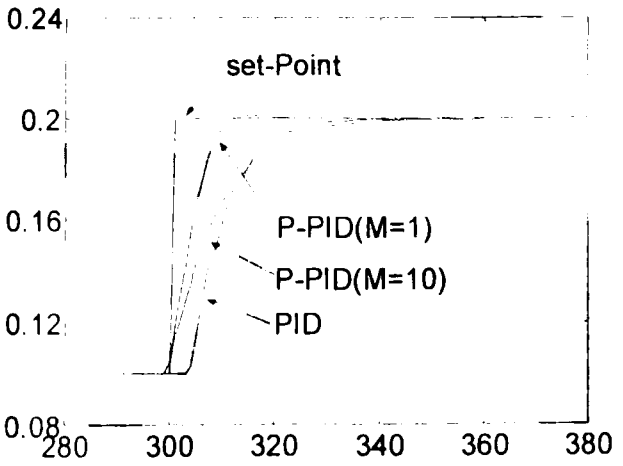

5.5b: The comparison of conventional PID with Proposed Method when the set point change is applied *d* second in advance.

Chapter 6

The MIMO Predictive PID Controller Design Problem

6.1 Introduction

Many industrial processes are inherently multivariable and need multivariable control to provide enhanced performance. This is a strong motivation to derive a simple and effective method for developing multivariable controller design methods. PID control is one of most common control schemes for MIMO plants.

This Chapter explain an extension of predictive PID controller, which was introduced in Chapter 5, to MIMO systems. The Chapter has been organised as follows: Section 2 describes the structure of MIMO PID type predictive controller and calculates the optimal values of the controller gains. Section 3 presents the decentralized predictive PID controllers. State space representation of predictive PID controller is discussed in section 4. In section 5, stability issues are discussed. A comparison between the proposed method and GPC technique using a simulated process is presented in Section 6. Finally, conclusions close the Chapter.

6.2 Polynomial Representation of the MIMO Predictive PID Controller

6.2.1 General form of PID for MIMO systems

Assume $K(s)$ is transfer function of a fully cross-coupled PID controller for a MIMO process under unity feedback as shown in Fig 6.1, where $G(s)$ is transfer function of system. The different representations of PID controllers are:

Continuous form of MIMO PID controllers

The input vector to the controller is $E(s)$ and output from the controller is $U(s)$:

$$U(s) = K(s)E(s) \tag{6.1}$$

where:

$$k_{ij}(s) = k_{ij}^{P} + \frac{k_{ij}^{I}}{s} + k_{ij}^{D}s$$

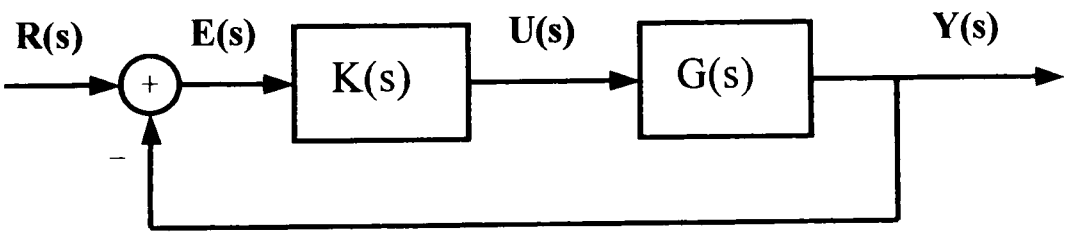

R(s): Set points of system E(s): Error

U(s): Control signal Y(s): Output

Fig 6.1: The closed loop block diagram of process and controller

$$K(s)=\begin{bmatrix} k_{11}(s) & \cdots & k_{1L}(s) \\ \vdots & \ddots & \vdots \\ k_{L1}(s) & \cdots & k_{LL}(s) \end{bmatrix} \quad \begin{aligned} U(s)&=\begin{bmatrix} u_1(s) & \cdots & u_L(s) \end{bmatrix}^T \\ E(s)&=\begin{bmatrix} e_1(s) & \cdots & e_L(s) \end{bmatrix}^T \end{aligned}$$

The *ij th* controller signal is:

$$u_{ij}(s)=(k_{ij}^P+\frac{k_{ij}^I}{s}+k_{ij}^D s)e_j(s) \qquad (i=1,\cdots,L; \quad j=1,\cdots,L) \tag{6.2}$$

The process is L-square multivariable system and $K(s)$ can be written as:

$$K(s)=K_P+\frac{K_I}{s}+K_D s$$

In time domain equation (6.1) will be:

$$U(t)=K_P e(t)+K_I\int_o^t e(\tau)d\tau+K_D\dot{e}(t) \tag{6.3}$$

where:

$$K_P=\begin{bmatrix} k_{11}^P & k_{12}^P & \cdots & k_{1L}^P \\ k_{21}^P & k_{22}^P & \cdots & k_{11}^P \\ \vdots & \vdots & \ddots & \vdots \\ k_{L1}^P & k_{L2}^P & \cdots & k_{LL}^P \end{bmatrix} \quad K_I=\begin{bmatrix} k_{11}^I & k_{12}^I & \cdots & k_{1L}^I \\ k_{21}^I & k_{22}^I & \cdots & k_{11}^I \\ \vdots & \vdots & \ddots & \vdots \\ k_{L1}^I & k_{L2}^I & \cdots & k_{LL}^I \end{bmatrix} \quad K_D=\begin{bmatrix} k_{11}^D & k_{12}^D & \cdots & k_{1L}^D \\ k_{21}^D & k_{22}^D & \cdots & k_{11}^D \\ \vdots & \vdots & \ddots & \vdots \\ k_{L1}^D & k_{L2}^D & \cdots & k_{LL}^D \end{bmatrix}$$

$K_P, K_I, K_D \in R^{L\times L}$ are the proportional, integral and derivates gains, respectively.

Chapter 6

Representation of Discrete MIMO PID controllers

The MIMO PID controller in discrete form can be represented by:

$$U(k) = K_P e(k) + K_I \sum_{j=1}^{k} e(j) + K_D[e(k) - e(k-1)] \tag{6.4}$$

where:

$$e(k) = \begin{bmatrix} e_1(k) & e_2(k) & \cdots & e_L(k) \end{bmatrix}^T \qquad e \in R^{L\times 1}$$

$$r(k) = \begin{bmatrix} r_1(k) & r_2(k) & \cdots & r_L(k) \end{bmatrix}^T \qquad r \in R^{L\times 1}$$

$$y(k) = \begin{bmatrix} y_1(k) & y_2(k) & \cdots & y_L(k) \end{bmatrix}^T \qquad y \in R^{L\times 1}$$

And the incremental representation of the controller is:

$$\begin{aligned} \Delta U(k) &= U(k) - U(k-1) = K_P[e(k) - e(k)] + K_I e(k) + K_D[e(k) - 2e(k-1) + e(k-2)] \\ &= (K_P + K_I + K_D)e(k) + (-K_P - 2K_D)e(k-1) + K_D e(k-2) \end{aligned} \tag{6.5}$$

In compact matrix form the equation (6.5) can be written as:

$$\Delta U(k) = KE(k) = K[R(k) - Y(k)] \tag{6.6}$$

where:

$$K = \begin{bmatrix} K_D & -2K_D - K_P & K_D + K_P + K_D \end{bmatrix} \qquad K \in R^{3L\times L}$$

$$\Delta U(k) = \begin{bmatrix} \Delta u_1(k) & \Delta u_2(k) & \cdots & \Delta u_L(k) \end{bmatrix}^T \qquad \Delta U \in R^{L\times 1}$$

$$E(k) = \begin{bmatrix} e^T(k-2) & e^T(k-1) & e^T(k) \end{bmatrix}^T$$

$$R(k) = \begin{bmatrix} r^T(k-2) & r^T(k-1) & r^T(k) \end{bmatrix}^T$$

$$Y(k) = \begin{bmatrix} y^T(k-2) & y^T(k-1) & y^T(k) \end{bmatrix}^T \qquad R, Y, E \in R^{3L\times 1}$$

6.2.2 Predictive form of MIMO PID controllers

The predictive PID controller is defined as follows:

$$\Delta u(k) = K\sum_{i=0}^{M} E(k+i) = K\sum_{i=0}^{M} R(k+i) - K\sum_{i=0}^{M} Y(k+i) \tag{6.7}$$

The controller consists of M parallel PID controllers as shown in Fig.6.2. For M=0, the controller is identical to the conventional PID in equation (6.6). For the M>0 the proposed controller has predictive capability similar to MPC where M is prediction horizon of PID controller. The horizon, M will be selected to find the best approximation to GPC solution. The controller signal in equation (6.7) can be decomposed as:

$$\begin{aligned}\Delta u(k) &= K\sum_{i=0}^{M} E(k+i) = K\{E(k) + E(k+1)+\cdots+E(k+M)\} \\ &= \Delta U(k) + \Delta U(k+1)+\cdots+\Delta U(k+M)\end{aligned} \tag{6.8}$$

It is clear from (6.8) and (6.6) that the controller consists of (M+1) PID controllers where the input of i th PID at time k depends on the error signal at time $(k+i)$. This implies that the current control signal value is a linear combination of the future predicted outputs. Then, the control signal can be written as:

$$\Delta u(k) = K\left\{\sum_{m=0}^{M} R(k+m) - \sum_{m=0}^{M} Y(k+m)\right\} \tag{6.9}$$

To calculate the control increment at time k, $\Delta u(k)$, the output for M step ahead needs to be predicted. The definition of the predictor is given in the next section.

Chapter 6

Future Output Predictor for Predictive PID

A CARIMA model for L-outputs, L-inputs multivariable process can be expressed as:

$$A(z^{-1})y(k) = B(z^{-1})u(k-1) \quad \text{or} \qquad A'(z^{-1})y(k) = B(z^{-1})\Delta u(k-1)$$

where:

$A(z^{-1})$ *and* $B(z^{-1})$ are $L \times L$ polynomial matrices defined as:

$$A(z^{-1}) = I + A_1 z^{-1} + \cdots + A_{n_a} z^{-n_a}$$

$$B(z^{-1}) = B_0 + B_1 z^{-1} + \cdots + B_{n_b} z^{-n_b}$$

$$A' = \Delta A \qquad I = I_{L\times L}$$

If the transfer matrix representation of system was available, using left matrix fraction algorithm, the transfer function will be changed to polynomial representation. This issue will be explained in section (6.3). The *m* step ahead prediction of output can be obtained from the following equation (Camacho and Bordons 1999):

$$y(k+m) = G^m(z^{-1})\Delta u(k+m-1) + G'^m(z^{-1})\Delta u(k-1) + F^m(z^{-1})y(k) \tag{6.10}$$

where:

$$\Delta u(k+m) = \left[\Delta u_1(k+m) \quad \Delta u_2(k+m) \quad \cdots \quad \Delta u_L(k+m)\right]^T$$

$$y(k-i) = \left[y_1(k-i) \quad y_2(k-i) \quad \cdots \quad y_L(k-i)\right]^T$$

$$\Delta u(k-i) = \left[\Delta u_1(k-i) \quad \Delta u_2(k-i) \quad \cdots \quad \Delta u_L(k-i)\right]^T$$

$$G^m(z^{-1}) = \begin{bmatrix} G_{11}^m(z^{-1}) & \cdots & G_{1L}^m(z^{-1}) \\ \vdots & \ddots & \vdots \\ G_{L1}^m(z^{-1}) & \cdots & G_{LL}^m(z^{-1}) \end{bmatrix} \quad G'^m(z^{-1}) = \begin{bmatrix} G_{11}'^m(z^{-1}) & \cdots & G_{1L}'^m(z^{-1}) \\ \vdots & \ddots & \vdots \\ G_{L1}'^m(z^{-1}) & \cdots & G_{LL}'^m(z^{-1}) \end{bmatrix}$$

$$F^m(z^{-1})=\begin{bmatrix} F_{11}^m(z^{-1}) & 0 & \cdots & 0 \\ 0 & F_{22}^m(z^{-1}) & \cdots & 0 \\ \vdots & \vdots & \ddots & \vdots \\ 0 & 0 & \cdots & F_{LL}^m(z^{-1}) \end{bmatrix}$$

$$G_{ij}^m(z^{-1}) = g_{ij}^0 + g_{ij}^1 z^{-1} + \cdots + g_{ij}^{m-1} z^{-(m-1)} \qquad i = (1, \cdots, L)$$

$$G_{ij}^{'m}(z^{-1}) = g_{ij}^m + g_{ij}^{m+1} z^{-1} + \cdots + g_{ij}^{m+n_{bij}-1} z^{-(n_{bij}-1)} \qquad j = (1, \cdots, L)$$

$$F_{jj}^m(z^{-1}) = f_{jj}^m(0) + f_{jj}^m(1) z^{-1} + \cdots + f_{jj}^m(n_{aj}) z^{-(n_{aj})}$$

$$C(z^{-1}) = E_m(z^{-1}) A'(z^{-1}) + z^{-m} F^m(z^{-1})$$

$$E_m(z^{-1}) B(z^{-1}) = G^m(z^{-1}) + z^{-i} G^{'m}(z^{-1})$$

n_{bij} : The order of ij th element in matrix $B(z^{-1})$

n_{aj} : The order of jj th element in matrix $A(z^{-1})$

$E_m(z^{-1})$ and $F_m(z^{-1})$ are a solution of the above Diophantine equation. In equation (6.10), it was assumed that the matrix $A(z^{-1})$ is diagonal, hence, matrices $E_m(z^{-1})$ and $F_m(z^{-1})$ are also diagonal matrices and the problem was reduced to the recursion of L scalar Diophanite equations, which are much simpler to program and require less computation.

The output prediction for the *m th* PID in each loop can be written as:

$$\begin{aligned} Y(k+m) &= \begin{bmatrix} y(k+m-2) \\ y(k+m-1) \\ y(k+m) \end{bmatrix} \\ &= \begin{bmatrix} G^{m-2}(z^{-1})\Delta u(k+m-2) + G^{'m-2}(z^{-1})\Delta u(k-1) + F^{m-2}(z^{-1}) y(k) \\ G^{m-1}(z^{-1})\Delta u(k+m-1) + G^{'m-1}(z^{-1})\Delta u(k-1) + F^{m-1}(z^{-1}) y(k) \\ G^{m}(z^{-1})\Delta u(k+m) + G^{'m}(z^{-1})\Delta u(k-1) + F^{m}(z^{-1}) y(k) \end{bmatrix} \end{aligned} \qquad (6.11)$$

Equation (6.11) can be simplified to:

$$Y(k+m)=\begin{bmatrix} y(k+m-2) \\ y(k+m-1) \\ y(k+m) \end{bmatrix}=\begin{bmatrix} G_{m-3} & \cdots & G_0 & 0 & 0 \\ G_{m-2} & G_{m-3} & \cdots & G_0 & 0 \\ G_{m-1} & G_{m-2} & G_{m-3} & \cdots & G_0 \end{bmatrix}\begin{bmatrix} \Delta u(k) \\ \Delta u(k+1) \\ \vdots \\ \Delta u(k+N_u-1) \end{bmatrix}$$
$$+\begin{bmatrix} F_0^{m-2} & F_1^{m-2} & \cdots & F_{n_a}^{m-2} \\ F_0^{m-1} & F_1^{m-1} & \cdots & F_{n_a}^{m-1} \\ F_0^{m} & F_1^{m} & \cdots & F_{n_a}^{m} \end{bmatrix}\begin{bmatrix} y(k) \\ y(k-1) \\ \vdots \\ y(k-n_a) \end{bmatrix} \qquad (6.12)$$
$$+\begin{bmatrix} G'_{(m-2)1} & G'_{(m-2)2} & \cdots & G'_{(m-2)n_b} \\ G'_{(m-1)1} & G'_{(m-1)2} & \cdots & G'_{(m-1)n_b} \\ G'_{m1} & G'_{m2} & \cdots & G'_{mn_b} \end{bmatrix}\begin{bmatrix} \Delta u(k-1) \\ \Delta u(k-2) \\ \vdots \\ \Delta u(k-n_b) \end{bmatrix}$$

where:

$$G_i=\begin{bmatrix} g_{11}^{\,i} & g_{12}^{\,i} & \cdots & g_{1L}^{\,i} \\ g_{21}^{\,i} & g_{22}^{\,i} & \cdots & g_{2L}^{\,i} \\ \vdots & \vdots & \ddots & \vdots \\ g_{L1}^{\,i} & g_{L2}^{\,i} & \cdots & g_{LL}^{\,i} \end{bmatrix}_{L\times L} \qquad G'_{i(j+1)}=\begin{bmatrix} g_{11}^{i+j} & g_{12}^{j+i} & \cdots & g_{1L}^{j+i} \\ g_{21}^{j+i} & g_{22}^{i+j} & \cdots & g_{2L}^{i+j} \\ \vdots & \vdots & \ddots & \vdots \\ g_{L1}^{j+i} & g_{L2}^{j+i} & \cdots & g_{LL}^{i+j} \end{bmatrix}_{L\times L}$$

$$F_j^i=\begin{bmatrix} f_{11}^i(j) & 0 & \cdots & 0 \\ 0 & f_{22}^i(j) & \cdots & 0 \\ \vdots & \vdots & \ddots & \vdots \\ 0 & 0 & \cdots & f_{LL}^i(j) \end{bmatrix}_{L\times L}$$

In equation (6.12), future control inputs $\{\Delta u(k+i) \quad i=1{:}(N_u-1)\}$ are needed to calculate the control input. Rewriting the output prediction gives straightforwardly:

$$Y(k+m)=G^m\Delta\hat{u}(k)+F^m y_0(k)+G'^m\Delta u_0(k) \qquad (6.13)$$

where:

$$G^m = \begin{bmatrix} G_{m-3} & \cdots & G_0 & 0 & 0 \\ G_{m-2} & G_{m-3} & \cdots & G_0 & 0 \\ G_{m-1} & G_{m-2} & G_{m-3} & \cdots & G_0 \end{bmatrix}_{(3\times L)\times(L\times N_u)}$$

$$G'^m = \begin{bmatrix} G'_{(m-2)1} & G'_{(m-2)2} & \cdots & G'_{(m-2)n_b} \\ G'_{(m-1)1} & G'_{(m-1)2} & \cdots & G'_{(m-1)n_b} \\ G'_{m1} & G'_{m2} & \cdots & G'_{mn_b} \end{bmatrix}_{(3\times L)\times(L\times n_b)}$$

$$F^m = \begin{bmatrix} F_0^{m-2} & F_1^{m-2} & \cdots & F_{n_a}^{m-2} \\ F_0^{m-1} & F_1^{m-1} & \cdots & F_{n_a}^{m-1} \\ F_0^m & F_1^m & \cdots & F_{n_a}^m \end{bmatrix}_{(3\times L)\times(L\times(n_a+1))}$$

$$\Delta\hat{u}(k) = \left[\Delta u^T(k) \quad \Delta u^T(k+1) \quad \cdots \quad \Delta u^T(k+N_u-1)\right]^T$$

$$\Delta u(j) = \left[\Delta u_1(j) \quad \Delta u_2(j) \quad \cdots \quad \Delta u_L(j)\right]^T$$

$$Y(k+m) = \left[y^T(k+m-2) \quad y^T(k+m-1) \quad y^T(k+m)\right]^T$$

$$y_0(k) = \left[y^{\circ T}(k) \quad y^{\circ T}(k-1) \quad \cdots \quad y^{\circ T}(k-n_a)\right]^T$$

$$y^\circ(j) = \left[y_1(j) \quad y_2(j) \quad \cdots \quad y_L(j)\right]^T$$

$$\Delta u_0(k) = \left[\Delta u^{\circ T}(k-1) \quad \Delta u^{\circ T}(k-2) \quad \cdots \quad \Delta u^{\circ T}(k-n_b)\right]^T$$

$$\Delta u^\circ(j) = \left[\Delta u_1(j) \quad \Delta u_2(j) \quad \cdots \quad \Delta u_L(j)\right]^T$$

Put equation (6.13) in the (6.9):

$$\begin{aligned} \Delta u(k) &= K\left\{R(k+m) - \sum_{m=0}^{M} Y(k+m)\right\} \\ &= K\left\{\sum_{m=0}^{M} R(k+m) - (\sum_{m=0}^{M} G^m)\Delta\hat{u}(k) + (\sum_{m=0}^{M} F^m)y_0(k) + (\sum_{m=0}^{M} G'^m)\Delta u_0(k)\right\} \end{aligned} \tag{6.14}$$

Equation (6.14) can be simplified to:

$$\Delta u(k) = K\left\{R_t(k) - \alpha\Delta\hat{u}(k) + F_f y_0(k) + G_g \Delta u_0(k)\right\} \tag{6.15}$$

where:

$$R_t(k) = \sum_{m=0}^{M} R(k+m) \qquad \alpha = \sum_{m=0}^{M} G^m \qquad F_f = \sum_{m=0}^{M} F^m \qquad G_g = \sum_{m=0}^{M} G^{'m}$$

System with time delay

For systems with time delays, d, the output of the process will not be affected by $\Delta u(k)$ until the time instant $(k+d+1)$, the previous outputs will be a part of the free response and there is no point in considering them as part of the objective function. In this case the control signal can be written as:

$$\Delta u(k-d) = K\left\{R_t(k) - \alpha\Delta\hat{u}(k) + F_f y_0(k) + G_g \Delta u_0(k)\right\} \tag{6.16}$$

Shifting the control signal for d step ahead gives:

$$\Delta u(k) = K\left\{R_{td}(k) - \alpha_d\Delta\hat{u}(k) + F_{fd} y_0(k) + G_{gd} \Delta u_0(k)\right\} \tag{6.17}$$

coefficient matrixes are:

$$R_{td}(k) = \sum_{m=d}^{d+M} R(k+m) \qquad \alpha_d = \sum_{m=d}^{d+M} G_m \qquad F_{fd} = \sum_{m=d}^{d+M} F_m \qquad G_{gd} = \sum_{m=d}^{d+M} G_m$$

6.2.3 Optimal Values of PID-type Predictive Gains

To obtain the optimal values of the gains, the GPC algorithm is used. For process control problems default setting of output cost horizon $\{N_1 : N_2\} = \{1 : N\}$, and the control cost horizon $N_u = 1$ can be used in GPC to give reasonable performance (Clarke *et al.*, 1987). GPC consists of applying a control sequence that minimises the following cost function:

$$\begin{aligned} J(1,N) &= \lambda \Delta u(k)^T \Delta u(k) + \\ &[Gu(k) + Fy_0(k) + G' \Delta u_0(k) - W(k)]^T [Gu(k) + Fy_0(k) + G' \Delta u_0(k) - W(k)] \end{aligned} \tag{6.18}$$

The minimum of J, assuming there are no constraints on the control signals, is obtained using the usual gradient analysis, which leads to (Camacho and Bordons, 1999):

$$\Delta u(k) = (G^T G + \lambda I)^{-1} G^T [W(k) - Fy_0(k) - G' \Delta u_0(k)] \tag{6.19}$$

which can be summarised as:

$$\Delta u(k) = K_{GPC} W(k) - K_{GPC} [F \quad G'] \begin{bmatrix} y_0(k) \\ \Delta u_0(k) \end{bmatrix} = K_{GPC} W(k) - K_0 \begin{bmatrix} y_0(k) \\ \Delta u_0(k) \end{bmatrix} \tag{6.20}$$

where:

$$K_0 = K_{GPC} [F \quad G']$$
$$K_{GPC} = (G^T G + \lambda I)^{-1} G^T$$
$$w(k) = \begin{bmatrix} w_1(k) & w_2(k) & \cdots & w_L(k) \end{bmatrix}^T$$
$$y_0(k) = \begin{bmatrix} y^T(k) & y^T(k-1) & \cdots & y^T(k-n_a) \end{bmatrix}^T$$

$$W(k) = \begin{bmatrix} w^T(k) & w^T(k+1) & \cdots & w^T(k+N) \end{bmatrix}^T$$

$$\Delta u_0(k) = \begin{bmatrix} \Delta u^T(k-1) & \Delta u^T(k-2) & \cdots & \Delta u^T(k-n_b) \end{bmatrix}^T$$

To compute the optimal values of predictive control PID gains with $N_u = 1$ $[\hat{u}(k) = u(k)]$, the PID control signals should then be made the same as GPC controller. This means using equation (6.15) and (6.19) the following optimal problem should be solved:

$$Min_{K \in K_{PID}^S, M} J(K, K_0) \tag{6.21}$$

$K_{PID}^S =$ Set of stability gain for PID

where:

$$J(K, K_0) = \left\| (I + K\alpha)^{-1} K[W - \begin{bmatrix} F_f & G_g \end{bmatrix} Z(K)] - \{K_{GPC} w - K_0[Z(K_0)\} \right\|_2$$

$Z = \begin{pmatrix} y_0(k) \\ \Delta u_0(k) \end{pmatrix}$ is dependent on the controls gains used

Write $Z(K) = Z(K_0) + \Delta Z$. Then the optimisation cost function can be stated as:

$$J(K, K_0) = \left\| (1 + K\alpha)^{-1} K[R_t(k) - \begin{bmatrix} F_f & G_g \end{bmatrix} Z(K)] - \{K_{GPC} W(k) - K_0[Z(K_0)\} \right\|_2$$

$$\leq \left\| (-(I + K\alpha)^{-1} K \begin{bmatrix} F_f & G_g \end{bmatrix} + K_0) Z(K_0) \right\|_2$$

$$+ \left\| -(I + K\alpha)^{-1} K \begin{bmatrix} F_f & G_g \end{bmatrix} \Delta Z \right\|_2 + \left\| (1 + K\alpha)^{-1} K R_t(k) - K_{GPC} W(k) \right\|_2$$

$$\leq \left\| (-(I + K\alpha)^{-1} K \begin{bmatrix} F_f & G_g \end{bmatrix} + K_0) \right\|_2 \left\| Z(K_0) \right\|_2$$

$$+ \left\| -(I + K\alpha)^{-1} K \begin{bmatrix} F_f & G_g \end{bmatrix} \right\|_2 \left\| \Delta Z \right\|_2 + \left\| (I + K\alpha)^{-1} K R_t(k) - K_{GPC} W(k) \right\|_2$$

Thus:

(i) A minimum norm solution is sought from:

$$\left\|-(I+K\alpha)^{-1}K\begin{bmatrix}F_f & G_g\end{bmatrix}+K_0\right\|_2$$

This is found as, $(I+K\alpha)^{-1}K\begin{bmatrix}F_f & G_g\end{bmatrix}=K_0$

(ii) It is assumed that it is possible to find suitable gain K close to K_0 so that $\|\Delta Z\|_2$ is suitably small.

(iii) It is assumed that $R_f(k)$ (rebuilt future set point) will be calculated as the following norm become minimum:

$$\left\|(I+K\alpha)^{-1}KR_f(k)-K_{GPC}W(k)\right\|_2=0$$

The above reasoning leads to:

$$J(K,K_0)=\left\|-(I+K\alpha)^{-1}K\begin{bmatrix}F_f & G_g\end{bmatrix}\Delta Z\right\|_2\le\left\|-(I+K\alpha)^{-1}K\begin{bmatrix}F_f & G_g\end{bmatrix}\right\|_2\|\Delta Z\|_2$$

if:

$$\begin{cases}(I+K\alpha)^{-1}KR_f(k)=K_{GPC}W(k)\\(I+K\alpha)^{-1}K\begin{bmatrix}F_f & G_g\end{bmatrix}=K_0\end{cases}\qquad(6.22)$$

To calculate the control signals, steady state values of the control inputs and outputs are used. These values are assumed to be almost constant at steady state plant operation, hence, the assumption (ii) will be satisfied, $\|\Delta Z\|_2$ is suitably small, and the cost function will be minimised.

The solution for K can be found in terms of K_0 from second equation of (6.22), and then W (rebuilt future set point) will be calculated from first equation. After some straightforward algebra:

$$K_0 = (I + K\alpha)^{-1} K\begin{bmatrix} F_f & G_g \end{bmatrix} \rightarrow K_0 = (I + K\alpha)^{-1} KS_0$$

After some straightforward calculation:

$$K_0(I + K\alpha) = KS_0 \rightarrow K(S_0 - \alpha K_0) = K_0 \tag{6.23}$$

where:

$$S_0 = \begin{bmatrix} F_f & G_g \end{bmatrix}$$

A unique solution to equation (6.23) always exists and takes the form:

$$K = K_0(S_0 - \alpha K_0)^T [(S_0 - \alpha K_0)(S_0 - \alpha K_0)^T]^{-1} \tag{6.24}$$

After calculation of K, from first equation in (6.22) the rebuilt future set point will be calculated:

$$R_f(k) = K^{-1}(I + K\alpha)K_{GPC}W(k) = K_S W(k) \tag{6.25}$$

where

$$K_S = K^{-1}(I + K\alpha)K_{GPC}$$

Chapter 6

Predictive Control Algorithm

The predictive PID controller can be implemented using the following procedure.

Algorithm 1: Predictive PID controller for MIMO process.

Step 1: Initialisation

1 Find a system model and calculate the discrete polynomials matrices, A and B

2 Chose the value of prediction horizon, *M*, and formulate the future set point vectors W

Step 2: Off line Calculation

1. Calculate the matrices α, F_f, G_g in equation (6.15) using equation (6.13)

2 Calculate the GPC gain, K_{GPC}, using equation (6.20)

3 Calculate the optimal value of predictive PID gains using equation (6.24)

4 Iterate over the value of *M* to minimize the cost function.

Step 3: On line Calculation

1 Calculate the following signals

a $\begin{bmatrix} F_f & G_g \end{bmatrix} Z(K)$

b $R_t(k)$ using equation (6.25)

2 Calculate the control increment

$$u(k) = u(k-1) + (I + K\alpha)^{-1} K[R_t(k) - \begin{bmatrix} F_f & G_g \end{bmatrix} Z(K)]$$

Step 4: Fine Tuning

1 Apply the control signal and check closed loop performance.

2 Fine tune the PID gains if necessary.

6.3 Decentralized Predictive PID Controllers

In practice, most industrial processes have multiple numbers of inputs and outputs. The inputs and outputs are arranged or paired to minimise the interaction between the control loops. Static or dynamic decoupling is also used to minimise the loop interactions and make the system diagonally dominant. Multiloop PID or non-interacting controllers can then be used to control MIMO processes. Koivo and Tanttu (1991) gave a survey of multivariable PID tuning techniques. When the process interactions are modest, a diagonal PID controller structure is often adequate. This structure is simple and easy to understand. In this section a kind of decentralised predictive PID controller will be introduced.

6.3.1. Decentralized Predictive PID Controller for MIMO Systems

Consider the following discrete MIMO system:

$$y(k) = G(z^{-1})u(k-1) \tag{6.26}$$

where:

$$G(z^{-1}) = \begin{bmatrix} g_{11}(z^{-1}) & \cdots & g_{1L}(z^{-1}) \\ \vdots & \ddots & \vdots \\ g_{L1}(z^{-1}) & \cdots & g_{LL}(z^{-1}) \end{bmatrix}$$

$$y(k) = [y_1(k) \quad y_2(k) \quad \cdots \quad y_L(k)]^T$$

$$u(k) = [u_1(k) \quad u_2(k) \quad \cdots \quad u_L(k)]^T$$

$$g_{ij}(z^{-1}) = \frac{b'_{ij}(z^{-1})}{a'_{ij}(z^{-1})}$$

$$a'_{ij}(z^{-1}) = 1 + a'^{1}_{ij} z^{-1} + \cdots + a'^{n_a}_{ij} z^{-n_a}$$

$$b'_{ij}(z^{-1}) = b'^{0}_{ij} + b'^{1}_{ij} z^{-1} + \cdots + b'^{n_b}_{ij} z^{-n_b}$$

A left matrix fraction description can be obtained by making matrix $A(z^{-1})$ equal to a diagonal elements equal to the least common multiple of the denominators of the corresponding row of the transfer function, resulting in:

$$A(z^{-1})y(k) = B(z^{-1})u(k-1) \tag{6.27}$$

where:

$$A(z^{-1}) = \begin{bmatrix} A_{11}(z^{-1}) & \cdots & 0 \\ \vdots & \ddots & \vdots \\ 0 & \cdots & A_{LL}(z^{-1}) \end{bmatrix}$$

$$B(z^{-1}) = \begin{bmatrix} b_{11}(z^{-1}) & \cdots & b_{1L}(z^{-1}) \\ \vdots & \ddots & \vdots \\ b_{L1}(z^{-1}) & \cdots & b_{LL}(z^{-1}) \end{bmatrix}$$

$$a_{ij}(z^{-1}) = 1 + a_{ij}^{1} z^{-1} + \cdots + a_{ij}^{Ln_a} z^{-Ln_a}$$

$$b_{ij}(z^{-1}) = b_{ij}^{0} + b_{ij}^{1} z^{-1} + \cdots + b_{ij}^{\Gamma} z^{-\Gamma}$$

$$\Gamma = [(L-1)n_a + n_b]$$

Using the following transformation:

$$\bar{u}(k-1) = B(z^{-1})u(k-1) \tag{6.28}$$

where:

$$\bar{u}(k) = \begin{bmatrix} \bar{u}_1(k) & \bar{u}_2(k) & \cdots & \bar{u}_L(k) \end{bmatrix}^T$$

The equation will be changed to:

$$A(z^{-1})y(k) = \bar{u}(k-1) \tag{6.29}$$

The equation (6.29) can be separated in L SISO systems:

$$\begin{cases} A_{11}(z^{-1})y_1(k) = \bar{u}_1(k-1) \\ \vdots \\ A_{LL}(z^{-1})y_L(k) = \bar{u}_L(k-1) \end{cases} \tag{6.30}$$

It has been shown (Katebi and Moradi, 2001b) that for each of these SISO systems the predictive PID controller can be design such that the controller has a similar performance to model based prediction control algorithm. The controller can be implemented by back calculating u(k) as:

$$u(k) = B^{0-1}[\bar{u}(k) - B^1 u(k-1) - \cdots - B^{\Gamma} u(k-\Gamma)] \tag{6.31}$$

where:

$$B^i = \begin{bmatrix} b_{11} & \cdots & b_{1\Gamma} \\ \vdots & \ddots & \vdots \\ b_{\Gamma 1} & \cdots & b_{\Gamma\Gamma} \end{bmatrix}$$

This means that for MIMO systems with the above transformation, the decentralized predictive PID controller can achieve GPC controller performance. The difference between this controller and GPC is that in GPC the minimization is for $u(k)$ and here the minimization is for $\bar{u}(k)$ in cost function. It has been assumed that B^{0-1} is exist.

6.3.2 Decentralized Predictive PID for Low Order 2I2O Systems

Consider the following discrete 2I2O second order system,

$$y(k) = G(z^{-1})u(k-1) \tag{6.32}$$

where:

$$y(k) = [y_1(k) \quad y_2(k)]^T \qquad a'_{ij}(z^{-1}) = 1 + a'^{1}_{ij} z^{-1}$$

$$u(k) = [u_1(k) \quad u_2(k)]^T \qquad b'_{ij}(z^{-1}) = b'^{0}_{ij}$$

$$G(z^{-1}) = \begin{bmatrix} g_{11}(z^{-1}) & g_{12}(z^{-1}) \\ g_{21}(z^{-1}) & g_{22}(z^{-1}) \end{bmatrix} \qquad g_{ij}(z^{-1}) = \frac{b'_{ij}(z^{-1})}{a'_{ij}(z^{-1})}$$

A left matrix fraction description can be obtained by making matrix $A(z^{-1})$ have diagonal elements equal to the least common multiple of the denominators of the corresponding row of the transfer function, resulting in:

$$A(z^{-1})y(k) = B(z^{-1})u(k-1) \tag{6.33}$$

where:

$$A(z^{-1}) = \begin{bmatrix} A_{11}(z^{-1}) & 0 \\ 0 & A_{22}(z^{-1}) \end{bmatrix}$$

$$B(z^{-1}) = \begin{bmatrix} b_{11}(z^{-1}) & b_{12}(z^{-1}) \\ b_{21}(z^{-1}) & b_{22}(z^{-1}) \end{bmatrix}$$

$$a_{ij}(z^{-1}) = 1 + a^1_{ij} z^{-1} + a^2_{ij} z^{-2}$$

$$b_{ij}(z^{-1}) = b^0_{ij} + b^1_{ij} z^{-1}$$

$A_{11}(z^{-1})$ is common denominator of $g_{11}(z^{-1})$ and $g_{12}(z^{-1})$

$A_{22}(z^{-1})$ is common denominator of $g_{21}(z^{-1})$ and $g_{22}(z^{-1})$

Using the following:

$$\bar{u}(k-1) = B(z^{-1})u(k-1)$$

Then equation (6.33) will be changed to:

$$A(z^{-1})y(k) = \bar{u}(k-1) \tag{6.34}$$

If the equation is given in element form:

$$\begin{cases} A_{11}(z^{-1})y_1(k) = \bar{u}_1(k-1) \\ A_{22}(z^{-1})y_2(k) = \bar{u}_2(k-1) \end{cases} \tag{6.35}$$

It has been shown (Katebi and Moradi, 2001b) for each of these second order system the predictive PID can be designed to have similar structure to the conventional PID. The optimisation is with respect to this new manipulated signal $\bar{u}(k)$. The controller can be implemented by back calculating $u(k)$ as:

$$\begin{bmatrix} u_1(k) \\ u_2(k) \end{bmatrix} = \begin{bmatrix} b_{11}^0 & b_{12}^0 \\ b_{21}^0 & b_{22}^0 \end{bmatrix}^{-1} \left(\begin{bmatrix} \bar{u}_1(k) \\ \bar{u}_2(k) \end{bmatrix} - \begin{bmatrix} b_{11}^1 & b_{12}^1 \\ b_{21}^1 & b_{22}^1 \end{bmatrix} \begin{bmatrix} u_1(k-1) \\ u_2(k-1) \end{bmatrix} \right) \tag{6.36}$$

This means that for 2I2O first order system using decentralized conventional PID controller could be designed to have similar performance to GPC controller.

Chapter 6

Summary: Decentralized Predictive PID Control Algorithm

In this section a new method to design a decentralised predictive PID controller was introduced. Using equation (6.28), the new control signal, $\bar{u}(k)$, will calculated, then, the minimization for this new control signal will be applied in the cost function. The drawback of this method is that the mathematical model of process is required. The predictive PID controller can be implemented using the following procedure.

Algorithm 2: Decentralized Predictive PID controller for MIMO process.

Step 1: Initialisation

1 Find a system model and calculate the discrete polynomials matrices (A, B).
2 Chose the value of prediction horizon, *M*, and formulate the future set point vectors w

Step 2: Control Signal Calculation

1 Using the transformation (6.28), transform the system for new control signal $\bar{u}(k)$
2 Calculate the $\bar{u}(k)$ in (6.30), Using the predictive PID algorithm for SISO systems.
3 Calculate $u(k)$, using equation (6.31).

Step 3: Fine Tuning

1 Apply the control signal and check closed loop performance.
2 Fine-tune the PID gains if necessary.

6.4 State Space Model Representation of Predictive PID

The state space representation has the advantage that it can be used for multi-variable processes in a straightforward manner. The control law is simply the feedback of a linear combination of state vectors. The calculations may be complicated with an additional necessity of including an observer if the states are not accessible. MPC has been formulated in the state space context by Morari, 1994.

6.4.1 System Representation

Consider the deterministic state space representation of the plant as follows:

$$\begin{aligned} x_p(k+1) &= A_p x_p(k) + B_p \Delta u(k) \\ y(k) &= C_p x_p(k) \end{aligned} \tag{6.37}$$

where:

$x_p(k)$: Process state vector $x_p(k) \in R^{n\times 1}$

A_p : State coefficient matrix $A_p \in R^{n\times n}$

B_p : Control coefficient matrix $B_p \in R^{n\times L}$

$\Delta u(k)$: Incremental Controller signal $\Delta u \in R^{L\times 1}$

$y(k)$: Output vector $y \in R^{L\times 1}$

C_p : Output coefficient matrix $C_p \in R^{L\times n}$

L: number of input and output

N: number of state

The system is assumed to be controllable and observable.

Chapter 6

Output Prediction

The output of the model for step *(k+i),* assuming that the state at step k and future control increments are known, can be computed by recursively applying equation (6.37) resulting in (Camacho and Bordons, 1999):

$$y(k+i) = C_p A_p^i x_p(k) + \begin{bmatrix} C_p A_p^{i-1} B_p & C_p A_p^{i-2} B_p & \cdots & C_p B_p \end{bmatrix} \begin{bmatrix} \Delta u(k) \\ \Delta u(k+1) \\ \vdots \\ \Delta u(k+i-1) \end{bmatrix} \tag{6.38}$$

6.4.2 Controller Representation

The MIMO PID controller was defined in equation (6.7):

$$\Delta u(k) = K \sum_{i=0}^{M} E(k+i) = K \sum_{i=0}^{M} R(k+i) - K \sum_{i=0}^{M} Y(k+i) \tag{6.39}$$

This implies that the current control signal value is a linear combination of the future predicted outputs. Using future output prediction in equation (6.38), $Y(k+i)$ can be written as:

$$Y(k+i) = \begin{bmatrix} y(k+i-2) \\ y(k+i-1) \\ y(k+i) \end{bmatrix} = \begin{bmatrix} C_p A_p^{i-2} \\ C_p A_p^{i-1} \\ C_p A_p^{i} \end{bmatrix} x_p(k) + \begin{bmatrix} C_p A_p^{i-3} B_p & \cdots & C_p B_p & 0 & 0 \\ C_p A_p^{i-2} B_p & \cdots & C_p A_p B_p & C_p B_p & 0 \\ C_p A_p^{i-1} B_p & \cdots & C_p A_p^2 B_p & C_p A_p B_p & C_p B_p \end{bmatrix} \begin{bmatrix} \Delta u(k) \\ \Delta u(k+1) \\ \vdots \\ \Delta u(k+i-1) \end{bmatrix} \tag{6.40}$$

which can be written as:

$$Y(k+i) = F_i x_p(k) + H_i U_i(k) \tag{6.41}$$

where the matrices and vectors are defined as:

$$Y(k+i) = \begin{bmatrix} y(k+i-2) \\ y(k+i-1) \\ y(k+i) \end{bmatrix} \quad F_i = \begin{bmatrix} C_p A_p^{i-2} \\ C_p A_p^{i-1} \\ C_p A_p^{i} \end{bmatrix} \qquad A_p^{i} = \begin{cases} A_p^{i} & i \geq 0 \\ 0 & i < 0 \end{cases}$$

$$H_i = \begin{bmatrix} C_p A_p^{i-3} B_p & \cdots & C_p B_p & 0 & 0 \\ C_p A_p^{i-2} B_p & \cdots & C_p A_p B_p & C_p B_p & 0 \\ C_p A_p^{i-1} B_p & \cdots & C_p A_p^2 B_p & C_p A_p B_p & C_p B_p \end{bmatrix} \quad U_i = \begin{bmatrix} \Delta u(k) \\ \Delta u(k+1) \\ \vdots \\ \Delta u(k+i-1) \end{bmatrix}$$

Inserting equation (6.41) in equation (6.39) gives:

$$\Delta u(k) = K \sum_{i=0}^{M} R(k+i) - K(\sum_{i=0}^{M} F_i) x_p(k) - K(\sum_{i=0}^{M} H_i^{'}) U_M(k) \tag{6.42}$$

where:

$$H_i^{'} = \begin{cases} [H_i \quad Zero(3, M-i)] & i < M \\ H_i & i \geq M \end{cases}$$

And if the control cost horizon N_u applies to equation (6.41) the matrices can be written:

$$Y(k+i) = \begin{bmatrix} y(k+i-2) \\ y(k+i-1) \\ y(k+i) \end{bmatrix} \quad F_i = \begin{bmatrix} C_p A_p^{i-2} \\ C_p A_p^{i-1} \\ C_p A_p^{i} \end{bmatrix} \quad U_i = \begin{bmatrix} \Delta u(k) \\ \Delta u(k+1) \\ \vdots \\ \Delta u(k+N_u-1) \end{bmatrix}$$

$$H_i = \begin{bmatrix} C_p A_p^{i-3} B_p & \cdots & C_p B_p & 0 & 0 \\ C_p A_p^{i-2} B_p & \cdots & C_p A_p B_p & C_p B_p & 0 \\ C_p A_p^{i-1} B_p & \cdots & C_p A_p^2 B_p & C_p A_p B_p & C_p B_p \end{bmatrix}_{3 \times N_u}$$

$$H_i' = \begin{cases} [H_i \;\; Zero(3, M-i)] & i < N_u \\ H_i & i \geq N_u \end{cases}$$

If $N_u = 1$ then the matrices are:

$$Y(k+i) = \begin{bmatrix} y(k+i-2) \\ y(k+i-1) \\ y(k+i) \end{bmatrix} \quad F_i = \begin{bmatrix} C_p A_p^{i-2} \\ C_p A_p^{i-1} \\ C_p A_p^{i} \end{bmatrix} \quad H_i' = \begin{bmatrix} C_p A_p^{i-3} B_p \\ C_p A_p^{i-2} B_p \\ C_p A_p^{i-1} B_p \end{bmatrix} \tag{6.43}$$

then for case $N_u = 1$ the equation (6.42) can be written as:

$$(I + KH_1)\Delta u(k) = KR_1 - KF_1 x_p(k) \tag{6.44}$$

where:

$$H_1 = \sum_{i=0}^{M} H_i' \qquad R_1(k) = \sum_{i=0}^{M} R(k+i) \qquad F_1 = \sum_{i=0}^{M} F_i$$

and after some straightforward algebra the controller can be written as:

$$\Delta u(k) = (I + KH_1)^{-1}[KR_1(k) - KF_1 x_p(k)] \tag{6.45}$$

6.4.3 GPC Control Design for State Space Representation

Consider the state space model of plant as has been shown in equation (6.37):

$$x_p(k+1) = A_p x_p(k) + B_p \Delta u(k)$$
$$y(k) = C_p x_p(k)$$

After some straightforward algebra the state prediction in i th step in future is:

$$x_p(k+i) = A_p^i x_p(k) + \begin{bmatrix} A_p^{i-1}B_p & A_p^{i-2}B_p & \cdots & B_p \end{bmatrix} \begin{bmatrix} \Delta u(k) \\ \Delta u(k+1) \\ \vdots \\ \Delta u(k+i-1) \end{bmatrix} \tag{6.46}$$

and for N step prediction ahead of states are:

$$X = \begin{bmatrix} x_p(k+1) \\ x_p(k+2) \\ \vdots \\ x_p(k+N) \end{bmatrix} = \begin{bmatrix} A_p \\ A_p^2 \\ \vdots \\ A_p^N \end{bmatrix} x_p(k) + \begin{bmatrix} B_p & 0 & \cdots & 0 \\ A_p B_p & B_p & \cdots & 0 \\ \vdots & \vdots & \ddots & \vdots \\ A_p^{N-1}B_p & A_p^{N-2}B_p & \cdots & B_p \end{bmatrix} \begin{bmatrix} \Delta u(k) \\ \Delta u(k+1) \\ \vdots \\ \Delta u(k+N-1) \end{bmatrix} \tag{6.47}$$

which can be written as:

$$X = F x_p(k) + HU \tag{6.48}$$

where H and F matrices are defined as:

$$H=\begin{bmatrix} B_p & 0 & \cdots & 0 \\ A_pB_p & B_p & \cdots & 0 \\ \vdots & \vdots & \ddots & \vdots \\ A_p^{N-1}B_p & A_p^{N-2}B_p & \cdots & B_p \end{bmatrix} \quad X=\begin{bmatrix} x_p(k+d+1) \\ x_p(k+d+2) \\ \vdots \\ x_p(k+d+N) \end{bmatrix} \quad U=\begin{bmatrix} \Delta u(k) \\ \Delta u(k+1) \\ \vdots \\ \Delta u(k+N-1) \end{bmatrix}$$

GPC consists of applying a control sequence that minimises the cost function. It is assumed that the costing horizon $\{N_1:N_2\}=\{1:N\}$, and the control horizon $N_u=1$. Assuming all the future control inputs are the same as $u(k)$, the cost function can be written as:

$$\begin{aligned} J=&[Fx_p(k+d)+Hu(k)-W(k)]^T[Fx_p(k+d)+Hu(k)-W(k)] \\ &+\lambda\Delta u^T(k)\Delta u(k) \end{aligned} \tag{6.49}$$

The minimum of J, assuming there are no constraints on the control signals, can be found by making the gradient of J equal to zero, which leads to:

$$\frac{\partial J}{\partial \Delta u}=2H^T[Fx_p(k+d)+Hu(k)-W(k)]+2\lambda(\Delta u(k))=0$$

which can solved for $\Delta u(k)$ as:

$$\begin{aligned} \Delta u(k)&=[H^TH+\lambda I]^{-1}H^T(W(k)-Fx_p(k)) \\ &=K_{GPC}(W(k)-Fx_p(k))=K_{GPC}W(k)-K_0x_p(k) \end{aligned} \tag{6.50}$$

where

$$K_{GPC}=[H^TH+\lambda I]^{-1}H^T \qquad K_0=K_{GPC}F$$

6.4.4 Optimal Values of Predictive PID Gains

Rewrite the MIMO predictive PID controller from (6.45) for constant set point as:

$$\Delta u(k) = (I + KH_t)^{-1}[KR_t(k) - KF_t x_p(k)] \tag{6.51}$$

To compute the optimal values of predictive control PID gains with $N_u = 1$ $[\hat{u}(k) = u(k)]$, the PID control signals should be made the same as GPC controller. This means using equation (6.50) and (6.51) the following optimal problem should be solved:

$$Min_{K \in K^S_{PID}, M} J(K, K_0) \tag{6.52}$$

K^S_{PID} = Set of stability gain matrices for PID

where

$$J(K, K_0) = \left\| (I + KH_t)^{-1} K[R_t(k) - F_t Z(K)] - \{K_{GPC} W(k) - K_0 Z(K)\} \right\|_2$$

$Z = x_p(k)$ is dependent on the controls gains used.

Using the same procedure that was explained in section 6.2.3, the PID gains and rebuilt set point will be calculated as:

$$K = K_0(F_t - H_t K_0)^T [(F_t - H_t K_0)(F_t - H_t K_0)^T]^{-1} \tag{6.53}$$

Calculated as the new set point for system can now be:

$$R_t(k) = K^{-1}(I + KH_t) K_{GPC} W(k) = K_S W(k) \tag{6.54}$$

where

$K_S = K^{-1}(1 + KH_t) K_{GPC}$

Chapter 6

Predictive Control Algorithm for State Space Representation

The predictive PID controller can be implemented using the following procedure.

Algorithm 3: Predictive PID controller for state space representation.

Step 1: Initialisation

1. Find a system model and calculate the discrete matrices, A_p, B_p, C_p
2. Chose the value of prediction horizon, *M*, and formulate the future set point vectors w

Step 2: Off line Calculation

1. Calculate the matrices H_t, F_t in equation (6.45) using equation (6.44)
2 Calculate the GPC gain, K_{GPC}, using equation (6.50)
3 Calculate the optimal value of predictive PID gains using equation (6.53)
4 Iterate over the value of *M* to minimize the cost function.

Step 3: On line Calculation

1 Calculate the following signals
   a $F_t Z(K)$
   b $R_t(k)$ using equation (6.54)
2 Calculate the control increment

$$u(k) = u(k-1) + (I + KH_t)^{-1} K[R_t(k) - F_t Z(K)]$$

Step 4: Fine Tuning

1 Apply the control signal and check closed loop performance.
2 Fine-tune the PID gains if necessary.

6.5 Stability Issues for MIMO Predictive PID Controllers

In spite of the great success of GPC in industry, there was an original lack of theoretical results about the properties of predictive control and initial gap in important questions such as stability and robustness. In fact, the majority of stability results are limited to the infinite horizon case and there is a lack of a clear theory relating the closed loop behaviour to design parameters, such as horizons and weighting sequences. A variation of the standard formulation of GPC appears developed by Clarke and Scattolini (1991), which allows stability and robustness results to be obtained for small horizons. Kouvaritakis and Rossister (1993) introduced the new algorithm called Stable Generalized Predictive Control (SGPC) and it is based on stabilizing the loop before the application of the control strategy. In this section, the closed loop system representation will be found for predictive PID controller and then effect of PID level (M) on stability regions for different systems will be discussed.

6.5.1 Closed Loop Representation of State Space Model

System Representation

The state space model for plant was shown in equation (6.37) as:

$$\begin{aligned} x_p(k+1) &= A_p x_p(k) + B_p \Delta u(k-d) \\ y(k) &= C_p x_p(k) \end{aligned} \tag{6.55}$$

Discrete MIMO PID Controller Representation

The discrete representation of MIMO PID controller can be calculated using continuous form of controller (see Appendix 6.1) and will be:

$$x_c(k+1) = A_c x_c(k) + B_c e(k)$$
$$\Delta u(k) = C_c x_c(k) + D_c e(k) \tag{6.56}$$

Where:

$e(k) = r(k) - y(k)$

$r(k)$ is the set point and d is delay of system

the relation between coefficient matrices are (see Appendix 6.2):

$A_c = (T_s A_c^{'} + I) \quad B_c = T_s B_c^{'}$.

Where:

T_s is sampling time.

$A_c^{'}, B_c^{'}$ are proper matrices in continuous form.

Then the closed loop system Fig 6.3 can be written:

$$\begin{bmatrix} x_p(k+1) \\ x_c(k+1) \end{bmatrix} = \begin{bmatrix} A_P - B_p D_c C_p & B_p C_c \\ -B_c C_p & A_c \end{bmatrix} \begin{bmatrix} x_p(k) \\ x_c(k) \end{bmatrix} + \begin{bmatrix} B_p D_c \\ B_c \end{bmatrix} r(k)$$
$$A_{cl} = \begin{bmatrix} A_P - B_p D_c C_p & B_p C_c \\ -B_c C_p & A_c \end{bmatrix} \tag{6.57}$$

The eigen-values of matrix A_{cl} are the poles of the closed loop system.

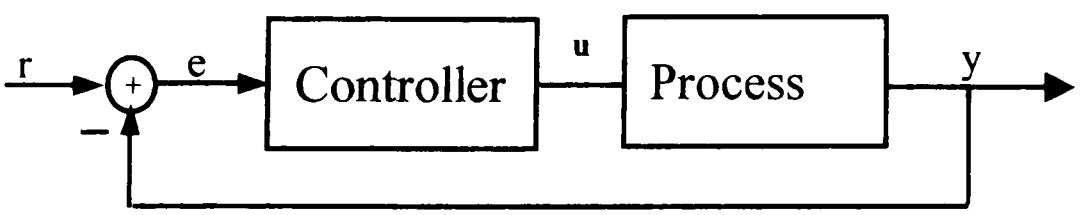

Fig 6.3: The closed loop block diagram of process and controller

6.5.2 Closed Loop Representation of Proposed Method

System Representation and Future Output Prediction

Form equation (6.55) the plant model is:

$$x_p(k+1) = A_p x_p(k) + B_p \Delta u(k)$$
$$y(k) = C_p x_p(k)$$

and from equation (6.38), the predicted output at step *(k+i)* is:

$$y(k+i) = C_p A_p^i x_p(k) + \begin{bmatrix} C_p A_p^{i-1} B_p & C_p A_p^{i-2} B_p & \cdots & C_p B_p \end{bmatrix} \begin{bmatrix} \Delta u(k) \\ \Delta u(k+1) \\ \vdots \\ \Delta u(k+i-1) \end{bmatrix}$$

M step prediction ahead of output in compact form will be:

$$Y_M(k) = F_M x_p(k) + H_M U_{M-1}(k) \tag{6.58}$$

where matrices are defined as:

$$Y_M(k) = \begin{bmatrix} y(k) \\ y(k+1) \\ y(k+2) \\ \vdots \\ y(k+M) \end{bmatrix} \quad F_M = \begin{bmatrix} C_p \\ C_p A_p \\ C_p A_p^2 \\ \vdots \\ C_p A_p^M \end{bmatrix} \quad U_{M-1}(k) = \begin{bmatrix} \Delta u(k) \\ \Delta u(k+1) \\ \vdots \\ \Delta u(k+M-1) \end{bmatrix}$$

$$H_M = \begin{bmatrix} 0 & 0 & 0 & 0 \\ C_p B_p & 0 & \cdots & 0 \\ C_p A_p B_p & C_p B_p & \cdots & 0 \\ \vdots & \vdots & \ddots & 0 \\ C_p A_p^{M-1} B_p & C_p A_p^{M-2} B_p & \cdots & C_p B_p \end{bmatrix}$$

Chapter 6

Representation of Predictive MIMO PID controllers

The controller consists of M parallel PID controllers as shown in Fig 6.2. For M=0, the closed loop system is identical to the conventional PID in equation (6.57). For M>0 the proposed controller has predictive capability similar to MPC where M is prediction horizon of PID controller. The state space representation of predictive PID controller can be achieved by the following two methods:

a) The conventional state space representation for PID is considered and the input to controller is sum of error signal from step k to step $(k+M)$, $\sum_{i=0}^{M} e(k+i)$, which depends on the future output of system (This means that the controller is using $\sum_{i=0}^{M} e(k+i)$ at step k, also, states and outputs of controller will be calculated using future output of system only).

$$x_c(k+1) = A_c x_c(k) + B_c \sum_{i=0}^{M} r(k+i) - B_c \sum_{i=0}^{M} y(k+i)$$
$$\Delta u(k) = C_c x_c(k) + D_c \sum_{i=0}^{M} r(k+i) - D_c \sum_{i=0}^{M} y(k+i) \qquad (6.59)$$

b) The conventional state space representation for predictive PID is considered and the input to controller at step k is sum of error signal from step k to step $(k+M)$, $\sum_{i=0}^{M} e(k+i)$, which depends on the future output of the system and the state of the controller at previous step (This means that controller will be fed by $e(k)$ from step k to step $(k+M)$, also, states and outputs of controller at each step will be calculated using future outputs of system and previous state of controller).

$$
\begin{aligned}
x_c(k+1) &= A_c x_c(k) + B_c \sum_{i=0}^{M} r(k+i) - B_c \sum_{i=0}^{M} y(k+i) \\
&\quad + \sum_{i=1}^{M} A_c^{i+1} x_c(k) + \sum_{i=1}^{M} \sum_{j=1}^{i} [A_c^j B_c e(k+i-j)] \\
\Delta u(k) &= C_c x_c(k) + D_c \sum_{i=0}^{M} r(k+i) - D_c \sum_{i=0}^{M} y(k+i) \\
&\quad + C_c \sum_{i=1}^{M} A_c^i x_c(k) + \sum_{i=1}^{M} \sum_{j=0}^{i-1} [C_c A_c^j B_c e(k+i-j)]
\end{aligned}
\tag{6.60}
$$

It seems that the method (a) is more reasonable and acceptable so we continue with this method (see appendix 6.3 for result of method b). To calculate $\Delta u(k)$ in equation (6.59), it is needed to predict $y(k+i)$ and from equation (6.58) to predict $y(k+i)$ it is necessary to specify $\Delta u(k+i)$. In other words, control signal at step k depend on future control signal, it is assumed that the system is causal then, there are two possibilities for $\Delta u(k+i)$ in equation (6.59):

1) $\Delta u(k+i) = 0 \qquad i > 0$

with this assumption the equation (6.58) can be written as:

$$y_t(k) = F_{Mt} x_p(k) + H_{Mt} \Delta u(k) \tag{6.61}$$

where:

$$y_t(k) = \sum_{i=0}^{M} y(k+i) \qquad F_{Mt} = C_p \sum_{i=0}^{M} A_p^i \qquad H_{Mt} = C_p (\sum_{i=0}^{M-1} A_p^i) B_p$$

2) $\Delta u(k+i) = \Delta u(k) \qquad i > 0$

After some straightforward algebra equation (6.58) can be written as:

$$y_t(k) = F_{Mt} x_p(k) + H_{Mt} \Delta u(k) \tag{6.62}$$

where:

$$y_t(k)=\sum_{i=0}^{M} y(k+i) \qquad F_{Mt}=C_p\sum_{i=0}^{M} A_p^i \qquad H_{Mt}=C_p(\sum_{i=0}^{M-1}\sum_{j=0}^{i} A_p^j)B_p$$

Inserting equation (6.61) or (6.62) in equation (6.59):

$$\begin{aligned} x_c(k+1) &= A_c x_c(k)+B_c\sum_{i=0}^{M} r(k+i)-B_c F_{Mt}x_p(k)-B_c H_{Mt}\Delta u(k) \\ \Delta u(k) &= C_c x_c(k)+D_c\sum_{i=0}^{M} r(k+i)-D_c F_{Mt}x_p(k)-D_c H_{Mt}\Delta u(k) \end{aligned} \tag{6.63}$$

Calculating $\Delta u(k)$ from equation (6.63)

$$(I+D_c H_{Mt})\Delta u(k)=C_c x_c(k)+D_c\sum_{i=0}^{M} r(k+i)-D_c F_{Mt}x_p(k)$$

$$\Delta u(k)=C_c^{'} x_c(k)+D_c^{'}\sum_{i=0}^{M} r(k+i)-D_c^{'} F_{Mt}x_p(k) \tag{6.64}$$

where:

$$C_c^{'}=(I+D_c H_{Mt})^{-1}C_c \qquad D_c^{'}=(I+D_c H_{Mt})^{-1}D_c$$

Put $\Delta u(k)$ in equation (6.63):

$$\begin{aligned} x_c(k+1) &= (A_c-B_c H_{Mt}C_c^{'})x_c(k)+(B_c-B_c H_{Mt}D_c^{'})\sum_{i=0}^{M} r(k+i) \\ &\quad -(B_c F_{Mt}-B_c H_{Mt}D_c^{'}F_{Mt})x_p(k) \end{aligned} \tag{6.65}$$

Rewriting equation (6.63) in compact form:

$$\begin{aligned} x_c(k+1) &= A_{cc}x_c(k)+B_{cc}\sum_{i=0}^{M} r(k+i)-A_{cp}x_p(k) \\ \Delta u(k) &= C_{cc}x_c(k)+D_c^{'}\sum_{i=0}^{M} r(k+i)-D_{cp}x_p(k) \end{aligned} \tag{6.66}$$

where

$$A_{cc} = (A_c - B_c H_{Mt} C_c^{'})$$
$$B_{cc} = (B_c - B_c H_{Mt} D_c^{'})$$
$$A_{cp} = (B_c F_{Mt} - B_c H_{Mt} D_c^{'} F_{Mt})$$
$$C_{cc} = C_c^{'} \qquad D_{cp} = D_c^{'} F_{Mt}$$

Using equation (6.55) and (6.66) the process and the controller can be rewritten as:

Plant:

$$x_p(k+1) = A_p x_p(k) + B_p \Delta u(k)$$
$$y(k) = C_p x_p(k)$$

Controller:

$$x_c(k+1) = A_{cc} x_c(k) + B_{cc} \sum_{i=0}^{M} r(k+i) - A_{cp} x_p(k)$$

$$\Delta u(k) = C_{cc} x_c(k) + D_c^{'} \sum_{i=0}^{M} r(k+i) - D_{cp} x_p(k)$$

then the closed loop system will be:

$$\begin{bmatrix} x_p(k+1) \\ x_c(k+1) \end{bmatrix} = \begin{bmatrix} A_P - B_p D_{cp} & B_p C_{cc} \\ -A_{cp} & A_{cc} \end{bmatrix} \begin{bmatrix} x_p(k) \\ x_c(k) \end{bmatrix}$$
$$A_{cl} = \begin{bmatrix} A_P - B_p D_{cp} & B_p C_{cc} \\ -A_{cp} & A_{cc} \end{bmatrix} \qquad (6.67)$$

To check the stability of system, all the eigen-values of the closed loop system (roots of characteristic equation of A_{cl} matrix) should be inside the unit circle.

6.6.Case Studies:

In this section, the stability regions of this method and performance comparison of proposed method and GPC for two industrial systems will be discussed, the systems are:

1- The small signal model of a stirred tank reactor, Fig 6.4a was described by the following transfer matrix (Camacho and Bordons, 1999):

$$g_1(s)=\begin{bmatrix} \dfrac{1}{1+0.7s} & \dfrac{5}{1+0.3s} \\ \dfrac{1}{1+0.5s} & \dfrac{2}{1+0.4s} \end{bmatrix} \tag{6.68}$$

where the manipulated variable $u_1(s)$ and $u_2(s)$ are the feed flow rate and the flow of coolant in the jacket respectively. The control variables $Y_1(s)$ and $Y_2(s)$ are the effluent concentration and the reactor temperature respectively.

2- The boiler model, Fig 6.4b, has been considered. (Katebi *et al*. 2000c)

$$g_2(s)=\begin{bmatrix} \dfrac{-.007s+.00078}{s^2+.0178s+.00055} & \dfrac{-.005s+7\times10^{-5}}{s^2+.017s+.0004} \\ \dfrac{-.0067s+.00062}{s^2+.017s+.00053} & \dfrac{s^2-.043s+.00065}{s^2+.067s+.0006} \end{bmatrix} \tag{6.69}$$

where the manipulated variable $u_1(s)$ and $u_2(s)$ are the feed/air demand and the control valve position respectively. The control variables $Y_1(s)$ and $Y_2(s)$ are throttle pressure and the steam flow respectively.

The table6.1 shows the continuous and discrete representation of systems.

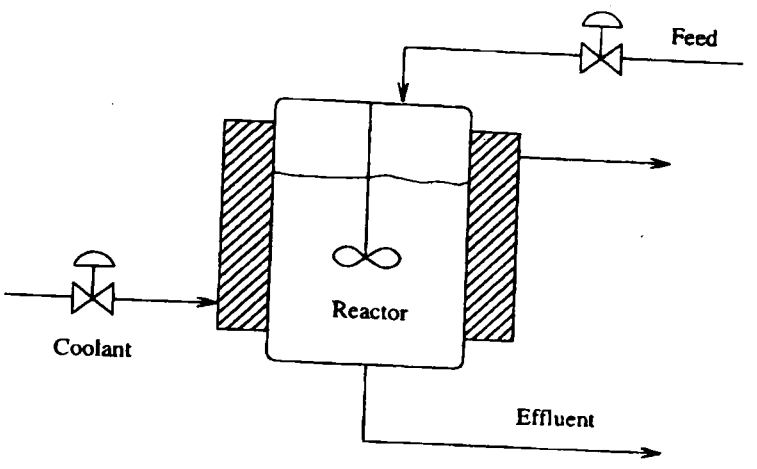

(a): Stirred tank reactor (Camacho and Bordons, 1999)

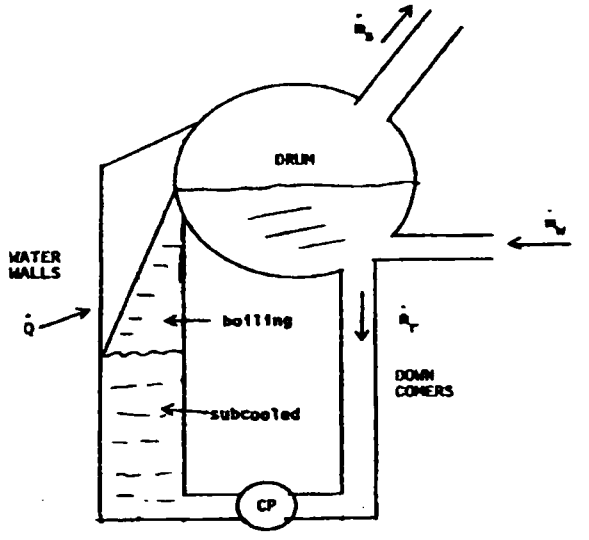

(b): System defining steam generation and pressure

Fig6.4: Two industrial system representation

6.6.1.Stability Study

The effect of M on PID parameters and variation of PID parameters on stability region for two types of systems has been considered. The results showed that for non-minimum phase system (boiler) the stability region is closed and bigger M causes the smaller stability region Fig 6.5b. For Stable systems the regions are not closed, but like non-minimum phase increasing M decreases the stability regions Fig 6.5a.

Remark:

It has been found empirically that bigger M decreases the PID coefficient and for stable system increases the possibility of stability. For non-minimum phase bigger M decreases the possibility of stability. And for unstable system increasing M increases the possibility of stability.

6.6.2.Performance Study

Performance of many different systems was studied and the proposed method showed satisfactory results compared to GPC. In this section, the closed loop performance of multivariable and multi-loop predictive PID will compare to GPC.

Multivariable Predictive PID Controller

GPC and Multivariable predictive PID methods were used to design the controller for two systems g1 and g2 with transfer function mentioned in equation (6.68) and (6.69) respectively. For GPC, the horizon prediction of output N=20, control input horizon N_u=1 were assumed. The controller gains for the two methods are shown in Table 6.2. It

is clear from the Table6.2 that for the first order 2I2O system conventional PID is enough to achieve the GPC performance (M=0). For second order 2I2O system also M=2 is sufficient to approximate the GPC performance. The step response of the closed loop system for two methods has been shown in Fig 6.6 and 6.7. The results show that the proposed method can achieve GPC performance levels provided M is chosen correctly.

Multi-loop Predictive PID Controller

GPC and Multi-loop predictive PID methods were used to design the controller for two systems described by equations (6.68) and (6.69). For GPC, the horizon prediction of output N=20, control input horizon N_u=1 ware assumed. The gains of two methods have been shown in Table 6.3. The step response of the closed loop system for two methods, control signals and the transformed control signals has been shown in Fig 6.8 and 6.9. The step response results show that for decentralized predictive PID design the interactions between loops has been removed and for first order 2I2O system conventional PID is enough to achieve the GPC performance (M=0) without interaction between loops. For second order 2I2O system, three levels of PID is sufficient to approximate the GPC performance (M=2).

6.7 Summary

The MIMO proposed predictive PID controller design was described in this chapter. A multivariable and multi-loop predictive PID controller was proposed which has important characteristics similar to the model based predictive control. The controller reduces to the same structure PID controller for first order 2I2O system. It was shown that the optimal values of PID gains might found using a scheme similar to a MPC. Various benchmark processes were employed to illustrate the stability and performance of the proposed method. The state space representation of method was shown. One of the main advantages of the proposed controller is that it can be used with systems of any order and the PID tuning can be used to adjust the controller performance.

Table 6.1: Continues and discrete representation of system.

Transfer Function of System	Z Transform presentation of system	Level of PID (M+1)	Description
$g_1(s) = \begin{bmatrix} \frac{1}{1+0.7s} & \frac{5}{1+0.3s} \\ \frac{1}{1+0.5s} & \frac{2}{1+0.4s} \end{bmatrix}$	$g_1(z^{-1}) = \begin{bmatrix} \frac{0.7603z^{-1}}{1-0.2397z^{-1}} & \frac{4.822z^{-1}}{1-0.036z^{-1}} \\ \frac{0.865z^{-1}}{1-0.1353z^{-1}} & \frac{1.84z^{-1}}{1-0.082z^{-1}} \end{bmatrix}$	1 5 20	a stirred tank reactor (Camacho and Bordons, 1999):
$g_2(s) = \begin{bmatrix} \frac{-.007s+.00078}{s^2+.0178s+.00055} & \frac{-.005s+7e-5}{s^2+.017s+.0004} \\ \frac{-.0067s+.00062}{s^2+.017s+.00053} & \frac{s^2-.043s+.00065}{s^2+.067s+.0006} \end{bmatrix}$	$g_2(z^{-1}) = \begin{bmatrix} \frac{-.007z^{-1}+0.007z^{-2}}{1-1.98z^{-1}+.98z^{-2}} & \frac{.005z^{-1}+0.005z^{-2}}{1-1.98z^{-1}+.98z^{-2}} \\ \frac{.006z^{-1}+0.007z^{-2}}{1-1.98z^{-1}+.98z^{-2}} & \frac{1-1.96z^{-1}+0.96z^{-2}}{1-1.93z^{-1}+.93z^{-2}} \end{bmatrix}$	0 1	The boiler model has been considered. (Moradi *et al*, 2000a)

Table 6.2: GPC and Proposed PID control design for: g1: Stirred tank reactor (Camacho and Bordons, 1999)
g2: Boiler model (Moradi *et al*, 2000a).

System	Level of PID (M+1)	GPC Gain	Predictive PID Gain $\begin{bmatrix} Kpid_{11} & Kpid_{12} \\ Kpid_{21} & Kpid_{22} \end{bmatrix}$
$g_1(z^{-1}) = \begin{bmatrix} \frac{0.7603z^{-1}}{1-0.2397z^{-1}} & \frac{4.822z^{-1}}{1-0.036z^{-1}} \\ \frac{0.865z^{-1}}{1-0.1353z^{-1}} & \frac{1.84z^{-1}}{1-0.082z^{-1}} \end{bmatrix}$	0	$\begin{bmatrix} -.072 & .285 & .019 & -.062 & -.0006 & .0031 & -.02 & .01 \\ .236 & .018 & -.064 & -.0038 & .002 & .0002 & -.008 & -.273 \end{bmatrix}$	$\begin{bmatrix} -.02 & -.054 & -.0006 & .055 & .23 & .003 \\ .06 & .174 & .002 & .0034 & .014 & .0002 \end{bmatrix}$
	10		$\begin{bmatrix} -.019 & -.029 & -.005 & .0067 & .038 & .0017 \\ -.037 & -.04 & .012 & -.013 & -.031 & .0026 \end{bmatrix}$
$g_2(z^{-1}) = \begin{bmatrix} \frac{-.007z^{-1}+0.007z^{-2}}{1-1.98z^{-1}+.98z^{-2}} & \frac{.005z^{-1}+0.005z^{-2}}{1-1.98z^{-1}+.98z^{-2}} \\ \frac{.006z^{-1}+0.007z^{-2}}{1-1.98z^{-1}+.98z^{-2}} & \frac{1-1.96z^{-1}+0.96z^{-2}}{1-1.93z^{-1}+.93z^{-2}} \end{bmatrix}$	1	$\begin{bmatrix} .087 & -.0 & .0597 & .0001 & .041 \\ -.003 & .026 & -.002 & .003 & -.0013 \\ .0001 & .011 & -.00 & .003 & .00 & .162 \\ .001 & -.0004 & -.002 & -.0001 & .0 & -.003 \end{bmatrix}$	$\begin{bmatrix} -0.05 & 0.14 & 0.04 & -0.0003 & -0.00031 & -0.0002 \\ 0.03 & 0.03 & 0.01 & -0.0034 & 0.0135 & -0.0058 \end{bmatrix}$
	5	$\begin{bmatrix} .033 & .055 & .014 & .015 & .003 \\ .27 & -.0087 & .056 & -.0005 & -.023 \end{bmatrix}$	$\begin{bmatrix} -0.004 & 0.05 & -0.013 & .0005 & .0015 & 0.0002 \\ .0005 & .0015 & .0002 & .017 & .047 & -0.061 \end{bmatrix}$

Table6.3: GPC and Proposed Decentralized PID control design for:two different system.

System	Level of PID (M+1)	GPC Gain	Predictive PID Gain $\begin{bmatrix} Kpid_{11} & 0 \\ 0 & Kpid_{22} \end{bmatrix}$
$g_1(z^{-1}) = \begin{bmatrix} \frac{0.7603z^{-1}}{1-0.2397z^{-1}} & \frac{4.822z^{-1}}{1-0.036z^{-1}} \\ \frac{0.865z^{-1}}{1-0.1353z^{-1}} & \frac{1.84z^{-1}}{1-0.082z^{-1}} \end{bmatrix}$	0	$\begin{bmatrix} .018 & .24 & -.004 & -.064 & -.0002 & .002 & -.27 & -.0075 \\ .285 & -.072 & -.062 & .0194 & .003 & -.0006 & .011 & -.018 \end{bmatrix}$	$\begin{bmatrix} .085 & .35 & .005 & 0 \\ 0 & .1225 & .35 & .004 \end{bmatrix}$
$g_2(z^{-1}) = \begin{bmatrix} \frac{.74z^{-1}+0.6z^{-2}}{1-0.84z^{-1}+.5z^{-2}} & \frac{.18z^{-1}+0.14z^{-2}}{1-0.82z^{-1}+.45z^{-2}} \\ \frac{.18z^{-1}+0.14z^{-2}}{1-0.82z^{-1}+.45z^{-2}} & \frac{.74z^{-1}+0.6z^{-2}}{1-0.84z^{-1}+.5z^{-2}} \end{bmatrix}$	3	$\begin{bmatrix} .53 & .126 & -.858 & -.235 & .777 & .256 & -.35 & -.14 \\ .0345 & .66 & -.056 & -1.2 & .03 & 1.3 & -0.026 & -.7 \\ .087 & .043 & .009 & .02 & .02 & .043 & .04 & .066 \\ .0056 & .22 & .028 & .15 & .027 & .23 & .061 & .26 \end{bmatrix}$	$\begin{bmatrix} -.01 & .046 & .085 & 0 \\ 0 & -.023 & .048 & .089 \end{bmatrix}$

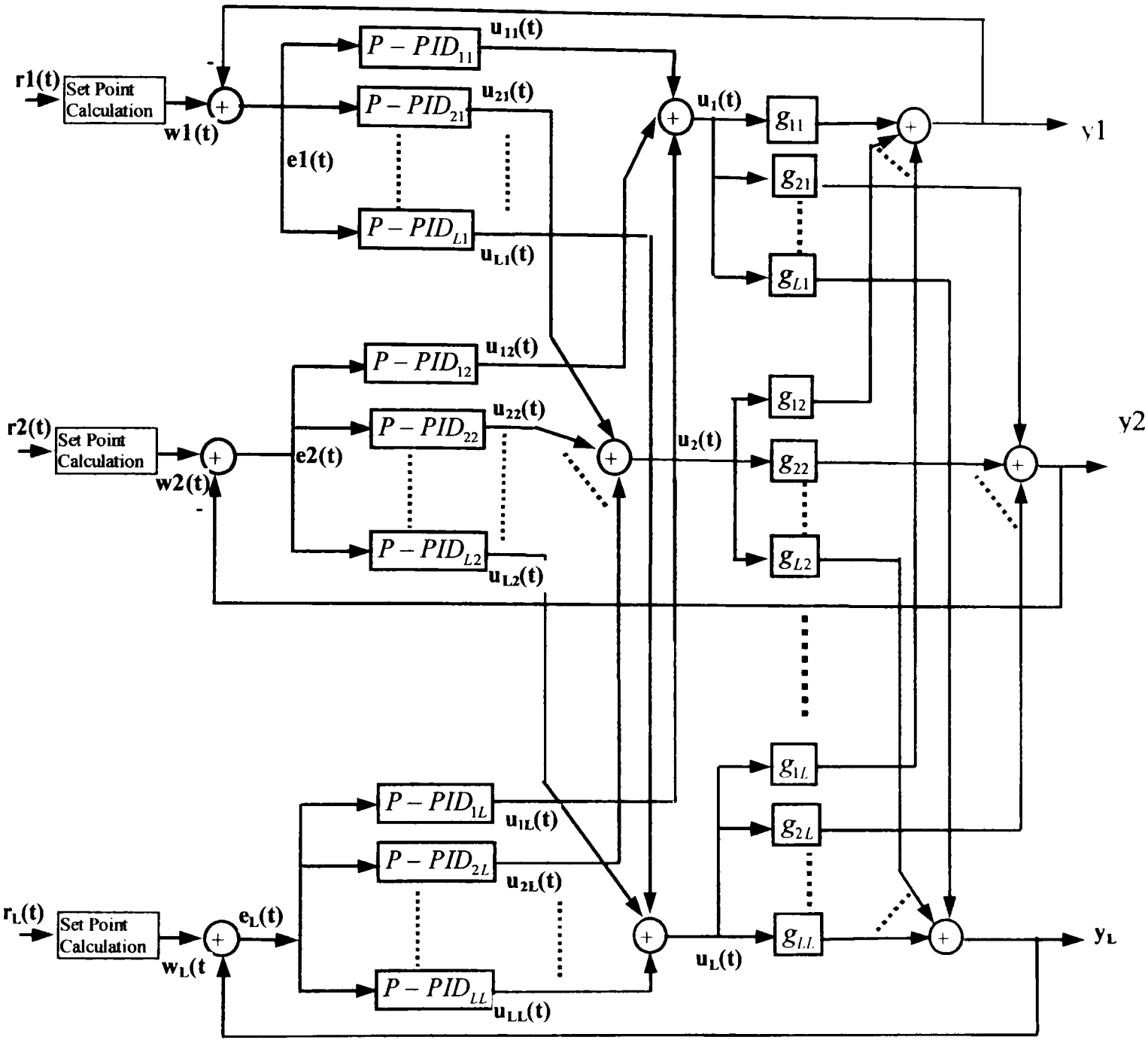

Fig 6.2a: The MIMO Predictive PID structure

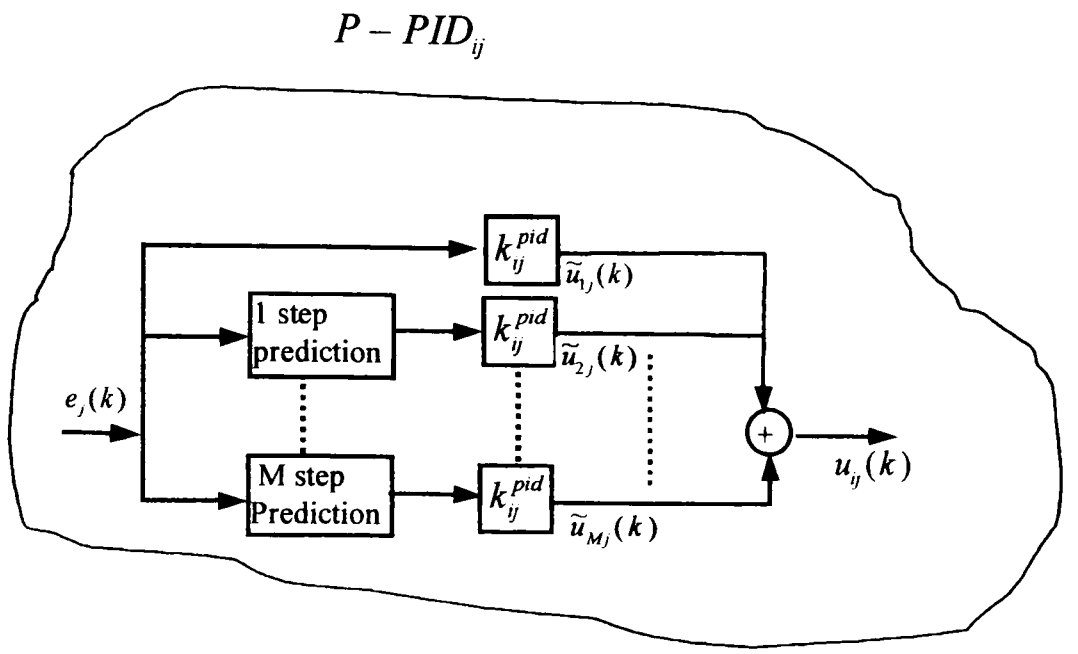

$$\widetilde{u}_{jl}(k) = k_{jl}^{p} e_l(k) + k_{jl}^{i} \sum_{m=1}^{k} e_l(m) + k_{jl}^{d}[e_l(k) - e_l(k-1)]$$

Fig 6.2b: The block diagram of ij th Predictive PID.

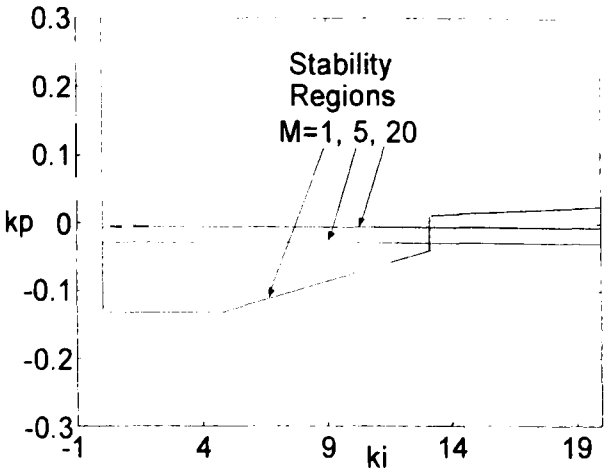

kd=constant

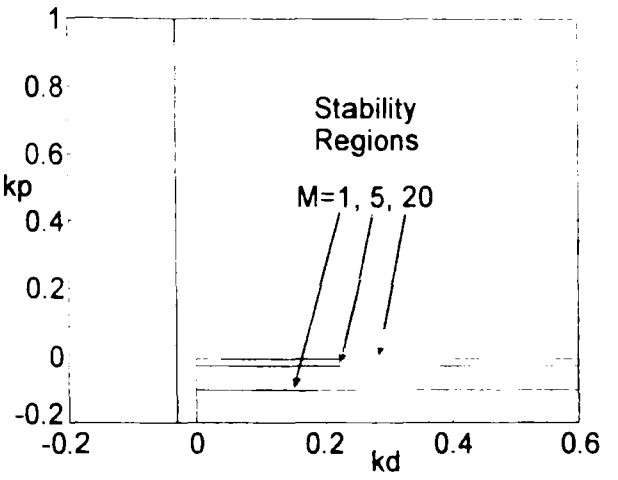

ki=constant

Fig6.5a: The stability Regions for the small signal model of a stirred tank reactor.

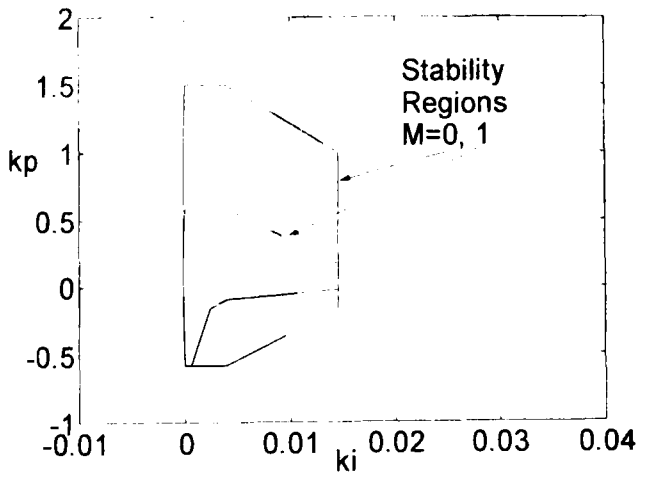

kd=constant

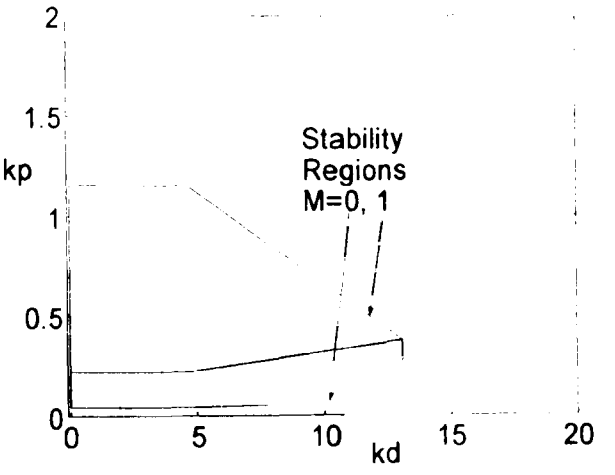

ki=constant

Fig6.5b: The stability Regions for the Boiler model

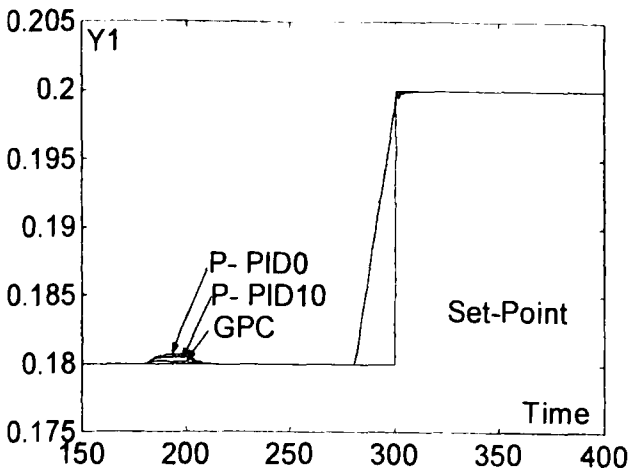

(a) Output 1

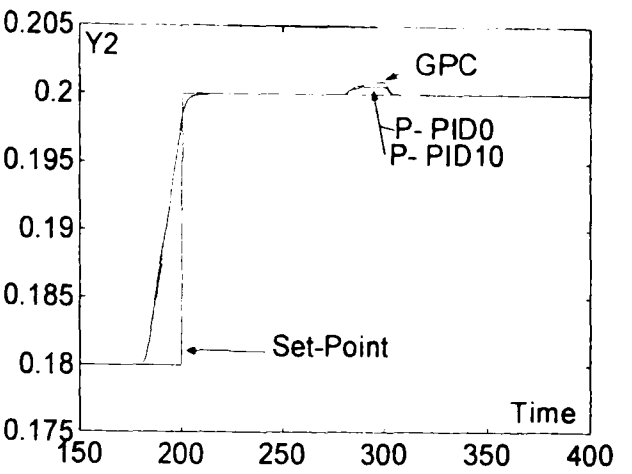

(b) Output 2

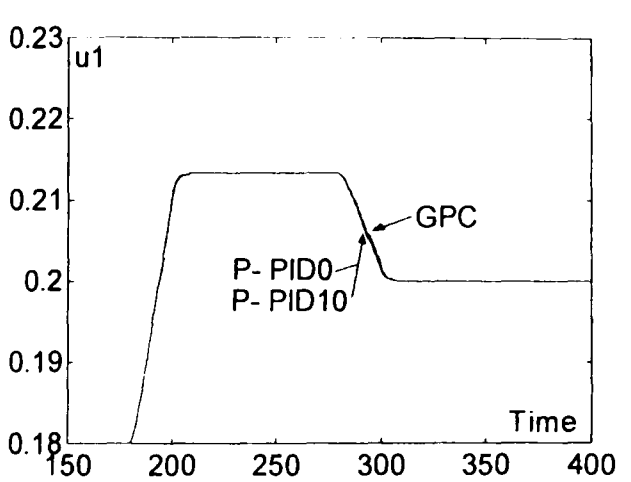

(c) Control signal 1

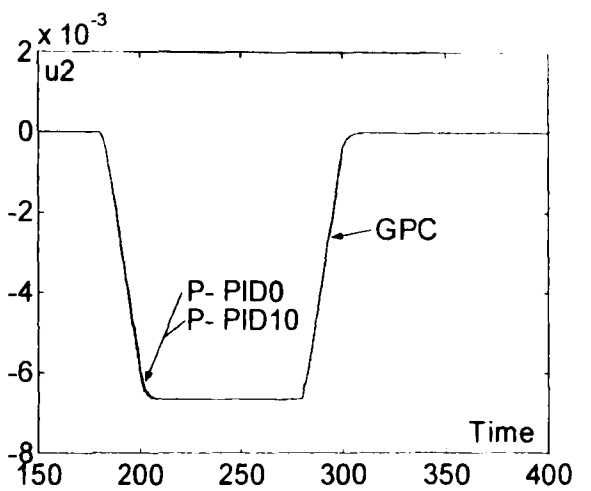

(d) Control signal 2

Fig.6.6: The comparison of GPC method with Proposed Predictive PID Method for g1

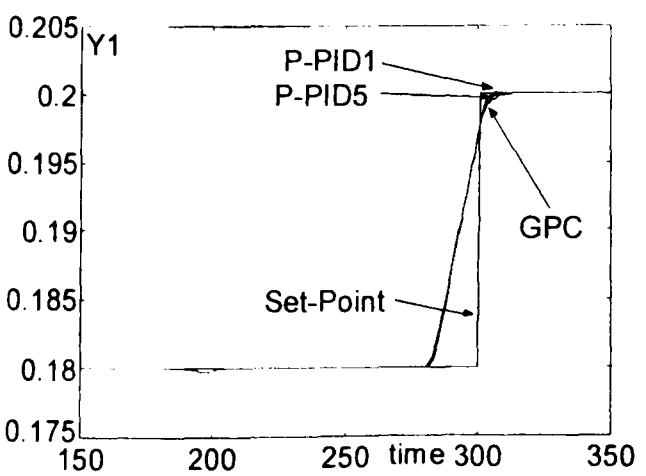

(a) Output 1

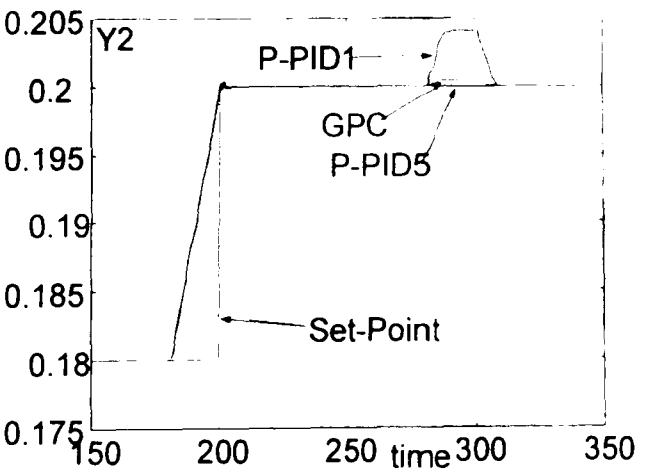

(b) Output 2

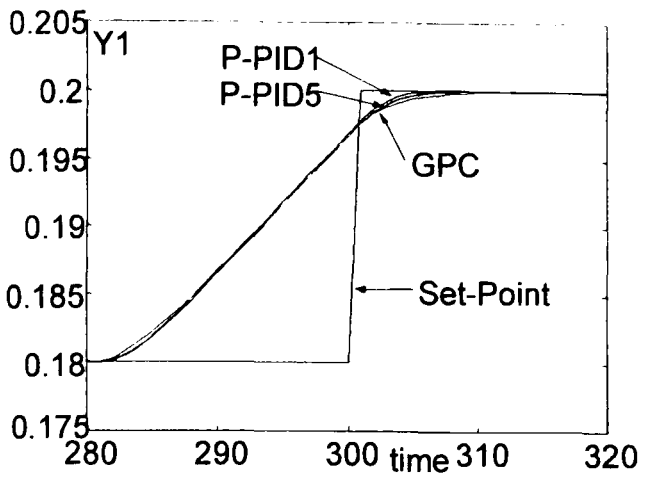

(c) Output 1

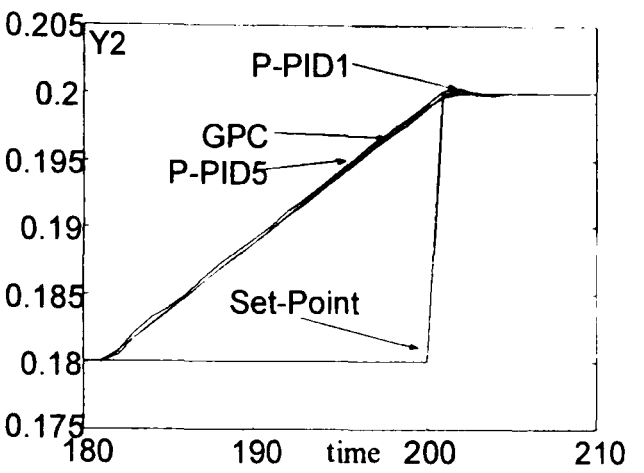

(d) Output 2

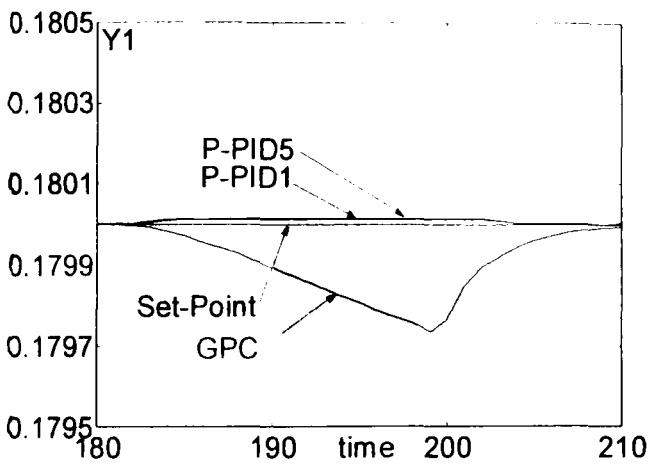

(e) Output 1

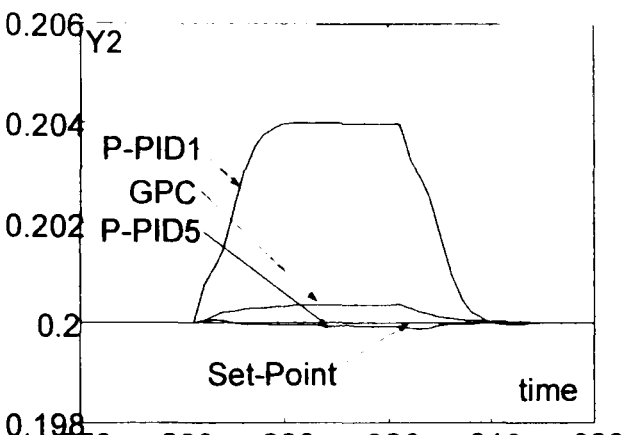

(f) Output 1

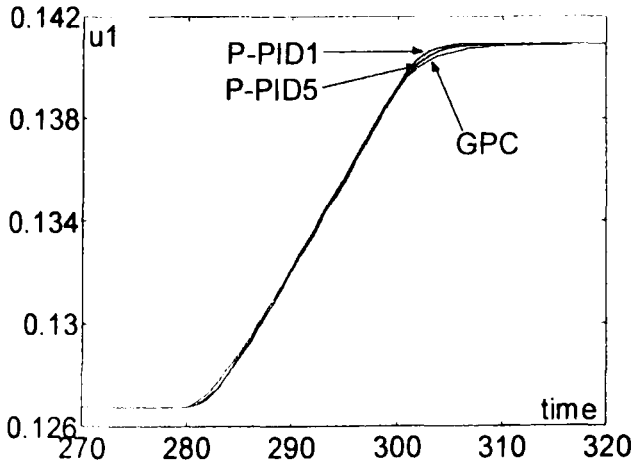

(g) Control signal 1

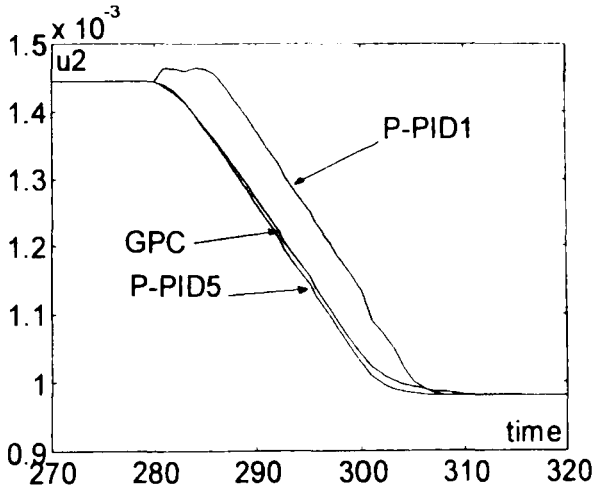

(h) Control signal 2

Fig.6.7: The comparison of GPC method with Proposed predictive PID Method for g2

.

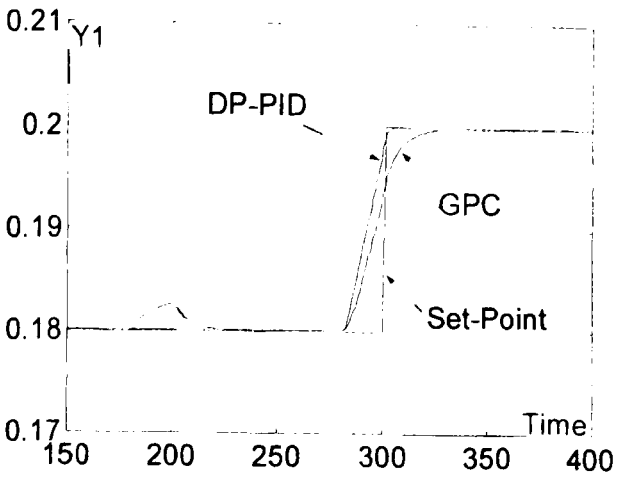

(a) Output 1

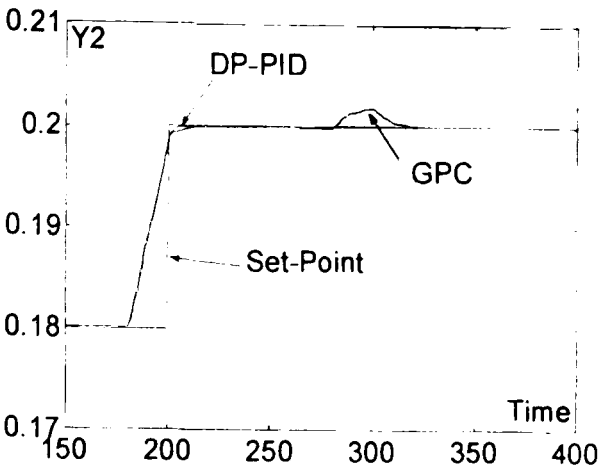

(b) Output 2

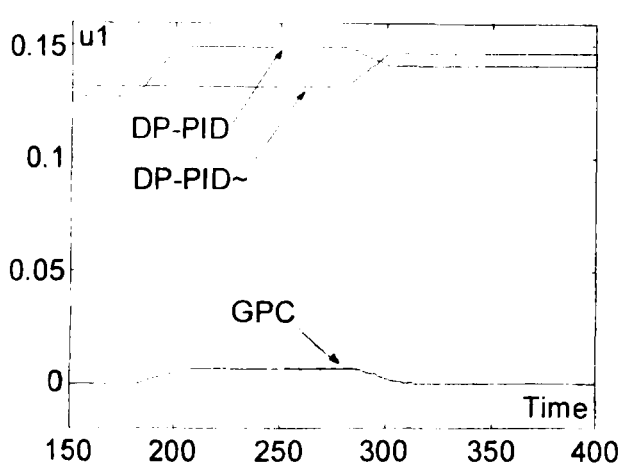

(c)

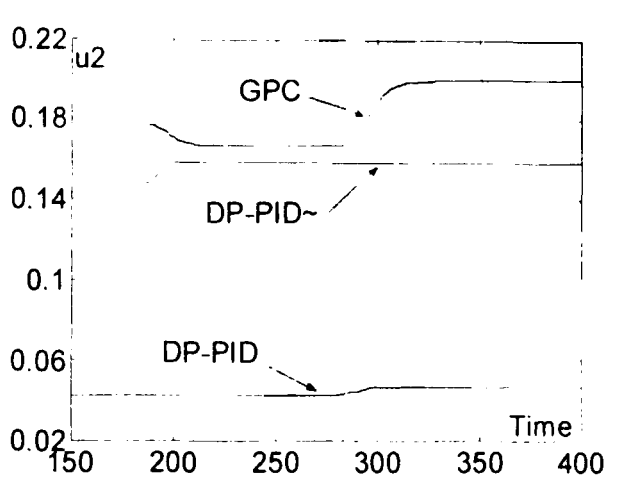

(d)

DP-PID: The control signal of the Decentralised Predictive PID Controller
DP-PID~: The transformed control signal of the Decentralised Predictive PID Controller

Fig.6.8: The comparison of GPC method with Proposed predictive PID Method for A stirred tank reactor (Camacho and Bordons, 1999).

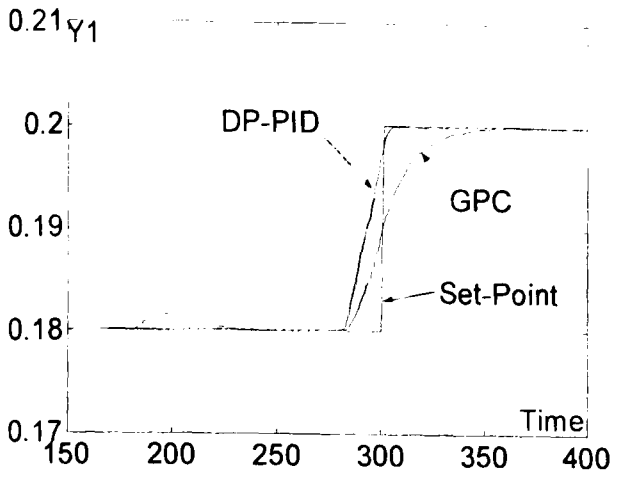

(a) Output 1

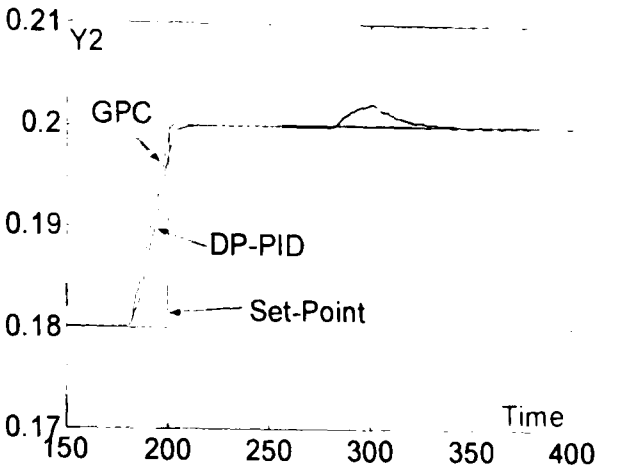

(b) Output 2

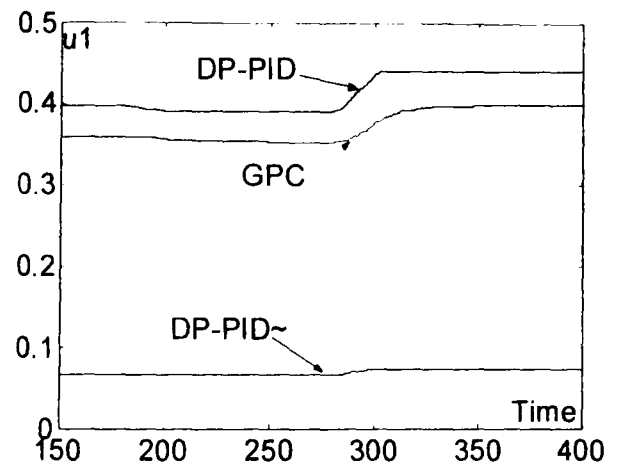

(c)

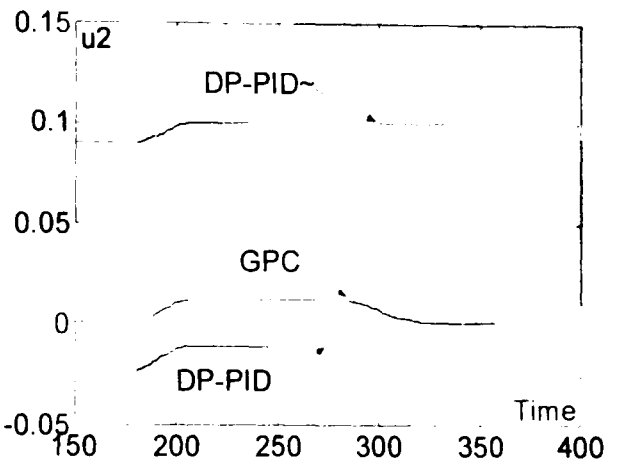

(d)

DP-PID: The control signal of the Decentralised Predictive PID Controller
DP-PID~: The transformed control signal of the Decentralised Predictive PID Controller

Fig.6.9: The comparison of GPC method with Proposed predictive PID Method for Boiler system.

Chapter 7

Conclusions

7.1 Introduction

PID tuning methods can be divided to following categories, where the classification is based on the availability of a process model, and the model type, Fig I (in Page x):

- Model Free Methods
- Non parametric Model Methods
- Parametric Model Methods

Model Free Methods

No model or any particular points of the process are identified.

Non-parametric model methods

In these methods, it is assumed that some particular points of the process such as critical points are available. This category can be further divided into:

Optimal non-parametric methods: In these methods the data of process is used to minimise a cost function. Very few methods exist in this area and more work should be done.

Non-optimal non-parametric methods: In these methods the data of particular points of process frequency response are used to calculate PID parameters. The well-known relay tests are in this category. Relay tests are used to identify the critical frequency data and then PID tuning rules such as the classical Ziegler-Nichols Rules are used to calculate the PID parameters.
Other data such as steady state gains, high frequency gains and bandwidth frequency gains can also be used to tune the PID controller. These methods were explained in Chapter 3, and a new relay tuning method was introduced in Chapter 4.

Parametric model methods

Parametric methods require a process model which is based on a parametric description. The model can be either nonlinear or linear in the process parameters. In this thesis most of the methods used a linear model of the process, a state space model, or a transfer function model over the frequency range of interest. The methods in this category are more suitable for off-line PID control tuning. Parametric methods can be divided to following methods:

- Non-Optimal Parametric Methods
- Optimal Methods one (Restricted Structure Control)
- Optimal Methods two (Control Signal Matching (Typically))

Non-Optimal parametric methods: In non-optimal parametric methods, it is assumed that the model of process is available. In some of these methods the PID controller is tuned so that the closed loop system meets specified system robustness (phase and gain margin) and performance values (Ho et al., 1998). Luyben (1986) devised the method of Biggest Log Modulus (BLT) to tune the PID gains. In this method, the PID gains are first found using well known methods and then these gains are retuned until BLT become less than a specified value. Internal Model Control (IMC) is another method of

non-optimal parametric, which will find the PID gains for each element of transfer function, G(s), and then tuning matrix for the MIMO system is computed. These methods were explained in Chapter 3.

Optimal parametric methods, Group 1 (Restricted Structure Control): In this optimal method, different ways are used to tune the PID parameters with respect to a criteria which is usually the minimization of a standard cost function:

$Min\ J_{Standard}$ with respect to k_p, k_i and k_d

where, k_p, k_i and k_d are the PID parameters.

Some possible design specifications are:

- Quadratic cost functions
- Minimum Input Energy cost
- Robust Stability cost functions
- Operational constraints

In recent years, Astrom *et al.* (1998) has presented a numerical method for designing PI controllers. Minimising the integrated control error has been used to obtain good load disturbance responses. Robustness was guaranteed by requiring that the maximum sensitivity is less than a specified value M_s. In their work, the design problem was formulated as a constrained optimisation problem and unique solutions for special cases of systems were introduced, but for complicated system the solution could be very complicated. This method has been simplified for first order system with delay by Hagglund and Astrom (2001).

Optimal parametric methods, Group 2 (Control Signal Matching (Typically)): Because of wide application of the PID controllers, many researchers have attempted to use advanced control techniques such as optimal control and GPC to restrict the structure of these controllers to retrieve the PID controller. In some of these methods the control signal of advanced technique has been approximated by PID control using a cost function, which usually is the norm of error between output of PID controller and advanced controller signal. These methods are called optimal methods *Group 2*. In these methods, Model Based Predictive control such as GPC, DMC are used to design controller for process and then PID parameters are fitted to minimize cost function like:

$$Min\ J = \left\| u_{PID}(k) - u_{OM}(k) \right\|_i$$
$$Sub\ to\ some\ constraints$$

where:

$u_{PID}(k)$ The control signal of PID

$u_{OM}(k)$ The control signal of other optimisation methods

i : The degree of the norm, usually 2 or ∞

One of the main aims of this thesis is to design a new optimal parametric PID tuning method (group two). In recent years these methods have been of interest to many researchers (Tan *et al.*, 2000; Moradi *et al* 2001). In these methods, much calculation is needed because the designer should solve an advanced control method, but the controller has PID structure so, it can be applied to the system easily. These methods are suitable for use when there is enough support to devote effort to the design of controller for more complex control problem, and also, where the simplicity and robustness of controllers are needed for controller application. In Chapter 5, an optimal parametric PID tuning method with control signal matching was introduced. This method was developed for MIMO systems in Chapter 6.

7.2 Summary of Achievements from the Research

The main aims and achievements of the research of this thesis are discussed below:

1. *Construct a simulation environment for combined cycle power plants.* MATLAB SIMULINK has been interfaced to simulate the dynamic of CCPPs. The simulation environment can be used for different configurations and different subsystems of CCPPs, to test performance, to compare alternative control solutions, and understand the dynamics of CCPPs. This has been achieved by developing a modular, hierarchical procedure, which is used to model these plants (Chapters 1 and 2). Then, the model was used in thesis as an industrial example. **This work was published as Moradi *et al* (2000a); Moradi *et al* (2000b); Katebi *et al* (2000c).**

2. *Propose a new robustness performance criterion.* A new criterion for robustness performance was introduced which assesses the robust performance of multi loop PID controller in number of frequencies along with considering the actuator variations. Different MIMO PID tuning methods were compared with respect to their performance and robustness using the proposed criterion (Chapter 3). **This work was published as Katebi *et al* (2000a); Katebi *et al* (2000b).**

3. *Introduce a new robust multi-loop PID tuning method.* The relay tuning method was used to calculate critical points of MIMO systems in this method. Then, gains of process at bandwidth frequency were used to calculate PID parameters. The performance and robustness of method was compared with an existing

well-known method (Chapter 4). The criteria, which were introduced in Chapter 3, were used to compare these methods. **This work was published as Moradi (2001a).**

4. *Contribute to design of PID tuning method.* A new formulation of the optimisation problem for PID tuning was proposed, and the stability of the solution was discussed (Chapter 5). The capabilities of PID control have been stretched to match the performance of the advanced control designs. A cost function, which minimises the difference between control signal of PID and GPC respect to PID parameters, was used. The design method could be considered as two steps; in the first step, the PID gains are calculated using an advanced technique. This step, which seems to be time consuming, is done off line and with high-speed processors this step is not time consuming. In step two, PID gains from step one will be applied to PID controller in real systems. **This work was published as Moradi and Katebi (2001); Moradi *et al* (2001); Katebi and Moradi (2001).**

5. *Improved the design of the predictive PID tuning method for multivariable processes.* The design method for predictive PID control was extended to MIMO processes. Decentralized predictive PID controllers were represented and stability issues for MIMO closed loop system were discussed (Chapter 6). Also, a state space representation of the method was introduced in this chapter. The Predictive PID method has been implemented in MATLAB. **This work was published as Moradi *et al* (2002a; 2002b).**

When there is enough support to devote much effort to design of controller and for complex control problem, the advanced techniques, such as GPC and IMC may achieve better performance. The problem with the advanced techniques is, that they are needed

more hardware, software and personnel training. Predictive PID controllers, which were a strong and important theme of the thesis, have the advantages of advanced control and when applied to industrial systems, they have the simplicity of PID.

7.3 Future Work

The future work can be divided in following areas:

- Modelling-Simulation
- Relay Technology-where next?
- PID Cost Functions
- Industrial Applications

Modelling and simulation:

The outputs of power plants system are usually connected to power system, which are modelled using per unit models. Therefore, it is suitable that the per unit model use to model the dynamic behaviour of the power plant.

Today, MATLAB is a powerful tool to simulate the different systems. Every few years, the new version of the power system toolbox will be available in the market. This improves the ability of MATLAB and SIMULINK to simulate the power plants and power systems. For controller design purposes, the MATLAB/SIMULINK environment seems to be adequate for most test and design purposes. In this thesis, MATLAB-SIMULINK has been used to construct a per unit model for CCPP's and to develop new controller methods without any problems. Another advantage of this software is that it is a worldwide tool. Consequently, the modelling and simulation work of the thesis provides a good framework for future research and development.

In recent years, use of auto tuning methods for control of process is increasing. Auto tuning methods can be applied on line and they are considered as non-parametric tuning methods, which need data of critical points of systems. This means future work could be focussed on introducing new non-parametric method or model free methods.

Relay technology:

Relay tests are closed loop tests used to identify the critical points. In recent years some researchers have tried to use relay tests for PID tuning methods whilst satisfying some additional performance or robustness constraints. For example, Tan *et al.* (Singapore) are currently trying to incorporate desired maximum sensitivity values for the controller via relay tests. This leads to more complicated control design specifications with more calculations but can give better closed-loop system behaviour. In the future relay experiments are likely to keep their position in system identification and they will be used with some additional system constraints.

PID cost function optimisation

The combination of PID controller and advanced control techniques make a very wide area of research. In this thesis a control signal matching method was introduced and used to tune PID parameters according to the GPC solution. The method gives an optimal PID control design, which needs same data of process as GPC design. This method with some changes could be used to approximate the other advanced technique; for example, Haeri (2001) used this method to approximate DMC method by PID. Various extensions of this basic technique can be anticipated. In this thesis, the cost function that was minimised was the norm of the difference of PID controller and GPC outputs. Future research could address the use of other cost functions, which include the outputs difference effect along with inputs difference of controllers. Also, other cost function norms can be minimized.

Industrial application:

One major motivation for the design of new PID controller was filling the gap between PID design methods, which are desirable for industry, and advanced technique controller design, which are suitable for complex systems. This new method has the advantages of advanced controller performance along with simplicity of PID in application. To apply predictive PID controllers to systems, which use PID controllers, small changes in input signal to PID controller are needed to include future data of set point. In computer simulation, this change has been done easily, but in practical work the set point should be changed. Thus, an interesting and important future research area concerns the steps needed to make the controller applicable in industry and make it practical.

References

Abdennour A.B. and K.Y.Lee (1996): "A decentralised controller design for a power plant using robust local controller and functional mapping" IEEE Trans. on Energy Conversion, Vol. 11, pp. 394-400.

Ahluvalia K.S. and R. Domenichini (1990): "Dynamic modelling of a combined cycle power plant." Trans. ASME Journal of Engineering for Gas Turbines and Power, Vol. 112, pp. 164-167.

Aling H and J. Heintze (1992): "Closed loop identification of a 600 MW Benson boiler" Proceedings of the 31st IEEE Conference on Decision and Control, Vol. 1, pp. 909 - 914.

Anderson P.M. and M. Mirheydar (1990): "A low order system frequency response model" IEEE Trans. on Power Systems, Vol. 5, No. 3, pp. 720-729.

Astrom K.J. and K. Eklund (1972): "A simplified non-linear model of a drum boiler-turbine unitl." International Journal of Control, Vol.16, pp.145-169.

Astrom K.J. and R.D. Bell (1988): "A Simple drum Boiler models." IFAC Power System modelling and Control Applications, Brussels, pp. 123-127.

Astrom K.J. and R.D. Bell (2000): "Drum-boiler dynamics." Automatica, No 36,pp.363-378.

Astrom K.J. and Hagglund, (1984): "Automatic tuning of simple regulator with specifications on phase and amplitude margins", Autimatica, Vol 20, pp. 645-651.

Astrom K.J. and T. Hagglund (1988): "Automatic tuning of PID controllers." Instrument Society of America, Research Triangle Park, NC.

Astrom,K.J. and T. Hagglund (1995): "PID controllers: Theory, Design and Tuning." Instrument Society of America, Research Triangle Park, NC, USA.

Astrom K. J., T. Hagglund, C. C. Hang, and W. K. Ho (1993): "Automatic tuning and adaptation for PID controllers- a survey." Control Engineering Practice, Vol. 1, pp. 699-714.

References

Astrom K.J., T.H. Lee, K.K. Tan and K.H. Johansson (1995): "Recent advances in relay feedback methods -A survey." IEEE, pp. 2616-2621.

Astrom,K.J., H. Panagopoulos and T. Hagglund (1998): Design of PI controllers based on non-convex optimization, Autimatica, Vol 34, pp. 585-601.

Atherton, D.P. (1975): "Non-linear Control Engineering." Van Nostrand Rienhold, London.

Bagnasco A., B. Delfino, G.B. Denegri and S. Massucco (1998): "Management and dynamic performances of combined cycle power plants during parallel and isolating operation." IEEE Trans. on Energy Conversion, Vol. 13, No. 2, pp. 194-201.

Basu R.N. and L.L. Cogger (1986): "Integrated approach to cogeneration planning, control and management." Proc. IFAC Symposium on Automation and Instrumentation for Power plants.

Bell R.D., K.J. Astrom (1996) "A fourth order non-linear model for drum-boiler dynamics." Preprints of the 13th IFAC World Congress, San Francisco, USA.

Boissenin Y. and A. Castanier (1988): "Choosing the right combined cycle power plant." Alsthom Gas Turbine Reference Library.

Camacho, E.F. and C. Bordons (1999): "Model Predictive Control." Springer-Verlag London.

Camporeale S.M., B. Fortunato and A. Dumas, (1997): "Non-linear simulation model and multivariable control of a regenerative single shaft gas turbine" Proceeding of the IEEE International Conference on Control Applications, pp. 721-723.

Chang S.H. and W.K. Dong (1995): "A design of robust two-degree-of-freedom boiler-turbine control systems using H_∞ optimization method." SICE, pp 1263-1268.

Chawdry P.K. and B.W. Hogg (1989): "Identification of boiler models." IEE Proc. C, Generation and Transmission and Distribution, Vol. 136(5), pp. 261-271.

Cheng C.M. and N.W. Rees (1996): "Application of the fuzzy dynamical model approach for identification of non linear drum-boiler process," Proceeding of the Fifth IEEE International Conference on Fuzzy Systems, Vol 1, pp. 726-731.

References

Cheres E. (1990): "Small and medium size drum boiler models suitable for long term dynamic response." IEEE Transactions on Energy Conversion. Vol 5 4. pp.686-692.

Cheung K.P., L.X. Wang (1998): "Comparison of fuzzy and PI controllers for a benchmark drum-boiler model." Proceeding of the 1998 IEEE international Conference on Control Applications, Vol 2, pp. 958-962.

Chien, I.L. (1988): "IMC-PID Controller Design-An Extension." IFAC Proceeding Series, 6, pp. 147-152.

Clarke, D.W., C.Mohtadi and P.S.Tuffs (1987): "Generalised Predictive Control' I & II." Automatica, 23(2): 137-160.

Clarke, D. W. and R. Scattolini (1991): "Constrained receiding-horizon predictive control." IEE Proceedings Part D, Vol. 138, No. 4, July, pp 347-354.

Clarke, D. W. (1988): "Application of generalized predictive control to industrial processes." IEEE Control Systems Magazine, Vol. 8, No. 2, pp. 49-55.

Cohen G.H. and G.A. Coon (1953): "Theoretical consideration of retarded control." Trans. ASME 75, pp. 827-834.

Cohen H., G.F.C. Rogers and H.I.H. Saravanamuttoo (1987): "Gas turbine theory." John Wiley and Sons, New York.

Crosa G., F. Pittaluga, A. Trucco, F. Beltrami, A. Trrolli and F. Traverso (1998): "Heavy-duty gas turbine plant aero-thermodynamic simulation using Simulink." Trans. on ASME, Vol. 120, pp. 550-555.

Daley S. and H. Wang (1994): "Adaptive gas turbine control using a singular system approach" IEE Conference on Control, No. 389, pp. 687-691.

Davison E. (1976): "Multivariable tuning regulators: the feed forward and robust control of a general servomechanism problem." IEEE Trans AC Vol. 21 No. 1, pp 35-47.

De Mello F.P. and C. Concordia (1969): "Concepts of synchronous machine stability as affected by excitation control." IEEE Trans. on PAS, Vol. 88, pp. 361-329.

De Mello F.P. (1991): "Boiler models for system dynamic performance." IEEE Trans. on Power Systems, No 61,pp. 66-74.

References

Dieck-Assad G., G.Y. Masada (1987): "Optimal set-point scheduling in a boiler-turbine system." IEEE Transactions on Energy Conversion, Vol. EC-2, No 3, pp 388-394.

Ding Z. and B.W. Hogg (1991): "Multivariable self-tuning control of a Boiler-Turbine system." IEE Con. on APSC, pp 498-501.

Dong J, C B. Brosilow: (1997): "Design of robust Multi-variable PID controllers via IMC." Proc. of the American Control Conference, pp 3380-3384.

Doughty R.L., L. Gise, E.W. Kalkstein and R.D. Willoughby (1989): "Electrical studies for an industrial gas turbine cogeneration facility." IEEE Trans. on Power Systems, Vol. 25, No. 4, pp. 750-765.

Doyle J C (1982): "Analysis of feedback systems with structured uncertainties." Proceeding of the Institution of Electrical Engineering, Part D, 129, 242-250.

Doyle J C, J.E. Wall and G Stein (1982): "Performance and Robustness analysis for structured uncertainty." In proc. IEEE Conf. On Decision and Control, Orlando FL, pp. 629-36.

Edmuns E.H. and B. Kouvaritakis (1974): "Extensions of the frame alignment technique and their use in the characteristic locus design method." International Journal of Control, Vol 29, pp. 787-796.

Finckh H.H. and H. Pfost (1992): "Development potential of combined cycle power plant with and without supplementary firing." Trans. ASME Journal of Engineering for Gas Turbines and Power, Vol. 114, pp. 653-659.

Gagnon E, A. Pomerleau and A. Desbiens (1999): "Mu-synthesis of robust decentralised PI controllers." IEE Proc Control Theory Appl., Vol. 146, No 4,pp. 289-294.

Gambini M and Guizzi G L (1989): "Re powering of steam power plants for medium-high increase of power generated." Proceeding of the 24th Intersociety IEEE on Energy Conversion, Vol. 5, pp. 2491-2498.

Garcia, C. E. and M. Morarl (1982): "Internal Model Control. 1. A unifying review and some new results." Ind. Eng. Chem. Process Des. Dev., Vol. 21, No. 2, 308-332.

References

Genichi E, A. Tsuda, T. Takeshita, M.T. Monical, S. Nakagawa and K. Fujita (1998): "Integrated large scale multi variable control and real time optimisation of a power plant" Proceeding of the IEEE International Conference on Control Application, pp. 1368-1372.

Gibbs B. P., D.S. Weber and D.W. Porter (1991): "Application of non-linear model based predictive control to fossil power plants" Proceeding of the 30th Conference on Decision and Control, Brighton, pp. 1850-1856.

Gorez R. and G. Calcev (1997): "A survey of PID auto-tuning methods." Proc. 11th International Conference on Control Systems and Computer Science, Vol. 1, pp. 18-27.

Grimble M.J. (1990): "LQG predictive optimal control for adaptive applications." Automatica, Vol.26, No.6, pp.949-961.

Grimble, M J, (1991): "H-infinity PID Controllers." Trans. IMC, Vol 13, No 5, pp 112-120.

Halevi Y., Palmor Z.J. and Efrati T. (1997): "Automatic tuning of decentralised PID controllers for MIMO Processes." Journal of Process Control, Vol 7, No. 2, pp. 119-128.

Hagglund T., K.J. Astrom (1991): "Industrial adaptive controllers based on frequency response techniques." Automatica, Vol. 27, pp.599-609.

Hang C.C., K.J. Astrom and W.K. Ho (1991): "Refinements of the Ziegler-Nichols tuning formula." IEE Proceeding-D, Vol. 138, No. 2, pp. 111-118.

Hannett L.N., J. George and B. Fardanesh (1995): "A governor/turbine model for a twin-shaft combustion turbine." IEEE Trans. on Power Systems, Vol. 10, No. 1, pp. 133-140.

Hannett L.H. and A. Khan (1993): "Combustion turbine dynamic model validation from tests" IEEE Trans. on Power Systems, Vol. 8, No. 1, pp. 152-158.

Harvey C.A., J.E. Wall (1981): "Multivariable design of robust controllers." Proc.JACC , USA, Paper Wp3c.

References

Heffron W.G. and R.A. Phillips (1952): "Effect of a modern voltage regulator on under-excited operation of large turbine generators." IEEE Trans, Vol PAS-71, pp. 687-691.

Hemmaplardh K., J.W. Lamont (1986): "Consideration for a long term dynamics simulation program." IEEE Trrans. PWRS-1, No. 1, pp. 129-135.

He, Q. and Garvay, S.D. (1996): "To automatically select structures for various electrical drive applications." IEE Colloquium on the Best PID in Machine Control, Digest No.: 287, pp. 2/1-2/4.

Hiyama T., N. Suzuki, H. Karino and K.Y. Lee (1999): "Artificial neural network based modelling of governor-turbine system" IEEE Winter Meeting of Power Engineering Society, Vol. 1, pp. 126-133.

Ho W.K. and W. Xu (1998): "Multivariable PID controllers design based on the direct nyquist array method." Proc. on American Control Conference, pp. 3524-3528.

Ho W.K., C.C. Hang and L.S. Cao (1995): "Tuning of PID controllers based on gain and phase margins specifications." Automatica, Vol. 31, No 3, pp. 497-502.

Ho A.P and V U. Vasnani (1992): "Multi loop controller design for multivariable plants." Proc. of the 31st Conference on Decision and Control, Arizona, pp. 181-182.

Hogg B.W. and N.M. Rabaie (1991): "Multivariable generalized predictive control of a boiler system." IEEE Trans. on Energy Conversion, Vol. 6 2, pp. 282-288.

Hussain A. and H. Seifi (1992): "Dynamic modelling of a single shaft gas turbine" IFAC Control of Power Plants and Power Systems, pp. 43-48.

IEEE Committee report (1973): "Dynamic Models for steam and Hydro turbines in power system studies." Trans. in Power Apparatus and systems, Vol. 92, No.6, pp. 1904-1915.

IEEE Committee report (1992): "IEEE recommended practice for excitation system models for power system stability studies." IEEE Standard 421.5.

References

Irwin G., M. Brown and B.Hogg (1995): "Neural network modelling of a 200 MW boiler system." IEE Proceedings Control Theory and Applications, Vol.142 6, pp. 529-536.

Ito K., R. Yokoyama and Y. Matsumoto (1997): "Effect of steam-injected gas turbines on the unit sizing of a cogeneration plant." Journal of Engineering for Gas Turbines and Power, Vol. 119, pp. 131-136.

Jericha H. and F. Hoeller (1991): "Combined cycle enhancement." Trans. ASME Journal of Engineering for Gas Turbines and Power, Vol. 113, pp. 198-202.

Kouvaritakis B. (1974): "Theory and practice of the characteristic locus design method." Proceedings of the Institution of electrical Engineers, Vol 126, pp. 542-548.

Kouvaritakis B. and J. A. Rossiter (1993). "Constrained Stable Generalized Predictive Control." Proc. IEE Pt-D, 140(4): 243-254.

Krasney N (1991): "A new algorithm for automatic tuning of decentralised PID controllers for 2I2O Processes." MSc thesis, Faculty of Mechanical Engineering, Techno Israel Institute of Technology.

Kundur P. (1993): "Power system stability and control." McGraw-Hill, New York.

Kuznetsov A.G., D.W. Clarke (1994): "Application of constrained GPC for improving performance of controlled plants." Advances in Model-Based Predictive Control, Oxford University Press, pp. 318-330.

Kwak S.W. and B. K. Kim (1995): "A study on automatic control of steam turbines of fossil power plant with thermal stress constraints in turbine rotors." IEEE, pp.1525-1530.

Landis E.D. (1977): " Load frequency control and economic dispatch by means of digital computer." Germany.

Larson E.D. and R.H. Williams (1987): "Steam-Injected gas turbines." ASME Journal of Engineering for Gas Turbines and Power, Vol. 109, pp. 55-63.

Lee K.Y., Y.Y. Yacoub, Y.M. Park (1996): "Optimal coordinated control of power plants." 13th Triennial IFAC World Congress, san Francisco, USA, pp. 151-156.

Levine W. (1996): "The Control Handbook Press."

References

Loh A.P., V.U. Vasnani (1994): "Describing function matrix for multivariable systems and its use in multi loop PI design." Journal Process Control, No. 4, pp 115-120.

Loh A. P., C. Hang, C. K. Quek and V. Vasnani (1993): "Auto tuning of multi-loop PI controllers using relay feedback." Ind. 'Eng. Chem. Res. 32, pp. 1102-1107.

Lieslehto J., J.T. Tanttu and H.N. Koivo (1991): "An expert system for multi-variable controller design." Proceedings of the ITAC, Singapore, pp. 211-216.

Luyben W. (1986): "Simple method for tuning SISO controllers in multi-variable systems." Ind. Eng. Chem. Process De. Dev., No 25, pp. 654-660.

Luyben W. (1990): "Process Modelling, Simulation and Control for Chemical Engineers, McGraw-Hill Pub. Company, USA.

Manayathara T and J. Bentsman (1994): "Application of stabilizing predictive control to boilers." Proceeding of the Third IEEE Conference on Control Applications,Vol:3, pp.1637-1642.

Mc Donald J.P., H.G. Kwanty and J.H. Spare (1971): "A non-linear model for reheat boiler-turbine-generator systems,Parts I & II, Proc. 12th JACC, St.Louis, USA,pp.219-236.

Maciejowski J.M. (1989): Multivariable feedback design, Addison-Wesley, Wokingham, England.

Maciejowski, J. M. (2001)." Predictive Control with constraints." Printice hall

Marcelle K., K.H. Chiang, P.K. Houpt and P.P. Bonissone (1994): "A Hierarchical controller for optimal load cycling of steam turbines." Proceedings of the 33rd Conference on Decision and Control, pp. 611-612.

Marques R. and M. Fliess (2000): "From PID to model predictive control a flatness-based approach." IFAC Workshop PID'00, Spain pp. 534-539.

Miller R.M., S.L. Shah, R.K. Wood and E.K. Kwok (1999): "Predictive PID." ISA Transactions, Vol. 38, pp. 11-23.

Morari, M (1994): "Advance in Model Predictive Control; Model Predictive Control." Oxford University Press.

Morari, M. and E. Zafiriou (1989): "Robust Process Control." Prentice Hall.

References

Nakamura H. and M. Uchida (1989): "Optimal regulation for thermal power plant." IEEE Control System Magazine, Vol: 9 1, pp. 33-38.

Nern H.J., H. Kreshman, F. Fischer and H.A.N. Eldin (1994): "Modelling of the long term dynamic performance of a gas turbo generator set" IEEE, p.p. 491-496.

Niederlinski A. (1971): "A heuristic approach to the design of linear multivariable interacting control system." Atomatica, Vol 7, pp 691-701.

Noymer P.D. and D.G. Wilson (1993): "Thermodynamic design considerations for steam-injected gas turbines." ASME, paper No. 93-GT-432.

Ollat X., R.S. Smoak, A.T. Alouani (1989): "Multi-variable control design for boiler furnace." IEEE , pp 93-97,1989.

Ordys A. and M.J. Grimble (1995): "State space dynamics performance predictive controller", Automatica.

Palmor,Z.J. and M. Blau, (1994): "An auto-tuner for Smith dead time compensator." Int. J. Control, Vol 60, pp. 117-135.

Palmor Z.J., Y.Halevi and N.Krasney (1995a): "Automatic tuning of decentralised PID controllers for 2I2O Processes." Automatica 31, No. 7, pp. 1001-1010.

Palmor Z.J., Halevi Y. and Efrati T.A. (1995b): "General and exact method for determining limit cycles in decentralized relay systems." Atomatica, Vol 31, No 9, pp 1333-1339.

Pegel S. and S. Engell (2001): "Multivariable PID controller design via approximation of the attainable performance." The 27th Conference of the IEEE Industrial Electronics Society, IECON'01, Colorado, USA, p.p. 724-729.

Pellegrinetti G., J. Bentsman (1996): "Non linear control oriented boiler modelling a benchmark problem for controller design." IEEE Transactions on Control Systems Technology, Vol 4, pp. 57-64.

Penttinen J. and H. N. Koivo (1980): "Multivariable tuning regulators for unknown systems." Automatica, Vol 16, pp. 393 -398.

References

Pidersen T.S., T. Hansen and M. Hangstrup (1996): "Process optimizing multivariable control of a boiler system." UKACC International Conference on Control, Vol. 2, pp. 787-792.

Prasad G., E. Swidenbank and Hogg B.W. (1996): "A multi variable predictive control strategy for economical fossil power plant operation." UKACC International Conference on control, Vol. 2, pp. 1444-1449,1996.

Ramirez, R. W. (1985): "The FFT: Fundamentals and Concepts." Prentice-Hall, Englewood Cliffs, NJ.

Rice I.G. (1993a): "Steam-injected gas turbine analysis: Part I-Steam rates." ASME Paper No. 93-GT-132.

Rice I.G. (1993b): "Steam-injected gas turbine analysis: Part II-Steam cycle efficiency." ASME Paper No. 93-GT-420.

Rice I.G. (1993c): "Steam-injected gas turbine analysis: Part III-Steam regenerated heat." ASME Paper No. 93-GT-421.

Ricketts B.E. (1997): "Modelling of gas turbine: a precursor to adaptive control." IEE Colloquium on Adaptive Controller in Practice, 1997.

Rivera D.E., S. Skogestad and M. Morari (1986): "Internal Model Control 4 PID Controller Design." Ind. Eng. Chem. Process Des. Dev, Vol 25, pp. 252-265.

Rosenbrock H.H. (1970): "State space and multivariable theory." London: Nelson.

Rosenbrock H.H. (1974): "Computer aided control system design." New York: Academic Press.

Rowen W.I. (1983): "Simplified mathematical representations of heavy duty gas turbines." Trans. of ASME, Vol. 105(1), pp. 865-869.

Rowen W.I. (1992): "Simplified mathematical representations of single shaft gas turbines in mechanical drive service." Turbo-Machinery International, pp. 26-32.

Rubashking A.S. and M. Khesin (1993): "Dynamic models for fossil power plant training simulator." Proceedings on. Amer. Power Conf., Chicago, IL.

Rusnak, I. (1999): "Generalized PID Controllers." The 7th IEEE Mediterranean Conference on Control & Automation, MED 99, Haifa, Israel.

References

Rusnak, I. (2000): "The Generalized PID Controllers and its Application to Control of Ultrasonic and Electric Motors." IFAC Workshop PID'00, Spain pp 125-130.

Saez D., A. Cipriano (1998): "Economic optimal control with environmental constraints for combined cycle power plants." IECON, Proceeding of the 24th Annual Conference of the IEEE, Vol. 2, pp. 640-645.

Safonov M.G. (1982): "Stability margins of diagonally perturbed multivariable feedback systems." Proc. IEE, Part D, 129, 251-6.

Schobeiri M.T., M. Attia and C. Lippke (1994): "GETRAN: A generic, modulary structured computer code for simulation of dynamic behavior of Aero- and power generation gas turbine engines", Trans. on ASME, Vol. 116, pp. 483-494.

Schobesberger R., G. Gasteiger and K. Budin (1991): "Combined cycle power plants with special respect to the heat recovery steam generator on the basis of the steyrermuhl power plant", ASME Cogen-Turbo IGTI, Vol. 6, pp. 461-470.

Scott P.H. and J.P. Russell (1994): "Modelling of a combined cycle conversion using Simulink." International Conference on Control, Vol. 1, pp. 368-373.

Shields C. (1989): "Current developments in gas turbine combined cycle power plant." Publication 453, Institution of Diesel and Gas Turbine Engineering.

Skogestad, S. and M. Morari (1989): "Robust performance of decentralized control systems by independent design." Automatica Vol. 25, pp. 119-125.

Soderstrom T. and P. Stoica (1989): "System Identification." Prentice Hall.

Sharma C. (1998): "Modelling of an island grid." IEEE Trans. on Power Systems, Vol. 13, No. 3, pp. 971-978.

Tan K.K., S.N. Huang and T.H. Lee (2000): "Development of a GPC-based PID controller for unstable systems with dead time." ISA Trans., Vol. 39, pp. 57-70.

Tan K.K., Q-G. Wang and C.C. Hang (1999): "Advances in PID Control, Springer Verlag London, ISBN-1-852333-138-0 .

Unbehauen H., U. Keuchel and I. Kocaarsian (1991): "Real-time adaptive control of electrical power and enthalpy for a 750 MW once-through boiler." Conference on International Control, Vol 1,pp 42-47.

References

Undrill J.M. (1984): "Power system simulator package program application guide." Power Technologies Inc. USA.

Wadey M.D. and D.P. Atherton (1984): "Periodic modes in multi variable system with relay and saturation elements." IMC Symposium on Applications of Multivariable Systems Techniques, Plymouth, pp. 157-161.

Wang F., G. Janka and G. Schellstede (1991): "Dynamic power system simulation for real time dispatcher training." 3rd International Conference of Power System Monitoring and Control, pp. 109-114.

Wang F., T. Y. Wu (1995): "Multi loop PID controllers tuning by goal attainment trade-off method." Trans Inst. MC, Vol 17, No 1, pp 27-34.

Wang Q., B. Zou, T. Lee, Q. Bi, C.K. Queek, V.U. Vasnani (1997): "Auto-tuning of Multivariable PID controllers from de-centralised relay feedback." Automatica 33,No 3, pp. 319-330.

Wang Q.G., C.C. Hang and X.P. Yang (2000): "Single -Loop controller design via IMC principles." In Proceeding Asian Control Conf. Shanghai, P.R.China.

Wiggin F.T.F. (1981): "Commercial/operational/performance effects of adding flexible multi fuel GT/fired HRB combined cycle to slough CHP utilities." IEE Conference Publication No 192.

Wood R.K. and M.W. Berry (1973): "Terminal composition control of a binary distillation column." Chem. Eng. Society, Vol. 28, pp. 1707-1727.

Working Group on Power Plants Response to Load Changes, (1973): "MW response of fossil fuelled steam units." IEEE Trans. on Power Apparatus and Systems, Vol. PAS- 92, No 2, pp. 455-463.

Working Group on Prime Mover and Energy Supply Models for System Dynamic Performance Studies, (1991): "Dynamic models for fossil fuelled steam units in power system studies." IEEE Trans. on PWRS, Vol. 9, No. 3, pp.753-761.

Working Group on Prime Mover and Energy Supply Models for System Dynamic Performance Studies, (1994): "Dynamic models for combined cycle plants in power systems studies." IEEE Trans. on PWRS, Vol. 9, No 3, pp. 1698-1708.

References

Yacobucci R.B. (1991): "A control system retrofit for a GE frame 5 turbine-generator unit." IEEE Trans. on Energy Conversion, Vol. 6, No 2, pp. 225-230.

Yu C.C. (1999): "Auto tuning of PID controllers." Springer-Verlag, New York.

Yusof, R, S Omatu and M Khalid, (1994): "Self-tuning PID Control: a Multivariable Derivation and Application." Automatica, Vol. 30, No. 12 pp. 1975-1981

Zaporowski B. (1996): "Modelling and simulation of energy conversion in combined gas-steam power plant integrated with coal gasification." Proceedings of the 31st IECEC, Vol. 3, pp 2056-2062.

Zhuang M. D., P. Atherton (1994): "PID controller design for a 2I2O system." IEE Proc. Control Theory Appl., Vol 141, No 2, pp 111-120.

Ziegler, J.G. and N.B.Nichols (1942): "Optimum setting for automatic controllers." Trans. ASME 64, 759-768.

Appendix 1.1: Physical methods for boiler modelling

Method	Linearity	Authors	Input	Output	Advantage	Control	Description
Analytical	Non-linear	Mcdonald *et al*, (1970)	CV,A/F Ssh, Srh, teta-sh teta-rh	P_d, T_d T_r, P_r, L P_t, T_t, $\dot{m}_s$	The model has been validated by real results.	PID	The model consists of 14 first order non-linear differential equation and 82 linear algebraic equations.
Physical	Non-linear	Pellegrinetti and Bentsman (1996)	A/F W_f	P_d, L_{wd}, O_e	Use to design a controller for training	PID	The model is fourth order non-linear and includes inverse response, time delay, measurement noise models
Physical	Non-linear	Manayathara and Bentsman (1994)	A/F W_f	Wl, O_e, Hp.		PID	The plant has two essential components, a combustion chamber and a drum.
Physical	Non-linear	Cheung and Wang (1998)1	A/F W_f	P_d, L_{wd}, O_e m_s.	Fast	Fuzzy Control	The performance of PI and fuzzy controller have been compared by the control of fuel flow and feed water rate.

Appendix 1.1: Physical methods for boiler modelling. (Continue)

Method	Linearity	Authors	Input	Output	Advantage	Control	Description
Physical	Non-linear	Astrom and Eklund (1973)	W_F	P_d	Simple	Local PID	The model is obtained from the global energy balance.
Physical	Non-linear	Astorm & Bell(1988)	$P_{ow}, W_F,$ $Tf, WA,$ $m_s,$	$L_d,$ $a_m,$	Low order		The model exhibits a complex behaviour in spite of low order.

Appendix 1.2: Identification methods for boiler modelling

Method	Linearity	Authors	Input	Output	Advantage	Control	Description
Auto-regressive (AR)	Linear	Nakamura and Unhida (1989)	$W_F,$ spray, gas-damper	T_{sh}, T_{rh}	High reliability, compensatd set-point	Digital control and PID	An autoregressive model is fitted to the plant input and output data, and steam temperatur is controlled.
Close Loop Iden.	Linear	Aling and Heintze (1992)	$W_F, Fs,$ $CV,$ G_d, C_f	$T_{sh1}, T_{sh2} T_{sh3}, P_a,$ L_c	More practical applications	PID	Once through, requires identification in parts, which is not required in open loop.
RLS	Linear	Chawdhry and Hogg (1989)	$W_A,$ $W_F, m_s,$ *	$P_d, L_d,$ $T_{re}, T_{sh},$ *	Quality of modelling	PID	The real data confirms the accuracy of model.
Fuzzy Ident.	Non-linear	Cheng and Rees (1996)	$m_s,$ $Q,$ $Q_f,$	$P_d,$ W_d	Evaluated under various load condition	Fuzzy and PID	The FDM is employed to link all the linear models together.

* The number of input/output depend on the order of model.

Appendix 1.3: Modelling of Steam Turbine

In Fig A1.3.1, the transfer function of a steam vessel and the expression for power developed by a turbine stage is derived as follow.

From continuity equation for the vessel:

$$\frac{dW}{dt} = V\frac{d\rho}{dt} = Q_{in} - Q_{out} \qquad \text{(A1.3.1)}$$

Assume the flow out to be proportional to pressure:

$$Q_{out} = \frac{Q_o}{P_o}P \qquad \text{(A1.3.2)}$$

Assume temperature is constant in the vessel:

$$\frac{d\rho}{dt} = \frac{dP}{dt}\frac{\partial\rho}{\partial P}$$

Then, from equation (A1.3.1) the continuity equation for the vessel will be:

$$Q_{in} - Q_{out} = V\frac{\partial\rho}{\partial P}\frac{dP}{dt} = V\frac{\partial\rho}{\partial P}\frac{P_o}{Q_o}\frac{dQ_{out}}{dt} = T_v\frac{dQ_{out}}{dt} \qquad \text{(A1.3.3)}$$

In Laplace Transform

$$Q_{in} - Q_{out} = T_v s Q_{out} \quad \text{or} \quad \frac{Q_{out}}{Q_{in}} = \frac{1}{1+T_v s} \qquad \text{(A1.3.4)}$$

Appendix

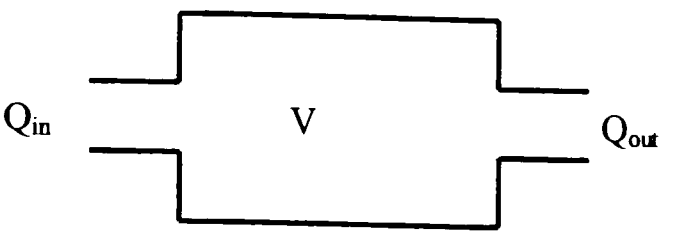

Fig A1.3.1: Steam Vessel

Where:

$$T_v = \frac{P_o}{Q_o} V \frac{\partial \rho}{\partial P}$$

W weight of steam in the vessel (kg)

V Volume of vessel (m^3)

ρ Density of steam (kg/ m^3)

Q Steam mass flow rate (kg/s), t= time (s)

P Pressure of steam in the vessel (kPa)

P_o Rated pressure

Q_o Rated flow out of vessel

In modern steam turbines the force on each rotor blade, and hence the turbine torque, is proportional to the steam flow rate. Thus $T_m=kQ$ where k is a proportional constant.

Appendix 1.4:Typical Parameters for Steam Turbine Models

	Time Constants				Fractions							
System Description	T_4	T_5	T_6	T_7	K_1	K_2	K_3	K_4	K_5	K_6	K_7	K_8
Non reheat	0.2-0.5	0	0	0	1	0	0	0	0	0	0	0
Tandem-compound single reheat	0.1-0.4	4-11	0.3-0.5	0	0.3	0	0.4	0	0.3	0	0	0
Tandem-compound Double reheat	0.1-0.4	4-11	4-11	0.3-0.5	0.22	0	0.22	0	0.3	0	0.3	0
Cross-compound single reheat	0.1-0.4	4-11	0.3-0.5	0	0.25	0	0	0.25	0.25	0.25	0	0
Cross-compound Double reheat	0.1-0.4	4-11	4-11	0.3-0.5	0.22	0	0	0.22	0.14	0.14	0.14	0.14

Appendix 1.5: The Comparison of single and twin shaft of open Cycle Gas Turbine.

	Advantage	Disadvantage	Description
Single Shaft	-Less over-speeding in the event of a loss of electrical load. -High output power levels in a dry cycle. -Simpler structure.	-The control system must be designed to minimize the connecting start up. -Narrow operating speed range. -Big starter unit.	-Consists of a compressor, a combustion chamber and a turbine.
Twin shaft	-Used for large-scale electricity generating units. -More flexibility of operation. -Small starter unit.	-The control system must be designed to prevent of rapid over-speeding.	-Consists of a compressor, a combustion chamber and two turbines and two shafts.

Appendix 1.6: The Comparison of Open and Close Cycle of Gas Turbine.

	Advantage	Disadvantage	Description
Open Cycle	-The danger of over-speeding in the event of a loss of electrical load is less. -Suitable at a fixed speed and fixed load condition. -Suitable to used in CC power generation.	-More erosion of the turbine blades and other detrimental effects due to the products of combustion. -The need for filtration of the incoming air.	-Fresh atmospheric air is drawn into the circuit continually and energy is added by the combustion of fuel in the working fluid itself.
Close Cycle	-Smaller compressor and Turbine. -Efficient control. -The use of gases other than air that having more desirable thermal properties. -More effective heat-exchange is possible. -Flexibility of operation.	-The need for an external heating system. -Used in the high temperature nuclear reactor only.	-The working fluid is repeatedly circulated through the machine and the fuel can not be burnt in the working fluid. The fuel is burnt in a separate air stream supplied by an auxiliary fan.

Appendix 1.7: Physical methods for Gas Turbine Modelling.

Model	Authors	Input	Output	Advantage	Control	Description
Physical Linear	Hossain and Seifi (1992)	ΔQ	ΔP_m	Suitable for stability studies.		Simple dynamic model of a single gas turbine using transfer function has been presented.
Physical Non-linear	Nern *et al.* (1994)	W_F & W_A	P_m $\dot{m}_s$	Long term study model	T_d, IGV, P,	The gas turbine design parameters have been appeared as model parameter.
Physical Non-linear	de Mello , and Ahner, (1994)	W_F & W_A	P_m & T_E	Use for power plant control studies.	N, T_E, W_F & W_A, IGV.	The model based on simplified non-linear equation is easy to use for power plant control.
Physical Non-linear	Badmus *et al.*(1995)			Useful in design of surge control and simulation		The generic model given are quasi one dimensional compressible flow model
Physical Non-linear	Camporeal and Fortunato, (1997)	W_F & IGV	N & T_{int}	Modular, linear and suitable for control	N & TIT	In order to synthesis the controller, The linear model of gas turbine has been developed from non-linear dynamic model

TIT : Turbine Inlet Temperature, IGV : Inlet Guide Vanes, T_{int} : Internal Temperature, P_m : Mechanical power, α : Acceleration, T_d : Time delay,

Appendix 1.8: Test methods for Gas Turbine Modelling.

Model	Authors	Input	Output	Advantage	Control	Description
Test data	Rowen .(1992)	W_A & W_F	P_m & T_E	Suitable for DPS studies	N , T_E , α , IGV ,	The model incorporates both the control and fuel system characteristics.
Test data	Hannet, and Khan, (1993)	W_F	P_m	Validation from test	N & T_E .	Dynamic models for two types of governor controllers have proposed
Test data	Hannet and Jee, (1995)	W_F	N_f , N , T_E	Suitable for Dynamic studies.	N , T_E , N_f .	Twin shaft gas turbine has been modelled by test.
Test data	Yokitomo *et al.* (1998)	W_F	P_m	Transfer function modelling	T_E &. W_w	The transfer function for gas turbine has been determined.
Test data	Bagnasco *et al.* (1998)	W_F	P_m , T_E , $\dot{m}_s$	Suitable for CC modelling.	N , α , IGV ,	The model has been tested on a realistic industrial CC power plant.
Test data	Sharma (1998)	W_F	P_m	Simple model	N	Model for the dynamic studies.

T_E : Exhaust gas temperature, W_A : Air flow, W_F : Fuel flow, P_m : Mechanical power, N_f : Free turbine speed, N : Engine speed.

DPS: Dynamic Power System, $\dot{m}_s$: mass flow, W_w : Water flow. P : Pressure.

Appendix

Appendix 2.1: Derivation steam temperature from steam pressure

To derive steam temperature the following equation has been used:

$$T_s = a_1 P_T^{\,2} + a_2 P_T + a_3$$

The coefficients are found from steam table. In Per-Unit for mentioned base in chapter 2, the equation is as follow:

$$T_s = -18.3657 P_{T,pu}^{\,2} + 107.746 P_{T,pu} + 131.5455$$

$$T_{s,pu} = -0.06333 P_{T,pu}^{\,2} + 0.37154 P_{T,pu} + 0.6923$$

To derive Drum Level the following equations has been used.

$$DL = (V_w + a_m V_r) / A$$

$$a_m = (r_w / r_{ws})(1 - \frac{r_s}{r_{ws} x_r}) \log((1 + \frac{r_{ws}}{r_s}) x_r)$$

$$r_{ws} = r_w - r_s$$

$$r_w = a_{b1} P_T^{\,2} + a_{b2} P_T + a_{b3}$$

$$r_S = a_{S1} P_T^{\,2} + a_{S2} P_T + a_{S3}$$

r_{ws}=r_w-r_s

where:

V_m Volume of water in the Drum

V_r Volume of riser

A Area of Drum

a_m Average steam water volume ratio

Appendix

r_w Level of water in riser:

r_S Level of steam in riser

x_r= Steam-water mass ratio at the riser outlet

Initial Values:

V_m= 13.521

V_r= 37

A= 20

x_r= 0.091263;

To derive coefficient of equation, the steam table has been used then:

a_{b1}=0.0810

a_{b2}=-3.4870

a_{b3}=718.1200

a_{s1}=0.2240

a_{s2}=2.6560

a_{s3}=6.4700

Appendix

Appendix 4.1:

Final value Theorem: If Laplace transform of *f(t)* be *F(s)*, and if *sF(s)* is an analytic on the imaginary axis and in the right half of the s-plane, then:

$$\lim_{t\to\infty} f(t) = \lim_{s\to 0} sF(s)$$

By using the system notation defined before, the steady state gain of the system is defined as:

$$\text{Steady state gain}=g_{11ss} = \frac{\textit{steady state output}}{\textit{steady state input}} = \frac{\lim_{t\to\infty} y_1(t)}{\lim_{t\to\infty} u_1(t)} = \lim_{t\to\infty} \frac{y_1(t)}{u_1(t)}\bigg|_{u_i(t)=0,\ i\neq 1}$$

By use of the final value theorem of the Laplace transform, the steady state gain of the system is:

$$g_{11ss} = \frac{\lim_{t\to\infty} y_1(t)}{\lim_{t\to\infty} u_1(t)}\bigg|_{u_i(t)=0,\ i\neq 1} = \frac{\lim_{s\to 0} sy_1(s)}{\lim_{s\to 0} su_1(s)}\bigg|_{u_i(s)=0,\ i\neq 1} = \frac{\lim_{s\to 0} y_1(s)}{\lim_{s\to 0} u_1(s)}\bigg|_{u_i(s)=0,\ i\neq 1} = \frac{y_1(0)}{u_1(0)}\bigg|_{u_i(s)=0,\ i\neq 1} = g_{11}(0)$$

With the same procedure, other steady state gains are:

$$G_{ss} = \begin{bmatrix} g_{11ss} & g_{12ss} & \cdots & g_{1Mss} \\ g_{21ss} & g_{22ss} & \cdots & g_{2Mss} \\ \vdots & \vdots & \ddots & \vdots \\ g_{M1ss} & g_{M2ss} & \cdots & g_{MMss} \end{bmatrix} = \begin{bmatrix} g_{11}(0) & g_{12}(0) & \cdots & g_{1M}(0) \\ g_{21}(0) & g_{22}(0) & \cdots & g_{2M}(0) \\ \vdots & \vdots & \ddots & \vdots \\ g_{M1}(0) & g_{M2}(0) & \cdots & g_{MM}(0) \end{bmatrix} = G(0)$$

Appendix

For the system shown in Fig.4.4, with at least one input non-zero means, the error signals $e_i(t)$ and $u_i(t)$ $(i = 1,\cdots,M)$ are also of non-zero mean. The steady state gains of process are identified simultaneously with the critical points, after M limit cycle experiments, as follow:

For first relay experiment:

Assume:

- $r_1^{\,1}(t) \neq 0,\ r_i^{\,1}(t) = 0$
- Limit cycle oscillation is exist
- G(s) is a linear time invariant system

$\therefore$ $y_1,\cdots,y_M$ *and* $u_1,\cdots,u_M$ are periodic

Define:

$$y_1,\cdots,y_M \in R \qquad y = \begin{bmatrix} y_1 & y_2 & \cdots & y_M \end{bmatrix}^T \in R^M$$

$$y(j\omega) = \begin{bmatrix} y_1(j\omega) \\ y_2(j\omega) \\ \vdots \\ y_M(j\omega) \end{bmatrix} \triangleq \begin{bmatrix} FT\, y_1(t) \\ FT\, y_2(t) \\ \vdots \\ FT\, y_M(t) \end{bmatrix} \qquad u(j\omega) \triangleq \begin{bmatrix} u_1(j\omega) \\ u_2(j\omega) \\ \vdots \\ u_M(j\omega) \end{bmatrix} \triangleq \begin{bmatrix} FT\, u_1(t) \\ FT\, u_2(t) \\ \vdots \\ FT\, u_M(t) \end{bmatrix} \tag{A4.1.1}$$

$$G(j\omega) \triangleq G(s)\big|_{s=j\omega} = \begin{bmatrix} g_{11}(j\omega) & g_{12}(j\omega) & \cdots & g_{1M}(j\omega) \\ g_{21}(j\omega) & g_{22}(j\omega) & \cdots & g_{2M}(j\omega) \\ \vdots & \vdots & \ddots & \vdots \\ g_{M1}(j\omega) & g_{M2}(j\omega) & \cdots & g_{MM}(j\omega) \end{bmatrix}$$

where:

The FT is Fourier Transform of signal, $\omega = \dfrac{2\pi}{T}$, T is period of signal

Appendix

The frequency response of output in compact form will be:

$$y(j\omega) = G(j\omega)x(j\omega) \tag{A4.1.2}$$

and y_1 could be written as follow:

$$y_1(j\omega) = g_{11}(j\omega)u_1(j\omega) + g_{12}(j\omega)u_2(j\omega) + \cdots + g_{1M}(j\omega)u_M(j\omega) \tag{A4.1.3}$$

Inserting $\omega = 0$ in equation (A4.1.3):

$$y_1(0) = g_{11}(0)u_1(0) + g_{12}(0)u_2(0) + \cdots + g_{1M}(0)u_M(0) \tag{A4.1.4}$$

where: $g_{11}(0), \cdots, g_{1M}(0)$ are steady state gain of transfer function. In the other hand, the mean value of output and inputs are:

$$\begin{aligned} \bar{u}_1 &= \frac{1}{T}\int_0^T u_1(t)dt = u_1(j\omega)\big|_{\omega=0} = u_1(0) \\ &\vdots \\ \bar{u}_M &= \frac{1}{T}\int_0^T u_M(t)dt = u_M(j\omega)\big|_{\omega=0} = u_M(0) \\ \bar{y}_1 &= \frac{1}{T}\int_0^T y_1(t)dt = y_1(j\omega)\big|_{\omega=0} = y_1(0) \end{aligned} \tag{A4.1.5}$$

Therefore, inserting equation (A4.1.5) in equation (A4.1.4), the result will be:

$$\bar{y}_1 = g_{11}(0)\bar{u}_1 + g_{12}(0)\bar{u}_2 + \cdots + g_{1M}(0)\bar{u}_M \tag{A4.1.6}$$

and with same manner output *i* will be:

Appendix

$$\bar{y}_i = g_{i1}(0)\bar{u}_1 + g_{i2}(0)\bar{u}_2 + \cdots + g_{iM}(0)\bar{u}_M \qquad \text{(A4.1.7)}$$

Showing equation (A4.1.6) and (A4.1.7) in compact form:

$$\bar{y} = G(0)\bar{u} \qquad \text{(A4.1.8)}$$

where:

$$\bar{y} = \begin{bmatrix} \bar{y}_1 \\ \bar{y}_2 \\ \vdots \\ \bar{y}_M \end{bmatrix} = \begin{bmatrix} \frac{1}{T}\int_0^T y_1(t)dt \\ \frac{1}{T}\int_0^T y_2(t)dt \\ \vdots \\ \frac{1}{T}\int_0^T y_M(t)dt \end{bmatrix} \qquad \bar{u} = \begin{bmatrix} \bar{u}_1 \\ \bar{u}_2 \\ \vdots \\ \bar{u}_M \end{bmatrix} = \begin{bmatrix} \frac{1}{T}\int_0^T u_1(t)dt \\ \frac{1}{T}\int_0^T u_2(t)dt \\ \vdots \\ \frac{1}{T}\int_0^T u_M(t)dt \end{bmatrix}$$

$$G(0) = \begin{bmatrix} g_{11}(0) & g_{12}(0) & \cdots & g_{1M}(0) \\ g_{21}(0) & g_{22}(0) & \cdots & g_{2M}(0) \\ \vdots & \vdots & \ddots & \vdots \\ g_{M1}(0) & g_{M2}(0) & \cdots & g_{MM}(0) \end{bmatrix}$$

The equation (A4.1.8) is not enough to identify steady state gain. Repeating the experiment M time more, with different reference signals, leads to

$$\begin{bmatrix} \bar{y}^1 & \bar{y}^2 & \cdots & \bar{y}^M \end{bmatrix} = G(0)\begin{bmatrix} \bar{u}^1 & \bar{u}^2 & \cdots & \bar{u}^M \end{bmatrix}$$

$$\begin{bmatrix} \bar{y}_1^1 & \bar{y}_1^2 & \cdots & \bar{y}_1^M \\ \bar{y}_2^1 & \bar{y}_2^2 & \cdots & \bar{y}_2^M \\ \vdots & \vdots & \ddots & \vdots \\ \bar{y}_M^1 & \bar{y}_M^2 & \cdots & \bar{y}_M^M \end{bmatrix} = G(0)\begin{bmatrix} \bar{u}_1^1 & \bar{u}_1^2 & \cdots & \bar{u}_1^M \\ \bar{u}_2^1 & \bar{u}_2^2 & \cdots & \bar{u}_2^M \\ \vdots & \vdots & \ddots & \vdots \\ \bar{u}_M^1 & \bar{u}_M^2 & \cdots & \bar{u}_M^M \end{bmatrix} \qquad \text{(A4.1.9)}$$

where: superscripts are number of experiments. $r_1, \cdots, r_M$ are chosen as the matrix $\bar{u}$ be non-singular, The steady state gains are identified using equation (A4.1.9) as follow:

$$G(0)=\begin{bmatrix} \bar{y}_1^1 & \bar{y}_1^2 & \cdots & \bar{y}_1^M \\ \bar{y}_2^1 & \bar{y}_2^2 & \cdots & \bar{y}_2^M \\ \vdots & \vdots & \ddots & \vdots \\ \bar{y}_M^1 & \bar{y}_M^2 & \cdots & \bar{y}_M^M \end{bmatrix}\begin{bmatrix} \bar{u}_1^1 & \bar{u}_1^2 & \cdots & \bar{u}_1^M \\ \bar{u}_2^1 & \bar{u}_2^2 & \cdots & \bar{u}_2^M \\ \vdots & \vdots & \ddots & \vdots \\ \bar{u}_M^1 & \bar{u}_M^2 & \cdots & \bar{u}_M^M \end{bmatrix}^{-1} \qquad \text{(A4.1.10)}$$

this means, the steady state gains of process will be identified, using M relay experiment and measuring the DC value of the control and output signals.

Determination of bandwidth frequency

As for SISO systems we define the bandwidth, as the frequency up to witch feedback is effective. For MIMO systems the bandwidth will depend on directions, and we have a bandwidth region between the lower frequency where the maximum singular value, $\bar{\sigma}(S)$, reaches .7 (the low-gain or worst case direction), and a higher frequency where the minimum singular value, $\underline{\sigma}(S)$, reaches 0.7 (the high gain or best direction). If we want to associate a single bandwidth frequency for a multivariable system, then we consider the worst-case (low-gain) direction and define:

- Bandwidth, ω_b : Frequency where $\bar{\sigma}(S)$ crosses 0.7 from below.

Appendix 4.2: Extension of Method for 3I3O systems

The improved method is summarized as follows:

Selection of DCP:

Select criteria's (A4.2.1) to choose desired critical point:

$$\tan\varphi_{d1} = \frac{C1}{1} = \frac{K_{2cr}g_{22}(0)}{K_{1cr}g_{11}(0)} \qquad \tan\varphi_{d2} = \frac{C2}{1} = \frac{K_{3cr}g_{33}(0)}{K_{1cr}g_{22}(0)} \qquad \text{(A4.2.1)}$$

Initialisation of first three critical points:

It is recommended to use following ratios in three relay experiments: $M_{R\max}$ and in the second $M_{R\min}$ is used.

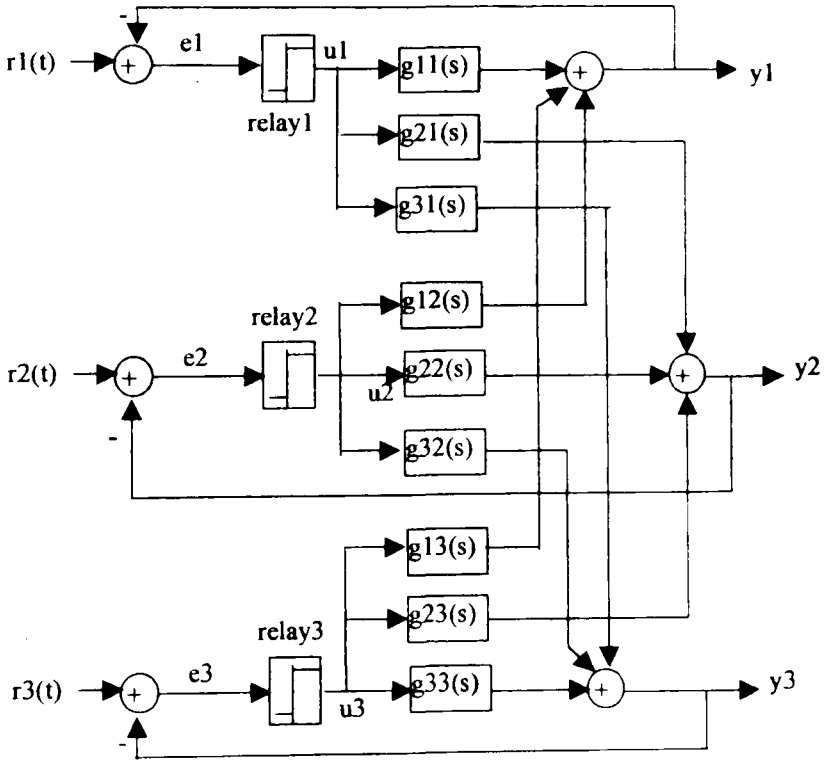

Fig A4.2.1a: A 3I3O decentralized relay system

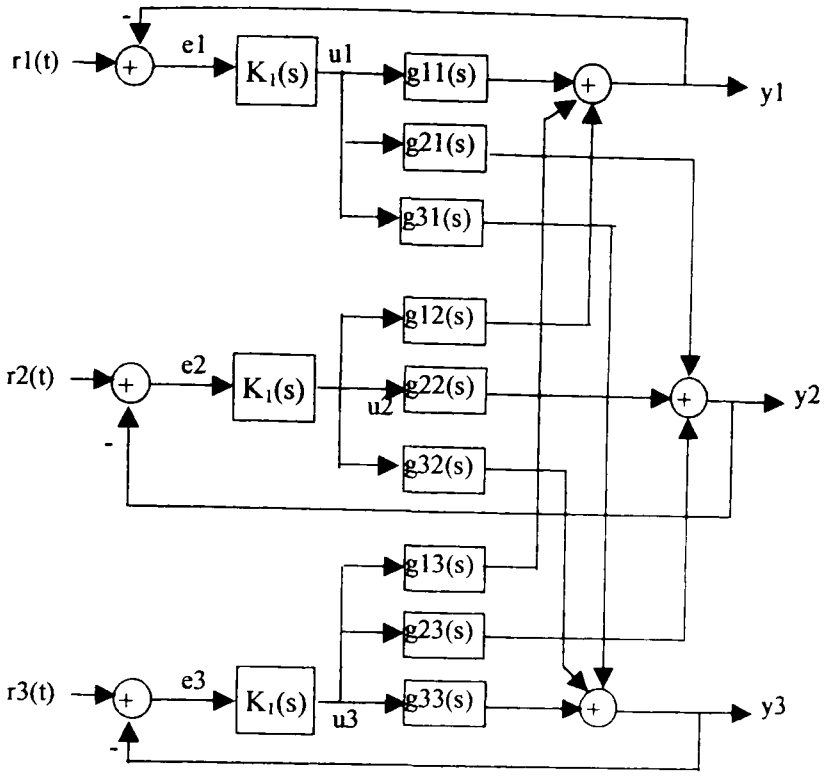

Fig 4.2.1b: The 3I3O system with multi-loop controller

Where:

$(i-2)$ *th* Experiment $\quad M_{R\max 12} = \dfrac{\overline{M_1}}{\underline{M_2}}, \quad M_{R\max 13} = \dfrac{\overline{M_1}}{\underline{M_3}}$ (A4.2.2)

$(i-1)$ *th* Experiment $\quad M_{R\max 21} = \dfrac{\overline{M_2}}{\underline{M_1}}, \quad M_{R\max 23} = \dfrac{\overline{M_2}}{\underline{M_3}}$

i th Experiment $M_{R\max 31} = \dfrac{\overline{M_3}}{\underline{M_1}}, \quad M_{R\max 32} = \dfrac{\overline{M_3}}{\underline{M_2}}$

These relay ratios will lead to three critical points, each on a different side of the DCP. These three critical points provide three good starting points for the next step, and are also close to the three independent single-loop critical points. A good approximation of a critical point is given by:

$$K_{1cr}(i) = \frac{4M_1(i)}{\pi a_1(i)} \qquad K_{2cr} = \frac{4M_2(i)}{\pi a_2(i)} \qquad K_{3cr}(i) = \frac{4M_3(i)}{\pi a_3(i)} \qquad \text{(A4.2.3)}$$

Appendix

Determination of steady state gains

The steady state gains of process are identified simultaneously with the critical points: after three relay experiments, using equation (A4.2.4) as follow.

$$G(0)=\begin{bmatrix} g_{11}(0) & g_{12}(0) & g_{13}(0) \\ g_{21}(0) & g_{22}(0) & g_{32}(0) \\ g_{31}(0) & g_{32}(0) & g_{33}(0) \end{bmatrix}=\begin{bmatrix} \bar{y}_1^1 & \bar{y}_1^2 & \bar{y}_1^3 \\ \bar{y}_2^1 & \bar{y}_2^2 & \bar{y}_2^3 \\ \bar{y}_3^1 & \bar{y}_3^2 & \bar{y}_3^3 \end{bmatrix}\begin{bmatrix} \bar{u}_1^1 & \bar{u}_1^2 & \bar{u}_1^3 \\ \bar{u}_2^1 & \bar{u}_2^2 & \bar{u}_2^3 \\ \bar{u}_3^1 & \bar{u}_3^2 & \bar{u}_3^3 \end{bmatrix}^{-1} \qquad \text{(A4.2.4)}$$

Linear Interpolation

From 3 relay experiments, 3 critical points will be identified as follow:

$(i-2)$ *th* Experiment $\quad M_1(i-2),\ M_2(i-2),\ M_3(i-2)$

$a_1(i-2),\ a_2(i-2),\ a_3(i-2)$

$$\therefore K_1(i-2)=\frac{4M_1(i-2)}{\pi a_1(i-2)} \qquad K_2(i-2)=\frac{4M_2(i-2)}{\pi a_2(i-2)} \quad K_3(i-2)=\frac{4M_3(i-2)}{\pi a_3(i-2)}$$

$(i-1)$ *th* Experiment $\quad M_1(i-1),\ M_2(i-1),\ M_3(i-1)$

$a_1(i-1),\ a_2(i-1),\ a_3(i-1)$

$$\therefore K_1(i-1)=\frac{4M_1(i-1)}{\pi a_1(i-1)} \qquad K_2(i-1)=\frac{4M_2(i-1)}{\pi a_2(i-1)} \quad K_3(i-1)=\frac{4M_3(i-1)}{\pi a_3(i-1)}$$

i th Experiment $\quad M_1(i),\ M_2(i),\ M_3(i)$

$a_1(i),\ a_2(i),\ a_3(i)$

$$\therefore K_1(i)=\frac{4M_1(i)}{\pi a_1(i)} \qquad K_2(i)=\frac{4M_2(i)}{\pi a_2(i)} \quad K_3(i)=\frac{4M_3(i)}{\pi a_3(i)}$$

Appendix

To find the relays ratio for next step:

$(i+1)\,th$ Experiment need $M_1(i+1),\ M_2(i+1)\,and\,M_3(i+1)$

Condition:

$$\tan\varphi_{d1} = \frac{K_2(i+1)}{K_1(i+1)}\frac{g_{22}(0)}{g_{11}(0)}$$

$$= \frac{4M_2(i+1)}{\pi a_2(i+1)}\frac{\pi a_1(i+1)}{4M_1(i+1)}\frac{g_{22}(0)}{g_{11}(0)}$$

$$\tan\varphi_{d2} = \frac{K_3(i+1)}{K_2(i+1)}\frac{g_{33}(0)}{g_{22}(0)}$$

$$= \frac{4M_3(i+1)}{\pi a_3(i+1)}\frac{\pi a_2(i+1)}{4M_2(i+1)}\frac{g_{33}(0)}{g_{22}(0)}$$

Introduce

$$a_{R1}(i+1) = \frac{a_1(i+1)}{a_2(i+1)} \qquad M_{R1}(i+1) = \frac{M_1(i+1)}{M_2(i+1)}$$

$$a_{R2}(i+1) = \frac{a_2(i+1)}{a_3(i+1)} \qquad M_{R2}(i+1) = \frac{M_2(i+1)}{M_3(i+1)}$$

$$\therefore \tan\varphi_{d1} = \frac{a_{R1}(i+1)}{M_{R1}(i+1)}\frac{g_{22}(0)}{g_{11}(0)} \qquad \tan\varphi_{d2} = \frac{a_{R2}(i+1)}{M_{R2}(i+1)}\frac{g_{33}(0)}{g_{22}(0)} \qquad \text{(A4.2.5)}$$

Recalling from above theorem that, along the stability limits, $a_{R1}(i) = f_k[M_{R1}(i), M_{R2}(i)]$ via some unknown implicit function f. A straight-line approximation to the function f is used, assumption:

$$a_{R1}(i) = b_{i11}M_{R1}(i) + b_{i12}M_{R2}(i) + b_{i13}$$

$$a_{R2}(i) = b_{i21}M_{R1}(i) + b_{i22}M_{R2}(i) + b_{i23} \qquad \text{(A4.2.6)}$$

Use $(i-2)\,th$, $(i-1)\,th$ and $i\,th$ experiments to find Matrix B:

in compact form Solve:

$$A_R = BM_R \rightarrow B = A_R M_R^{-1} \tag{A4.2.7}$$

where:

$$A_R = \begin{bmatrix} a_{R1}(i) & a_{R1}(i-1) & a_{R1}(i-2) \\ a_{R2}(i) & a_{R2}(i-1) & a_{R2}(i-2) \end{bmatrix} \quad B = \begin{bmatrix} b_{i11} & b_{i12} & b_{i13} \\ b_{i21} & b_{i22} & b_{i23} \end{bmatrix}$$

$$M_R = \begin{bmatrix} M_{R1}(i) & M_{R1}(i-1) & M_{R1}(i-2) \\ M_{R2}(i) & M_{R2}(i-1) & M_{R1}(i-2) \\ 1 & 1 & 1 \end{bmatrix}$$

After calculation of B the new relay ratios, $M_R(i+1)$ from equation (A4.2.8) will be:

$$M_R(i+1) = [B_t - B_1]^{-1} B_2 \tag{A4.2.8}$$

where:

$$M_R(i+1) = \begin{bmatrix} M_{R1}(i+1) \\ M_{R2}(i+1) \end{bmatrix} \quad B_t = \begin{bmatrix} \tan\varphi_{d1} \dfrac{g_{11}(0)}{g_{22}(0)} & 0 \\ 0 & \tan\varphi_{d2} \dfrac{g_{22}(0)}{g_{33}(0)} \end{bmatrix}$$

$$B_1 = \begin{bmatrix} b_{i11} & b_{i12} \\ b_{i21} & b_{i22} \end{bmatrix} \quad B_2 = \begin{bmatrix} b_{i13} \\ b_{i23} \end{bmatrix}$$

If the approximation (A4.2.6) is perfectly accurate then $M_{R12}(i+1)$ *and* $M_{R23}(i+1)$ leads exactly to the desired critical point. Since it is not, there will be some error. A tolerance ε_i is defined, and algorithm is stopped when $|\varphi - \varphi_{dk}| < \varepsilon_i$ (i=1,2). Otherwise, the procedure is continued in the same fashion as in experiment (i+1). Where the best three experiments, i.e. those that are closer to φ_{dk} play the role of experiments $(i-2),(i-1)$ *and* i equations (A4.2.5)-(A4.2.8). This simple algorithm shows excellent convergence properties.

PID Tuning: Once the DCP has been found, the setting of the PID controllers can be determined in a straightforward manner. A simple choice is to use the ZN rules.

Appendix

Appendix 6.1: Discrete MIMO PID Controller Representation

z transforming equation of discrete PID can be written as:

$$U(z) = \frac{[q_0 z^2 + q_1 z + q_2]}{z^2 - z} E(z) \qquad \text{(A6.3.1)}$$

where:

$$q_0 = (k_P + k_I + k_D), \quad q_1 = -(k_P + 2k_D) \quad q_2 = k_D$$

In time scale and incremental from:

$$u(k+2) - u(k+1) = q_0 e(k+2) + q_1 e(k+1) + q_2 e(k) \qquad \text{(A6.3.2)}$$

Define the state as follow:

$$\begin{cases} x_1(k) = u(k) - q_0 e(k) \\ x_2(k) = x_1(k+1) - q_1 e(k) \end{cases} \qquad \text{(A6.3.3)}$$

$$x_1(k+1) = u(k+1) - q_0 e(k+1) = x_2(k) + q_1 e(k)$$
$$x_2(k+1) = x_1(k+2) - q_1 e(k+1) = u(k+2) - q_0 e(k+2) - q_1 e(k+1) =$$
$$u(k+1) + q_2 e(k) = x_1(k) + q_0 e(k) + q_2 e(k)$$

$$\begin{cases} x_1(k+1) = x_2(k) + q_1 e(k) \\ x_2(k+1) = x_1(k) + (q_0 + q_2) e(k) \end{cases} \qquad \text{(A6.3.4)}$$

Appendix

$$\begin{cases} x_1(k+1) = x_2(k) + q_1 e(k) \\ x_2(k+1) = x_1(k) + (q_0 + q_2) e(k) \end{cases} \qquad \text{(A6.3.5)}$$
$$u(k) = x_1(k) + q_0 e(k)$$

Therefore the state space presentation is:

$$\begin{aligned} x_c(k+1) &= A_c x_c(k) + B_c e(k) \\ u(k) &= C_c x_c(k) + D_c e(k) \end{aligned} \qquad \text{(A6.3.6)}$$

where:

$$x_c(k) = \begin{bmatrix} x_1(k) \\ x_2(k) \end{bmatrix} \quad A_c = \begin{bmatrix} 0 & 1 \\ 1 & 0 \end{bmatrix} \quad B_c = \begin{bmatrix} q_1 \\ q_0 + q_2 \end{bmatrix} \quad C_c = \begin{bmatrix} 1 & 0 \end{bmatrix} \quad D_c = q_0$$

Appendix 6.2: The Relation Between Continuous and Discrete Matrices of MIMO PID Controller Representation

The MIMO PID controller in continuous form can be represented by:

$$\begin{aligned} \dot{x}_c(t) &= A_c^{'} x_c(t) + B_c^{'} e(t) \\ \Delta u(t) &= C_c x_c(t) + D_c e(t) \end{aligned} \qquad \text{(A6.2.1)}$$

where:

$A_c^{'}, B_c^{'}, C_c$ and D_c are coefficient matrices of the appropriate dimensions.

The basic definition of a derivative is:

$$\dot{x}_c(t) = \lim_{\Delta t \to 0} \frac{x_c(t+\Delta t) - x_c(t)}{\Delta t} \qquad \text{(A6.2.2)}$$

It is considered $\Delta t = T$, thus, approximating the derivative as:

$$\dot{x}_c = \frac{x_c(t+T) - x_c(t)}{T} \qquad \text{(A6.2.3)}$$

Substituting in above equation to obtain:

$$\frac{x_c(t+T) - x_c(t)}{T} = A_c^{'} x_c(t) + B_c^{'} e(t) \qquad \text{(A6.2.4)}$$

Appendix

Solving for $x_c(t+T)$, it will be:

$$x_c(t+T) = T_s A_c' x_c(t) + x_c(t) + T_s B_c' e(t) = (T_s A_c' + I)x_c(t) + T_s B_c' e(t) \qquad \text{(A6.2.5)}$$

where:

t is divided into intervals of width T_s

Therefore the time t is written as $t = kT_s$, where k is an integer index so that $k = 0,1,2,\cdots$

then the above equation is written as:

$$\begin{aligned} x_c[(k+1)T_s] &= (T_s A_c' + I)x_c(kT_s) + T_s B_c' e(kT_s) \\ \Delta u(kT_s) &= C_c x_c(kT_s) + D_c e(kT_s) \end{aligned} \qquad \text{(A6.2.6)}$$

this equation can be rewritten as:

$$\begin{aligned} x_c(k+1) &= A_c x_c(k) + B_c e(k) \\ \Delta u(k) &= C_c x_c(k) + D_c e(k) \end{aligned} \qquad \text{(A6.2.7)}$$

where:

$$A_c = (T_s A_c' + I) \quad B_c = T_s B_c'$$

The symbol T_s is omitted from the arguments of the variables.

Appendix 6.3: The Control Signal Calculation of Predictive PID

The state space presentation of predictive PID controller is:

$$\begin{aligned} x_c(k+1) &= A_c x_c(k) + B_c e(k) \\ u(k) &= \sum_{i=0}^{M} \tilde{u}(k+i) = \sum_{i=0}^{M} C_c x_c(k+i) + D_c e(k+i) \end{aligned} \tag{A6.1.1}$$

The state space presentation of deferent level of PID is:

Level 0: (conventional PID)

$$\begin{aligned} x_c(k+1) &= A_c x_c(k) + B_c e(k) \\ \tilde{u}(k) &= C_c x_c(k) + D_c e(k) \end{aligned} \tag{A6.1.2}$$

Level 1:

$$\begin{aligned} x_c(k+2) &= A_c x_c(k+1) + B_c e(k+1) = A_c^2 x_c(k) + A_c B_c e(k) + B_c e(k+1) \\ \tilde{u}(k+1) &= C_c x_c(k+1) + D_c e(k+1) = C_c A_c x_c(k) + C_c B_c e(k) + D_c e(k+1) \end{aligned}$$

Level 2:

$$\begin{aligned} x_c(k+3) &= A_c x_c(k+2) + B_c e(k+2) = A_c^3 x_c(k) + A_c^2 B_c e(k) + A_c B_c e(k+1) + B_c e(k+2) \\ \tilde{u}(k+2) &= C_c x_c(k+2) + D_c e(k+2) = C_c A_c^2 x_c(k) + C_c A_c B_c e(k) + C_c B_c e(k+1) + D_c e(k+2) \end{aligned}$$

Level 3:

$$\begin{aligned} x_c(k+4) &= A_c x_c(k+3) + B_c e(k+3) \\ &= A_c^4 x_c(k) + A_c^3 B_c e(k) + A_c^2 B_c e(k+1) + A_c B_c e(k+2) + B_c e(k+3) \\ \tilde{u}(k+3) &= C_c x_c(k+3) + D_c e(k+3) \\ &= C_c A_c^3 x_c(k) + C_c A_c^2 B_c e(k) + C_c A_c B_c e(k+1) + C_c B_c e(k+2) + D_c e(k+3) \end{aligned}$$

$\vdots$

Appendix

Level M:

$$\begin{cases} x_c(k+i+1) = A_c^{(i+1)} x_c(k) + \sum_{j=0}^{i} A_c^j B_c e(k+i-j) \\ \tilde{u}(k+i) = C_c A_c^i x_c(k) + \sum_{j=0}^{i-1} C_c A_c^i B_c e(k+i-j-1) + D_c e(k+i) \end{cases} \tag{A6.1.3}$$

and for M level of PID controller the control signal is:

$$X_c = \begin{bmatrix} x_c(k+1) \\ x_c(k+2) \\ x_c(k+3) \\ \vdots \\ x_c(k+M+1) \end{bmatrix} = \begin{bmatrix} A_c \\ A_c^2 \\ A_c^3 \\ \vdots \\ A_c^{M+1} \end{bmatrix} x_c(k) + \begin{bmatrix} B_c & 0 & \cdots & 0 & 0 \\ A_c B_c & B_c & \cdots & 0 & 0 \\ A_c^2 B_c & A_c B_c & \cdots & 0 & 0 \\ \vdots & \vdots & \ddots & \vdots & \vdots \\ A_c^M B_c & A_c^{M-1} B_c & \cdots & A_c B_c & B_c \end{bmatrix} \begin{bmatrix} e(k) \\ e(k+1) \\ e(k+2) \\ \vdots \\ e(k+M) \end{bmatrix} \tag{A6.1.4}$$

$$\tilde{U}_M = \begin{bmatrix} \tilde{u}(k) \\ \tilde{u}(k+1) \\ \tilde{u}(k+2) \\ \vdots \\ \tilde{u}(k+M) \end{bmatrix} = \begin{bmatrix} C_c \\ C_c A_c \\ C_c A_c^2 \\ \vdots \\ C_c A_c^M \end{bmatrix} x_c(k) - \begin{bmatrix} D_c & 0 & \cdots & 0 & 0 \\ C_c B_c & D_c & \cdots & 0 & 0 \\ C_c A_c B_c & C_c B_c & \cdots & 0 & 0 \\ \vdots & \vdots & \ddots & \vdots & \vdots \\ C_c A_c^{M-1} B_c & C_c A_c^{M-2} B_c & \cdots & C_c B_c & D_c \end{bmatrix} \begin{bmatrix} y(k) \\ y(k+1) \\ y(k+2) \\ \vdots \\ y(k+M) \end{bmatrix}$$

$$+ \begin{bmatrix} D_c & 0 & \cdots & 0 & 0 \\ C_c B_c & D_c & \cdots & 0 & 0 \\ C_c A_c B_c & C_c B_c & \cdots & 0 & 0 \\ \vdots & \vdots & \ddots & \vdots & \vdots \\ C_c A_c^{M-1} B_c & C_c A_c^{M-2} B_c & \cdots & C_c B_c & D_c \end{bmatrix} \begin{bmatrix} r(k) \\ r(k+1) \\ r(k+2) \\ \vdots \\ r(k+M) \end{bmatrix} \tag{A6.1.5}$$

which can be expressed as:

$$X_c = G_c x_c(k) + H_p R_M(k) - H_p Y_M(k)$$

$$\tilde{U}_M = F_c x_c(k) + L_p R_M(k) - L_p Y_M(k) \tag{A6.1.6}$$

Appendix

Calculating control signal from equation (A6.1.6) will give us:

$$x_c(k+1) = \sum_{i=1}^{M+1} X_c(i,:) = \sum_{i=1}^{M+1} G_c(i,:)x_c(k) + \sum_{i=1}^{M+1}\sum_{j=1}^{i} H_p(i,j)e(k+j-1)$$

$$x_c(k+1) = \sum_{i=1}^{M+1} \tilde{x}_c(k+i) = \sum_{i=0}^{M} A_c^{i+1}x_c(k) + \sum_{i=0}^{M}\sum_{j=0}^{i}[A_c^j B_c e(k+i-j)] \qquad \text{(A6.1.7)}$$

$$u(k) = \sum_{i=1}^{M+1} \tilde{U}_M(i,:) = \sum_{i=1}^{M+1} F_c(i,:)x_c(k) + \sum_{i=1}^{M+1}\sum_{j=1}^{i} L_p(i,j)r(k+j-1) - \sum_{i=1}^{M+1}\sum_{j=1}^{i} L_p(i,j)y(k+j-1)$$

$$u(k) = C_c\sum_{i=0}^{M} A_c^{i+1}x_c(k) + D_c\sum_{i=0}^{M} e(k+i) + \sum_{i=1}^{M}\sum_{j=0}^{i-1}[C_c A_c^j B_c e(k+i-j)] \qquad \text{(A6.1.8)}$$